NASA/TP–2010-216726

Nondimensional Parameters and Equations for Nonlinear and Bifurcation Analyses of Thin Anisotropic Quasi-Shallow Shells

Michael P. Nemeth
Langley Research Center, Hampton, Virginia

July 2010

NASA STI Program . . . in Profile

Since its founding, NASA has been dedicated to the advancement of aeronautics and space science. The NASA scientific and technical information (STI) program plays a key part in helping NASA maintain this important role.

The NASA STI program operates under the auspices of the Agency Chief Information Officer. It collects, organizes, provides for archiving, and disseminates NASA's STI. The NASA STI program provides access to the NASA Aeronautics and Space Database and its public interface, the NASA Technical Report Server, thus providing one of the largest collections of aeronautical and space science STI in the world. Results are published in both non-NASA channels and by NASA in the NASA STI Report Series, which includes the following report types:

- TECHNICAL PUBLICATION. Reports of completed research or a major significant phase of research that present the results of NASA programs and include extensive data or theoretical analysis. Includes compilations of significant scientific and technical data and information deemed to be of continuing reference value. NASA counterpart of peer-reviewed formal professional papers, but having less stringent limitations on manuscript length and extent of graphic presentations.

- TECHNICAL MEMORANDUM. Scientific and technical findings that are preliminary or of specialized interest, e.g., quick release reports, working papers, and bibliographies that contain minimal annotation. Does not contain extensive analysis.

- CONTRACTOR REPORT. Scientific and technical findings by NASA-sponsored contractors and grantees.

- CONFERENCE PUBLICATION. Collected papers from scientific and technical conferences, symposia, seminars, or other meetings sponsored or co-sponsored by NASA.

- SPECIAL PUBLICATION. Scientific, technical, or historical information from NASA programs, projects, and missions, often concerned with subjects having substantial public interest.

- TECHNICAL TRANSLATION. English-language translations of foreign scientific and technical material pertinent to NASA's mission.

Specialized services also include creating custom thesauri, building customized databases, and organizing and publishing research results.

For more information about the NASA STI program, see the following:

- Access the NASA STI program home page at *http://www.sti.nasa.gov*

- E-mail your question via the Internet to help@sti.nasa.gov

- Fax your question to the NASA STI Help Desk at 443-757-5803

- Phone the NASA STI Help Desk at 443-757-5802

- Write to:
  NASA STI Help Desk
  NASA Center for AeroSpace Information
  7115 Standard Drive
  Hanover, MD 21076-1320

NASA/TP–2010-216726

Nondimensional Parameters and Equations for Nonlinear and Bifurcation Analyses of Thin Anisotropic Quasi-Shallow Shells

Michael P. Nemeth
Langley Research Center, Hampton, Virginia

National Aeronautics and
Space Administration

Langley Research Center
Hampton, Virginia 23681-2199

July 2010

Available from:

NASA Center for AeroSpace Information
7115 Standard Drive
Hanover, MD 21076-1320
443-757-5802

Contents

List of Tables

List of Figures

Summary

A comprehensive development of nondimensional parameters and equations for nonlinear and bifurcation analyses of quasi-shallow shells, based on the Donnell-Mushtari-Vlasov theory for thin anisotropic shells, is presented. A complete set of field equations for geometrically imperfect shells that includes kinematic equations, isothermal constitutive equations for generally laminated shells, equilibrium equations, boundary conditions, and the compatibility equation is presented in terms of general lines-of-curvature coordinates. In addition, the corresponding virtual work statement is presented. A systematic nondimensionalization of these equations is developed, several new nondimensional parameters are defined, and a comprehensive stress-function formulation is presented that includes variational principles for equilibrium and compatibility. Bifurcation analysis is applied to the nondimensional nonlinear field equations and a comprehensive set of bifurcation equations are given that include the effects of pre-bifurcation rotations, which are commonly neglected. These bifurcation equations also include a stress-function formulation with variational principles for equilibrium and compatibility of the adjacent equilibrium states.

An extensive collection of tables and figures is presented that shows the effects of lamina material properties and stacking sequence on the nondimensional parameters. In particular, results are presented for nine lamina material systems and several stacking sequences, and are independent of the shell geometry. These stacking sequences include balanced symmetric angle-ply laminates, balanced antisymmetric angle-ply laminates, symmetric quasi-isotropic laminates, antisymmetric quasi-isotropic laminates, and unsymmetric quasi-isotropic laminates. Results are also given for unbalanced, unsymmetric laminates composed of perpendicular unidirectional plies aligned with the shell coordinate curves and angle plies.

Introduction

A common structural element of aerospace vehicles is the thin-walled shell. Often, aerospace shell structures are tailored from fiber-reinforced, laminated-composite materials to reduce structural weight, increase strength and stiffness, and improve one or more performance characteristics of a vehicle. In a tailoring process, it is desirable to know the "landscape" of the design space so that a designer can assess the sensitivity of a candidate optimal design to the variations in structural characteristics that may occur in a manufacturing process or in a design change introduced to accommodate some other vehicle attribute. This point is particularly true for laminated-composite structures, which offer a much larger design space than metals because of the plethora of material systems available and the laminate constructions that are possible. As a result, nondimensional parameters are sometimes used to navigate the design space. In particular, many different laminate constuctions may correspond to the same set of nondimensional parameters, and the relative magnitudes of the parameters can be used to identify special cases in which one or more parameters are negligible. This correspondance effectively reduces the dimensionality of the design space to something that can be managed by designers. As a result, nondimensional parameters also provide insight into the development of scaling technology used to reduce the cost of experimental validation and certification of large-scale structures.

Several early works have been published that use nondimensional parameters to characterize structural behavior and to faciliate design. For example, Seydel used nondimensional parameters to characterize the shear-buckling behavior of orthogonally stiffened long, flat plate strips made of metal or plywood in the early 1930s.[1, 2] In his study, the parameters were identified by modeling the stiffened plate strip as a homogeneous orthotropic plate and by using the corresponding differential equation for buckling, derived by Huber around 1923.[3] Seydel's parameters and results appeared in a compilation of design technology for airplane design in 1935.[4] Similarly, in 1946, Cozzone and Melcon[5] presented column buckling results in terms of nondimensional parameters. Their work was driven by the need to address the numerous new aluminum and steel alloys being used in airplane design. Perhaps one of the most well known nondimensional parameters to appear in the 1940s is the "Z" parameter introduced by Batdorf, which characterizes the effects of length, thickness, and radius of curvature on the linear bifurcation buckling of isotropic cylinders.[6-10]

Around 1950, Thielemann[11] presented an in-depth study of the buckling behavior of generally orthotropic plates subjected to compression and shear loads. This class of plates is similar to symmetrically laminated plates in that they exhibit anisotropy in the form of coupling between pure bending and twisting deformations. More specifically, Thielemann presented numerous results for specially orthotropic plates in terms of one of Seydel's nondimensional parameters, and introduces two additional nondimensional parameters to characterize the effects of anisotropy on the buckling of generally orthotropic plates. In 1952, Wittrick[12] used nondimensional parameters to simplify the buckling design of rectangular specially orthotropic plates subjected to compression loads. A similar study was presented by Shuleshko in 1957.[13] In 1960, Thielemann[14] presented another in-depth study that focuses on the buckling and postbuckling behavior of specially orthotropic, thin-walled cylinders with initial geometric imperfections and subjected to compression, shear, and internal pressure. In this reference, the nonlinear and buckling responses are obtained by using a single equilibrium equation and a single strain-compatibility equation. Several nondimensional parameters, in addition to those used for specially orthotropic plates, that are needed to characterize the response trends are also identified. Similar studies were presented by Geier[15] in 1965 and Seggelke and Geier[16] in 1967 that also addresses the effects of stiffener eccentricity on the buckling response of cylinders.

As the weight saving potential of fiber-reinforced and fabric-reinforced plastics started becoming apparent, the use of nondimensional parameters to characterize common response trends and behavior also increased. In 1968, Brukva[17] presented buckling results, in terms of nondimensional parameters, for specially orthotropic plates subjected to axial compression and with various combinations of clamped and simply supported edges. The results of his study were aimed at understanding the behavior of plates made from a glass-reinforced plastic material. In 1968-1970, Khot[18, 19] and Khot and Venkayya[20] used nondimensional parameters to characterize the imperfection sensitivity of generally laminated, fiber-reinforced shells subjected to axial compression and with small initial geometric imperfections. In these references, the nonlinear and buckling responses are obtained by using a single equilibrium equation and a single strain-compatibility equation. These two equations were shown to be significantly more complicated than the corresponding equations for generally orthotropic plates. Nondimensional parameters

were also identified that represent the anisotropies associated with coupling between membrane dilatation and distortion, coupling between pure bending and twisting deformations, and coupling between membrane and bending deformations. The relative magnitude of these parameters provide measures of the relative importance of each type of coupling, and when some coupling terms can be deemed negligible, analytical solutions can sometimes be obtained. Also in 1970, Johns[21] presented a review of results for the shear buckling of isotropic, specially orthotropic, and generally orthotropic rectangular plates. This review gives numerous generic results, useful for design, in terms of Seydel's nondimensional parameters and nondimensional buckling coefficients. Nondimensional parameters and results are also given that characterize the effects of edge rotational restraint on the buckling resistance. A similar in-depth study with numerous general results was given by Housner & Stein in 1975.[22]

Later, in 1977, Wiggenraad[23] used nondimensional parameters and buckling coefficients to study the effects of anistropy associated with coupling between pure bending and twisting deformations on the buckling of rectangular symmetrically laminated plates subjected to compression and shear loads. The nondimensional parameters used to characterize the anisotropy are different than those presented by Thielemann. A large number of results are presented in this reference that illustrate the sensitivity of the buckling response to variations in the nondimensional orthotropy and anisotropy parameters. An extensive study of the generic buckling and vibration behavior of specially orthotropic rectangular and circular plates was presented by Oyibo[24] in 1981 that uses affine transformations. This approach yields the plate response in terms of two independent nondimensional parameters, referred to as the generalized Poisson's ratio and the generalized rigidity ratio by Oyibo. The generalized rigidity ratio for rectangular plates is the reciprocal of the parameter defined by Seidel[1,2] in the 1930s. Likewise, a substantial amount of generic buckling-design data was presented by Fogg[25] in 1982 for laminated composite plates and curved panels in terms of nondimensional parameters and by Brunelle and Oyibo[26] in 1983 for specially orthotropic rectangular plates. Oyibo[27-29] and Stein[30] also presented a substantial amount of generic results for flutter and postbuckling, respectively, of specially orthotropic rectangular plates in 1983. Also in 1983, Nemeth[31] presented nondimensional parameters that characterize the effects of anistropy associated with coupling between pure bending and twisting deformations on the buckling of rectangular symmetrically laminated plates subjected to compression loads. The parameters given in this reference are identical to those previously given by Wiggenraad.[23] A couple of years later, Oyibo and Berman[32] and Nemeth[33, 34] published indentical forms of the anisotropy parameters that are different from, but similar to, those previously given by Wiggenraad[23] and by Nemeth.[31] These nondimensional parameters have been used extensively by Nemeth[35-42] to develop generic design data for buckling of laminated composite plates subjected to various loading conditions. Moreover, the nondimensionl parameters given in these references are used to quantify just how "close" various families of quasi-isotropic laminate are to being isotropic. In 1985, Stein[43,44] extended his earlier work to include plates subjected to shear and combined loads. Likewise, Brunelle[45-47] extended his earlier work in 1985 by examining the values of his nondimensional parameters for several orthotropic materials, and in 1986 by using nondimensional parameters to develop similarity rules for buckling and vibration and by deriving nondimensional parameters and equations for large deflections of specially orthotropic plates. Vibration analysis and generic results for specially orthotropic circular plates were also given by Oyibo and Brunelle[48] in 1985. Additional generic

results for the bending, buckling, large deflection, postbuckling, and linear and nonlinear vibration of symmetrically and unsymmetrically laminated, angle-ply and cross-ply rectangular plates were presented by Yang, Shieh, Liu, and Kuo in 1987 through 1989.[49-56] Moreover, the work presented in references 49-52 and 55 is based on the Reissner-Mindlin first-order transverse-shear-deformation plate theory. Brunelle and Shin presented detailed studies of the postbuckling behavior of rectangular specially orthotropic plates, also in 1989, by using affine transformations and nondimensional parameters to obtain generic response trends.[57-59]

In the 1990s, Nemeth[60, 61] extended his previous work to develop nondimensional parameters and equations for linear bifurcation buckling of symmetrically laminated shallow shells with double curvature. The analysis presented in these references uses a single equilibrium equation and a single strain-compatibility equation, and the nondimensionalization procedure used was heavily influenced by the previous work done by Stein[30] on postbuckling of specially orthotropic plates. In addition to the nondimensional parameters presented in references 30 and 34, parameters that characterize the anisotropy associated coupling between membrane dilatation and distortion were given, and analogues of the Batdorf "Z" parameter were derived. In addition, generalizations of Donnell's and Batdorf's equations for cylinder buckling (see references 6, 7, and 10) were presented. Also in the 1990s, Radloff et. al.[62] developed a nondimensional buckling analysis for symmetrically laminated trapezoidal plates subjected to uniaxial compression. A study of the generic bending, buckling, and vibration behavior of antisymmetric angle-ply laminates was presented by Lee and Yang[63] in 1996. In 2000, Nemeth and Smeltzer[64] presented formulas for the attenuation length of a bending boundary layer in generally laminated shells. In this reference, the attenuation length of the bending boundary layer is characterized by two nondimensional parameters; that is, one for the shell orthotropy and one for the general anisotropy. Values of these two parameters are also presented for nine different lamina material systems and several laminate stacking sequences. Later, in 2001, Hilburger et.al.[65] used nondimensional parameters, based on the Reissner-Mindlin first-order shear-deformation plate theory, to obtain scaling laws for a representative portion of a blended-wing-body transport aircraft.

From 2002-2008, Weaver and his colleagues[66-75] made extensive use of nondimensionalization procedures and parameters to gain insight into the behavior of laminated-composite structures. In particular, "knockdown" factors that account for the effects of flexural-twist and extension-twist anisotropies on the buckling of compression-loaded cylindrical shells are given in references 66-68. The results presented in reference 67 indicate that the importance of flexural-twist anisotropy depends strongly on the cylinder curvature. A similar finding was obtained by Nemeth[60, 61] for doubly curved shells subjected to shear loading. Also, design-oriented approximate solutions for compression-loaded long plates, in terms of nondimensional parameters, are given in references 70 and 74 for buckling and in references 69 and 72 for postbuckling. Moreover, a design-oriented approximate solution for compression-loaded, generally laminated cylindrical shells is given in reference 71, that uses the reduced bending stiffnesses obtained when the partially inverted form of the constitutive equations is used. In 2007, Weaver and Nemeth[76] presented bounds on the nondimensional parameters that govern symmetrically laminated plate buckling behavior, which provide insight into the potential gains in buckling resistance that are possible through laminate tailoring and composite-material

development. Similarly, in 2008, Weaver and Nemeth[77] presented design-oriented nondimensional buckling interaction curves for specially orthotropic plates subjected to combined loads. These curves represent a broad range of plate-bending orthotropy and inherently indicate the corresponding design sensitivities.

Recently, Mittelstedt and Beerhorst[78] presented nondimensional buckling curves for specially orthotropic compression-loaded plates with finite length and elastically supported edges. These results are expressed in terms of the reciprocal of Seidel's orthotropy parameter and a nodimensional measure of edge restraint, and are used for the design of stiffened panels. Also recently, Nemeth and Mikulas[79] presented simple formulas and results for use in determining the buckling resistance and stiffness design of laminated-composite cylinders subjected to compression loads. Their work is based on the nondimensional parameters and equations given in reference 60. One noteworthy aspect of this work is that the validation of the simple formulas presented is simplified significantly by establishing a simple parametric relationship between two of the nondimensional parameters governing the response.

The literature discussed previously in the present study indicates clearly the potential for simplifying and unifying design criteria for laminated-composite structures by using nondimensional parameters and equations. Although a lot has been done in this regard to develop generic design technology, the task is monumental and much more remains to be done, particularly for shell structures. Thus, one goal of the present study is to extend the nondimensionalization procedure given in references 60 and 61 for geometrically perfect, symmetrically laminated, quasi-shallow shells to include generally laminated quasi-shallow shells, with initial geometric imperfections, undergoing small strains and moderately small rotations. Herein, the term, "quasi-shallow shell," is used (e.g., see Brush and Almroth[80], p. 143), to denote shallow shell panels that are relatively flat and nonshallow shells that exhibit deformations that are rapidly varying functions of the reference-surface coordinates. These equations, and the corresponding nondimensional parameters, should be useful in the development of generic design technology that represents the effects of geometry and laminate construction on the imperfection sensitivity of shells subjected to destabilizing loads. Another goal is to present a collection of data for the nondimensional parameters presented subsequently that shows the effects of lamina material properties and laminate stacking sequence on their values and that are independent of the shell geometry. To accomplish these goals, equations of quasi-shallow shell theory that govern the nonlinear deformations of geometrically imperfect shells are presented first. Then, nondimensionalization of the kinematic equations, constitutive equations, equilibrium equations, boundary conditions, compatibility equation, and virtual work is presented and several new nondimensional parameters are defined. Next a nondimensional stress-function formulation of the nonlinear boundary-value problem is presented that yields extensions to the Donnell-Stein equations given previously in references 60 and 61. In addition, nondimensional stress-function formulations of the principles of virtual work and complementary virtual work are given. Nondimensional bifurcation equations follow that also include kinematic equations, constitutive equations, equilibrium equations, boundary conditions, the compatibility equation, and the virtual work associated with equilibrium states adjacent to a primary equilibrium path. Then, a nondimensional stress-function formulation of the boundary-eigenvalue problem is presented that includes variational principles for equilibrium and compatibility. For all these analytical developments, an extensive list of symbols is given in the Appendix. Finally an

extensive collection of nondimensional-parameter data is presented for nine lamina material systems and several laminate stacking sequences that should be useful to design-technology developers.

Equations for Nonlinear Deformations

The basic equations for nonlinear deformations of doubly curved quasi-shallow (e.g., see Brush and Almroth[80], p. 196) shells with uniform thickness h are presented subsequently in terms of the orthogonal, lines-of-curvature, curvilinear coordinates (ξ_1,ξ_2,ζ) that are depicted in figure 1 for a generic shell reference surface A. Associated with each point **p** of the reference surface, with coordinates $(\xi_1,\xi_2,0)$, are three perpendicular, unit-magnitude vector fields $\hat{e}_1$, $\hat{e}_2$, and $\hat{n}$. The vectors $\hat{e}_1$ and $\hat{e}_2$ are tangent to the ξ_1 -and ξ_2-coordinate curves, respectively, and reside in the tangent plane at the point **p**. The vector $\hat{n}$ is tangent to the ζ-coordinate curve at point **p** and perpendicular to the tangent plane. This class of parametric coordinates permits substantial simplification of the shell equations and has many practical applications.

Lines-of-curvature coordinates form an orthogonal coordinate mesh and are identified by examining how the vectors $\hat{e}_1$, $\hat{e}_2$, and $\hat{n}$ change as the coordinate curves are traversed by an infinitesimal amount. In particular, at every point **q** that is infinitesimally close to point **p** there is another set of vectors $\hat{e}_1$, $\hat{e}_2$, and $\hat{n}$ with similar attributes; that is, the vectors $\hat{e}_1$ and $\hat{e}_2$ are orthogonal and tangent to the ξ_1 -and ξ_2-coordinate curves at **q**, respectively, and reside in the tangent plane at the point **q**. Likewise, vector $\hat{n}$ is tangent to the ζ-coordinate curve at point **q** and perpendicular to the tangent plane at point **q**. Next, consider the finite portion of the tangent plane at point **p** shown in figure 1. Because of the identical properties of the vectors $\hat{e}_1$, $\hat{e}_2$, and $\hat{n}$ at every point of the surface, an identical, corresponding planar region exists at point **q**. Therefore, the vectors $\hat{e}_1$, $\hat{e}_2$, and $\hat{n}$ at point **q** can be obtained by moving the vectors $\hat{e}_1$, $\hat{e}_2$, and $\hat{n}$ at point **p** to point **q**. In addition, the plane region at point **p** moves into coincidence with the corresponding plane region at point **q** as the surface is traversed from point **p** to point **q**. During this process, the plane region at point **p** undergoes roll, pitch, and yaw (rotation about the normal line to the surface) motions. The roll and pitch motions are caused by surface twist (torsion) and curvature, respectively. The yaw motion is associated with the geodesic curvature of the surface curve traversed in going from point **p** to **q**. When a line-of-curvature coordinate curve is traversed in going from point **p** to **q**, the planar region at point **p** undergoes only pitch and yaw motions as it moves into coincidence with the corresponding region at point **q**. Rolling motion associated with local surface torsion does not occur.

These shell equations used subsequently in the present study are relatively well known (e.g., see the classic paper by Sanders[81]) and are referred to commonly as the equations of Donnell-Mushtari-Vlasov shell theory (see the textbooks by Brush & Almroth[80] and Novozhilov[82]). Moreover, these equations are based on the fundamental assumptions of classical Love-Kirchhoff

shell theory, which neglects transverse-shear flexibility. First, the kinematic equations are presented, which include the displacement-field distribution, and the strain-displacement relations. Then, the stress resultants, constitutive equations, virtual work, and the work-conjugate nonlinear equilibrium equations and corresponding boundary conditions are presented, followed by the strain compatibility equation. These equations represent a simple, approximate representation of nonlinear shell behavior that has seen wide practical application. For each group of equations, the generalization to include a known distribution of initial geometric imperfection is given. The imperfection is manifested as a "small" displacement normal to the idealized shell reference surface.

Kinematic Equations

In the Donnell-Mushtari-Vlasov theory of quasi-shallow shells, the components of the displacement vector field of the material points comprising a shell are denoted by $\mathcal{U}_1(\xi_1,\xi_2,\zeta)$, $\mathcal{U}_2(\xi_1,\xi_2,\zeta)$, and $\mathcal{U}_3(\xi_1,\xi_2,\zeta)$, where (ξ_1, ξ_2, ζ) are orthogonal curvilinear coordinates for points of three-dimensional Euclidean space. In addition, the coordinates are defined for $a_1 \le \xi_1 \le b_1$, $a_2 \le \xi_2 \le b_2$, and $-\frac{h}{2} \le \zeta \le \frac{h}{2}$ (see figure 2), where h is shell thickness. Similarly, the displacement components of points of the two-dimensional shell reference surface, defined by $\zeta = 0$, are denoted by $u_1(\xi_1, \xi_2)$, $u_2(\xi_1, \xi_2)$, and $w(\xi_1, \xi_2)$, where (ξ_1, ξ_2) are orthogonal curvilinear Gaussian coordinates for the reference surface. These surface displacements are usually measured with respect to a given geometrically perfect, idealized shell reference surface.

To analyze to response of a shell with relatively small initial geometric imperfections, measured with respect to the idealized shell reference surface, Donnell[83] (see p. 349) introduced an "imperfection" function $w_I(\xi_1, \xi_2)$. This imperfection function represents a distribution of small deviations in the ζ-coordinate direction, measured perpendicular to the tangent plane at each point of the shell reference surface, for an unloaded shell that is stress and strain free. Under the application of loads, the shell normal displacement associated with deformation from the idealized configuration is given by $w_I(\xi_1, \xi_2) + w(\xi_1, \xi_2)$. The corresponding relationships between the three-dimensional displacement-field components and the surface-displacement-field components of the Donnell-Mushtari-Vlasov quasi-shallow shell theory are given by

$$\mathcal{U}_1(\xi_1, \xi_2, \zeta) = u_1(\xi_1, \xi_2) + \zeta \left[\psi_1(\xi_1, \xi_2) + \beta^I_1(\xi_1, \xi_2)\right] \tag{1}$$

$$\mathcal{U}_2(\xi_1, \xi_2, \zeta) = u_2(\xi_1, \xi_2) + \zeta \left[\psi_2(\xi_1, \xi_2) + \beta^I_2(\xi_1, \xi_2)\right] \tag{2}$$

$$\mathcal{U}_3(\xi_1, \xi_2, \zeta) = w(\xi_1, \xi_2) + w_I(\xi_1, \xi_2) \tag{3}$$

where

$$\beta^I_1 = -\frac{1}{A_1}\frac{\partial w_I}{\partial \xi_1} \tag{4}$$

and

$$\beta_2^I = -\frac{1}{A_2}\frac{\partial w_I}{\partial \xi_2} \tag{5}$$

are fields that define the initial stress- and strain-free rotation of a material line element that is tangent to the shell reference surface, at a given point of the reference surface. Similarly, $\psi_1 + \beta_1^I$ and $\psi_2 + \beta_2^I$ are fields that define the net rotation of a material line element that is perpendicular to the shell reference surface, at a given point of the reference surface, with respect to the undeformed idealized configuration. The symbols A_1 and A_2 are the coefficients of the first fundamental form of the shell reference surface that are defined by

$$(ds)^2 = (A_1 d\xi_1)^2 + (A_2 d\xi_2)^2 \tag{6}$$

where ds is the differential arc length between two infinitesimally neighboring points of the surface.

The normal-strain fields for a three-dimensional shell body are denoted by $\varepsilon_{11}(\xi_1,\xi_2,\zeta)$, $\varepsilon_{22}(\xi_1,\xi_2,\zeta)$, and $\varepsilon_{33}(\xi_1,\xi_2,\zeta)$, and the corresponding shearing strains are denoted by $\gamma_{12}(\xi_1,\xi_2,\zeta)$, $\gamma_{13}(\xi_1,\xi_2,\zeta)$, and $\gamma_{23}(\xi_1,\xi_2,\zeta)$. The relationships between the three-dimensional shell strains and the reference-surface strains in the Donnell-Mushtari-Vlasov theory are given by

$$\varepsilon_{11}(\xi_1, \xi_2, \zeta) = \varepsilon_{11}^{o}(\xi_1, \xi_2) + \zeta\, \kappa_{11}^{o}(\xi_1, \xi_2) \tag{7a}$$

$$\varepsilon_{22}(\xi_1, \xi_2, \zeta) = \varepsilon_{22}^{o}(\xi_1, \xi_2) + \zeta\, \kappa_{22}^{o}(\xi_1, \xi_2) \tag{7b}$$

$$\varepsilon_{33}(\xi_1, \xi_2, \zeta) = 0 \tag{7c}$$

$$\gamma_{12}(\xi_1, \xi_2, \zeta) = \gamma_{12}^{o}(\xi_1, \xi_2) + \zeta\, \kappa_{12}^{o}(\xi_1, \xi_2) \tag{7d}$$

$$\gamma_{13}(\xi_1, \xi_2, \zeta) = \gamma_{13}^{o}(\xi_1, \xi_2) \tag{7e}$$

$$\gamma_{23}(\xi_1, \xi_2, \zeta) = \gamma_{23}^{o}(\xi_1, \xi_2) \tag{7f}$$

where ε_{11}^{o}, ε_{11}^{o}, and γ_{12}^{o} are the membrane reference-surface strains; κ_{11}^{o} and κ_{22}^{o} are the changes in surface curvature; κ_{12}^{o} is the change in surface torsion; and γ_{13}^{o} and γ_{23}^{o} are the transverse shearing strains. The strain expressions result from substituting equations (1)-(3) into the corresponding strain-displacement relations of the theory of elasticity (see Novozhilov[84], pp. 56-60) and simplifying the results according to the presumptions of the Donnell-Mushtari-Vlasov theory. This process yields

$$\varepsilon_{11}^{\circ} = \frac{1}{A_1}\frac{\partial u_1}{\partial \xi_1} + \frac{u_2}{A_1 A_2}\frac{\partial A_1}{\partial \xi_2} + \frac{w}{R_1} + \frac{1}{2}(\beta_1)^2 + \beta_1^I \beta_1 \tag{8a}$$

$$\varepsilon_{22}^{\circ} = \frac{1}{A_2}\frac{\partial u_2}{\partial \xi_2} + \frac{u_1}{A_1 A_2}\frac{\partial A_2}{\partial \xi_1} + \frac{w}{R_2} + \frac{1}{2}(\beta_2)^2 + \beta_2^I \beta_2 \tag{8b}$$

$$\gamma_{12}^{\circ} = \frac{1}{A_2}\frac{\partial u_1}{\partial \xi_2} - \frac{u_2}{A_1 A_2}\frac{\partial A_2}{\partial \xi_1} + \frac{1}{A_1}\frac{\partial u_2}{\partial \xi_1} - \frac{u_1}{A_1 A_2}\frac{\partial A_1}{\partial \xi_2} + \beta_1 \beta_2 + \beta_1^I \beta_2 + \beta_2^I \beta_1 \tag{8c}$$

$$\kappa_{11}^{\circ} = \frac{1}{A_1}\frac{\partial \psi_1}{\partial \xi_1} + \frac{\psi_2}{A_1 A_2}\frac{\partial A_1}{\partial \xi_2} \tag{9a}$$

$$\kappa_{22}^{\circ} = \frac{1}{A_2}\frac{\partial \psi_2}{\partial \xi_2} + \frac{\psi_1}{A_1 A_2}\frac{\partial A_2}{\partial \xi_1} \tag{9b}$$

$$\kappa_{12}^{\circ} = \frac{1}{A_2}\frac{\partial \psi_1}{\partial \xi_2} - \frac{\psi_2}{A_1 A_2}\frac{\partial A_2}{\partial \xi_1} + \frac{1}{A_1}\frac{\partial \psi_2}{\partial \xi_1} - \frac{\psi_1}{A_1 A_2}\frac{\partial A_1}{\partial \xi_2} \tag{9c}$$

$$\gamma_{13}^{\circ} = \psi_1 - \beta_1 \tag{10a}$$

$$\gamma_{23}^{\circ} = \psi_2 - \beta_2 \tag{10b}$$

where

$$\beta_1 = -\frac{1}{A_1}\frac{\partial w}{\partial \xi_1} \tag{11a}$$

$$\beta_2 = -\frac{1}{A_2}\frac{\partial w}{\partial \xi_2} \tag{11b}$$

are fields that define the rotation of a material line element that is tangent to the imperfect-shell reference surface, at a given point of the reference surface. The symbols R_1 and R_2 represent the principal radii of curvature of the shell reference surface along the ξ_1 and ξ_2 coordinate directions, respectively. Expressions for the rotations, ψ_1 and ψ_2, are obtained in the Donnell-Mushtari-Vlasov thin-shell theory by enforcing the presumption that the transverse shearing strains are negligible compared to the other strains. This consideration gives $\psi_1 = \beta_1$ and $\psi_2 = \beta_2$. As pointed out by Donnell[83] (see p. 349), strain-like terms associated with the "imperfection" function w_I are subtracted from the corresponding terms associated with $w + w_I$ to obtain equations (8)-(10). This subtraction process enforces the requirement of a strain-free state in the absence of applied loads.

Stress Resultants and Constitutive Equations

The linear elastic constitutive equations for a laminated composite shell depend on the specific definition for the two-dimensional stress resultants that are used to represent the internal stresses, and on the presumed strain distribution. In the Donnell-Mushtari-Vlasov theory, the stress resultants are defined by

$$\begin{Bmatrix} N_{11} \\ N_{22} \\ N_{12} \end{Bmatrix} = \int_{-\frac{h}{2}}^{+\frac{h}{2}} \begin{Bmatrix} \sigma_{11} \\ \sigma_{22} \\ \sigma_{12} \end{Bmatrix} d\zeta \tag{12a}$$

$$\begin{Bmatrix} M_{11} \\ M_{22} \\ M_{12} \end{Bmatrix} = \int_{-\frac{h}{2}}^{+\frac{h}{2}} \begin{Bmatrix} \sigma_{11} \\ \sigma_{22} \\ \sigma_{12} \end{Bmatrix} \zeta \, d\zeta \tag{12b}$$

and

$$\begin{Bmatrix} Q_1 \\ Q_2 \end{Bmatrix} = \int_{-\frac{h}{2}}^{+\frac{h}{2}} \begin{Bmatrix} \sigma_{13} \\ \sigma_{23} \end{Bmatrix} d\zeta \tag{13}$$

where σ_{11}, σ_{22}, σ_{12}, σ_{13}, and σ_{23} are stresses. Equations (7) define the strain distribution, which is expressed in matrix form as

$$\begin{Bmatrix} \varepsilon_{11} \\ \varepsilon_{22} \\ \gamma_{12} \end{Bmatrix} = \begin{Bmatrix} \varepsilon^{o}_{11} \\ \varepsilon^{o}_{22} \\ \gamma^{o}_{12} \end{Bmatrix} + \zeta \begin{Bmatrix} \kappa^{o}_{11} \\ \kappa^{o}_{22} \\ \kappa^{o}_{12} \end{Bmatrix} \tag{14}$$

The state of stress in a shell is presumed to be a state of plane stress, and is represented by

$$\begin{Bmatrix} \sigma_{11} \\ \sigma_{22} \\ \sigma_{12} \end{Bmatrix} = \begin{bmatrix} \overline{Q}_{11} & \overline{Q}_{12} & \overline{Q}_{16} \\ \overline{Q}_{12} & \overline{Q}_{22} & \overline{Q}_{26} \\ \overline{Q}_{16} & \overline{Q}_{26} & \overline{Q}_{66} \end{bmatrix} \begin{Bmatrix} \varepsilon_{11} \\ \varepsilon_{22} \\ \gamma_{12} \end{Bmatrix} \tag{15}$$

where the subscripted $\overline{Q}$ symbols denote the transformed, reduced stiffness coefficients (reduced for a state of plane stress) and are found in the well-known book by Jones.[85] Note that all quantities that appear in equation (15) are functions of the ζ coordinate. The two-dimensional constitutive equations for a shell are obtained by substituting equation (14) into equation (15) first and then by substituting the resulting expression into equations (12a) and (12b). This procedure

yields

$$\left\{\begin{array}{c} N_{11} \\ N_{22} \\ N_{12} \\ \hline M_{11} \\ M_{22} \\ M_{12} \end{array}\right\} = \left[\begin{array}{ccc|ccc} A_{11} & A_{12} & A_{16} & B_{11} & B_{12} & B_{16} \\ A_{12} & A_{22} & A_{26} & B_{12} & B_{22} & B_{26} \\ A_{16} & A_{26} & A_{66} & B_{16} & B_{26} & B_{66} \\ \hline B_{11} & B_{12} & B_{16} & D_{11} & D_{12} & D_{16} \\ B_{12} & B_{22} & B_{26} & D_{12} & D_{22} & D_{26} \\ B_{16} & B_{26} & B_{66} & D_{16} & D_{26} & D_{66} \end{array}\right] \left\{\begin{array}{c} \varepsilon_{11}^{o} \\ \varepsilon_{22}^{o} \\ \gamma_{12}^{o} \\ \hline \kappa_{11}^{o} \\ \kappa_{22}^{o} \\ \kappa_{12}^{o} \end{array}\right\} \tag{16}$$

where

$$\left[\begin{array}{ccc} A_{11} & A_{12} & A_{16} \\ A_{12} & A_{22} & A_{26} \\ A_{16} & A_{26} & A_{66} \end{array}\right] = \int_{-\frac{h}{2}}^{+\frac{h}{2}} \left[\begin{array}{ccc} \overline{Q}_{11} & \overline{Q}_{12} & \overline{Q}_{16} \\ \overline{Q}_{12} & \overline{Q}_{22} & \overline{Q}_{26} \\ \overline{Q}_{16} & \overline{Q}_{26} & \overline{Q}_{66} \end{array}\right] d\zeta \tag{17}$$

$$\left[\begin{array}{ccc} B_{11} & B_{12} & B_{16} \\ B_{12} & B_{22} & B_{26} \\ B_{16} & B_{26} & B_{66} \end{array}\right] = \int_{-\frac{h}{2}}^{+\frac{h}{2}} \left[\begin{array}{ccc} \overline{Q}_{11} & \overline{Q}_{12} & \overline{Q}_{16} \\ \overline{Q}_{12} & \overline{Q}_{22} & \overline{Q}_{26} \\ \overline{Q}_{16} & \overline{Q}_{26} & \overline{Q}_{66} \end{array}\right] \zeta \, d\zeta \tag{18}$$

$$\left[\begin{array}{ccc} D_{11} & D_{12} & D_{16} \\ D_{12} & D_{22} & D_{26} \\ D_{16} & D_{26} & D_{66} \end{array}\right] = \int_{-\frac{h}{2}}^{+\frac{h}{2}} \left[\begin{array}{ccc} \overline{Q}_{11} & \overline{Q}_{12} & \overline{Q}_{16} \\ \overline{Q}_{12} & \overline{Q}_{22} & \overline{Q}_{26} \\ \overline{Q}_{16} & \overline{Q}_{26} & \overline{Q}_{66} \end{array}\right] \zeta^{2} \, d\zeta \tag{19}$$

In equations (17) through (21), the symbol h denotes the shell thickness and the reference surface is the middle surface of the shell. For a laminated-composite shell with thin layers, the layer properties are presumed constant and the integrands that are indicated in equations (17) through (19) are piecewise constant. Thus, the integrations are replaced by summations of the appropriate layer attributes over the number of layers that comprise a specific shell.

To gain insight into the nondimensionalization process presented herein, and for comparisons with other works, it is useful to express the constitutive equations in the partially inverted form

$$\left\{\begin{array}{c} \varepsilon_{11}^{o} \\ \varepsilon_{22}^{o} \\ \gamma_{12}^{o} \end{array}\right\} = \left[\begin{array}{ccc} a_{11} & a_{12} & a_{16} \\ a_{12} & a_{22} & a_{26} \\ a_{16} & a_{26} & a_{66} \end{array}\right] \left\{\begin{array}{c} N_{11} \\ N_{22} \\ N_{12} \end{array}\right\} + \left[\begin{array}{ccc} b_{11} & b_{12} & b_{16} \\ b_{12} & b_{22} & b_{26} \\ b_{16} & b_{26} & b_{66} \end{array}\right] \left\{\begin{array}{c} \kappa_{11}^{o} \\ \kappa_{22}^{o} \\ \kappa_{12}^{o} \end{array}\right\} \tag{20a}$$

$$\begin{Bmatrix} M_{11} \\ M_{22} \\ M_{12} \end{Bmatrix} = -\begin{bmatrix} b_{11} & b_{12} & b_{16} \\ b_{12} & b_{22} & b_{26} \\ b_{16} & b_{26} & b_{66} \end{bmatrix}^{\mathbf{T}} \begin{Bmatrix} N_{11} \\ N_{22} \\ N_{12} \end{Bmatrix} + \begin{bmatrix} d_{11} & d_{12} & d_{16} \\ d_{12} & d_{22} & d_{26} \\ d_{16} & d_{26} & d_{66} \end{bmatrix} \begin{Bmatrix} \kappa^{\circ}_{11} \\ \kappa^{\circ}_{22} \\ \kappa^{\circ}_{12} \end{Bmatrix} \tag{20b}$$

where

$$\begin{bmatrix} a_{11} & a_{12} & a_{16} \\ a_{12} & a_{22} & a_{26} \\ a_{16} & a_{26} & a_{66} \end{bmatrix} = \begin{bmatrix} A_{11} & A_{12} & A_{16} \\ A_{12} & A_{22} & A_{26} \\ A_{16} & A_{26} & A_{66} \end{bmatrix}^{-1} \tag{21a}$$

$$\begin{bmatrix} b_{11} & b_{12} & b_{16} \\ b_{12} & b_{22} & b_{26} \\ b_{16} & b_{26} & b_{66} \end{bmatrix} = -\begin{bmatrix} A_{11} & A_{12} & A_{16} \\ A_{12} & A_{22} & A_{26} \\ A_{16} & A_{26} & A_{66} \end{bmatrix}^{-1} \begin{bmatrix} B_{11} & B_{12} & B_{16} \\ B_{12} & B_{22} & B_{26} \\ B_{16} & B_{26} & B_{66} \end{bmatrix} \tag{21b}$$

$$\begin{bmatrix} d_{11} & d_{12} & d_{16} \\ d_{12} & d_{22} & d_{26} \\ d_{16} & d_{26} & d_{66} \end{bmatrix} = \begin{bmatrix} D_{11} & D_{12} & D_{16} \\ D_{12} & D_{22} & D_{26} \\ D_{16} & D_{26} & D_{66} \end{bmatrix} - \begin{bmatrix} B_{11} & B_{12} & B_{16} \\ B_{12} & B_{22} & B_{26} \\ B_{16} & B_{26} & B_{66} \end{bmatrix} \begin{bmatrix} A_{11} & A_{12} & A_{16} \\ A_{12} & A_{22} & A_{26} \\ A_{16} & A_{26} & A_{66} \end{bmatrix}^{-1} \begin{bmatrix} B_{11} & B_{12} & B_{16} \\ B_{12} & B_{22} & B_{26} \\ B_{16} & B_{26} & B_{66} \end{bmatrix} \tag{21c}$$

Nonlinear Equilibrium Equations and Boundary Conditions

Equilibrium equations and boundary conditions that are work conjugate to the strains given by equations (7)-(10) are obtained by applying the principle of virtual work. The statement of this principle for the Donnell-Mushtari-Vlasov theory of quasi-shallow shells is obtained by using equations (7), (12), and (13) with the general virtual work statement for a three-dimensional solid undergoing "small" strains and "moderately small" rotations (e.g., see Washizu[86], pp. 325-327). The resulting expression is given by

$$\int\int_{A} \delta W_{int}\, A_1 A_2 d\xi_1 d\xi_2 = \int\int_{A} \delta W_{ext}\, A_1 A_2 d\xi_1 d\xi_2 + \int_{\partial A} \delta W^{B}_{ext}\, ds \tag{22}$$

where δW_{int} is the virtual work of the internal stresses and δW_{ext} is the virtual work of the external surface tractions acting at each point of the shell reference surface A depicted in figure 1. The symbol δW^{B}_{ext} represents the virtual work of the external tractions acting on the curve ∂A that encloses the region A, as shown in figure 1. The internal virtual work is given by

$$\delta W_{int} = N_{11}\,\delta\varepsilon^{\circ}_{11} + N_{12}\,\delta\gamma^{\circ}_{12} + N_{22}\,\delta\varepsilon^{\circ}_{22} + M_{11}\,\delta\kappa^{\circ}_{11} + M_{12}\,\delta\kappa^{\circ}_{12} + M_{22}\,\delta\kappa^{\circ}_{22} + Q_1\delta\gamma^{\circ}_{13} + Q_2\delta\gamma^{\circ}_{23} \tag{23a}$$

In this expression, the virtual strains $\delta\varepsilon^{\circ}_{11}$, etc. are obtained by taking the first variation of the strains given by equations (8)-(10). The pointwise external virtual work of the tangential surface

tractions q_1 and q_2 and the normal surface traction q_3 is

$$\delta W_{ext} = q_1 \delta u_1 + q_2 \delta u_2 + q_3 \delta w \tag{23b}$$

The surface tractions q_1, q_2, and q_3 are presumed positive-valued in the positive ξ_1, ξ_2, and ζ coordinate directions, respectively, as shown in figure 2. The boundary integral in equation (22) represents the virtual work of forces per unit length that are applied to the boundary ∂A of the region A, and it is implied that the integrand is evaluated on the boundary. The symbol ds denotes the boundary differential arc-length coordinate, which is traversed in accordance with the surface divergence theorem of Calculus. In the present study, the domain of the surface A is given by $a_1 \le \xi_1 \le b_1$ and $a_2 \le \xi_2 \le b_2$, and the boundary curve ∂A consists of four smooth arcs given by the constant values of the coordinates ξ_1 and ξ_2, as depicted in figure 2. For this case, the boundary integral is expressed more precisely as

$$\begin{aligned}\int_{\partial A} \delta W_{ext}^{B}\, ds = &\int_{a_2}^{b_2} \left[N(\xi_2)\delta u_1 + S(\xi_2)\delta u_2 + V(\xi_2)\delta w - M(\xi_2)\frac{1}{A_1}\frac{\partial \delta w}{\partial \xi_1} \right]_{a_1}^{b_1} A_2 d\xi_2 + \\ &\int_{a_1}^{b_1} \left[S(\xi_1)\delta u_1 + N(\xi_1)\delta u_2 + V(\xi_1)\delta w - M(\xi_1)\frac{1}{A_2}\frac{\partial \delta w}{\partial \xi_2} \right]_{a_2}^{b_2} A_1 d\xi_1\end{aligned} \tag{23c}$$

In equation (23c); N, S, and V represent external forces per unit length that are applied normal, tangential, and transverse to the given edge, respectively, as shown in figure 2. Likewise, M is a moment per unit length with an axis of rotation that is parallel to the given edge, at the given point of the boundary. In addition, V contains a contribution due to an applied twisting moment per unit length, consistent with the definition of the Kirchhoff shear stress resultant used in classical plate and shell theory.

The equilibrium equations and boundary conditions are obtained by applying "integration-by-parts" formulas, obtained by specialization of the surface divergence theorem, to the first integral in equation (22). For two arbitrary differentiable functions $f(\xi_1,\xi_2)$ and $g(\xi_1,\xi_2)$, the "integration-by-parts" formulas are given in general form by

$$\iint_A \frac{\partial f}{\partial \xi_1}(g)\, d\xi_1 d\xi_2 = -\iint_A (f)\frac{\partial g}{\partial \xi_1}\, d\xi_1 d\xi_2 + \int_{\partial A} \frac{fg}{A_2}\left(\hat{N} \bullet \hat{e}_1\right) ds \tag{24a}$$

$$\iint_A \frac{\partial f}{\partial \xi_2}(g)\, d\xi_1 d\xi_2 = -\iint_A (f)\frac{\partial g}{\partial \xi_2}\, d\xi_1 d\xi_2 + \int_{\partial A} \frac{fg}{A_1}\left(\hat{N} \bullet \hat{e}_2\right) ds \tag{24b}$$

where $\hat{N}$ is the outward unit-magnitude vector field perpendicular to A and ∂A, and $\hat{e}_1$ and $\hat{e}_2$ are unit-magnitude vector fields that are tangent to the ξ_1 and ξ_2 coordinate curves, respectively, at every point of A and ∂A, as shown in figure 1. Thus, at a given point of ∂A, $\hat{N}$ lies in the surface tangent plane at that point. For the specific surface domain given by $a_1 \le \xi_1 \le b_1$ and $a_2 \le \xi_2 \le b_2$, and enclosed by the four smooth arcs given by the constant values of the coordinates ξ_1 and ξ_2, equations (24) are expressed as

$$\iint_A \frac{\partial f}{\partial \xi_1}(g)\, d\xi_1 d\xi_2 = -\iint_A (f)\frac{\partial g}{\partial \xi_1}\, d\xi_1 d\xi_2 + \int_{a_2}^{b_2} \{fg\}_{a_1}^{b_1} d\xi_2 \tag{25a}$$

$$\iint_A \frac{\partial f}{\partial \xi_2}(g)\, d\xi_1 d\xi_2 = -\iint_A (f)\frac{\partial g}{\partial \xi_2}\, d\xi_1 d\xi_2 + \int_{a_1}^{b_1} \{fg\}_{a_2}^{b_2} d\xi_1 \tag{25b}$$

where

$$\{fg\}_{a_1}^{b_1} \equiv f(b_1,\xi_2)\, g(b_1,\xi_2) - f(a_1,\xi_2)\, g(a_1,\xi_2) \tag{25c}$$

$$\{fg\}_{a_2}^{b_2} \equiv f(\xi_1,b_2)\, g(\xi_1,b_2) - f(\xi_1,a_2)\, g(\xi_1,a_2) \tag{25d}$$

The notation defined by equations (25) is used throughout the present study.

The virtual strains appearing in equation (23a) are given by

$$\delta\varepsilon_{11}^{\circ} = \frac{1}{A_1}\frac{\partial \delta u_1}{\partial \xi_1} + \frac{\delta u_2}{A_1 A_2}\frac{\partial A_1}{\partial \xi_2} + \frac{\delta w}{R_1} - \left(\beta_1 + \beta_1^{I}\right)\frac{1}{A_1}\frac{\partial \delta w}{\partial \xi_1} \tag{26a}$$

$$\delta\varepsilon_{22}^{\circ} = \frac{1}{A_2}\frac{\partial \delta u_2}{\partial \xi_2} + \frac{\delta u_1}{A_1 A_2}\frac{\partial A_2}{\partial \xi_1} + \frac{\delta w}{R_2} - \left(\beta_2 + \beta_2^{I}\right)\frac{1}{A_2}\frac{\partial \delta w}{\partial \xi_2} \tag{26b}$$

$$\begin{aligned}\delta\gamma_{12}^{\circ} = {} & \frac{1}{A_2}\frac{\partial \delta u_1}{\partial \xi_2} - \frac{\delta u_2}{A_1 A_2}\frac{\partial A_2}{\partial \xi_1} + \frac{1}{A_1}\frac{\partial \delta u_2}{\partial \xi_1} - \frac{\delta u_1}{A_1 A_2}\frac{\partial A_1}{\partial \xi_2} \\ & - \left(\beta_1 + \beta_1^{I}\right)\frac{1}{A_2}\frac{\partial \delta w}{\partial \xi_2} - \left(\beta_2 + \beta_2^{I}\right)\frac{1}{A_1}\frac{\partial \delta w}{\partial \xi_1}\end{aligned} \tag{26c}$$

$$\delta\kappa_{11}^{\circ} = \frac{1}{A_1}\frac{\partial \delta\psi_1}{\partial \xi_1} + \frac{\delta\psi_2}{A_1 A_2}\frac{\partial A_1}{\partial \xi_2} \tag{27a}$$

$$\delta\kappa^{\circ}_{22} = \frac{1}{A_2}\frac{\partial\delta\psi_2}{\partial\xi_2} + \frac{\delta\psi_1}{A_1A_2}\frac{\partial A_2}{\partial\xi_1} \tag{27b}$$

$$\delta\kappa^{\circ}_{12} = \frac{1}{A_2}\frac{\partial\delta\psi_1}{\partial\xi_2} - \frac{\delta\psi_2}{A_1A_2}\frac{\partial A_2}{\partial\xi_1} + \frac{1}{A_1}\frac{\partial\delta\psi_2}{\partial\xi_1} - \frac{\delta\psi_1}{A_1A_2}\frac{\partial A_1}{\partial\xi_2} \tag{27c}$$

$$\delta\gamma^{\circ}_{13} = \delta\psi_1 + \frac{1}{A_1}\frac{\partial\delta w}{\partial\xi_1} \tag{28a}$$

$$\delta\gamma^{\circ}_{23} = \delta\psi_2 + \frac{1}{A_2}\frac{\partial\delta w}{\partial\xi_2} \tag{28b}$$

By using these virtual strain expressions, applying equations (25) to the first integral in equation (22), and enforcing the *Fundamental Lemma of the Calculus of Variations* (see Reddy[87], pp. 107-108), the equilibrium equations are found to be

$$\frac{\partial}{\partial\xi_1}(N_{11}A_2) + \frac{\partial}{\partial\xi_2}(N_{12}A_1) - N_{22}\frac{\partial A_2}{\partial\xi_1} + N_{12}\frac{\partial A_1}{\partial\xi_2} + A_1A_2q_1 = 0 \tag{29a}$$

$$\frac{\partial}{\partial\xi_1}(N_{12}A_2) + \frac{\partial}{\partial\xi_2}(N_{22}A_1) - N_{11}\frac{\partial A_1}{\partial\xi_2} + N_{12}\frac{\partial A_2}{\partial\xi_1} + A_1A_2q_2 = 0 \tag{29b}$$

$$\frac{\partial}{\partial\xi_1}(Q_1A_2) + \frac{\partial}{\partial\xi_2}(Q_2A_1) + A_1A_2\left(q_3 - \frac{N_{11}}{R_1} - \frac{N_{22}}{R_2} + P_m\right) = 0 \tag{29c}$$

$$\frac{\partial}{\partial\xi_1}(M_{11}A_2) + \frac{\partial}{\partial\xi_2}(M_{12}A_1) - M_{22}\frac{\partial A_2}{\partial\xi_1} + M_{12}\frac{\partial A_1}{\partial\xi_2} - A_1A_2Q_1 = 0 \tag{29d}$$

$$\frac{\partial}{\partial\xi_1}(M_{12}A_2) + \frac{\partial}{\partial\xi_2}(M_{22}A_1) - M_{11}\frac{\partial A_1}{\partial\xi_2} + M_{12}\frac{\partial A_2}{\partial\xi_1} - A_1A_2Q_2 = 0 \tag{29e}$$

where the nonlinear terms are contained in

$$\begin{aligned} A_1A_2P_m = &-\frac{\partial}{\partial\xi_1}\left[A_2\left(\left[\beta_1 + \beta_1^I\right]N_{11} + \left[\beta_2 + \beta_2^I\right]N_{12}\right)\right] \\ &-\frac{\partial}{\partial\xi_2}\left[A_1\left(\left[\beta_1 + \beta_1^I\right]N_{12} + \left[\beta_2 + \beta_2^I\right]N_{22}\right)\right] \end{aligned} \tag{30}$$

Expanding the derivative terms gives

$$
\begin{aligned}
P_m = &- \left[\frac{1}{A_1}\frac{\partial N_{11}}{\partial \xi_1} + \frac{1}{A_2}\frac{\partial N_{12}}{\partial \xi_2} + \frac{N_{11}}{A_2}\left(\frac{1}{A_1}\frac{\partial A_2}{\partial \xi_1}\right) + \frac{N_{12}}{A_1}\left(\frac{1}{A_2}\frac{\partial A_1}{\partial \xi_2}\right)\right]\left(\beta_1 + \beta_1^I\right) \\
&- \left[\frac{1}{A_1}\frac{\partial N_{12}}{\partial \xi_1} + \frac{1}{A_2}\frac{\partial N_{22}}{\partial \xi_2} + \frac{N_{12}}{A_2}\left(\frac{1}{A_1}\frac{\partial A_2}{\partial \xi_1}\right) + \frac{N_{22}}{A_1}\left(\frac{1}{A_2}\frac{\partial A_1}{\partial \xi_2}\right)\right]\left(\beta_2 + \beta_2^I\right) \\
&- N_{11}\left(\frac{1}{A_1}\frac{\partial}{\partial \xi_1}\left(\beta_1 + \beta_1^I\right)\right) - N_{22}\left(\frac{1}{A_2}\frac{\partial}{\partial \xi_2}\left(\beta_2 + \beta_2^I\right)\right) \\
&- N_{12}\left[\frac{1}{A_1}\frac{\partial}{\partial \xi_1}\left(\beta_2 + \beta_2^I\right) + \frac{1}{A_2}\frac{\partial}{\partial \xi_2}\left(\beta_1 + \beta_1^I\right)\right]
\end{aligned}
\tag{31}
$$

and using equations (29a) and (29b) gives the alternate form

$$
\begin{aligned}
P_m = &\, q_1\left(\beta_1 + \beta_1^I\right) + q_2\left(\beta_2 + \beta_2^I\right) \\
&- N_{11}\left[\frac{\left(\beta_2 + \beta_2^I\right)}{A_1}\left(\frac{1}{A_2}\frac{\partial A_1}{\partial \xi_2}\right) - \frac{1}{A_1}\frac{\partial}{\partial \xi_1}\left(\beta_1 + \beta_1^I\right)\right] \\
&- N_{22}\left[\frac{\left(\beta_1 + \beta_1^I\right)}{A_2}\left(\frac{1}{A_1}\frac{\partial A_2}{\partial \xi_1}\right) - \frac{1}{A_2}\frac{\partial}{\partial \xi_2}\left(\beta_2 + \beta_2^I\right)\right] \\
&- N_{12}\left[\frac{1}{A_2}\frac{\partial}{\partial \xi_2}\left(\beta_1 + \beta_1^I\right) - \frac{\left(\beta_1 + \beta_1^I\right)}{A_1}\left(\frac{1}{A_2}\frac{\partial A_1}{\partial \xi_2}\right)\right] \\
&- N_{12}\left[\frac{1}{A_1}\frac{\partial}{\partial \xi_1}\left(\beta_2 + \beta_2^I\right) - \frac{\left(\beta_2 + \beta_2^I\right)}{A_2}\left(\frac{1}{A_1}\frac{\partial A_2}{\partial \xi_1}\right)\right]
\end{aligned}
\tag{32}
$$

The boundary conditions that result from enforcing the *Fundamental Lemma of the Calculus of Variations* (see Reddy[87], pp. 107-108) consist of two groups. On the edges given by $\xi_1 = a_1$ and $\xi_1 = b_1$, the boundary conditions are

$$N_{11} = N(\xi_2) \quad \text{or} \quad u_1 = \Delta_1(\xi_2) \tag{33a}$$

$$N_{12} = S(\xi_2) \quad \text{or} \quad u_2 = \Delta_2(\xi_2) \tag{33b}$$

$$Q_1 + \frac{1}{A_2}\frac{\partial M_{12}}{\partial \xi_2} - \left[\left(\beta_1 + \beta_1^I\right)N_{11} + \left(\beta_2 + \beta_2^I\right)N_{12}\right] = V(\xi_2) \quad \text{or} \quad w = \Delta_n(\xi_2) \tag{33c}$$

$$M_{11} = M(\xi_2) \quad \text{or} \quad \beta_1 = \Phi(\xi_2) \tag{33d}$$

where

$$Q_1 = \frac{1}{A_1}\frac{\partial M_{11}}{\partial \xi_1} + \frac{1}{A_2}\frac{\partial M_{12}}{\partial \xi_2} + \frac{M_{11} - M_{22}}{A_2}\left(\frac{1}{A_1}\frac{\partial A_2}{\partial \xi_1}\right) + \frac{2M_{12}}{A_1}\left(\frac{1}{A_2}\frac{\partial A_1}{\partial \xi_2}\right) \tag{33e}$$

where $\Delta_1(\xi_2)$, $\Delta_2(\xi_2)$, and $\Delta_n(\xi_2)$ are applied displacements and $\Phi(\xi_2)$ is an applied rotation. On the edges given by $\xi_2 = a_2$ and $\xi_2 = b_2$, the boundary conditions are

$$N_{22} = N(\xi_1) \quad \text{or} \quad u_2 = \Delta_2(\xi_1) \tag{34a}$$

$$N_{12} = S(\xi_1) \quad \text{or} \quad u_1 = \Delta_1(\xi_1) \tag{34b}$$

$$Q_2 + \frac{1}{A_1}\frac{\partial M_{12}}{\partial \xi_1} - \left[\left(\beta_1 + \beta_1^I\right)N_{12} + \left(\beta_2 + \beta_2^I\right)N_{22}\right] = V(\xi_1) \quad \text{or} \quad w = \Delta_n(\xi_1) \tag{34c}$$

$$M_{22} = M(\xi_1) \quad \text{or} \quad \beta_2 = \Phi(\xi_1) \tag{34d}$$

where

$$Q_2 = \frac{1}{A_1}\frac{\partial M_{12}}{\partial \xi_1} + \frac{1}{A_2}\frac{\partial M_{22}}{\partial \xi_2} + \frac{M_{22} - M_{11}}{A_1}\left(\frac{1}{A_2}\frac{\partial A_1}{\partial \xi_2}\right) + \frac{2M_{12}}{A_2}\left(\frac{1}{A_1}\frac{\partial A_2}{\partial \xi_1}\right) \tag{34e}$$

where $\Delta_1(\xi_1)$, $\Delta_2(\xi_1)$, and $\Delta_n(\xi_1)$ are applied displacements and $\Phi(\xi_1)$ is an applied rotation. In addition, "corner conditions" arise that must be satisifed; that is, either M_{12} or w must be specified at the points (a_1, a_2), (a_1, b_2), (b_1, a_2), and (b_1, b_2).

Nonlinear Compatibility Equation

The compatibility equation of the Donnell-Mushtari-Vlasov theory for a geometrically perfect shell is presented in the book by Wempner[88] (see p. 616), in terms of tensor analysis. The corresponding equation for an imperfect shell is obtained from this equation by replacing the shell normal displacement with $w_I(\xi_1, \xi_2) + w(\xi_1, \xi_2)$, and then by noting that when $w(\xi_1, \xi_2) = 0$ the strains vanish and compatibility must be satisfied. The resulting equation for lines-of-curvature coordinates, using the notation herein, is given by

$$\begin{aligned} &\frac{1}{A_1A_2}\left\{\mathscr{C}_{11}\left[\varepsilon_{11}^o\right] + \mathscr{C}_{22}\left[\varepsilon_{22}^o\right] + \mathscr{C}_{12}\left[\gamma_{12}^o\right]\right\} + \\ &\qquad \frac{\kappa_{22}^o}{R_1} + \frac{\kappa_{11}^o}{R_2} - \kappa_{11}^o\kappa_{22}^o + \frac{1}{4}\left(\kappa_{12}^o\right)^2 - \kappa_{11}^o\kappa_{22}^I - \kappa_{11}^I\kappa_{22}^o + \frac{1}{2}\kappa_{12}^o\kappa_{12}^I = 0 \end{aligned} \tag{35}$$

where

$$\mathscr{C}_{11}\left[\varepsilon^{o}_{11}\right] = -\frac{\partial}{\partial\xi_1}\left[\frac{1}{A_1}\frac{\partial A_2}{\partial\xi_1}\,\varepsilon^{o}_{11}\right] + \frac{\partial}{\partial\xi_2}\left[\frac{A_1}{A_2}\,\frac{\partial\varepsilon^{o}_{11}}{\partial\xi_2} + \frac{1}{A_2}\frac{\partial A_1}{\partial\xi_2}\,\varepsilon^{o}_{11}\right] \tag{36a}$$

$$\mathscr{C}_{22}\left[\varepsilon^{o}_{22}\right] = -\frac{\partial}{\partial\xi_2}\left[\frac{1}{A_2}\frac{\partial A_1}{\partial\xi_2}\,\varepsilon^{o}_{22}\right] + \frac{\partial}{\partial\xi_1}\left[\frac{A_2}{A_1}\,\frac{\partial\varepsilon^{o}_{22}}{\partial\xi_1} + \frac{1}{A_1}\frac{\partial A_2}{\partial\xi_1}\,\varepsilon^{o}_{22}\right] \tag{36b}$$

$$\mathscr{C}_{12}\left[\gamma^{o}_{12}\right] = -\frac{\partial}{\partial\xi_1}\left[\frac{1}{2}\,\frac{\partial\gamma^{o}_{12}}{\partial\xi_2} + \frac{1}{A_1}\,\frac{\partial A_1}{\partial\xi_2}\,\gamma^{o}_{12}\right] - \frac{\partial}{\partial\xi_2}\left[\frac{1}{2}\,\frac{\partial\gamma^{o}_{12}}{\partial\xi_1} + \frac{1}{A_2}\,\frac{\partial A_2}{\partial\xi_1}\,\gamma^{o}_{12}\right] \tag{36c}$$

$$\kappa^{I}_{11} = -\frac{1}{A_1}\frac{\partial}{\partial\xi_1}\left(\frac{1}{A_1}\frac{\partial w_I}{\partial\xi_1}\right) - \frac{1}{A_1\left(A_2\right)^2}\frac{\partial A_1}{\partial\xi_2}\,\frac{\partial w_I}{\partial\xi_2} \tag{37a}$$

$$\kappa^{I}_{22} = -\frac{1}{A_2}\frac{\partial}{\partial\xi_2}\left(\frac{1}{A_2}\frac{\partial w_I}{\partial\xi_2}\right) - \frac{1}{A_2\left(A_1\right)^2}\frac{\partial A_2}{\partial\xi_1}\,\frac{\partial w_I}{\partial\xi_1} \tag{37b}$$

$$\kappa^{I}_{12} = -\frac{A_2}{A_1}\frac{\partial}{\partial\xi_1}\left(\frac{1}{\left(A_2\right)^2}\frac{\partial w_I}{\partial\xi_2}\right) - \frac{A_1}{A_2}\frac{\partial}{\partial\xi_2}\left(\frac{1}{\left(A_1\right)^2}\frac{\partial w_I}{\partial\xi_1}\right) \tag{37c}$$

Equation (35) gives the necessary and sufficient conditions for compatible displacements in a simply connected domain. For a multiply connected domain, single-valuedness of the displacements around each curve enclosing a cutout must be enforced, in addition to equation (35) to have compatible displacement fields.

Nondimensional Fields Equations and Parameters

The nondimensionalization procedure used herein follows that given in references 60 and 61 for symmetrically laminated shells, modified to accomodate generally laminated shells. In particular, the only differences in the equations for symmetrically laminated and generally laminated shells appear in the constitutive equations. The underyling premise of this procedure is to make the field variables and their derivatives quantities with magnitudes on the order of unity, to minimize the number of parameters required to characterize the behavior, and to avoid introducing a preferential direction, or bias, into the nondimensional equations. This approach is intended to enable one to assess the relative importance of terms in the nondimensional field equations, and to provide a means for rationalizing similar response characteristics of shells with different material composition and geometry. Based on this approach, it follows that it is convenient to define the nondimensional normal displacement W for a generally laminated shell also by $W \equiv \left[a_{11}a_{22}D_{11}D_{22}\right]^{-\frac{1}{4}} w$. In addition, to facilitate nondimensionalization of the Donnell-Mushtari-Vlasov equations, it is convenient to introduce the nondimensional arc-length Gaussian coordinates $\left(z_1, z_2\right)$ of references 60 and 61 given by $\xi_1 = L_1 z_1$ and $\xi_2 = L_2 z_2$, where L_1 and

L_2 are characteristic dimensions of the reference surface that can be picked to faciliate solution of a specific problem. For these coordinates, the surface metric coefficients A_1 and A_2 are equal to unity, which greatly simplifies the shell equations. In the analysis that follows, it is presumed that the shell stiffnesses defined in equation (16), and the corresponding compliances, are independent of the (ξ_1, ξ_2) surface coordinates. Unlike previously published studies on nondimensional parameters, a complete set of nondimensional field equations are presented subsequently.

Nondimensional Kinematic Equations

First, consider the rotation of the reference surface given by equation (11a). Introducing the nondimensional normal displacement $W \equiv \left[a_{11}a_{22}D_{11}D_{22}\right]^{-\frac{1}{4}} w$ and the coordinates (z_1, z_2) into equation (11a) gives

$$\beta_1 = -\frac{1}{L_1}\left[a_{11}a_{22}D_{11}D_{22}\right]^{\frac{1}{4}} \frac{\partial W}{\partial z_1} \tag{38}$$

Defining the nondimensional rotation as

$$\Omega_1 = \beta_1 L_1 \left[a_{11}a_{22}D_{11}D_{22}\right]^{-\frac{1}{4}} \tag{39}$$

yields

$$\Omega_1 = -\frac{\partial W}{\partial z_1} \tag{40}$$

Similarly,

$$\Omega_2 = \beta_2 L_2 \left[a_{11}a_{22}D_{11}D_{22}\right]^{-\frac{1}{4}} \tag{41}$$

and

$$\Omega_2 = -\frac{\partial W}{\partial z_2} \tag{42}$$

Likewise, introducing $W \equiv \left[a_{11}a_{22}D_{11}D_{22}\right]^{-\frac{1}{4}} w$ and the coordinates (z_1, z_2) into equation (8a) gives

$$\frac{\varepsilon^{o}_{11} L_1^2}{\left[a_{11}a_{22}D_{11}D_{22}\right]^{\frac{1}{2}}} = \frac{L_1}{\left[a_{11}a_{22}D_{11}D_{22}\right]^{\frac{1}{2}}} \frac{\partial u_1}{\partial z_1} + \frac{L_1^2}{R_1\left[a_{11}a_{22}D_{11}D_{22}\right]^{\frac{1}{4}}} W + \frac{1}{2}\left(\frac{\partial W}{\partial z_1}\right)^2 + \frac{\partial W}{\partial z_1}\frac{\partial W_I}{\partial z_1} \tag{43}$$

where $W_I \equiv \left[a_{11}a_{22}D_{11}D_{22}\right]^{-\frac{1}{4}} w_I$ is a nondimensional initial geometric imperfection function. By defining a nondimensional strain E_{11}, a nondimensional displacement U_1 given by

$$U_1 \equiv \frac{u_1 L_1}{\left[a_{11}a_{22}D_{11}D_{22}\right]^{\frac{1}{2}}} \tag{44}$$

and introducing the Batdorf-Stein parameter, previously defined in references 60 and 61, as

$$Z_1 \equiv \frac{L_1^2}{\sqrt{12}R_1\left[a_{11}a_{22}D_{11}D_{22}\right]^{\frac{1}{4}}} = \left(\frac{L_1}{R_1}\right)^2\left(\frac{R_1}{h}\right)\left[\frac{h}{\sqrt{12}\left[a_{11}a_{22}D_{11}D_{22}\right]^{\frac{1}{4}}}\right] \tag{45}$$

equation (43) is expressed as

$$E_{11} \equiv \frac{\varepsilon_{11}^{\circ} L_1^2}{\left[a_{11}a_{22}D_{11}D_{22}\right]^{\frac{1}{2}}} = \frac{\partial U_1}{\partial z_1} + \sqrt{12}Z_1 W + \frac{1}{2}\left(\frac{\partial W}{\partial z_1}\right)^2 + \frac{\partial W}{\partial z_1}\frac{\partial W_I}{\partial z_1} \tag{46a}$$

Similarly,

$$E_{22} \equiv \frac{\varepsilon_{22}^{\circ} L_2^2}{\left[a_{11}a_{22}D_{11}D_{22}\right]^{\frac{1}{2}}} = \frac{\partial U_2}{\partial z_2} + \sqrt{12}Z_2 W + \frac{1}{2}\left(\frac{\partial W}{\partial z_2}\right)^2 + \frac{\partial W}{\partial z_2}\frac{\partial W_I}{\partial z_2} \tag{46b}$$

$$G_{12} \equiv \frac{\gamma_{12}^{\circ} L_1 L_2}{\left[a_{11}a_{22}D_{11}D_{22}\right]^{\frac{1}{2}}} = \frac{\partial U_1}{\partial z_2} + \frac{\partial U_2}{\partial z_1} + \frac{\partial W}{\partial z_1}\frac{\partial W}{\partial z_2} + \frac{\partial W_I}{\partial z_1}\frac{\partial W}{\partial z_2} + \frac{\partial W_I}{\partial z_2}\frac{\partial W}{\partial z_1} \tag{46c}$$

where

$$U_2 \equiv \frac{u_2 L_2}{\left[a_{11}a_{22}D_{11}D_{22}\right]^{\frac{1}{2}}} \tag{47}$$

and

$$Z_2 \equiv \frac{L_2^2}{\sqrt{12}R_2\left[a_{11}a_{22}D_{11}D_{22}\right]^{\frac{1}{4}}} = \left(\frac{L_2}{R_2}\right)^2\left(\frac{R_2}{h}\right)\left[\frac{h}{\sqrt{12}\left[a_{11}a_{22}D_{11}D_{22}\right]^{\frac{1}{4}}}\right] \tag{48}$$

Furthermore, similar nondimensionalization of the bending strains given by equations (9) yields

$$\varkappa_{11} \equiv \frac{\kappa_{11}^{\circ} L_1^2}{\left[a_{11}a_{22}D_{11}D_{22}\right]^{\frac{1}{4}}} = -\frac{\partial^2 W}{\partial z_1^2} \tag{49a}$$

$$\varkappa_{22} \equiv \frac{\kappa_{22}^{\circ} L_2^2}{\left[a_{11}a_{22}D_{11}D_{22}\right]^{\frac{1}{4}}} = -\frac{\partial^2 W}{\partial z_2^2} \tag{49b}$$

$$\mathcal{K}_{12} \equiv \frac{\kappa^{\circ}_{12} L_1 L_2}{\left[a_{11} a_{22} D_{11} D_{22}\right]^{\frac{1}{4}}} = -2 \frac{\partial^2 W}{\partial z_1 \partial z_2} \tag{49c}$$

Nondimensional Constitutive Equations

In deriving a set of nondimensional constitutive equations, it is desirable to keep the number of parameters that characterize the material behavior to a minimum. To achieve this goal, and to bring clarity to the nondimensionalization procedure, nondimensional constitutive equations symmetrically laminated shells are derived first. With these baseline constitutive equations established, the approach is extended to obtain nondimensional constitutive equations generally laminated shells. The guiding principles for this second case is to develop nondimensional constitutive equations for generally laminated shells with as few new nondimensional parameters as possible and that retain the nondimensional parameters for symmetrically laminated shells as an explicit subset. For example, Khot and Venkayya[20] define several nondimensional parameters for generally laminated shells in terms of the "reduced" bending stiffnesses defined by equation (21c). With their approach, the nondimensional parameters for symmetrically laminated shells do not appear explicitly. The signficance of this difference will be indicated subsequently.

Symmetrically laminated shells. For this class of laminates, the first partially inverted constitutive equation appearing in equation (20a) reduces to

$$\varepsilon^{\circ}_{11} = a_{11} N_{11} + a_{12} N_{22} + a_{16} N_{12} \tag{50}$$

Multiplying this equation by $L_1^2 \left[a_{11} a_{22} D_{11} D_{22}\right]^{-\frac{1}{2}}$ and using equation (46a) gives

$$E_{11} = L_1^2 \frac{a_{11} N_{11} + a_{12} N_{22} + a_{16} N_{12}}{\left[a_{11} a_{22} D_{11} D_{22}\right]^{\frac{1}{2}}} \tag{51}$$

This equation, and the others that follow, are simplified further by using the parameters

$$\alpha_m \equiv \frac{L_2}{L_1} \left(\frac{a_{22}}{a_{11}}\right)^{\frac{1}{4}} \tag{52a}$$

$$\mu \equiv \frac{2a_{12} + a_{66}}{2\sqrt{a_{11} a_{22}}} \tag{52b}$$

$$\gamma_m \equiv -\frac{a_{26}}{\left[a_{11} a_{22}^3\right]^{\frac{1}{4}}} \tag{52c}$$

$$\delta_m \equiv -\frac{a_{16}}{\left[a_{11}^3 a_{22}\right]^{\frac{1}{4}}} \tag{52d}$$

previously defined in references 60 and 61 and by introducing the generalized Poisson's ratio associated with membrane action defined as

$$\nu_m \equiv -\frac{a_{12}}{\sqrt{a_{11}a_{22}}} \tag{52e}$$

That is, equation (51) becomes

$$E_{11} = \frac{\pi^2}{\alpha_m^2}\frac{N_{11}L_2^2}{\pi^2\sqrt{D_{11}D_{22}}} - \pi^2\nu_m\frac{N_{22}L_1^2}{\pi^2\sqrt{D_{11}D_{22}}} - \pi^2\frac{\delta_m}{\alpha_m}\frac{L_1}{L_2}\left(\frac{D_{22}}{D_{11}}\right)^{\frac{1}{4}}\frac{N_{12}L_2^2}{\pi^2\left[D_{11}D_{22}^3\right]^{1/4}} \tag{53}$$

Equation (53), and others that follow, are simplified further by introducing the nondimensional stress resultants

$$\mathcal{N}_{11} \equiv \frac{N_{11}L_2^2}{\pi^2\sqrt{D_{11}D_{22}}} \tag{54a}$$

$$\mathcal{N}_{22} \equiv \frac{N_{22}L_1^2}{\pi^2\sqrt{D_{11}D_{22}}} \tag{54b}$$

$$\mathcal{N}_{12} \equiv \frac{N_{12}L_2^2}{\pi^2\left[D_{11}D_{22}^3\right]^{1/4}} \tag{54c}$$

and using the parameter α_b defined in references 60 and 61 as

$$\alpha_b \equiv \frac{L_2}{L_1}\left(\frac{D_{11}}{D_{22}}\right)^{\frac{1}{4}} \tag{55}$$

Specifically, equation (53) becomes

$$E_{11} = \pi^2\left(\frac{1}{\alpha_m^2}\mathcal{N}_{11} - \nu_m\mathcal{N}_{22} - \frac{\delta_m}{\alpha_m}\frac{\mathcal{N}_{12}}{\alpha_b}\right) \tag{56a}$$

Similarly,

$$E_{22} = \pi^2\left(- \nu_m \mathcal{N}_{11} + \alpha_m^2 \mathcal{N}_{22} - \alpha_m \gamma_m \frac{\mathcal{N}_{12}}{\alpha_b} \right) \tag{56b}$$

$$G_{12} = \pi^2\left(- \frac{\delta_m}{\alpha_m} \mathcal{N}_{11} - \alpha_m \gamma_m \mathcal{N}_{22} + 2(\mu + \nu_m) \frac{\mathcal{N}_{12}}{\alpha_b} \right) \tag{56c}$$

Next, consider the constitiutive equation (see equation(16))

$$M_{11} = D_{11}\kappa_{11}^{\circ} + D_{12}\kappa_{22}^{\circ} + D_{16}\kappa_{12}^{\circ} \tag{57}$$

Using equations (49) and multiplying by $L_2^2\left[a_{11}a_{22}D_{11}^3D_{22}^3\right]^{-\frac{1}{4}}$ gives

$$\frac{M_{11}L_2^2}{\left[a_{11}a_{22}D_{11}^3D_{22}^3\right]^{\frac{1}{4}}} = -\left(\frac{L_2^2}{L_1^2}\left(\frac{D_{11}}{D_{22}}\right)^{\frac{1}{2}} \frac{\partial^2 W}{\partial z_1^2} + \frac{D_{12}}{\sqrt{D_{11}D_{22}}} \frac{\partial^2 W}{\partial z_2^2} + 2\frac{D_{16}}{\sqrt{D_{11}D_{22}}} \frac{L_2}{L_1} \frac{\partial^2 W}{\partial z_1 \partial z_2} \right) \tag{58}$$

Equation (58), and others that follow, are simplified further by using equation (55), and by using the parameters β, γ_b, and δ_b defined in references 60 and 61 as

$$\beta \equiv \frac{D_{12} + 2D_{66}}{\sqrt{D_{11}D_{22}}} \tag{59a}$$

$$\gamma_b \equiv \frac{D_{16}}{\left[D_{11}^3 D_{22}\right]^{\frac{1}{4}}} \tag{59b}$$

$$\delta_b \equiv \frac{D_{26}}{\left[D_{11}D_{22}^3\right]^{\frac{1}{4}}} \tag{59c}$$

In addition, a generalized Poisson's ratio associated with anticlastic bending action is defined by

$$\nu_b \equiv \frac{D_{12}}{\sqrt{D_{11}D_{22}}} \tag{59d}$$

Specifically, equation (58) becomes

$$\mathcal{M}_{11} \equiv \frac{M_{11}L_2^2}{\left[a_{11}a_{22}D_{11}^3D_{22}^3\right]^{\frac{1}{4}}} = -\left(\alpha_b^2 \frac{\partial^2 W}{\partial z_1^2} + \nu_b \frac{\partial^2 W}{\partial z_2^2} + 2\alpha_b\gamma_b \frac{\partial^2 W}{\partial z_1 \partial z_2} \right) \tag{60a}$$

Similarly,

$$\mathcal{M}_{22} \equiv \frac{M_{22}L_1^2}{\left[a_{11}a_{22}D_{11}^3D_{22}^3\right]^{\frac{1}{4}}} = -\left(\nu_b \frac{\partial^2 W}{\partial z_1^2} + \frac{1}{\alpha_b^2}\frac{\partial^2 W}{\partial z_2^2} + 2\frac{\delta_b}{\alpha_b}\frac{\partial^2 W}{\partial z_1 \partial z_2}\right) \tag{60b}$$

$$\mathcal{M}_{12} \equiv \frac{M_{12}L_1L_2}{\left[a_{11}a_{22}D_{11}^3D_{22}^3\right]^{\frac{1}{4}}} = -\left(\alpha_b\gamma_b \frac{\partial^2 W}{\partial z_1^2} + \frac{\delta_b}{\alpha_b}\frac{\partial^2 W}{\partial z_2^2} + \left(\beta - \nu_b\right)\frac{\partial^2 W}{\partial z_1 \partial z_2}\right) \tag{60c}$$

Now, equations (56) and (60) have the matrix representations

$$\begin{Bmatrix} E_{11} \\ E_{22} \\ G_{12} \end{Bmatrix} = \pi^2 \begin{bmatrix} \frac{1}{\alpha_m^2} & -\nu_m & -\frac{\delta_m}{\alpha_m} \\ -\nu_m & \alpha_m^2 & -\alpha_m\gamma_m \\ -\frac{\delta_m}{\alpha_m} & -\alpha_m\gamma_m & 2\left(\mu + \nu_m\right) \end{bmatrix} \begin{Bmatrix} \mathcal{N}_{11} \\ \mathcal{N}_{22} \\ \frac{\mathcal{N}_{12}}{\alpha_b} \end{Bmatrix} \tag{61a}$$

$$\begin{Bmatrix} \mathcal{M}_{11} \\ \mathcal{M}_{22} \\ \mathcal{M}_{12} \end{Bmatrix} = -\begin{bmatrix} \alpha_b^2 & \nu_b & \alpha_b\gamma_b \\ \nu_b & \frac{1}{\alpha_b^2} & \frac{\delta_b}{\alpha_b} \\ \alpha_b\gamma_b & \frac{\delta_b}{\alpha_b} & \frac{\beta - \nu_b}{2} \end{bmatrix} \begin{Bmatrix} \frac{\partial^2 W}{\partial z_1^2} \\ \frac{\partial^2 W}{\partial z_2^2} \\ 2\frac{\partial^2 W}{\partial z_1 \partial z_2} \end{Bmatrix} \tag{61b}$$

Generally laminated shells. For this general class of shells, consider the constitutive equations given by equations (20a) written in the form

$$\begin{Bmatrix} \varepsilon_{11}^o \\ \varepsilon_{22}^o \\ \gamma_{12}^o \end{Bmatrix} = \begin{bmatrix} a_{11} & a_{12} & a_{16} \\ a_{12} & a_{22} & a_{26} \\ a_{16} & a_{26} & a_{66} \end{bmatrix} \begin{Bmatrix} N_{11} \\ N_{22} \\ N_{12} \end{Bmatrix} - \begin{bmatrix} a_{11} & a_{12} & a_{16} \\ a_{12} & a_{22} & a_{26} \\ a_{16} & a_{26} & a_{66} \end{bmatrix} \begin{bmatrix} B_{11} & B_{12} & B_{16} \\ B_{12} & B_{22} & B_{26} \\ B_{16} & B_{26} & B_{66} \end{bmatrix} \begin{Bmatrix} \kappa_{11}^o \\ \kappa_{22}^o \\ \kappa_{12}^o \end{Bmatrix} \tag{62}$$

by using equations (21). To obtain the desired additional nondimensional parameters, equations (46), (49), and (54) are expressed as

$$\begin{Bmatrix} \varepsilon_{11}^{o} \\ \varepsilon_{22}^{o} \\ \gamma_{12}^{o} \end{Bmatrix} = \left[a_{11}a_{22}D_{11}D_{22}\right]^{\frac{1}{2}} \begin{bmatrix} \frac{1}{L_1^2} & 0 & 0 \\ 0 & \frac{1}{L_2^2} & 0 \\ 0 & 0 & \frac{1}{L_1 L_2} \end{bmatrix} \begin{Bmatrix} E_{11} \\ E_{22} \\ G_{12} \end{Bmatrix} \tag{63}$$

$$\begin{Bmatrix} \kappa_{11}^{o} \\ \kappa_{22}^{o} \\ \kappa_{12}^{o} \end{Bmatrix} = \left[a_{11}a_{22}D_{11}D_{22}\right]^{\frac{1}{4}} \begin{bmatrix} \frac{1}{L_1^2} & 0 & 0 \\ 0 & \frac{1}{L_2^2} & 0 \\ 0 & 0 & \frac{1}{L_1 L_2} \end{bmatrix} \begin{Bmatrix} \mathcal{K}_{11} \\ \mathcal{K}_{22} \\ \mathcal{K}_{12} \end{Bmatrix} \tag{64}$$

$$\begin{Bmatrix} N_{11} \\ N_{22} \\ N_{12} \end{Bmatrix} = \pi^2 \sqrt{D_{11}D_{22}} \begin{bmatrix} \frac{1}{L_2^2} & 0 & 0 \\ 0 & \frac{1}{L_1^2} & 0 \\ 0 & 0 & \frac{1}{L_1 L_2} \end{bmatrix} \begin{Bmatrix} \mathcal{N}_{11} \\ \mathcal{N}_{22} \\ \frac{\mathcal{N}_{12}}{\alpha_b} \end{Bmatrix} \tag{65}$$

With these expressions, matrix equation (62) becomes

$$\begin{Bmatrix} E_{11} \\ E_{22} \\ G_{12} \end{Bmatrix} = \frac{\pi^2}{\sqrt{a_{11}a_{22}}} \begin{bmatrix} L_1^2 & 0 & 0 \\ 0 & L_2^2 & 0 \\ 0 & 0 & L_1 L_2 \end{bmatrix} \begin{bmatrix} a_{11} & a_{12} & a_{16} \\ a_{12} & a_{22} & a_{26} \\ a_{16} & a_{26} & a_{66} \end{bmatrix} \begin{bmatrix} \frac{1}{L_2^2} & 0 & 0 \\ 0 & \frac{1}{L_1^2} & 0 \\ 0 & 0 & \frac{1}{L_1 L_2} \end{bmatrix} \begin{Bmatrix} \mathcal{N}_{11} \\ \mathcal{N}_{22} \\ \frac{\mathcal{N}_{12}}{\alpha_b} \end{Bmatrix}$$
$$- \frac{1}{\left[a_{11}a_{22}D_{11}D_{22}\right]^{\frac{1}{4}}} \begin{bmatrix} L_1^2 & 0 & 0 \\ 0 & L_2^2 & 0 \\ 0 & 0 & L_1 L_2 \end{bmatrix} \begin{bmatrix} a_{11} & a_{12} & a_{16} \\ a_{12} & a_{22} & a_{26} \\ a_{16} & a_{26} & a_{66} \end{bmatrix} \begin{bmatrix} B_{11} & B_{12} & B_{16} \\ B_{12} & B_{22} & B_{26} \\ B_{16} & B_{26} & B_{66} \end{bmatrix} \begin{bmatrix} \frac{1}{L_1^2} & 0 & 0 \\ 0 & \frac{1}{L_2^2} & 0 \\ 0 & 0 & \frac{1}{L_1 L_2} \end{bmatrix} \begin{Bmatrix} \mathcal{K}_{11} \\ \mathcal{K}_{22} \\ \mathcal{K}_{12} \end{Bmatrix} \tag{66}$$

Inspection of equations (61) and (66) indicates

$$\begin{bmatrix} \frac{1}{\alpha_m^2} & -\nu_m & -\frac{\delta_m}{\alpha_m} \\ -\nu_m & \alpha_m^2 & -\alpha_m\gamma_m \\ -\frac{\delta_m}{\alpha_m} & -\alpha_m\gamma_m & 2(\mu+\nu_m) \end{bmatrix} = \frac{1}{\sqrt{a_{11}a_{22}}} \begin{bmatrix} L_1^2 & 0 & 0 \\ 0 & L_2^2 & 0 \\ 0 & 0 & L_1L_2 \end{bmatrix} \begin{bmatrix} a_{11} & a_{12} & a_{16} \\ a_{12} & a_{22} & a_{26} \\ a_{16} & a_{26} & a_{66} \end{bmatrix} \begin{bmatrix} \frac{1}{L_2^2} & 0 & 0 \\ 0 & \frac{1}{L_1^2} & 0 \\ 0 & 0 & \frac{1}{L_1L_2} \end{bmatrix} \tag{67}$$

Using equation (67) and the identity

$$\begin{bmatrix} a_{11} & a_{12} & a_{16} \\ a_{12} & a_{22} & a_{26} \\ a_{16} & a_{26} & a_{66} \end{bmatrix} = \begin{bmatrix} a_{11} & a_{12} & a_{16} \\ a_{12} & a_{22} & a_{26} \\ a_{16} & a_{26} & a_{66} \end{bmatrix} \begin{bmatrix} \frac{1}{L_2^2} & 0 & 0 \\ 0 & \frac{1}{L_1^2} & 0 \\ 0 & 0 & \frac{1}{L_1L_2} \end{bmatrix} \begin{bmatrix} L_2^2 & 0 & 0 \\ 0 & L_1^2 & 0 \\ 0 & 0 & L_1L_2 \end{bmatrix} \tag{68}$$

with equation (66) yields

$$\begin{Bmatrix} E_{11} \\ E_{22} \\ G_{12} \end{Bmatrix} = \begin{bmatrix} \frac{1}{\alpha_m^2} & -\nu_m & -\frac{\delta_m}{\alpha_m} \\ -\nu_m & \alpha_m^2 & -\alpha_m\gamma_m \\ -\frac{\delta_m}{\alpha_m} & -\alpha_m\gamma_m & 2(\mu+\nu_m) \end{bmatrix} \left[\pi^2 \begin{Bmatrix} \mathcal{N}_{11} \\ \mathcal{N}_{22} \\ \frac{\mathcal{N}_{12}}{\alpha_b} \end{Bmatrix} - \begin{bmatrix} \mathcal{C}_{11} & \mathcal{C}_{12} & \mathcal{C}_{16} \\ \mathcal{C}_{12} & \mathcal{C}_{22} & \mathcal{C}_{26} \\ \mathcal{C}_{16} & \mathcal{C}_{26} & \mathcal{C}_{66} \end{bmatrix} \begin{Bmatrix} \mathcal{K}_{11} \\ \mathcal{K}_{22} \\ \mathcal{K}_{12} \end{Bmatrix} \right] \tag{69a}$$

where

$$\begin{bmatrix} \mathcal{C}_{11} & \mathcal{C}_{12} & \mathcal{C}_{16} \\ \mathcal{C}_{12} & \mathcal{C}_{22} & \mathcal{C}_{26} \\ \mathcal{C}_{16} & \mathcal{C}_{26} & \mathcal{C}_{66} \end{bmatrix} = \left[\frac{a_{11}a_{22}}{D_{11}D_{22}} \right]^{\frac{1}{4}} \begin{bmatrix} L_2^2 & 0 & 0 \\ 0 & L_1^2 & 0 \\ 0 & 0 & L_1L_2 \end{bmatrix} \begin{bmatrix} B_{11} & B_{12} & B_{16} \\ B_{12} & B_{22} & B_{26} \\ B_{16} & B_{26} & B_{66} \end{bmatrix} \begin{bmatrix} \frac{1}{L_1^2} & 0 & 0 \\ 0 & \frac{1}{L_2^2} & 0 \\ 0 & 0 & \frac{1}{L_1L_2} \end{bmatrix} \tag{69b}$$

or

$$\begin{bmatrix} \mathcal{C}_{11} & \mathcal{C}_{12} & \mathcal{C}_{16} \\ \mathcal{C}_{12} & \mathcal{C}_{22} & \mathcal{C}_{26} \\ \mathcal{C}_{16} & \mathcal{C}_{26} & \mathcal{C}_{66} \end{bmatrix} = \left[\frac{a_{11}a_{22}}{D_{11}D_{22}} \right]^{\frac{1}{4}} \begin{bmatrix} B_{11}\frac{L_2^2}{L_1^2} & B_{12} & B_{16}\frac{L_2}{L_1} \\ B_{12} & B_{22}\frac{L_1^2}{L_2^2} & B_{26}\frac{L_1}{L_2} \\ B_{16}\frac{L_2}{L_1} & B_{26}\frac{L_1}{L_2} & B_{66} \end{bmatrix} \tag{69c}$$

Now, consider the constitutive equation

$$\begin{Bmatrix} M_{11} \\ M_{22} \\ M_{12} \end{Bmatrix} = \begin{bmatrix} B_{11} & B_{12} & B_{16} \\ B_{12} & B_{22} & B_{26} \\ B_{16} & B_{26} & B_{66} \end{bmatrix} \begin{Bmatrix} \varepsilon_{11}^{o} \\ \varepsilon_{22}^{o} \\ \gamma_{12}^{o} \end{Bmatrix} + \begin{bmatrix} D_{11} & D_{12} & D_{16} \\ D_{12} & D_{22} & D_{26} \\ D_{16} & D_{26} & D_{66} \end{bmatrix} \begin{Bmatrix} \kappa_{11}^{o} \\ \kappa_{22}^{o} \\ \kappa_{12}^{o} \end{Bmatrix} \tag{70}$$

To obtain the desired additional nondimensional parameters, equations (60) are used to get

$$\begin{Bmatrix} M_{11} \\ M_{22} \\ M_{12} \end{Bmatrix} = \left[a_{11} a_{22} D_{11}^{3} D_{22}^{3} \right]^{\frac{1}{4}} \begin{bmatrix} \frac{1}{L_2^2} & 0 & 0 \\ 0 & \frac{1}{L_1^2} & 0 \\ 0 & 0 & \frac{1}{L_1 L_2} \end{bmatrix} \begin{Bmatrix} \mathcal{M}_{11} \\ \mathcal{M}_{22} \\ \mathcal{M}_{12} \end{Bmatrix} \tag{71}$$

Using equations (63), (64), and (71), matrix equation (70) is expressed as

$$\begin{aligned} \begin{Bmatrix} \mathcal{M}_{11} \\ \mathcal{M}_{22} \\ \mathcal{M}_{12} \end{Bmatrix} = & \left[\frac{a_{11} a_{22}}{D_{11} D_{22}} \right]^{\frac{1}{4}} \begin{bmatrix} L_2^2 & 0 & 0 \\ 0 & L_1^2 & 0 \\ 0 & 0 & L_1 L_2 \end{bmatrix} \begin{bmatrix} B_{11} & B_{12} & B_{16} \\ B_{12} & B_{22} & B_{26} \\ B_{16} & B_{26} & B_{66} \end{bmatrix} \begin{bmatrix} \frac{1}{L_1^2} & 0 & 0 \\ 0 & \frac{1}{L_2^2} & 0 \\ 0 & 0 & \frac{1}{L_1 L_2} \end{bmatrix} \begin{Bmatrix} E_{11} \\ E_{22} \\ G_{12} \end{Bmatrix} + \\ & \frac{1}{\sqrt{D_{11} D_{22}}} \begin{bmatrix} L_2^2 & 0 & 0 \\ 0 & L_1^2 & 0 \\ 0 & 0 & L_1 L_2 \end{bmatrix} \begin{bmatrix} D_{11} & D_{12} & D_{16} \\ D_{12} & D_{22} & D_{26} \\ D_{16} & D_{26} & D_{66} \end{bmatrix} \begin{bmatrix} \frac{1}{L_1^2} & 0 & 0 \\ 0 & \frac{1}{L_2^2} & 0 \\ 0 & 0 & \frac{1}{L_1 L_2} \end{bmatrix} \begin{Bmatrix} \mathcal{K}_{11} \\ \mathcal{K}_{22} \\ \mathcal{K}_{12} \end{Bmatrix} \end{aligned} \tag{72}$$

Inspection of equations (49), (61), and (72) indicates

$$\begin{bmatrix} \alpha_b^2 & \nu_b & \alpha_b \gamma_b \\ \nu_b & \frac{1}{\alpha_b^2} & \frac{\delta_b}{\alpha_b} \\ \alpha_b \gamma_b & \frac{\delta_b}{\alpha_b} & \frac{\beta - \nu_b}{2} \end{bmatrix} = \frac{1}{\sqrt{D_{11} D_{22}}} \begin{bmatrix} L_2^2 & 0 & 0 \\ 0 & L_1^2 & 0 \\ 0 & 0 & L_1 L_2 \end{bmatrix} \begin{bmatrix} D_{11} & D_{12} & D_{16} \\ D_{12} & D_{22} & D_{26} \\ D_{16} & D_{26} & D_{66} \end{bmatrix} \begin{bmatrix} \frac{1}{L_1^2} & 0 & 0 \\ 0 & \frac{1}{L_2^2} & 0 \\ 0 & 0 & \frac{1}{L_1 L_2} \end{bmatrix} \tag{73}$$

Thus, using equations (69b) and (73) with equation (72) yields

$$\begin{Bmatrix} \mathcal{M}_{11} \\ \mathcal{M}_{22} \\ \mathcal{M}_{12} \end{Bmatrix} = \begin{bmatrix} \mathcal{b}_{11} & \mathcal{b}_{12} & \mathcal{b}_{16} \\ \mathcal{b}_{12} & \mathcal{b}_{22} & \mathcal{b}_{26} \\ \mathcal{b}_{16} & \mathcal{b}_{26} & \mathcal{b}_{66} \end{bmatrix} \begin{Bmatrix} E_{11} \\ E_{22} \\ G_{12} \end{Bmatrix} + \begin{bmatrix} \alpha_b^2 & \nu_b & \alpha_b\gamma_b \\ \nu_b & \dfrac{1}{\alpha_b^2} & \dfrac{\delta_b}{\alpha_b} \\ \alpha_b\gamma_b & \dfrac{\delta_b}{\alpha_b} & \dfrac{\beta - \nu_b}{2} \end{bmatrix} \begin{Bmatrix} \mathcal{K}_{11} \\ \mathcal{K}_{22} \\ \mathcal{K}_{12} \end{Bmatrix} \tag{74}$$

At this point in the analysis, it is convenient to express equation (69c) as

$$\begin{bmatrix} \mathcal{b}_{11} & \mathcal{b}_{12} & \mathcal{b}_{16} \\ \mathcal{b}_{12} & \mathcal{b}_{22} & \mathcal{b}_{26} \\ \mathcal{b}_{16} & \mathcal{b}_{26} & \mathcal{b}_{66} \end{bmatrix} = \begin{bmatrix} \alpha_m\alpha_b e_{11} & e_{12} & \alpha_m e_{16} \\ e_{12} & \dfrac{e_{22}}{\alpha_m\alpha_b} & \dfrac{e_{26}}{\alpha_m} \\ \alpha_m e_{16} & \dfrac{e_{26}}{\alpha_m} & e_{66} \end{bmatrix} \tag{75a}$$

where

$$e_{11} \equiv B_{11}\left(\frac{a_{11}}{D_{11}}\right)^{\frac{1}{2}} \tag{75b}$$

$$e_{12} \equiv B_{12}\left[\frac{a_{11}a_{22}}{D_{11}D_{22}}\right]^{\frac{1}{4}} \tag{75c}$$

$$e_{22} \equiv B_{22}\left(\frac{a_{22}}{D_{22}}\right)^{\frac{1}{2}} \tag{75d}$$

$$e_{16} \equiv B_{16}\left[\frac{a_{11}^2}{D_{11}D_{22}}\right]^{\frac{1}{4}} \tag{75e}$$

$$e_{26} \equiv B_{26}\left[\frac{a_{22}^2}{D_{11}D_{22}}\right]^{\frac{1}{4}} \tag{75f}$$

$$e_{66} \equiv B_{66}\left[\frac{a_{11}a_{22}}{D_{11}D_{22}}\right]^{\frac{1}{4}} \tag{75g}$$

are defined as *load-path eccentricity parameter*s. The partially inverted form of the nondimensional constitutive equations derived herein is obtained by expressing equation (69a) as

$$\begin{Bmatrix} E_{11} \\ E_{22} \\ G_{12} \end{Bmatrix} = \pi^2 \begin{bmatrix} \frac{1}{\alpha_m^2} & -\nu_m & -\frac{\delta_m}{\alpha_m} \\ -\nu_m & \alpha_m^2 & -\alpha_m\gamma_m \\ -\frac{\delta_m}{\alpha_m} & -\alpha_m\gamma_m & 2(\mu+\nu_m) \end{bmatrix} \begin{Bmatrix} \mathcal{N}_{11} \\ \mathcal{N}_{22} \\ \frac{\mathcal{N}_{12}}{\alpha_b} \end{Bmatrix} + \begin{bmatrix} \mathcal{B}_{11} & \mathcal{B}_{12} & \mathcal{B}_{16} \\ \mathcal{B}_{21} & \mathcal{B}_{22} & \mathcal{B}_{26} \\ \mathcal{B}_{61} & \mathcal{B}_{62} & \mathcal{B}_{66} \end{bmatrix} \begin{Bmatrix} \frac{\partial^2 W}{\partial z_1^2} \\ \frac{\partial^2 W}{\partial z_2^2} \\ 2\frac{\partial^2 W}{\partial z_1 \partial z_2} \end{Bmatrix} \tag{76a}$$

where

$$\begin{bmatrix} \mathcal{B}_{11} & \mathcal{B}_{12} & \mathcal{B}_{16} \\ \mathcal{B}_{21} & \mathcal{B}_{22} & \mathcal{B}_{26} \\ \mathcal{B}_{61} & \mathcal{B}_{62} & \mathcal{B}_{66} \end{bmatrix} = \begin{bmatrix} \frac{1}{\alpha_m^2} & -\nu_m & -\frac{\delta_m}{\alpha_m} \\ -\nu_m & \alpha_m^2 & -\alpha_m\gamma_m \\ -\frac{\delta_m}{\alpha_m} & -\alpha_m\gamma_m & 2(\mu+\nu_m) \end{bmatrix} \begin{bmatrix} \mathcal{b}_{11} & \mathcal{b}_{12} & \mathcal{b}_{16} \\ \mathcal{b}_{12} & \mathcal{b}_{22} & \mathcal{b}_{26} \\ \mathcal{b}_{16} & \mathcal{b}_{26} & \mathcal{b}_{66} \end{bmatrix} \tag{76b}$$

Using equation (75a) gives

$$\mathcal{B}_{11} = \frac{\alpha_b}{\alpha_m} e_{11} - \nu_m e_{12} - \delta_m e_{16} \tag{77a}$$

$$\mathcal{B}_{12} = \frac{1}{\alpha_m^2}\left(e_{12} - \frac{\nu_m\alpha_m}{\alpha_b} e_{22} - \delta_m e_{26} \right) \tag{77b}$$

$$\mathcal{B}_{16} = \frac{1}{\alpha_m}\left(e_{16} - \nu_m e_{26} - \delta_m e_{66} \right) \tag{77c}$$

$$\mathcal{B}_{21} = \alpha_m^2\left(e_{12} - \frac{\nu_m\alpha_b}{\alpha_m} e_{11} - \gamma_m e_{16} \right) \tag{77d}$$

$$\mathcal{B}_{22} = \frac{\alpha_m}{\alpha_b} e_{22} - \nu_m e_{12} - \gamma_m e_{26} \tag{77e}$$

$$\mathcal{B}_{26} = \alpha_m\left(e_{26} - \nu_m e_{16} - \gamma_m e_{66} \right) \tag{77f}$$

$$\mathcal{B}_{61} = \alpha_m\left(2(\mu+\nu_m) e_{16} - \frac{\delta_m\alpha_b}{\alpha_m} e_{11} - \gamma_m e_{12} \right) \tag{77g}$$

$$\mathcal{B}_{62} = \frac{1}{\alpha_m}\left(2(\mu+\nu_m) e_{26} - \delta_m e_{12} - \frac{\alpha_m\gamma_m}{\alpha_b} e_{22} \right) \tag{77h}$$

$$\mathcal{B}_{66} = 2(\mu+\nu_m) e_{66} - \delta_m e_{16} - \gamma_m e_{26} \tag{77i}$$

where it is noted that all of equations (77) vanish for symmetrically laminated shells. Now, substituting equation (76a) into equation (74), and using equation (75a) yields

$$\begin{Bmatrix} \mathcal{M}_{11} \\ \mathcal{M}_{22} \\ \mathcal{M}_{12} \end{Bmatrix} = \pi^2 \begin{bmatrix} \mathcal{B}_{11} & \mathcal{B}_{21} & \mathcal{B}_{61} \\ \mathcal{B}_{12} & \mathcal{B}_{22} & \mathcal{B}_{62} \\ \mathcal{B}_{16} & \mathcal{B}_{26} & \mathcal{B}_{66} \end{bmatrix} \begin{Bmatrix} \mathcal{N}_{11} \\ \mathcal{N}_{22} \\ \dfrac{\mathcal{N}_{12}}{\alpha_b} \end{Bmatrix} - \begin{bmatrix} \mathcal{A}_{11} & \mathcal{A}_{12} & \mathcal{A}_{16} \\ \mathcal{A}_{12} & \mathcal{A}_{22} & \mathcal{A}_{26} \\ \mathcal{A}_{16} & \mathcal{A}_{26} & \mathcal{A}_{66} \end{bmatrix} \begin{Bmatrix} \dfrac{\partial^2 W}{\partial z_1^2} \\ \dfrac{\partial^2 W}{\partial z_2^2} \\ 2\dfrac{\partial^2 W}{\partial z_1 \partial z_2} \end{Bmatrix} \tag{78a}$$

where

$$\begin{bmatrix} \mathcal{A}_{11} & \mathcal{A}_{12} & \mathcal{A}_{16} \\ \mathcal{A}_{21} & \mathcal{A}_{22} & \mathcal{A}_{26} \\ \mathcal{A}_{61} & \mathcal{A}_{62} & \mathcal{A}_{66} \end{bmatrix} = \begin{bmatrix} \alpha_b^2 & \nu_b & \alpha_b\gamma_b \\ \nu_b & \dfrac{1}{\alpha_b^2} & \dfrac{\delta_b}{\alpha_b} \\ \alpha_b\gamma_b & \dfrac{\delta_b}{\alpha_b} & \dfrac{\beta - \nu_b}{2} \end{bmatrix} - \begin{bmatrix} \alpha_m\alpha_b e_{11} & e_{12} & \alpha_m e_{16} \\ e_{12} & \dfrac{e_{22}}{\alpha_m\alpha_b} & \dfrac{e_{26}}{\alpha_m} \\ \alpha_m e_{16} & \dfrac{e_{26}}{\alpha_m} & e_{66} \end{bmatrix} \begin{bmatrix} \mathcal{B}_{11} & \mathcal{B}_{12} & \mathcal{B}_{16} \\ \mathcal{B}_{21} & \mathcal{B}_{22} & \mathcal{B}_{26} \\ \mathcal{B}_{61} & \mathcal{B}_{62} & \mathcal{B}_{66} \end{bmatrix} \tag{78b}$$

In expanded form,

$$\mathcal{A}_{11} = \alpha_b^2\left(1 - e_{11}^2\right) + \alpha_m^2\left[2\,\frac{\alpha_b\nu_m}{\alpha_m}\,e_{11}e_{12} - e_{12}^2 + 2\left(\frac{\alpha_b\delta_m}{\alpha_m}\,e_{11} + \gamma_m\,e_{12}\right)e_{16} - 2\left(\mu + \nu_m\right)e_{16}^2\right] \tag{79a}$$

$$\begin{aligned} \mathcal{A}_{12} = \nu_b + \nu_m\left(e_{11}e_{22} + e_{12}^2\right) - \left(\frac{\alpha_b}{\alpha_m}\,e_{11} + \frac{\alpha_m}{\alpha_b}\,e_{22}\right)e_{12} + \delta_m\left(\frac{\alpha_b}{\alpha_m}\,e_{11}e_{26} + e_{12}e_{16}\right) + \\ \gamma_m\left(\frac{\alpha_m}{\alpha_b}\,e_{16}e_{22} + e_{12}e_{26}\right) - 2\left(\mu + \nu_m\right)e_{16}e_{26} \end{aligned} \tag{79b}$$

$$\begin{aligned} \mathcal{A}_{16} = \alpha_b\left[\gamma_b + \left(\,\delta_m\,e_{66} - e_{16} + \nu_m\,e_{26}\right)e_{11}\right] + \alpha_m\left[\gamma_m\,e_{66} - e_{26} + \nu_m\,e_{16}\right]e_{12} \\ + \alpha_m\left[\delta_m\,e_{16} + \gamma_m\,e_{26} - 2\left(\mu + \nu_m\right)e_{66}\right]e_{16} \end{aligned} \tag{79c}$$

$$\mathcal{A}_{22} = \frac{1}{\alpha_b^2}\left(1 - e_{22}^2\right) + \frac{1}{\alpha_m^2}\left[2\,\frac{\alpha_m\nu_m}{\alpha_b}\,e_{12}e_{22} - e_{12}^2 + 2\left(\frac{\alpha_m\gamma_m}{\alpha_b}\,e_{22} + \delta_m\,e_{12}\right)e_{26} - 2\left(\mu + \nu_m\right)e_{26}^2\right] \tag{79d}$$

$$\begin{aligned} \mathcal{A}_{26} = \frac{1}{\alpha_b}\left[\delta_b + \left(\gamma_m e_{66} + \nu_m\,e_{16} - e_{26}\right)e_{22}\right] + \frac{1}{\alpha_m}\left[\delta_m\,e_{66} - e_{16} + \nu_m\,e_{26}\right]e_{12} \\ + \frac{1}{\alpha_m}\left[\delta_m\,e_{16} + \gamma_m\,e_{26} - 2\left(\mu + \nu_m\right)e_{66}\right]e_{26} \end{aligned} \tag{79e}$$

$$\mathcal{A}_{66} = \frac{1}{2}(\beta - \nu_b) - 2(\mu + \nu_m)e_{66}^2 + 2\nu_m e_{16}e_{26} - e_{16}^2 - e_{26}^2 + 2\left(\delta_m e_{16} + \gamma_m e_{26}\right)e_{66} \tag{79f}$$

Equations (76a) and (78a) define a set of partially inverted constitutive equations that are expressed in terms of the nondimensional parameters defined in references 60 and 61 for symmetrically laminated shells and six new nondimensional parameters defined by equations (75) that characterize the anisotropies associated with coupling between membrane and bending deformations. This formulation is different from those used in references 18-20 and 71 in that all of the nondimensional parameters are defined in terms of the stiffnesses appearing in equation (16) and not the reduced stiffnesses appearing in equations (20b), defined by equations (21c). The utility of the formulation presented herein is revealed by inspection of equations (77) and (79); that is, the equations contain the fewest number of parameters needed to characterize fully the load path eccentricity associated with subscripted b-terms appearing in the constitutive equations given by equations (20). Moreover, equations (77) and (79) show explicitly the coupling between all forms of orthotropy and anisotropy that can occur in a generally laminated shell.

Nondimensional Equilibrium Equations

In this section of the present study, nondimensional equilibrium equations are obtained by direct nondimensionalization of the equilibrium equations given by equations (29). Specifically, introducing the coordinates (z_1, z_2) into equation (29a) gives

$$\frac{1}{L_1}\frac{\partial N_{11}}{\partial z_1} + \frac{1}{L_2}\frac{\partial N_{12}}{\partial z_2} + q_1 = 0 \tag{80}$$

Multiplying by $\dfrac{L_1 L_2^2}{\pi^2\sqrt{D_{11}D_{22}}}$ and using equations (54) gives

$$\frac{\partial \mathcal{N}_{11}}{\partial z_1} + \frac{1}{\alpha_b}\frac{\partial \mathcal{N}_{12}}{\partial z_2} + \mathcal{q}_1 = 0 \tag{81}$$

where

$$\mathcal{q}_1 \equiv \frac{q_1 L_1 L_2^2}{\pi^2\sqrt{D_{11}D_{22}}} \tag{82}$$

Similarly, equation (29b) becomes

$$\frac{1}{\alpha_b}\frac{\partial \mathcal{N}_{12}}{\partial z_1} + \frac{\partial \mathcal{N}_{22}}{\partial z_2} + \mathcal{q}_2 = 0 \tag{83}$$

where

$$\mathcal{g}_2 \equiv \frac{q_2 L_1^2 L_2}{\pi^2 \sqrt{D_{11} D_{22}}} \tag{84}$$

Next, introducing the coordinates (z_1, z_2) into equation (29d) gives

$$\frac{1}{L_1}\frac{\partial M_{11}}{\partial z_1} + \frac{1}{L_2}\frac{\partial M_{12}}{\partial z_2} - Q_1 = 0 \tag{85}$$

Multiplying equation (85) by $L_1 L_2^2 \left[a_{11} a_{22} D_{11}^3 D_{22}^3\right]^{-\frac{1}{4}}$ and then using equations (60) gives

$$\frac{\partial \mathcal{M}_{11}}{\partial z_1} + \frac{\partial \mathcal{M}_{12}}{\partial z_2} - \mathcal{Q}_1 = 0 \tag{86}$$

where

$$\mathcal{Q}_1 \equiv \frac{Q_1 L_1 L_2^2}{\left[a_{11} a_{22} D_{11}^3 D_{22}^3\right]^{\frac{1}{4}}} \tag{87}$$

Similarly, equation (29e) becomes

$$\frac{\partial \mathcal{M}_{12}}{\partial z_1} + \frac{\partial \mathcal{M}_{22}}{\partial z_2} - \mathcal{Q}_2 = 0 \tag{88}$$

where

$$\mathcal{Q}_2 \equiv \frac{Q_2 L_1^2 L_2}{\left[a_{11} a_{22} D_{11}^3 D_{22}^3\right]^{\frac{1}{4}}} \tag{89}$$

Likewise, introducing the coordinates (z_1, z_2) into equation (29c) gives

$$\frac{1}{L_1}\frac{\partial Q_1}{\partial z_1} + \frac{1}{L_2}\frac{\partial Q_2}{\partial z_2} + q_3 - \frac{N_{11}}{R_1} - \frac{N_{22}}{R_2} + P_m = 0 \tag{90}$$

Multiplying equation (90) by $L_1^2 L_2^2 \left[a_{11} a_{22} D_{11}^3 D_{22}^3\right]^{-\frac{1}{4}}$ and using equations (87) and (89) gives

$$\frac{\partial \mathcal{Q}_1}{\partial z_1} + \frac{\partial \mathcal{Q}_2}{\partial z_2} + \mathcal{g}_3 + L_1^2 L_2^2 \left[a_{11} a_{22} D_{11}^3 D_{22}^3\right]^{-\frac{1}{4}} \left(P_m - \frac{N_{11}}{R_1} - \frac{N_{22}}{R_2}\right) = 0 \tag{91}$$

where

$$\mathcal{g}_3 \equiv \frac{q_3 L_1^2 L_2^2}{\left[a_{11} a_{22} D_{11}^3 D_{22}^3\right]^{\frac{1}{4}}} \tag{92}$$

Next, using equations (45), (48), and (54) with equation (91) gives

$$\frac{\partial \mathcal{Z}_1}{\partial z_1} + \frac{\partial \mathcal{Z}_2}{\partial z_2} + \mathcal{g}_3 - \pi^2 \sqrt{12}\left(\mathcal{N}_{11} Z_1 + \mathcal{N}_{22} Z_2\right) + \mathcal{P}_m = 0 \tag{93}$$

where

$$\mathcal{P}_m \equiv \frac{P_m L_1^2 L_2^2}{\left[a_{11} a_{22} D_{11}^3 D_{22}^3\right]^{\frac{1}{4}}} \tag{94}$$

The specific form of $\mathcal{P}_m$ is obtained by first introducing the coordinates (z_1, z_2) into equation (30), which gives

$$\begin{aligned} P_m = &-\frac{1}{L_1}\frac{\partial}{\partial z_1}\left[\left(\left[\beta_1 + \beta_1^I\right]N_{11} + \left[\beta_2 + \beta_2^I\right]N_{12}\right)\right] \\ &-\frac{1}{L_2}\frac{\partial}{\partial z_2}\left[\left(\left[\beta_1 + \beta_1^I\right]N_{12} + \left[\beta_2 + \beta_2^I\right]N_{22}\right)\right] \end{aligned} \tag{95}$$

By using equations (39)-(42), (54), and (94); and noting that

$$\beta_1^I = -\frac{1}{L_1}\left[a_{11} a_{22} D_{11} D_{22}\right]^{\frac{1}{4}} \frac{\partial W_I}{\partial z_1} \tag{96a}$$

$$\beta_2^I = -\frac{1}{L_2}\left[a_{11} a_{22} D_{11} D_{22}\right]^{\frac{1}{4}} \frac{\partial W_I}{\partial z_2} \tag{96b}$$

equation (95) yields

$$\begin{aligned} \mathcal{P}_m = &\pi^2 \frac{\partial}{\partial z_1}\left[\mathcal{N}_{11}\frac{\partial}{\partial z_1}\left(W + W_I\right) + \frac{\mathcal{N}_{12}}{\alpha_b}\frac{\partial}{\partial z_2}\left(W + W_I\right)\right] \\ &+ \pi^2 \frac{\partial}{\partial z_2}\left[\frac{\mathcal{N}_{12}}{\alpha_b}\frac{\partial}{\partial z_1}\left(W + W_I\right) + \mathcal{N}_{22}\frac{\partial}{\partial z_2}\left(W + W_I\right)\right] \end{aligned} \tag{97a}$$

Expanding the derivatives of the bracketed terms and using equations (81) and (83) give the alternate form

$$\mathcal{P}_m = -\pi^2\left[\mathcal{g}_1\frac{\partial}{\partial z_1}\left(W + W_I\right) + \mathcal{g}_2\frac{\partial}{\partial z_2}\left(W + W_I\right)\right] + \pi^2\left[\mathcal{N}_{11}\frac{\partial^2}{\partial z_1^2}\left(W + W_I\right) + \mathcal{N}_{22}\frac{\partial^2}{\partial z_2^2}\left(W + W_I\right) + 2\frac{\mathcal{N}_{12}}{\alpha_b}\frac{\partial^2}{\partial z_1 \partial z_2}\left(W + W_I\right)\right] \tag{97b}$$

Nondimensional Boundary Conditions

In terms of the nondimensional coordinates, the boundary conditions are defined at the edges given by constant values of z_1 and z_2. On the edges given by $z_1 = a_1 / L_1$ and $z_1 = b_1 / L_1$, the boundary conditions given by equations (33) become

$$\mathcal{N}_{11} = \frac{N(z_2)L_2^2}{\pi^2\sqrt{D_{11}D_{22}}} \equiv \bar{N}(z_2) \quad \text{or} \quad U_1 = \frac{\Delta_1(z_2)L_1}{\left[a_{11}a_{22}D_{11}D_{22}\right]^{\frac{1}{2}}} \equiv \bar{\Delta}_1(z_2) \tag{98a}$$

$$\mathcal{N}_{12} = \frac{S(z_2)L_2^2}{\pi^2\left[D_{11}D_{22}^3\right]^{1/4}} \equiv \bar{S}(z_2) \quad \text{or} \quad U_2 = \frac{\Delta_2(z_2)L_2}{\left[a_{11}a_{22}D_{11}D_{22}\right]^{\frac{1}{2}}} \equiv \bar{\Delta}_2(z_2) \tag{98b}$$

$$\mathcal{Z}_1 + \frac{\partial \mathcal{M}_{12}}{\partial z_2} + \pi^2\mathcal{N}_{11}\frac{\partial}{\partial z_1}\left(W + W_I\right) + \frac{\pi^2}{\alpha_b}\mathcal{N}_{12}\frac{\partial}{\partial z_2}\left(W + W_I\right) = \frac{V(z_2)L_1L_2^2}{\left[a_{11}a_{22}D_{11}^3D_{22}^3\right]^{\frac{1}{4}}} \equiv \bar{V}(z_2)$$

$$\text{or} \qquad W = \frac{\Delta_n(z_2)}{\left[a_{11}a_{22}D_{11}D_{22}\right]^{\frac{1}{4}}} \equiv \bar{\Delta}_n(z_2) \tag{98c}$$

$$\mathcal{M}_{11} = \frac{M(z_2)L_2^2}{\left[a_{11}a_{22}D_{11}^3D_{22}^3\right]^{\frac{1}{4}}} \equiv \bar{M}(z_2) \quad \text{or} \quad -\frac{\partial W}{\partial z_1} = \frac{\Phi(z_2)L_1}{\left[a_{11}a_{22}D_{11}D_{22}\right]^{\frac{1}{4}}} \equiv \bar{\Phi}(z_2) \tag{98d}$$

where $\mathcal{Z}_1$ is given by equation (86). On the edges given by $z_2 = a_2 / L_2$ and $z_2 = b_2 / L_2$, the boundary conditions specified by equations (34) become

$$\mathcal{N}_{22} = \frac{N(z_1)L_1^2}{\pi^2\sqrt{D_{11}D_{22}}} \equiv \bar{N}(z_1) \quad \text{or} \quad U_2 = \frac{\Delta_2(z_1)L_2}{\left[a_{11}a_{22}D_{11}D_{22}\right]^{\frac{1}{2}}} \equiv \bar{\Delta}_2(z_1) \tag{99a}$$

$$\mathcal{N}_{12} = \frac{S(z_1)L_2^2}{\pi^2\left[D_{11}D_{22}^3\right]^{1/4}} \equiv \bar{S}(z_1) \quad \text{or} \quad U_1 = \frac{\Delta_1(z_1)L_1}{\left[a_{11}a_{22}D_{11}D_{22}\right]^{\frac{1}{2}}} \equiv \bar{\Delta}_1(z_1) \tag{99b}$$

$$\mathcal{Z}_2 + \frac{\partial \mathcal{M}_{12}}{\partial z_1} + \frac{\pi^2}{\alpha_b}\,\mathcal{N}_{12}\,\frac{\partial}{\partial z_1}\left(W + W_I\right) + \pi^2\,\mathcal{N}_{22}\,\frac{\partial}{\partial z_2}\left(W + W_I\right) = \frac{V(z_1)L_1^2 L_2}{\left[a_{11}a_{22}D_{11}^3 D_{22}^3\right]^{\frac{1}{4}}} \equiv \overline{V}(z_1)$$

$$\text{or} \qquad W = \frac{\Lambda_n(z_1)}{\left[a_{11}a_{22}D_{11}D_{22}\right]^{\frac{1}{4}}} \equiv \overline{\Lambda}_n(z_1) \tag{99c}$$

$$\mathcal{M}_{22} = \frac{M(z_1)L_1^2}{\left[a_{11}a_{22}D_{11}^3 D_{22}^3\right]^{\frac{1}{4}}} \equiv \overline{M}(z_1) \quad \text{or} \quad -\frac{\partial W}{\partial z_2} = \frac{\Phi(z_1)L_2}{\left[a_{11}a_{22}D_{11}D_{22}\right]^{\frac{1}{4}}} \equiv \overline{\Phi}(z_1) \tag{99d}$$

where $\mathcal{Z}_2$ is given by equation (88).

Nondimensional Compatibility Equation

Nondimensional compatibility equations for geometrically imperfect shells are obtained by introducing the nondimensional arc-length Gaussian coordinates (z_1, z_2) into equations (36) and (37). This step gives

$$\mathcal{C}_{11}\left[\varepsilon_{11}^{o}\right] = \frac{1}{L_2^2}\,\frac{\partial^2 \varepsilon_{11}^{o}}{\partial z_2^2} \tag{100a}$$

$$\mathcal{C}_{22}\left[\varepsilon_{22}^{o}\right] = \frac{1}{L_1^2}\,\frac{\partial^2 \varepsilon_{22}^{o}}{\partial z_1^2} \tag{100b}$$

$$\mathcal{C}_{12}\left[\gamma_{12}^{o}\right] = -\frac{1}{L_1 L_2}\,\frac{\partial^2 \gamma_{12}^{o}}{\partial z_1 \partial z_2} \tag{100c}$$

$$\kappa_{11}^{I} = -\frac{1}{L_1^2}\frac{\partial^2 w_I}{\partial z_1^2} \tag{101a}$$

$$\kappa_{22}^{I} = -\frac{1}{L_2^2}\frac{\partial^2 w_I}{\partial z_2^2} \tag{101b}$$

$$\kappa_{12}^{I} = -\frac{2}{L_1 L_2}\frac{\partial^2 w_I}{\partial z_1 \partial z_2} \tag{101c}$$

Using equations (100), it follows that the first three terms of equation (35) becomes

$$\frac{1}{A_1A_2}\left\{\mathscr{C}_{11}\left[\varepsilon^{\circ}_{11}\right]+\mathscr{C}_{22}\left[\varepsilon^{\circ}_{22}\right]+\mathscr{C}_{12}\left[\gamma^{\circ}_{12}\right]\right\}=\frac{1}{L_2^2}\frac{\partial^2\varepsilon^{\circ}_{11}}{\partial z_2^2}+\frac{1}{L_1^2}\frac{\partial^2\varepsilon^{\circ}_{22}}{\partial z_1^2}-\frac{1}{L_1L_2}\frac{\partial^2\gamma^{\circ}_{12}}{\partial z_1\partial z_2} \tag{102}$$

and using the definitions in equations (46) with the previous expression gives

$$\frac{1}{A_1A_2}\left\{\mathscr{C}_{11}\left[\varepsilon^{\circ}_{11}\right]+\mathscr{C}_{22}\left[\varepsilon^{\circ}_{22}\right]+\mathscr{C}_{12}\left[\gamma^{\circ}_{12}\right]\right\}=\frac{\left[a_{11}a_{22}D_{11}D_{22}\right]^{\frac{1}{2}}}{L_1^2L_2^2}\left(\frac{\partial^2E_{11}}{\partial z_2^2}+\frac{\partial^2E_{22}}{\partial z_1^2}-\frac{\partial^2G_{12}}{\partial z_1\partial z_2}\right) \tag{103}$$

Similarly, substituting $w_I=\left[a_{11}a_{22}D_{11}D_{22}\right]^{\frac{1}{4}}W_I$ into equations (101) and then using the results with equations (45), (48), and (49) gives the second part of equation (35) as

$$\begin{aligned}&\frac{\kappa^{\circ}_{22}}{R_1}+\frac{\kappa^{\circ}_{11}}{R_2}-\kappa^{\circ}_{11}\kappa^{\circ}_{22}+\frac{1}{4}\left(\kappa^{\circ}_{12}\right)^2-\kappa^{\circ}_{11}\kappa^{I}_{22}-\kappa^{I}_{11}\kappa^{\circ}_{22}+\frac{1}{2}\kappa^{\circ}_{12}\kappa^{I}_{12}=\\&\qquad-\frac{\left[a_{11}a_{22}D_{11}D_{22}\right]^{\frac{1}{2}}}{L_1^2L_2^2}\sqrt{12}\left[Z_1\frac{\partial^2W}{\partial z_2^2}+Z_2\frac{\partial^2W}{\partial z_1^2}\right]\\&+\frac{\left[a_{11}a_{22}D_{11}D_{22}\right]^{\frac{1}{2}}}{L_1^2L_2^2}\left[\left(\frac{\partial^2W}{\partial z_1\partial z_2}\right)^2-\frac{\partial^2W}{\partial z_1^2}\frac{\partial^2W}{\partial z_2^2}-\frac{\partial^2W}{\partial z_1^2}\frac{\partial^2W_I}{\partial z_2^2}-\frac{\partial^2W}{\partial z_2^2}\frac{\partial^2W_I}{\partial z_1^2}+2\frac{\partial^2W}{\partial z_1\partial z_2}\frac{\partial^2W_I}{\partial z_1\partial z_2}\right]\end{aligned} \tag{104}$$

Substituting equations (103) and (104) into equation (35) gives the nondimensional compatibility equation

$$\begin{aligned}\frac{\partial^2E_{11}}{\partial z_2^2}+\frac{\partial^2E_{22}}{\partial z_1^2}-\frac{\partial^2G_{12}}{\partial z_1\partial z_2}&=\sqrt{12}\left(Z_1\frac{\partial^2W}{\partial z_2^2}+Z_2\frac{\partial^2W}{\partial z_1^2}\right)+\frac{\partial^2W}{\partial z_1^2}\frac{\partial^2W}{\partial z_2^2}-\left(\frac{\partial^2W}{\partial z_1\partial z_2}\right)^2\\&\quad+\frac{\partial^2W}{\partial z_1^2}\frac{\partial^2W_I}{\partial z_2^2}+\frac{\partial^2W}{\partial z_2^2}\frac{\partial^2W_I}{\partial z_1^2}-2\frac{\partial^2W}{\partial z_1\partial z_2}\frac{\partial^2W_I}{\partial z_1\partial z_2}\end{aligned} \tag{105}$$

Nondimensional Virtual Work

A nondimensional form of the principle of virtual work given by equation (22) is obtained by by first taking the variation of the nondimensional displacements given by equations (44), (47), and the definition $w\equiv\left[a_{11}a_{22}D_{11}D_{22}\right]^{\frac{1}{4}}W$; and strains given by equations (46) and (49). This step produces

$$\delta U_1\equiv\frac{\delta u_1L_1}{\left[a_{11}a_{22}D_{11}D_{22}\right]^{\frac{1}{2}}} \tag{106a}$$

$$\delta U_2 \equiv \frac{\delta u_2 L_2}{\left[a_{11}a_{22}D_{11}D_{22}\right]^{\frac{1}{2}}} \tag{106b}$$

$$\delta W \equiv \frac{\delta w}{\left[a_{11}a_{22}D_{11}D_{22}\right]^{\frac{1}{4}}} \tag{106c}$$

$$\delta E_{11} \equiv \frac{\delta \varepsilon^{\circ}_{11} L_1^2}{\left[a_{11}a_{22}D_{11}D_{22}\right]^{\frac{1}{2}}} = \frac{\partial \delta U_1}{\partial z_1} + \sqrt{12} Z_1 \, \delta W + \left(\frac{\partial W}{\partial z_1} + \frac{\partial W_I}{\partial z_1}\right)\frac{\partial \delta W}{\partial z_1} \tag{107a}$$

$$\delta E_{22} \equiv \frac{\delta \varepsilon^{\circ}_{22} L_2^2}{\left[a_{11}a_{22}D_{11}D_{22}\right]^{\frac{1}{2}}} = \frac{\partial \delta U_2}{\partial z_2} + \sqrt{12} Z_2 \, \delta W + \left(\frac{\partial W}{\partial z_2} + \frac{\partial W_I}{\partial z_2}\right)\frac{\partial \delta W}{\partial z_2} \tag{107b}$$

$$\delta G_{12} \equiv \frac{\delta \gamma^{\circ}_{12} L_1 L_2}{\left[a_{11}a_{22}D_{11}D_{22}\right]^{\frac{1}{2}}} = \frac{\partial \delta U_1}{\partial z_2} + \frac{\partial \delta U_2}{\partial z_1} + \left(\frac{\partial W}{\partial z_2} + \frac{\partial W_I}{\partial z_2}\right)\frac{\partial \delta W}{\partial z_1} + \left(\frac{\partial W}{\partial z_1} + \frac{\partial W_I}{\partial z_1}\right)\frac{\partial \delta W}{\partial z_2} \tag{107c}$$

$$\delta \mathcal{K}_{11} \equiv \frac{\delta \kappa^{\circ}_{11} L_1^2}{\left[a_{11}a_{22}D_{11}D_{22}\right]^{\frac{1}{4}}} = -\frac{\partial^2 \delta W}{\partial z_1^2} \tag{108a}$$

$$\delta \mathcal{K}_{22} \equiv \frac{\delta \kappa^{\circ}_{22} L_2^2}{\left[a_{11}a_{22}D_{11}D_{22}\right]^{\frac{1}{4}}} = -\frac{\partial^2 \delta W}{\partial z_2^2} \tag{108b}$$

$$\delta \mathcal{K}_{12} \equiv \frac{\delta \kappa^{\circ}_{12} L_1 L_2}{\left[a_{11}a_{22}D_{11}D_{22}\right]^{\frac{1}{4}}} = -2\,\frac{\partial^2 \delta W}{\partial z_1 \partial z_2} \tag{108c}$$

Using these definitions and the definitions in equations (54) and (60) with the internal virtual work per unit area given by equation (23a) and requiring the transverse shearing strains to vanish gives

$$\delta \mathcal{W}_{\text{int}} \equiv \frac{\delta W_{\text{int}} L_1^2 L_2^2}{\left[a_{11}a_{22}\right]^{\frac{1}{2}} D_{11}D_{22}} = \pi^2 \mathcal{N}_{11}\,\delta E_{11} + \frac{\pi^2}{\alpha_b}\mathcal{N}_{12}\,\delta G_{12} + \pi^2 \mathcal{N}_{22}\,\delta E_{22} + \mathcal{M}_{11}\,\delta \mathcal{K}_{11} + \mathcal{M}_{12}\,\delta \mathcal{K}_{12} + \mathcal{M}_{22}\,\delta \mathcal{K}_{22} \tag{109a}$$

Similarly, the external work per unit area given by equation (23b) becomes

$$\delta \mathcal{W}_{\text{ext}} \equiv \frac{\delta W_{\text{ext}} L_1^2 L_2^2}{\left[a_{11}a_{22}\right]^{\frac{1}{2}} D_{11}D_{22}} = \pi^2 \mathcal{Z}_1\,\delta U_1 + \pi^2 \mathcal{Z}_2\,\delta U_2 + \mathcal{Z}_3 \delta W \tag{109b}$$

Multiplying equation (22) by $\dfrac{L_1 L_2}{\left[a_{11}a_{22}\right]^{\frac{1}{2}} D_{11}D_{22}}$ gives the principle of virtual work in nondimensional form as

$$\int\int_{\mathcal{A}} \delta\mathcal{W}_{\text{int}}\, dz_1 dz_2 = \int\int_{\mathcal{A}} \delta\mathcal{W}_{\text{ext}}\, dz_1 dz_2 + \int_{\partial\mathcal{A}} \delta\mathcal{W}^{B}_{\text{ext}}\, d\mathcal{s} \tag{110}$$

where $\mathcal{A}$ is the nondimensional domain given by $\frac{a_1}{L_1} \le z_1 \le \frac{b_1}{L_1}$ and $\frac{a_2}{L_2} \le z_2 \le \frac{b_2}{L_2}$, $\partial\mathcal{A}$ denotes the boundary of $\mathcal{A}$, $d\mathcal{s}$ denotes the nondimensional arc-length coordinate for $\partial\mathcal{A}$, and where

$$\int_{\partial\mathcal{A}} \delta\mathcal{W}^{B}_{\text{ext}}\, d\mathcal{s} \equiv \frac{L_1 L_2}{\left[a_{11}a_{22}\right]^{\frac{1}{2}} D_{11}D_{22}} \int_{\partial A} \delta W^{B}_{\text{ext}}\, ds \tag{111}$$

The explicit expression for virtual work of the applied loads acting on $\partial\mathcal{A}$ is obtained from equation (23c) as follows. From equations (38)-(42) it follows that

$$\delta\beta_1 = -\frac{1}{L_1}\left[a_{11}a_{22}D_{11}D_{22}\right]^{\frac{1}{4}} \frac{\partial\delta W}{\partial z_1} \tag{112a}$$

$$\delta\beta_2 = -\frac{1}{L_2}\left[a_{11}a_{22}D_{11}D_{22}\right]^{\frac{1}{4}} \frac{\partial\delta W}{\partial z_2} \tag{112b}$$

Introducing the nondimensional coordinates (z_1, z_2) and substituting equations (106) and (112) into equation (111), and making use of the notation for the nondimensional boundary loads defined in equations (98) and (99) yields

$$\begin{aligned}\int_{\partial\mathcal{A}} \delta\mathcal{W}^{B}_{\text{ext}}\, d\mathcal{s} = &\int_{\frac{a_2}{L_2}}^{\frac{b_2}{L_2}} \left[\pi^2\overline{N}(z_2)\,\delta U_1 + \frac{\pi^2}{\alpha_b}\overline{S}(z_2)\,\delta U_2 + \overline{V}(z_2)\,\delta W - \overline{M}(z_2)\frac{\partial\delta W}{\partial z_1}\right]_{\frac{a_1}{L_1}}^{\frac{b_1}{L_1}} dz_2 \\ &+ \int_{\frac{a_1}{L_1}}^{\frac{b_1}{L_1}} \left[\frac{\pi^2}{\alpha_b}\overline{S}(z_1)\,\delta U_1 + \pi^2\overline{N}(z_1)\,\delta U_2 + \overline{V}(z_1)\,\delta W - \overline{M}(z_1)\frac{\partial\delta W}{\partial z_2}\right]_{\frac{a_2}{L_2}}^{\frac{b_2}{L_2}} dz_1\end{aligned} \tag{113}$$

Nondimensional Stress-Function Formulation

The stress-function formulation of the Donnell-Mushtari-Vlasov equations is often used to facilitiate solution of practical problems by reducing the number of unknown functions to two. These two unknowns are the normal displacement $w(\xi_1, \xi_2)$ and a stress function $F(\xi_1, \xi_2)$. In particular, the stress resultants N_{11}, N_{22}, and N_{12} are defined in terms of derivatives of a stress function such that the equilibrium equations given by equations (29a) and (29b) are satisfied identically. As a result, the compatibility equation given by equation (35) must be satisfied. Similarly, moment equilibrium equations (21d) and (21e) are used to eliminate the transverse shear stress resultants in the force equilibrium equation given by equation (29c). In addition, N_{11} and N_{22} in the force equilibrium equation are expressed in terms of the stress function. Next, the constitutive equations given by equations (20a), the bending strains given by equations (8), and the rotations defined by equations (10), neglecting transverse shearing deformations, is used to express the membrane strains in terms of $w(\xi_1, \xi_2)$ and $F(\xi_1, \xi_2)$. Likewise, equations (20b) give the bending stress resultants in terms of $w(\xi_1, \xi_2)$ and $F(\xi_1, \xi_2)$. With these modified constitutive equations, the compatibility equation and the transverse force equilibrium equation are expressed as two coupled nonlinear partial differential equations in terms of the normal displacement $w(\xi_1, \xi_2)$ and the stress function $F(\xi_1, \xi_2)$. A similar process that uses the nondimensional field equations derived herein directly is presented in this section first. Then, the corresponding expressions for the virtual work and complementary virtual work, are presented that are useful for for solving boundary-value problems by direct variational methods. A similar similar approach has been given by Zhang and Matthews[89] that uses the basic integral forms that are used to derive the principles of virtual work and complementary virtual work (see Washizu[86], pp. 18-32 for a general treatment). In the last part of this section, simplifications to the stress-function formulation are presented for cases of practical importance.

Field Equations in terms of W and $\mathcal{F}$

The nondimensional stress-function formulation is obtained by first using equations (86) and (88) to reduce the number of independent equilibrium equations to three force balance equations by eliminating $\mathcal{Q}_1$ and $\mathcal{Q}_2$. This step yields

$$\frac{\partial^2 \mathcal{M}_{11}}{\partial Z_1^2} + 2\,\frac{\partial^2 \mathcal{M}_{12}}{\partial Z_1 \partial Z_2} + \frac{\partial^2 \mathcal{M}_{22}}{\partial Z_2^2} + \mathcal{G}_3 - \pi^2 \sqrt{12}\left(\mathcal{N}_{11} Z_1 + \mathcal{N}_{22} Z_2\right) + \mathcal{P}_m = 0 \tag{114}$$

for the force balance, in the direction normal to the tangent plane at a given point of the shell reference surface, given by equation (93). Next, a stress function is defined that satisfies the tangential-equilibrium equations, equations (81) and (83), indentically. Let $\mathcal{F} = \mathcal{F}(Z_1, Z_2)$ denote the stress function defined by

$$\pi^2 \mathcal{N}_{11} = \frac{\partial^2 \mathcal{F}}{\partial Z_2^2} - \pi^2 \int \mathcal{G}_1 \, dZ_1 \tag{115a}$$

$$\pi^2 \mathcal{N}_{22} = \frac{\partial^2 \mathcal{F}}{\partial z_1^2} - \pi^2 \int \mathcal{g}_2 \, dz_2 \tag{115b}$$

$$\frac{\pi^2}{\alpha_b} \mathcal{N}_{12} = - \frac{\partial^2 \mathcal{F}}{\partial z_1 \partial z_2} \tag{115c}$$

such that equations (81) and (83) are satisfied identically. Equation (114) becomes

$$\frac{\partial^2 \mathcal{M}_{11}}{\partial z_1^2} + 2 \frac{\partial^2 \mathcal{M}_{12}}{\partial z_1 \partial z_2} + \frac{\partial^2 \mathcal{M}_{22}}{\partial z_2^2} + \mathcal{g}_3 - \sqrt{12} \left(Z_1 \frac{\partial^2 \mathcal{F}}{\partial z_2^2} + Z_2 \frac{\partial^2 \mathcal{F}}{\partial z_1^2} \right) + \mathcal{P}_m = \mathcal{P}_T \tag{116a}$$

where $\mathcal{P}_T$ is a known function given by

$$\mathcal{P}_T = - \pi^2 \sqrt{12} \left(Z_1 \int \mathcal{g}_1 \, dz_1 + Z_2 \int \mathcal{g}_2 \, dz_2 \right) = \mathcal{P}_T(z_1, z_2) \tag{116b}$$

In addition, equation (97a) becomes

$$\mathcal{P}_m = - \mathcal{D}_g (W + W_I) + \mathcal{L}(\mathcal{F}, W + W_I) \tag{117a}$$

where $\mathcal{D}_g$ is a linear differential operator defined as

$$\mathcal{D}_g (W + W_I) \equiv \pi^2 \frac{\partial}{\partial z_1} \left[\int \mathcal{g}_1 \, dz_1 \, \frac{\partial}{\partial z_1} (W + W_I) \right] + \pi^2 \frac{\partial}{\partial z_2} \left[\int \mathcal{g}_2 \, dz_2 \, \frac{\partial}{\partial z_2} (W + W_I) \right] \tag{117b}$$

and $\mathcal{L}$ is a bilinear differential operator defined as

$$\mathcal{L}(\mathcal{F}, W + W_I) \equiv \frac{\partial^2 \mathcal{F}}{\partial z_2^2} \frac{\partial^2}{\partial z_1^2} (W + W_I) + \frac{\partial^2 \mathcal{F}}{\partial z_1^2} \frac{\partial^2}{\partial z_2^2} (W + W_I) - 2 \frac{\partial^2 \mathcal{F}}{\partial z_1 \partial z_2} \frac{\partial^2}{\partial z_1 \partial z_2} (W + W_I) \tag{117c}$$

The next step in the stress-function formulation is to express the partially inverted constitutive equations, equations (76a) and (78a), in terms of the stress function. This action yields

$$\begin{Bmatrix} E_{11} \\ E_{22} \\ G_{12} \end{Bmatrix} = \begin{bmatrix} \frac{1}{\alpha_m^2} & -\nu_m & -\frac{\delta_m}{\alpha_m} \\ -\nu_m & \alpha_m^2 & -\alpha_m\gamma_m \\ -\frac{\delta_m}{\alpha_m} & -\alpha_m\gamma_m & 2(\mu+\nu_m) \end{bmatrix} \begin{Bmatrix} \frac{\partial^2 \mathcal{F}}{\partial z_2^2} \\ \frac{\partial^2 \mathcal{F}}{\partial z_1^2} \\ -\frac{\partial^2 \mathcal{F}}{\partial z_1 \partial z_2} \end{Bmatrix} + \begin{bmatrix} \mathcal{B}_{11} & \mathcal{B}_{12} & \mathcal{B}_{16} \\ \mathcal{B}_{21} & \mathcal{B}_{22} & \mathcal{B}_{26} \\ \mathcal{B}_{61} & \mathcal{B}_{62} & \mathcal{B}_{66} \end{bmatrix} \begin{Bmatrix} \frac{\partial^2 W}{\partial z_1^2} \\ \frac{\partial^2 W}{\partial z_2^2} \\ 2\frac{\partial^2 W}{\partial z_1 \partial z_2} \end{Bmatrix} - \begin{Bmatrix} \mathcal{P}_1 \\ \mathcal{P}_2 \\ \mathcal{P}_3 \end{Bmatrix} \tag{118}$$

where

$$\begin{Bmatrix} \mathcal{P}_1 \\ \mathcal{P}_2 \\ \mathcal{P}_3 \end{Bmatrix} = \begin{bmatrix} \frac{1}{\alpha_m^2} & -\nu_m & -\frac{\delta_m}{\alpha_m} \\ -\nu_m & \alpha_m^2 & -\alpha_m\gamma_m \\ -\frac{\delta_m}{\alpha_m} & -\alpha_m\gamma_m & 2(\mu+\nu_m) \end{bmatrix} \begin{Bmatrix} \pi^2 \int \mathcal{G}_1 \, dz_1 \\ \pi^2 \int \mathcal{G}_2 \, dz_2 \\ 0 \end{Bmatrix} \tag{119}$$

and

$$\begin{Bmatrix} \mathcal{M}_{11} \\ \mathcal{M}_{22} \\ \mathcal{M}_{12} \end{Bmatrix} = \begin{bmatrix} \mathcal{B}_{11} & \mathcal{B}_{21} & \mathcal{B}_{61} \\ \mathcal{B}_{12} & \mathcal{B}_{22} & \mathcal{B}_{62} \\ \mathcal{B}_{16} & \mathcal{B}_{26} & \mathcal{B}_{66} \end{bmatrix} \begin{Bmatrix} \frac{\partial^2 \mathcal{F}}{\partial z_2^2} \\ \frac{\partial^2 \mathcal{F}}{\partial z_1^2} \\ -\frac{\partial^2 \mathcal{F}}{\partial z_1 \partial z_2} \end{Bmatrix} - \begin{bmatrix} \mathcal{A}_{11} & \mathcal{A}_{12} & \mathcal{A}_{16} \\ \mathcal{A}_{12} & \mathcal{A}_{22} & \mathcal{A}_{26} \\ \mathcal{A}_{16} & \mathcal{A}_{26} & \mathcal{A}_{66} \end{bmatrix} \begin{Bmatrix} \frac{\partial^2 W}{\partial z_1^2} \\ \frac{\partial^2 W}{\partial z_2^2} \\ 2\frac{\partial^2 W}{\partial z_1 \partial z_2} \end{Bmatrix} - \begin{Bmatrix} \mathcal{M}_1 \\ \mathcal{M}_2 \\ \mathcal{M}_3 \end{Bmatrix} \tag{120}$$

where

$$\begin{Bmatrix} \mathcal{M}_1 \\ \mathcal{M}_2 \\ \mathcal{M}_3 \end{Bmatrix} = \begin{bmatrix} \mathcal{B}_{11} & \mathcal{B}_{21} & \mathcal{B}_{61} \\ \mathcal{B}_{12} & \mathcal{B}_{22} & \mathcal{B}_{62} \\ \mathcal{B}_{16} & \mathcal{B}_{26} & \mathcal{B}_{66} \end{bmatrix} \begin{Bmatrix} \pi^2 \int \mathcal{G}_1 \, dz_1 \\ \pi^2 \int \mathcal{G}_2 \, dz_2 \\ 0 \end{Bmatrix} \tag{121}$$

Substituting equations (120) into equation (116a), and using equations (116b) and (117), give the stress-function form of the transverse equilibrium equation as

$$\begin{aligned} &\mathcal{D}_b(W) + \sqrt{12}\,\mathcal{D}_c(\mathcal{F}) - \mathcal{D}_\varepsilon(\mathcal{F}) = \\ &\qquad \mathcal{L}(\mathcal{F}, W + W_I) - \mathcal{D}_g(W + W_I) + \mathcal{G}_3 - \mathcal{P}_T - \left(\frac{\partial^2 \mathcal{M}_1}{\partial z_1^2} + 2\frac{\partial^2 \mathcal{M}_3}{\partial z_1 \partial z_2} + \frac{\partial^2 \mathcal{M}_2}{\partial z_2^2} \right) \end{aligned} \tag{122a}$$

where $\mathcal{D}_b$, $\mathcal{D}_c$, and $\mathcal{D}_\varepsilon$ are linear differential operators defined as

$$\mathcal{D}_b(W) \equiv \mathcal{A}_{11}\frac{\partial^4 W}{\partial z_1^4} + 4\mathcal{A}_{16}\frac{\partial^4 W}{\partial z_1^3 \partial z_2} + 2\left(\mathcal{A}_{12} + 2\mathcal{A}_{66}\right)\frac{\partial^4 W}{\partial z_1^2 \partial z_2^2} + 4\mathcal{A}_{26}\frac{\partial^4 W}{\partial z_1 \partial z_2^3} + \mathcal{A}_{22}\frac{\partial^4 W}{\partial z_2^4} \tag{122b}$$

$$\mathcal{D}_c(\mathcal{F}) \equiv Z_1\frac{\partial^2 \mathcal{F}}{\partial z_2^2} + Z_2\frac{\partial^2 \mathcal{F}}{\partial z_1^2} \tag{122c}$$

and

$$\begin{aligned}\mathcal{D}_\varepsilon(\mathcal{F}) \equiv \mathcal{B}_{21}\frac{\partial^4 \mathcal{F}}{\partial z_1^4} + \left(2\mathcal{B}_{26} - \mathcal{B}_{61}\right)\frac{\partial^4 \mathcal{F}}{\partial z_1^3 \partial z_2} + \left(\mathcal{B}_{11} + \mathcal{B}_{22} - 2\mathcal{B}_{66}\right)\frac{\partial^4 \mathcal{F}}{\partial z_1^2 \partial z_2^2} \\ + \left(2\mathcal{B}_{16} - \mathcal{B}_{62}\right)\frac{\partial^4 \mathcal{F}}{\partial z_1 \partial z_2^3} + \mathcal{B}_{12}\frac{\partial^4 \mathcal{F}}{\partial z_2^4}\end{aligned} \tag{122d}$$

Since the tangential equilibrium equations are satisfied identically, the tangential strains must satisfy the compatibility equation given by equation (105). By using the operators defined by equations (117c) and (122c), the compatibility equation given by equation (105) is expressed as

$$\frac{\partial^2 E_{11}}{\partial z_2^2} + \frac{\partial^2 E_{22}}{\partial z_1^2} - \frac{\partial^2 G_{12}}{\partial z_1 \partial z_2} = \sqrt{12}\,\mathcal{D}_c(W) - \frac{1}{2}\mathcal{L}\left(W,\, W + 2W_I\right) \tag{123a}$$

where, in particular,

$$\frac{1}{2}\mathcal{L}\left(W,\, W + 2W_I\right) = \frac{\partial^2 W}{\partial z_1^2}\frac{\partial^2 W}{\partial z_2^2} - \left(\frac{\partial^2 W}{\partial z_1 \partial z_2}\right)^2 + \frac{\partial^2 W}{\partial z_1^2}\frac{\partial^2 W_I}{\partial z_2^2} + \frac{\partial^2 W}{\partial z_2^2}\frac{\partial^2 W_I}{\partial z_1^2} - 2\frac{\partial^2 W}{\partial z_1 \partial z_2}\frac{\partial^2 W_I}{\partial z_1 \partial z_2} \tag{123b}$$

Substituting equations (118) into equation (123a) gives the nondimensional compatibility equation

$$\begin{aligned}\mathcal{D}_m(\mathcal{F}) + \mathcal{D}_\varepsilon(W) - \sqrt{12}\,\mathcal{D}_c(W) \\ + \frac{1}{2}\mathcal{L}\left(W,\, W + 2W_I\right) = \frac{\partial^2 \mu_1}{\partial z_2^2} + \frac{\partial^2 \mu_2}{\partial z_1^2} - \frac{\partial^2 \mu_3}{\partial z_1 \partial z_2}\end{aligned} \tag{124a}$$

where

$$\mathcal{D}_m(\mathcal{F}) \equiv \alpha_m^2\frac{\partial^4 \mathcal{F}}{\partial z_1^4} + 2\alpha_m\gamma_m\frac{\partial^4 \mathcal{F}}{\partial z_1^3 \partial z_2} + 2\mu\frac{\partial^4 \mathcal{F}}{\partial z_1^2 \partial z_2^2} + 2\frac{\delta_m}{\alpha_m}\frac{\partial^4 \mathcal{F}}{\partial z_1 \partial z_2^3} + \frac{1}{\alpha_m^2}\frac{\partial^4 \mathcal{F}}{\partial z_2^4} \tag{124b}$$

Expressions for the tangential displacements U_1 and U_2 are obtained from the nondimensional strain-displacement relations, equations (46); that is

$$\frac{\partial U_1}{\partial z_1} = E_{11} - \sqrt{12}Z_1 W - \frac{1}{2}\left(\frac{\partial W}{\partial z_1}\right)^2 - \frac{\partial W}{\partial z_1}\frac{\partial W_I}{\partial z_1} \tag{125}$$

$$\frac{\partial U_2}{\partial z_2} = E_{22} - \sqrt{12} Z_2 W - \frac{1}{2}\left(\frac{\partial W}{\partial z_2}\right)^2 - \frac{\partial W}{\partial z_2}\frac{\partial W_I}{\partial z_2} \tag{126}$$

$$\frac{\partial U_1}{\partial z_2} + \frac{\partial U_2}{\partial z_1} = G_{12} - \frac{\partial W}{\partial z_1}\frac{\partial W}{\partial z_2} - \frac{\partial W_I}{\partial z_1}\frac{\partial W}{\partial z_2} - \frac{\partial W_I}{\partial z_2}\frac{\partial W}{\partial z_1} \tag{127}$$

Substituting equations (118) into these three expressions gives

$$\begin{aligned}\frac{\partial U_1}{\partial z_1} = \frac{1}{\alpha_m^2}\frac{\partial^2 \mathcal{F}}{\partial z_2^2} - \nu_m \frac{\partial^2 \mathcal{F}}{\partial z_1^2} + \frac{\delta_m}{\alpha_m}\frac{\partial^2 \mathcal{F}}{\partial z_1 \partial z_2} + \mathcal{B}_{11}\frac{\partial^2 W}{\partial z_1^2} + \mathcal{B}_{12}\frac{\partial^2 W}{\partial z_2^2} + 2\mathcal{B}_{16}\frac{\partial^2 W}{\partial z_1 \partial z_2} \\ - \mathcal{P}_1 - \sqrt{12} Z_1 W - \frac{1}{2}\left(\frac{\partial W}{\partial z_1}\right)^2 - \frac{\partial W}{\partial z_1}\frac{\partial W_I}{\partial z_1}\end{aligned} \tag{128}$$

$$\begin{aligned}\frac{\partial U_2}{\partial z_2} = -\nu_m \frac{\partial^2 \mathcal{F}}{\partial z_2^2} + \alpha_m^2 \frac{\partial^2 \mathcal{F}}{\partial z_1^2} + \alpha_m \gamma_m \frac{\partial^2 \mathcal{F}}{\partial z_1 \partial z_2} + \mathcal{B}_{21}\frac{\partial^2 W}{\partial z_1^2} + \mathcal{B}_{22}\frac{\partial^2 W}{\partial z_2^2} + 2\mathcal{B}_{26}\frac{\partial^2 W}{\partial z_1 \partial z_2} \\ - \mathcal{P}_2 - \sqrt{12} Z_2 W - \frac{1}{2}\left(\frac{\partial W}{\partial z_2}\right)^2 - \frac{\partial W}{\partial z_2}\frac{\partial W_I}{\partial z_2}\end{aligned} \tag{129}$$

$$\begin{aligned}\frac{\partial U_1}{\partial z_2} + \frac{\partial U_2}{\partial z_1} = -\frac{\delta_m}{\alpha_m}\frac{\partial^2 \mathcal{F}}{\partial z_2^2} - \alpha_m \gamma_m \frac{\partial^2 \mathcal{F}}{\partial z_1^2} - 2(\mu + \nu_m)\frac{\partial^2 \mathcal{F}}{\partial z_1 \partial z_2} + \mathcal{B}_{61}\frac{\partial^2 W}{\partial z_1^2} + \mathcal{B}_{62}\frac{\partial^2 W}{\partial z_2^2} \\ + 2\mathcal{B}_{66}\frac{\partial^2 W}{\partial z_1 \partial z_2} - \mathcal{P}_3 - \frac{\partial W}{\partial z_1}\frac{\partial W}{\partial z_2} - \frac{\partial W_I}{\partial z_1}\frac{\partial W}{\partial z_2} - \frac{\partial W_I}{\partial z_2}\frac{\partial W}{\partial z_1}\end{aligned} \tag{130}$$

The nondimensional tangential displacements are represented in terms of W and $\mathcal{F}$, to within a rigid-body motion, by the integrals of these three equations.

Next, the desired form of the boundary conditions are obtained by using equations (86) and (88) to express the nondimensional transverse shear stress resultants in terms of the nondimensional bending stress resultants, by using equations (115) to express the nondimensional membrane stress resultants in terms of $\mathcal{F}$, and by using equations (120) to express the nondimensional bending stress resultants in term of W and $\mathcal{F}$. On the edges given by $z_1 = a_1 / L_1$ and $z_1 = b_1 / L_1$, the boundary conditions given by equations (98) become

$$\frac{\partial^2 \mathcal{F}}{\partial z_2^2} = \pi^2 \overline{N}(z_2) + \pi^2 \left[\int \mathcal{G}_1 \, dz_1\right]_{z_1 = \text{constant}} \qquad \text{or} \qquad U_1 = \overline{\Delta}_1(z_2) \tag{131a}$$

$$-\frac{\partial^2 \mathcal{F}}{\partial z_1 \partial z_2} = \frac{\pi^2}{\alpha_b}\overline{S}(z_2) \qquad \text{or} \qquad U_2 = \overline{\Delta}_2(z_2) \tag{131b}$$

$$\mathcal{B}_{21}\frac{\partial^3\mathcal{F}}{\partial z_1^3}+\left(2\mathcal{B}_{26}-\mathcal{B}_{61}\right)\frac{\partial^3\mathcal{F}}{\partial z_1^2\partial z_2}+\left(\mathcal{B}_{11}-2\mathcal{B}_{66}\right)\frac{\partial^3\mathcal{F}}{\partial z_1\partial z_2^2}+2\mathcal{B}_{16}\frac{\partial^3\mathcal{F}}{\partial z_2^3}-\mathcal{A}_{11}\frac{\partial^3 W}{\partial z_1^3}-4\mathcal{A}_{16}\frac{\partial^3 W}{\partial z_1^2\partial z_2}$$
$$-\left(\mathcal{A}_{12}+4\mathcal{A}_{66}\right)\frac{\partial^3 W}{\partial z_1\partial z_2^2}-2\mathcal{A}_{26}\frac{\partial^3 W}{\partial z_2^3}+\left(\frac{\partial^2\mathcal{F}}{\partial z_2^2}-\pi^2\int g_1\,dz_1\right)\frac{\partial}{\partial z_1}\left(W+W_I\right)$$
$$-\frac{\partial^2\mathcal{F}}{\partial z_1\partial z_2}\frac{\partial}{\partial z_2}\left(W+W_I\right)=\overline{V}(z_2)+\frac{\partial m_1}{\partial z_1}+2\frac{\partial m_3}{\partial z_2}$$

$$\text{or}\qquad W=\overline{\Delta}_n(z_2) \tag{131c}$$

$$\mathcal{B}_{11}\frac{\partial^2\mathcal{F}}{\partial z_2^2}+\mathcal{B}_{21}\frac{\partial^2\mathcal{F}}{\partial z_1^2}-\mathcal{B}_{61}\frac{\partial^2\mathcal{F}}{\partial z_1\partial z_2}-\mathcal{A}_{11}\frac{\partial^2 W}{\partial z_1^2}-\mathcal{A}_{12}\frac{\partial^2 W}{\partial z_2^2}-2\mathcal{A}_{16}\frac{\partial^2 W}{\partial z_1\partial z_2}=\overline{M}(z_2)+m_1$$

$$\text{or}\qquad -\frac{\partial W}{\partial z_1}=\overline{\Phi}(z_2) \tag{131d}$$

On the edges given by $z_2 = a_2 / L_2$ and $z_2 = b_2 / L_2$, the boundary conditions given by equations (99) become

$$2\mathcal{B}_{26}\frac{\partial^3\mathcal{F}}{\partial z_1^3}+\left(\mathcal{B}_{22}-2\mathcal{B}_{66}\right)\frac{\partial^3\mathcal{F}}{\partial z_1^2\partial z_2}+\left(2\mathcal{B}_{16}-\mathcal{B}_{62}\right)\frac{\partial^3\mathcal{F}}{\partial z_1\partial z_2^2}+\mathcal{B}_{12}\frac{\partial^3\mathcal{F}}{\partial z_2^3}-2\mathcal{A}_{16}\frac{\partial^3 W}{\partial z_1^3}$$
$$-\left(\mathcal{A}_{12}+4\mathcal{A}_{66}\right)\frac{\partial^3 W}{\partial z_1^2\partial z_2}-4\mathcal{A}_{26}\frac{\partial^3 W}{\partial z_1\partial z_2^2}-\mathcal{A}_{22}\frac{\partial^3 W}{\partial z_2^3}+\left(\frac{\partial^2\mathcal{F}}{\partial z_1^2}-\pi^2\int g_2\,dz_2\right)\frac{\partial}{\partial z_2}\left(W+W_I\right)$$
$$-\frac{\partial^2\mathcal{F}}{\partial z_1\partial z_2}\frac{\partial}{\partial z_1}\left(W+W_I\right)=\overline{V}(z_1)+\frac{\partial m_2}{\partial z_2}+2\frac{\partial m_3}{\partial z_1}$$

$$\text{or}\qquad W=\overline{\Delta}_n(z_1) \tag{132c}$$

$$\mathcal{B}_{12}\frac{\partial^2\mathcal{F}}{\partial z_2^2}+\mathcal{B}_{22}\frac{\partial^2\mathcal{F}}{\partial z_1^2}-\mathcal{B}_{62}\frac{\partial^2\mathcal{F}}{\partial z_1\partial z_2}-\mathcal{A}_{12}\frac{\partial^2 W}{\partial z_1^2}-\mathcal{A}_{22}\frac{\partial^2 W}{\partial z_2^2}-2\mathcal{A}_{26}\frac{\partial^2 W}{\partial z_1\partial z_2}=\overline{M}(z_1)+m_2$$

$$\text{or}\qquad -\frac{\partial W}{\partial z_2}=\overline{\Phi}(z_1) \tag{132d}$$

Virtual Work in terms of W and $\mathcal{F}$

The virtual work statement given by equations (107) - (110) is expressed in terms of the stress function $\mathcal{F}$ and the displacement W by using equations (115) and the integration-by-parts

formulas, equations (25), specialized for the nondimensional coordinates (z_1, z_2). In particular, applying equations (25) to the terms $\pi^2 \mathcal{N}_{11} \dfrac{\partial \delta U_1}{\partial z_1}$, $\pi^2 \mathcal{N}_{22} \dfrac{\partial \delta U_2}{\partial z_2}$, and $\dfrac{\pi^2}{\alpha_b} \mathcal{N}_{12} \left(\dfrac{\partial \delta U_1}{\partial z_2} + \dfrac{\partial \delta U_2}{\partial z_1} \right)$ appearing in $\pi^2 \mathcal{N}_{11} \delta E_{11}$, $\pi^2 \mathcal{N}_{22} \delta E_{22}$, and $\dfrac{\pi^2}{\alpha_b} \mathcal{N}_{12} \delta G_{12}$, respectively, and using equations (81), (83), and (108) yield the variational statement

$$\int\int_{\mathcal{A}} \left\{ \left[\mathcal{G}_3 - \pi^2 \sqrt{12} \left\lfloor Z_1 \; Z_2 \; 0 \right\rfloor \{\mathcal{N}\} \right] \delta W - \{\mathcal{M}\}^T \{\delta \mathcal{K}\} \right. \\ \left. - \pi^2 \left[\{\Omega\} + \{\Omega_I\} \right]^T [\mathcal{N}] \{\delta \Omega\} \right\} dz_1 dz_2 + \mathcal{I}_1^B + \mathcal{I}_2^B = 0 \tag{133}$$

where

$$\mathcal{I}_1^B = \int_{\frac{a_2}{L_2}}^{\frac{b_2}{L_2}} \left\{ \pi^2 \left[\bar{N}(z_2) - \mathcal{N}_{11} \right] \delta U_1 + \frac{\pi^2}{\alpha_b} \left[\bar{S}(z_2) - \mathcal{N}_{12} \right] \delta U_2 + \bar{V}(z_2) \, \delta W - \bar{M}(z_2) \frac{\partial \delta W}{\partial z_1} \right\}_{\frac{a_1}{L_1}}^{\frac{b_1}{L_1}} dz_2 \tag{134a}$$

$$\mathcal{I}_2^B = \int_{\frac{a_1}{L_1}}^{\frac{b_1}{L_1}} \left\{ \frac{\pi^2}{\alpha_b} \left[\bar{S}(z_1) - \mathcal{N}_{12} \right] \delta U_1 + \pi^2 \left[\bar{N}(z_1) - \mathcal{N}_{22} \right] \delta U_2 + \bar{V}(z_1) \, \delta W - \bar{M}(z_1) \frac{\partial \delta W}{\partial z_2} \right\}_{\frac{a_2}{L_2}}^{\frac{b_2}{L_2}} dz_1 \tag{134b}$$

where the subscripts and superscripts on the braces indicate the integrand evaluated at the upper limit minus the integrand evaluated at the lower limit, and where

$$\{\mathcal{N}\}^T = \left\lfloor \mathcal{N}_{11} \;\; \mathcal{N}_{22} \;\; \frac{\mathcal{N}_{12}}{\alpha_b} \right\rfloor \tag{135a}$$

$$\{\mathcal{M}\}^T = \left\lfloor \mathcal{M}_{11} \;\; \mathcal{M}_{22} \;\; \mathcal{M}_{12} \right\rfloor \tag{135b}$$

$$[\mathcal{N}] = \begin{bmatrix} \mathcal{N}_{11} & \dfrac{\mathcal{N}_{12}}{\alpha_b} \\ \dfrac{\mathcal{N}_{12}}{\alpha_b} & \mathcal{N}_{22} \end{bmatrix} \tag{135c}$$

$$\{\Omega\}^T = \begin{bmatrix} -\dfrac{\partial W}{\partial z_1} & -\dfrac{\partial W}{\partial z_2} \end{bmatrix} \tag{136a}$$

$$\{\Omega_I\}^T = \begin{bmatrix} -\dfrac{\partial W_I}{\partial z_1} & -\dfrac{\partial W_I}{\partial z_2} \end{bmatrix} \tag{136b}$$

$$\{\delta\Omega\}^T = \begin{bmatrix} -\dfrac{\partial \delta W}{\partial z_1} & -\dfrac{\partial \delta W}{\partial z_2} \end{bmatrix} \tag{136c}$$

$$\{\delta\mathcal{K}\}^T = \begin{bmatrix} -\dfrac{\partial^2 \delta W}{\partial z_1^2} & -\dfrac{\partial^2 \delta W}{\partial z_2^2} & -2\dfrac{\partial^2 \delta W}{\partial z_1 \partial z_2} \end{bmatrix} \tag{136d}$$

In particular, the last term of the integrand in equation (133) becomes

$$\begin{aligned} \pi^2\left[\{\Omega\} + \{\Omega_I\}\right]^T[\mathcal{N}]\{\delta\Omega\} = &\left[\pi^2\mathcal{N}_{11}\frac{\partial}{\partial z_1}\left(W + W_I\right) + \frac{\pi^2}{\alpha_b}\mathcal{N}_{12}\frac{\partial}{\partial z_2}\left(W + W_I\right)\right]\frac{\partial \delta W}{\partial z_1} + \\ &\left[\frac{\pi^2}{\alpha_b}\mathcal{N}_{12}\frac{\partial}{\partial z_1}\left(W + W_I\right) + \pi^2\mathcal{N}_{22}\frac{\partial}{\partial z_2}\left(W + W_I\right)\right]\frac{\partial \delta W}{\partial z_2} \end{aligned} \tag{136e}$$

Typically, the stress function is selected to satisfy the tangential boundary conditions and, as a result, the boundary integrals reduce to

$$\mathcal{I}_1^B = \int_{\frac{a_2}{L_2}}^{\frac{b_2}{L_2}} \left\{ \overline{V}(z_2)\,\delta W - \overline{M}(z_2)\frac{\partial \delta W}{\partial z_1} \right\}_{\frac{a_1}{L_1}}^{\frac{b_1}{L_1}} dz_2 \tag{137a}$$

$$\mathcal{I}_2^B = \int_{\frac{a_1}{L_1}}^{\frac{b_1}{L_1}} \left\{ \overline{V}(z_1)\,\delta W - \overline{M}(z_1)\,\frac{\partial \delta W}{\partial z_2} \right\}_{\frac{a_2}{L_2}}^{\frac{b_2}{L_2}} dz_1 \tag{137b}$$

for that special case. Next, it is convenient to express equation (120) as

$$\{\mathcal{M}\} = [\mathcal{B}]^T \{\partial \mathcal{F}\} + [\mathcal{A}]\{\mathcal{K}\} - \{\mathcal{M}\} \tag{138}$$

where

$$\{\mathcal{K}\}^T = \left[-\frac{\partial^2 W}{\partial z_1^2} \quad -\frac{\partial^2 W}{\partial z_2^2} \quad -2\,\frac{\partial^2 W}{\partial z_1 \partial z_2} \right] \tag{139a}$$

$$[\mathcal{B}] = \begin{bmatrix} \mathcal{B}_{11} & \mathcal{B}_{12} & \mathcal{B}_{16} \\ \mathcal{B}_{21} & \mathcal{B}_{22} & \mathcal{B}_{26} \\ \mathcal{B}_{61} & \mathcal{B}_{62} & \mathcal{B}_{66} \end{bmatrix} \tag{139b}$$

$$[\mathcal{A}] = \begin{bmatrix} \mathcal{A}_{11} & \mathcal{A}_{12} & \mathcal{A}_{16} \\ \mathcal{A}_{12} & \mathcal{A}_{22} & \mathcal{A}_{26} \\ \mathcal{A}_{16} & \mathcal{A}_{26} & \mathcal{A}_{66} \end{bmatrix} \tag{139c}$$

$$\{\mathcal{M}\}^T = \begin{bmatrix} \mathcal{M}_1 & \mathcal{M}_2 & \mathcal{M}_3 \end{bmatrix} \tag{139d}$$

$$\{\partial \mathcal{F}\}^T = \left[\frac{\partial^2 \mathcal{F}}{\partial z_2^2} \quad \frac{\partial^2 \mathcal{F}}{\partial z_1^2} \quad -\frac{\partial^2 \mathcal{F}}{\partial z_1 \partial z_2} \right] \tag{139e}$$

By using these equations, and noting that equations (115) give

$$\pi^2 \{\mathcal{N}\} = \{\partial \mathcal{F}\} - \pi^2 \{\tilde{\mathcal{G}}\} \tag{140a}$$

with

$$\{\tilde{\mathcal{G}}\}^T = \left[\int \mathcal{G}_1\, dz_1 \quad \int \mathcal{G}_2\, dz_2 \quad 0 \right] \tag{140b}$$

equation (133) is expressed as

$$\iint_{\mathcal{A}} \left\{ \left[\mathcal{g}_3 - \sqrt{12} \left| \mathrm{Z}_1 \, \mathrm{Z}_2 \;\; 0 \right| \left\{ \left\{ \partial \mathcal{F} \right\} - \pi^2 \left\{ \tilde{\mathcal{g}} \right\} \right\} \right] \delta \mathrm{W} - \left\{ \left\{ \partial \mathcal{F} \right\}^{\mathrm{T}} \left[\mathcal{B} \right] + \left\{ \mathcal{K} \right\}^{\mathrm{T}} \left[\mathcal{d} \right] - \left\{ \mathcal{m} \right\}^{\mathrm{T}} \right\} \left\{ \delta \mathcal{K} \right\} \right.$$
$$\left. - \left[\left\{ \Omega \right\} + \left\{ \Omega_{\mathrm{I}} \right\} \right]^{\mathrm{T}} \left[\left[\partial \mathcal{F} \right] - \pi^2 \left[\tilde{\mathcal{g}} \right] \right] \left\{ \delta \Omega \right\} \right\} \mathrm{dz}_1 \mathrm{dz}_2 + \mathcal{V}_1^{\mathrm{B}} + \mathcal{V}_2^{\mathrm{B}} = 0 \tag{141}$$

where

$$\left[\partial \mathcal{F} \right] \equiv \begin{bmatrix} \dfrac{\partial^2 \mathcal{F}}{\partial \mathrm{z}_2^2} & -\dfrac{\partial^2 \mathcal{F}}{\partial \mathrm{z}_1 \partial \mathrm{z}_2} \\ -\dfrac{\partial^2 \mathcal{F}}{\partial \mathrm{z}_1 \partial \mathrm{z}_2} & \dfrac{\partial^2 \mathcal{F}}{\partial \mathrm{z}_1^2} \end{bmatrix} \tag{142a}$$

$$\left[\tilde{\mathcal{g}} \right] \equiv \begin{bmatrix} \displaystyle\int \mathcal{g}_1 \, \mathrm{dz}_1 & 0 \\ 0 & \displaystyle\int \mathcal{g}_2 \, \mathrm{dz}_2 \end{bmatrix} \tag{142b}$$

Equations (141) and (137) constitute the virtual work in terms of the two unknowns, the stress function $\mathcal{F}$ and the displacement W, and can be used as an alternative to equilibrium equation (122a).

Complementary Virtual Work in terms of W and $\mathcal{F}$

The complementary virtual work is obtained by considering the work of incompatible tangential strains and violated kinematic boundary conditions generated when the shell is subjected to statically admissible internal stresses. The statically admissible stress resultants are denoted by $\pi^2 \delta \mathcal{N}^*_{11}$, $\pi^2 \delta \mathcal{N}^*_{22}$, and $\dfrac{\pi^2}{\alpha_{\mathrm{b}}} \delta \mathcal{N}^*_{12}$; and as a result satisfy the equilibrium equations

$$\frac{\partial \delta \mathcal{N}^*_{11}}{\partial \mathrm{z}_1} + \frac{1}{\alpha_{\mathrm{b}}} \frac{\partial \delta \mathcal{N}^*_{12}}{\partial \mathrm{z}_2} = 0 \tag{143a}$$

$$\frac{1}{\alpha_{\mathrm{b}}} \frac{\partial \delta \mathcal{N}^*_{12}}{\partial \mathrm{z}_1} + \frac{\partial \delta \mathcal{N}^*_{22}}{\partial \mathrm{z}_2} = 0 \tag{143b}$$

the boundary conditions

$$\delta \mathcal{N}^*_{11} = 0 \tag{144a}$$

$$\delta\mathcal{N}^*_{12} = 0 \tag{144b}$$

on the edges given by $z_1 = a_1 / L_1$ and $z_1 = b_1 / L_1$, and the boundary conditions

$$\delta\mathcal{N}^*_{12} = 0 \tag{145a}$$

$$\delta\mathcal{N}^*_{22} = 0 \tag{145b}$$

the edges given by $z_2 = a_2 / L_2$ and $z_2 = b_2 / L_2$. For this case, the nondimensional form of the principle of complementary virtual work is stated as

$$\int\int_{\mathcal{A}} \delta\mathcal{W}^*_{\text{int}} dz_1 dz_2 + \delta\mathcal{W}^{*\,\text{B}} = 0 \tag{146}$$

where

$$\begin{aligned}\delta\mathcal{W}^*_{\text{int}} = &\left[E_{11} - \frac{\partial U_1}{\partial z_1} - \sqrt{12} Z_1 W - \frac{1}{2}\left(\frac{\partial W}{\partial z_1}\right)^2 - \frac{\partial W}{\partial z_1}\frac{\partial W_I}{\partial z_1}\right]\pi^2 \delta\mathcal{N}^*_{11} \\ &+ \left[E_{22} - \frac{\partial U_2}{\partial z_2} - \sqrt{12} Z_2 W - \frac{1}{2}\left(\frac{\partial W}{\partial z_2}\right)^2 - \frac{\partial W}{\partial z_2}\frac{\partial W_I}{\partial z_2}\right]\pi^2 \delta\mathcal{N}^*_{22} \\ &+ \left[G_{12} - \frac{\partial U_1}{\partial z_2} - \frac{\partial U_2}{\partial z_1} - \frac{\partial W}{\partial z_1}\frac{\partial W}{\partial z_2} - \frac{\partial W_I}{\partial z_1}\frac{\partial W}{\partial z_2} - \frac{\partial W_I}{\partial z_2}\frac{\partial W}{\partial z_1}\right]\frac{\pi^2}{\alpha_b}\,\delta\mathcal{N}^*_{12}\end{aligned} \tag{147a}$$

and

$$\begin{aligned}\delta\mathcal{W}^{*\,\text{B}} = &\int_{\frac{a_1}{L_1}}^{\frac{b_1}{L_1}} \left\{\left[U_1 - \bar{\Delta}_1(z_1)\right]\frac{\pi^2}{\alpha_b}\,\delta\mathcal{N}^*_{12} + \left[U_2 - \bar{\Delta}_2(z_1)\right]\pi^2 \delta\mathcal{N}^*_{22}\right\}_{\frac{a_2}{L_2}}^{\frac{b_2}{L_2}} dz_1 \\ &+ \int_{\frac{a_2}{L_2}}^{\frac{b_2}{L_2}} \left\{\left[U_1 - \bar{\Delta}_1(z_2)\right]\pi^2 \delta\mathcal{N}^*_{11} + \left[U_2 - \bar{\Delta}_2(z_2)\right]\frac{\pi^2}{\alpha_b}\delta\mathcal{N}^*_{12}\right\}_{\frac{a_1}{L_1}}^{\frac{b_1}{L_1}} dz_2\end{aligned} \tag{147b}$$

Using the integration-by-parts formulas, specialized for the nondimensional coordinates (z_1, z_2), to eliminate the derivatives of the tangential displacements and enforcing equations (143), equation (146) is transformed into

$$\int\int_{\mathcal{A}} \delta\tilde{\mathcal{W}}^*_{\text{int}} dz_1 dz_2 - \delta\tilde{\mathcal{W}}^{*\,B} = 0 \tag{148}$$

where

$$\begin{aligned}\delta\tilde{\mathcal{W}}^*_{\text{int}} = &\left[E_{11} - \sqrt{12}Z_1 W - \frac{1}{2}\left(\frac{\partial W}{\partial z_1}\right)^2 - \frac{\partial W}{\partial z_1}\frac{\partial W_I}{\partial z_1}\right]\pi^2\delta\mathcal{N}^*_{11} \\ &+ \left[E_{22} - \sqrt{12}Z_2 W - \frac{1}{2}\left(\frac{\partial W}{\partial z_2}\right)^2 - \frac{\partial W}{\partial z_2}\frac{\partial W_I}{\partial z_2}\right]\pi^2\delta\mathcal{N}^*_{22} \\ &+ \left[G_{12} - \frac{\partial W}{\partial z_1}\frac{\partial W}{\partial z_2} - \frac{\partial W_I}{\partial z_1}\frac{\partial W}{\partial z_2} - \frac{\partial W_I}{\partial z_2}\frac{\partial W}{\partial z_1}\right]\frac{\pi^2}{\alpha_b}\delta\mathcal{N}^*_{12}\end{aligned} \tag{149a}$$

and

$$\begin{aligned}\delta\tilde{\mathcal{W}}^{*\,B} = &\int_{\frac{a_1}{L_1}}^{\frac{b_1}{L_1}} \left\{\left[\bar{\Delta}_1(z_1)\right]\frac{\pi^2}{\alpha_b}\delta\mathcal{N}^*_{12} + \left[\bar{\Delta}_2(z_1)\right]\pi^2\delta\mathcal{N}^*_{22}\right\}_{\frac{a_2}{L_2}}^{\frac{b_2}{L_2}} dz_1 \\ &+ \int_{\frac{a_2}{L_2}}^{\frac{b_2}{L_2}} \left\{\left[\bar{\Delta}_1(z_2)\right]\pi^2\delta\mathcal{N}^*_{11} + \left[\bar{\Delta}_2(z_2)\right]\frac{\pi^2}{\alpha_b}\delta\mathcal{N}^*_{12}\right\}_{\frac{a_1}{L_1}}^{\frac{b_1}{L_1}} dz_2\end{aligned} \tag{149b}$$

It is important to note that when only traction boundary conditions are specified, $\delta\tilde{\mathcal{W}}^{*\,B}$ vanishes. Next, a virtual stress function is defined such that equations (143) are satisfied identically; that is,

$$\pi^2\delta\mathcal{N}^*_{11} = \frac{\partial^2\delta\mathcal{F}}{\partial z_2^2} \tag{150a}$$

$$\pi^2\delta\mathcal{N}^*_{22} = \frac{\partial^2\delta\mathcal{F}}{\partial z_1^2} \tag{150b}$$

$$\frac{\pi^2}{\alpha_b}\delta\mathcal{N}^*_{12} = -\frac{\partial^2\delta\mathcal{F}}{\partial z_1 \partial z_2} \tag{150c}$$

Substituting equations (150) into equation (149a) gives

$$\delta\tilde{\mathcal{W}}^{*}_{\text{int}} = \left(\left\{ E \right\}^{T} - \sqrt{12} W \left[Z_1 \;\; Z_2 \;\; 0 \right] - \frac{1}{2} \left\{ \Omega \right\}^{T} \left(\left[\Omega \right] - 2 \left[\Omega_I \right] \right) \right) \left\{ \partial \delta \mathcal{F} \right\} \tag{151a}$$

where

$$\left\{ E \right\}^{T} = \left[E_{11} \;\; E_{22} \;\; G_{12} \right] \tag{151b}$$

$$\left[\Omega \right] \equiv \begin{bmatrix} -\dfrac{\partial W}{\partial z_1} & 0 & -\dfrac{\partial W}{\partial z_2} \\ 0 & -\dfrac{\partial W}{\partial z_2} & -\dfrac{\partial W}{\partial z_1} \end{bmatrix} \tag{151c}$$

$$\left[\Omega_I \right] \equiv \begin{bmatrix} -\dfrac{\partial W_I}{\partial z_1} & 0 & -\dfrac{\partial W_I}{\partial z_2} \\ 0 & -\dfrac{\partial W_I}{\partial z_2} & -\dfrac{\partial W_I}{\partial z_1} \end{bmatrix} \tag{151d}$$

$$\left\{ \partial \delta \mathcal{F} \right\}^{T} = \left[\frac{\partial^2 \delta \mathcal{F}}{\partial z_2^2} \;\; \frac{\partial^2 \delta \mathcal{F}}{\partial z_1^2} \;\; -\frac{\partial^2 \delta \mathcal{F}}{\partial z_1 \partial z_2} \right] \tag{151e}$$

and where $\left\{ \Omega \right\}$ is defined by equation (136a). Likewise, equation (149b) becomes

$$\begin{aligned} \delta\tilde{\mathcal{W}}^{*\,B} = & \int_{\frac{a_1}{L_1}}^{\frac{b_1}{L_1}} \left\{ \left[\bar{\Delta}_2(z_1) \right] \frac{\partial^2 \delta \mathcal{F}}{\partial z_1^2} - \left[\bar{\Delta}_1(z_1) \right] \frac{\partial^2 \delta \mathcal{F}}{\partial z_1 \partial z_2} \right\}_{\frac{a_2}{L_2}}^{\frac{b_2}{L_2}} dz_1 \\ & + \int_{\frac{a_2}{L_2}}^{\frac{b_2}{L_2}} \left\{ \left[\bar{\Delta}_1(z_2) \right] \frac{\partial^2 \delta \mathcal{F}}{\partial z_2^2} - \left[\bar{\Delta}_2(z_2) \right] \frac{\partial^2 \delta \mathcal{F}}{\partial z_1 \partial z_2} \right\}_{\frac{a_1}{L_1}}^{\frac{b_1}{L_1}} dz_2 \end{aligned} \tag{152}$$

Next, equation (118) is expressed as

$$\{E\} = \left[\mathcal{a}\right]\{\partial\mathcal{F}\} - \left[\mathcal{B}\right]\{\mathcal{K}\} - \left\{\mathcal{p}\right\} \tag{153}$$

where

$$\left[\mathcal{a}\right] \equiv \begin{bmatrix} \frac{1}{\alpha_m^2} & -\nu_m & -\frac{\delta_m}{\alpha_m} \\ -\nu_m & \alpha_m^2 & -\alpha_m\gamma_m \\ -\frac{\delta_m}{\alpha_m} & -\alpha_m\gamma_m & 2(\mu+\nu_m) \end{bmatrix} \tag{154a}$$

$$\left\{\mathcal{p}\right\}^T = \left[\mathcal{p}_1 \quad \mathcal{p}_2 \quad \mathcal{p}_3\right] \tag{154b}$$

and where $[\mathcal{B}]$, $\{\partial\mathcal{F}\}$, and $\{\mathcal{K}\}$ are defined by equations (139). Substituting equation (153) into equation (151a) gives the desired variational principle

$$\delta\tilde{\mathcal{W}}^*_{int} = \left(\left\{\partial\mathcal{F}\right\}^T\left[\mathcal{a}\right] - \left\{\mathcal{K}\right\}^T\left[\mathcal{B}\right]^T - \left\{\mathcal{p}\right\}^T - \sqrt{12}W\left[Z_1 \;\; Z_2 \;\; 0\right] - \frac{1}{2}\left\{\Omega\right\}^T\left(\left[\,\Omega\,\right] - 2\left[\,\Omega_I\,\right]\right)\right)\left\{\partial\delta\mathcal{F}\right\} \tag{155}$$

Equations (148), (152), and (155) constitute the principle of complementary virtual work for the stress-function formulation. Further integration by parts of equations (148) and (149), with the virtual stress resultants given by equations (150), yields

$$\begin{aligned} &\int\int_{\mathcal{A}} \left[\frac{\partial^2 E_{22}}{\partial z_1^2} + \frac{\partial^2 E_{11}}{\partial z_2^2} - \frac{\partial^2 G_{12}}{\partial z_1 \partial z_2} - \sqrt{12}\mathcal{D}_c(W) + \frac{1}{2}\mathcal{L}(W, W + 2W_I) \right] \delta\mathcal{F}\, dz_1 dz_2 + \\ &+ \int_{\frac{a_2}{L_2}}^{\frac{b_2}{L_2}} \left\{ -\bar{\Delta}_1(z_2)\frac{\partial^2\delta\mathcal{F}}{\partial z_2^2} + \bar{\Delta}_2(z_2)\frac{\partial^2\delta\mathcal{F}}{\partial z_1 \partial z_2} + S_{22}\frac{\partial\delta\mathcal{F}}{\partial z_1} - \frac{1}{2}S_{12}\frac{\partial\delta\mathcal{F}}{\partial z_2} + \left(\frac{1}{2}\frac{\partial S_{12}}{\partial z_2} - \frac{\partial S_{22}}{\partial z_1}\right)\delta\mathcal{F} \right\}_{\frac{a_1}{L_1}}^{\frac{b_1}{L_1}} dz_2 \\ &+ \int_{\frac{a_1}{L_1}}^{\frac{b_1}{L_1}} \left\{ -\bar{\Delta}_2(z_1)\frac{\partial^2\delta\mathcal{F}}{\partial z_1^2} + \bar{\Delta}_1(z_1)\frac{\partial^2\delta\mathcal{F}}{\partial z_1 \partial z_2} + S_{11}\frac{\partial\delta\mathcal{F}}{\partial z_2} - \frac{1}{2}S_{12}\frac{\partial\delta\mathcal{F}}{\partial z_1} + \left(\frac{1}{2}\frac{\partial S_{12}}{\partial z_1} - \frac{\partial S_{11}}{\partial z_2}\right)\delta\mathcal{F} \right\}_{\frac{a_2}{L_2}}^{\frac{b_2}{L_2}} dz_1 = 0 \end{aligned} \tag{156}$$

where

$$S_{11} = E_{11} - \sqrt{12} Z_1 W - \frac{1}{2}\left(\frac{\partial W}{\partial z_1}\right)^2 - \frac{\partial W}{\partial z_1}\frac{\partial W_I}{\partial z_1} \tag{157a}$$

$$S_{22} = E_{22} - \sqrt{12} Z_2 W - \frac{1}{2}\left(\frac{\partial W}{\partial z_2}\right)^2 - \frac{\partial W}{\partial z_2}\frac{\partial W_I}{\partial z_2} \tag{157b}$$

$$S_{12} = G_{12} - \frac{\partial W}{\partial z_1}\frac{\partial W}{\partial z_2} - \frac{\partial W_I}{\partial z_1}\frac{\partial W}{\partial z_2} - \frac{\partial W_I}{\partial z_2}\frac{\partial W}{\partial z_1} \tag{157c}$$

and the integrand of the double integral is the nondimensional compatibility equation given by equations (123) and (122c). When only traction boundary conditions are applied to the shell, equations (144) and (145) must be satisfied by $\delta\mathcal{F}$. This task is done by noting that only the second derivatives of $\delta\mathcal{F}$ are required to be unique in order to obtain unique stress resultants. Thus, it is convenient to enforce $\delta\mathcal{F} = 0$ on the shell boundary, to require $\frac{\partial \delta\mathcal{F}}{\partial z_1} = 0$ on the edges $z_1 = a_1 / L_1$ and $z_1 = b_1 / L_1$, and to require $\frac{\partial \delta\mathcal{F}}{\partial z_2} = 0$ on the edges $z_2 = a_2 / L_2$ and $z_2 = b_2 / L_2$. For these choices, equation (156) reduces to

$$\int\int_{\mathcal{A}} \left[\frac{\partial^2 E_{22}}{\partial z_1^2} + \frac{\partial^2 E_{11}}{\partial z_2^2} - \frac{\partial^2 G_{12}}{\partial z_1 \partial z_2} - \sqrt{12}\,\mathcal{D}_c(W) + \frac{1}{2}\mathcal{L}\left(W, W + 2W_I\right) \right] \delta\mathcal{F}\, dz_1 dz_2 = 0 \tag{158}$$

For the case of displacement boundary conditions, the boundary integrals in equation (156) can be converted, by further integration by parts, into expressions that require satisfaction of the tangential-strain-displacement relations and continuity of the displacements and their derivatives on the boundary when the *Fundamental Lemma of the Calculus of Variations* is enforced.

Equations for Special Cases

Significant simplification of the equations for stress-function formulation can be obtained for several cases of practical importance. For example, when the tangential surface tractions q_1 and q_2 are negligible, the transverse equilibrium equation given by equation (122a) reduces to

$$\mathcal{D}_b(W) + \sqrt{12}\,\mathcal{D}_c(\mathcal{F}) - \mathcal{D}_\varepsilon(\mathcal{F}) = \mathcal{L}\left(\mathcal{F}, W + W_I\right) + \mathcal{G}_3 \tag{159}$$

and the compatibility equation given by equation (124a) reduces to

$$\mathcal{D}_m(\mathcal{F}) + \mathcal{D}_\varepsilon(W) - \sqrt{12}\,\mathcal{D}_c(W) = \frac{1}{2}\mathcal{L}\left(W, W + 2W_I\right) \tag{160}$$

Likewise, the boundary conditions on the edges $z_1 = a_1 / L_1$ and $z_1 = b_1 / L_1$, given by equations (131), reduce to

$$\frac{\partial^2 \mathcal{F}}{\partial z_2^2} = \pi^2 \overline{N}(z_2) \qquad \text{or} \qquad U_1 = \overline{\Delta}_1(z_2) \tag{161a}$$

$$-\frac{\partial^2 \mathcal{F}}{\partial z_1 \partial z_2} = \frac{\pi^2}{\alpha_b} \overline{S}(z_2) \qquad \text{or} \qquad U_2 = \overline{\Delta}_2(z_2) \tag{161b}$$

$$\begin{aligned} \mathcal{B}_{21} \frac{\partial^3 \mathcal{F}}{\partial z_1^3} + \left(2\mathcal{B}_{26} - \mathcal{B}_{61}\right) \frac{\partial^3 \mathcal{F}}{\partial z_1^2 \partial z_2} + \left(\mathcal{B}_{11} - 2\mathcal{B}_{66}\right) \frac{\partial^3 \mathcal{F}}{\partial z_1 \partial z_2^2} + 2\mathcal{B}_{16} \frac{\partial^3 \mathcal{F}}{\partial z_2^3} - \mathcal{A}_{11} \frac{\partial^3 W}{\partial z_1^3} - 4\mathcal{A}_{16} \frac{\partial^3 W}{\partial z_1^2 \partial z_2} \\ - \left(\mathcal{A}_{12} + 4\mathcal{A}_{66}\right) \frac{\partial^3 W}{\partial z_1 \partial z_2^2} - 2\mathcal{A}_{26} \frac{\partial^3 W}{\partial z_2^3} + \frac{\partial^2 \mathcal{F}}{\partial z_2^2} \frac{\partial}{\partial z_1}\left(W + W_I\right) \\ - \frac{\partial^2 \mathcal{F}}{\partial z_1 \partial z_2} \frac{\partial}{\partial z_2}\left(W + W_I\right) = \overline{V}(z_2) \end{aligned}$$

$$\text{or} \qquad W = \overline{\Delta}_n(z_2) \tag{161c}$$

$$\mathcal{B}_{11} \frac{\partial^2 \mathcal{F}}{\partial z_2^2} + \mathcal{B}_{21} \frac{\partial^2 \mathcal{F}}{\partial z_1^2} - \mathcal{B}_{61} \frac{\partial^2 \mathcal{F}}{\partial z_1 \partial z_2} - \mathcal{A}_{11} \frac{\partial^2 W}{\partial z_1^2} - \mathcal{A}_{12} \frac{\partial^2 W}{\partial z_2^2} - 2\mathcal{A}_{16} \frac{\partial^2 W}{\partial z_1 \partial z_2} = \overline{M}(z_2)$$

$$\text{or} \qquad -\frac{\partial W}{\partial z_1} = \overline{\Phi}(z_2) \tag{161d}$$

On the edges $z_2 = a_2 / L_2$ and $z_2 = b_2 / L_2$, given by equations (132), reduce to

$$\frac{\partial^2 \mathcal{F}}{\partial z_1^2} = \pi^2 \overline{N}(z_1) \qquad \text{or} \qquad U_2 = \overline{\Delta}_2(z_1) \tag{162a}$$

$$-\frac{\partial^2 \mathcal{F}}{\partial z_1 \partial z_2} = \frac{\pi^2}{\alpha_b} \overline{S}(z_1) \qquad \text{or} \qquad U_1 = \overline{\Delta}_1(z_1) \tag{162b}$$

$$\begin{aligned} 2\mathcal{B}_{26} \frac{\partial^3 \mathcal{F}}{\partial z_1^3} + \left(\mathcal{B}_{22} - 2\mathcal{B}_{66}\right) \frac{\partial^3 \mathcal{F}}{\partial z_1^2 \partial z_2} + \left(2\mathcal{B}_{16} - \mathcal{B}_{62}\right) \frac{\partial^3 \mathcal{F}}{\partial z_1 \partial z_2^2} + \mathcal{B}_{12} \frac{\partial^3 \mathcal{F}}{\partial z_2^3} - 2\mathcal{A}_{16} \frac{\partial^3 W}{\partial z_1^3} \\ - \left(\mathcal{A}_{12} + 4\mathcal{A}_{66}\right) \frac{\partial^3 W}{\partial z_1^2 \partial z_2} - 4\mathcal{A}_{26} \frac{\partial^3 W}{\partial z_1 \partial z_2^2} - \mathcal{A}_{22} \frac{\partial^3 W}{\partial z_2^3} + \frac{\partial^2 \mathcal{F}}{\partial z_1^2} \frac{\partial}{\partial z_2}\left(W + W_I\right) \\ - \frac{\partial^2 \mathcal{F}}{\partial z_1 \partial z_2} \frac{\partial}{\partial z_1}\left(W + W_I\right) = \overline{V}(z_1) \end{aligned}$$

$$\text{or} \qquad W = \overline{\Delta}_n(z_1) \tag{162c}$$

$$\mathcal{B}_{12}\frac{\partial^2\mathcal{F}}{\partial z_2^2}+\mathcal{B}_{22}\frac{\partial^2\mathcal{F}}{\partial z_1^2}-\mathcal{B}_{62}\frac{\partial^2\mathcal{F}}{\partial z_1\partial z_2}-\mathcal{A}_{12}\frac{\partial^2 W}{\partial z_1^2}-\mathcal{A}_{22}\frac{\partial^2 W}{\partial z_2^2}-2\mathcal{A}_{26}\frac{\partial^2 W}{\partial z_1\partial z_2}=\overline{M}(z_1)$$

$$\text{or}\quad -\frac{\partial W}{\partial z_2}=\overline{\Phi}(z_1) \tag{162d}$$

where the tangential displacements are obtained from equations (128)-(130) with $\mathcal{P}_1=\mathcal{P}_2=\mathcal{P}_3=0$. For this special case, with $q_1 = q_2 = 0$, the virtual work given by equation (141) reduces to

$$\int\!\!\int_{\mathcal{A}}\left\{\left[\mathcal{P}_3-\sqrt{12}\left[\,Z_1\;Z_2\;0\,\right]\left\{\partial\mathcal{F}\right\}\right]\delta W-\left\{\left\{\partial\mathcal{F}\right\}^T\left[\mathcal{B}\right]+\left\{\mathcal{K}\right\}^T\left[\mathcal{A}\right]\right\}\left\{\delta\mathcal{K}\right\}\right.$$
$$\left.-\left[\left\{\Omega\right\}+\left\{\Omega_I\right\}\right]^T\left[\partial\mathcal{F}\right]\left\{\delta\Omega\right\}\right\}dz_1dz_2+\mathcal{I}_1^B+\mathcal{I}_2^B=0 \tag{163}$$

and the complementary virtual work term given by equation (155) becomes

$$\delta\tilde{\mathcal{W}}^*_{\text{int}}=\left(\left\{\partial\mathcal{F}\right\}^T\left[\mathcal{A}\right]-\left\{\mathcal{K}\right\}^T\left[\mathcal{B}\right]^T-\sqrt{12}\,W\left[Z_1\;Z_2\;0\right]-\frac{1}{2}\left\{\Omega\right\}^T\left(\left[\,\Omega\,\right]-2\left[\,\Omega_I\,\right]\right)\right)\left\{\partial\delta\mathcal{F}\right\} \tag{164}$$

When the tangential surface tractions q_1 and q_2 are negligible and the shell is symmetrically laminated, the transverse equilibrium equation given by equation (159) reduces to

$$\mathcal{D}_b(W)+\sqrt{12}\,\mathcal{D}_c(\mathcal{F})=\mathcal{L}\left(\mathcal{F},\,W+W_I\right)+\mathcal{P}_3 \tag{165}$$

and the compatibility equation given by equation (160) reduces to

$$\mathcal{D}_m(\mathcal{F})-\sqrt{12}\,\mathcal{D}_c(W)+\frac{1}{2}\mathcal{L}\left(W,\,W+2W_I\right)=0 \tag{166}$$

with the additional simplification

$$\mathcal{D}_b(W)=\alpha_b^2\frac{\partial^4 W}{\partial z_1^4}+4\alpha_b\gamma_b\frac{\partial^4 W}{\partial z_1^3\partial z_2}+2\beta\frac{\partial^4 W}{\partial z_1^2\partial z_2^2}+4\frac{\delta_b}{\alpha_b}\frac{\partial^4 W}{\partial z_1\partial z_2^3}+\frac{1}{\alpha_b^2}\frac{\partial^4 W}{\partial z_2^4} \tag{167}$$

Likewise, the boundary conditions on the edges $z_1 = a_1 / L_1$ and $z_1 = b_1 / L_1$, given by equations (161), reduce to

$$\frac{\partial^2\mathcal{F}}{\partial z_2^2}=\pi^2\overline{N}(z_2)\qquad\text{or}\qquad U_1=\overline{\Delta}_1(z_2) \tag{168a}$$

$$-\frac{\partial^2 \mathcal{F}}{\partial z_1 \partial z_2} = \frac{\pi^2}{\alpha_b}\,\bar{S}(z_2) \qquad \text{or} \qquad U_2 = \bar{\Delta}_2(z_2) \tag{168b}$$

$$\begin{aligned} &-\alpha_b^2 \frac{\partial^3 W}{\partial z_1^3} - 4\alpha_b\gamma_b \frac{\partial^3 W}{\partial z_1^2 \partial z_2} - \left(2\beta - \nu_b\right)\frac{\partial^3 W}{\partial z_1 \partial z_2^2} - 2\frac{\delta_b}{\alpha_b}\frac{\partial^3 W}{\partial z_2^3} \\ &\qquad + \frac{\partial^2 \mathcal{F}}{\partial z_2^2}\frac{\partial}{\partial z_1}\left(W + W_I\right) - \frac{\partial^2 \mathcal{F}}{\partial z_1 \partial z_2}\frac{\partial}{\partial z_2}\left(W + W_I\right) = \bar{V}(z_2) \end{aligned} \qquad \text{or} \quad W = \bar{\Delta}_n(z_2) \tag{168c}$$

$$-\alpha_b^2 \frac{\partial^2 W}{\partial z_1^2} - \nu_b \frac{\partial^2 W}{\partial z_2^2} - 2\alpha_b\gamma_b \frac{\partial^2 W}{\partial z_1 \partial z_2} = \bar{M}(z_2) \quad \text{or} \quad -\frac{\partial W}{\partial z_1} = \bar{\Phi}(z_2) \tag{168d}$$

On the edges $z_2 = a_2 / L_2$ and $z_2 = b_2 / L_2$, the boundary conditions given by equations (162) reduce to

$$\frac{\partial^2 \mathcal{F}}{\partial z_1^2} = \pi^2 \bar{N}(z_1) \qquad \text{or} \qquad U_2 = \bar{\Delta}_2(z_1) \tag{169a}$$

$$-\frac{\partial^2 \mathcal{F}}{\partial z_1 \partial z_2} = \frac{\pi^2}{\alpha_b}\,\bar{S}(z_1) \qquad \text{or} \qquad U_1 = \bar{\Delta}_1(z_1) \tag{169b}$$

$$\begin{aligned} &-2\alpha_b\gamma_b \frac{\partial^3 W}{\partial z_1^3} - \left(2\beta - \nu_b\right)\frac{\partial^3 W}{\partial z_1^2 \partial z_2} - 4\frac{\delta_b}{\alpha_b}\frac{\partial^3 W}{\partial z_1 \partial z_2^2} - \frac{1}{\alpha_b^2}\frac{\partial^3 W}{\partial z_2^3} \\ &\qquad + \frac{\partial^2 \mathcal{F}}{\partial z_1^2}\frac{\partial}{\partial z_2}\left(W + W_I\right) - \frac{\partial^2 \mathcal{F}}{\partial z_1 \partial z_2}\frac{\partial}{\partial z_1}\left(W + W_I\right) = \bar{V}(z_1) \end{aligned} \qquad \text{or} \quad W = \bar{\Delta}_n(z_1) \tag{169c}$$

$$-\nu_b \frac{\partial^2 W}{\partial z_1^2} - \frac{1}{\alpha_b^2}\frac{\partial^2 W}{\partial z_2^2} - 2\frac{\delta_b}{\alpha_b}\frac{\partial^2 W}{\partial z_1 \partial z_2} = \bar{M}(z_1) \quad \text{or} \quad -\frac{\partial W}{\partial z_2} = \bar{\Phi}(z_1) \tag{169d}$$

where the tangential displacements are obtained from

$$\frac{\partial U_1}{\partial z_1} = \frac{1}{\alpha_m^2}\frac{\partial^2 \mathcal{F}}{\partial z_2^2} - \nu_m \frac{\partial^2 \mathcal{F}}{\partial z_1^2} + \frac{\delta_m}{\alpha_m}\frac{\partial^2 \mathcal{F}}{\partial z_1 \partial z_2} - \sqrt{12}Z_1 W - \frac{1}{2}\left(\frac{\partial W}{\partial z_1}\right)^2 - \frac{\partial W}{\partial z_1}\frac{\partial W_I}{\partial z_1} \tag{170}$$

$$\frac{\partial U_2}{\partial z_2} = -\nu_m \frac{\partial^2 \mathcal{F}}{\partial z_2^2} + \alpha_m^2 \frac{\partial^2 \mathcal{F}}{\partial z_1^2} + \alpha_m\gamma_m \frac{\partial^2 \mathcal{F}}{\partial z_1 \partial z_2} - \sqrt{12}Z_2 W - \frac{1}{2}\left(\frac{\partial W}{\partial z_2}\right)^2 - \frac{\partial W}{\partial z_2}\frac{\partial W_I}{\partial z_2} \tag{171}$$

$$\frac{\partial U_1}{\partial z_2} + \frac{\partial U_2}{\partial z_1} = -\frac{\delta_m}{\alpha_m}\frac{\partial^2 \mathcal{F}}{\partial z_2^2} - \alpha_m\gamma_m \frac{\partial^2 \mathcal{F}}{\partial z_1^2} - 2\left(\mu + \nu_m\right)\frac{\partial^2 \mathcal{F}}{\partial z_1 \partial z_2} - \frac{\partial W}{\partial z_1}\frac{\partial W}{\partial z_2} - \frac{\partial W_I}{\partial z_1}\frac{\partial W}{\partial z_2} - \frac{\partial W_I}{\partial z_2}\frac{\partial W}{\partial z_1} \tag{172}$$

The virtual work given by equation (163) reduces to

$$\int\int_{\mathcal{A}} \left\{ \left[\mathcal{G}_3 - \sqrt{12} \left[Z_1 \; Z_2 \; 0 \right] \left\{ \partial \mathcal{F} \right\} \right] \delta W - \left\{ \mathcal{K} \right\}^T \left[\mathcal{A} \right] \left\{ \delta \mathcal{K} \right\} \right.$$
$$\left. - \left[\left\{ \Omega \right\} + \left\{ \Omega_I \right\} \right]^T \left[\partial \mathcal{F} \right] \left\{ \delta \Omega \right\} \right\} dz_1 dz_2 + \mathcal{I}_1^B + \mathcal{I}_2^B = 0 \tag{173}$$

and the complementary virtual work term given by equation (164) becomes

$$\delta \tilde{\mathcal{W}}^*_{\text{int}} = \left(\left\{ \partial \mathcal{F} \right\}^T \left[\mathcal{A} \right] - \sqrt{12} W \left[Z_1 \; Z_2 \; 0 \right] - \frac{1}{2} \left\{ \Omega \right\}^T \left(\left[\Omega \right] - 2 \left[\Omega_I \right] \right) \right) \left\{ \partial \delta \mathcal{F} \right\} \tag{174}$$

Nondimensional Bifurcation Equations

Bifurcation analysis presumes the existence of a known continuous set of primary equilibrium states, called the primary or fundamental equilibrium path, for a geometrically perfect shell whose continuity is manifested by a continuously varying loading parameter $\tilde{p}$. In addition, each primary equilibrium state is presumed to be governed by a linear boundary-value problem. In the present study, each primary equilibrium state, determined by the specific value of $\tilde{p}$, is represented by the displacement fields $\overset{(0)}{U}_1(z_1, z_2, \tilde{p})$, $\overset{(0)}{U}_2(z_1, z_2, \tilde{p})$, and $\overset{(0)}{W}(z_1, z_2, \tilde{p})$. Here, the superscript (0) denotes quantites associated with the primary equilibrium states prior to bifurcation. Bifurcation analysis also presumes the existence of a critical value of $\tilde{p}$, denoted by $\tilde{p}_{cr}$, for which one or more solutions to the corresponding nonlinear boundary-value problem intersect the primary equilibrium path. Therefore, in the "small" neighborhood of a bifurcation, the shell response is represented by the displacement fields

$$U_1 = \overset{(0)}{U}_1 + \varepsilon \overset{(1)}{U}_1 \tag{175a}$$

$$U_2 = \overset{(0)}{U}_2 + \varepsilon \overset{(1)}{U}_2 \tag{175b}$$

$$W = \overset{(0)}{W} + \varepsilon \overset{(1)}{W} \tag{175c}$$

where $|\varepsilon| << 1$ and the superscript (1) denotes quantites associated with equilibrium states that are adjacent to the unique primary equilibrium state at the bifurcation point, given by $\tilde{p} = \tilde{p}_{cr}$. It is important to note that although $\tilde{p} = \tilde{p}_{cr}$ defines a unique point of the primary equilibrium path,

the displacement fields $\overset{(1)}{U}_1$, $\overset{(1)}{U}_2$, and $\overset{(1)}{W}$ are not unique; that is, more than one adjacent equilibrium state may correspond to the same value of $\tilde{p}_{cr}$. Bifurcation points of this type are typically referred to as points of compound bifurcation.

Equations for the Primary Equilibrium Path

The rotation and strain fields associated with each primary equilibrium state are obtained directly from linearization of equations (40), (42), (46), and (49); which gives

$$\overset{(0)}{\Omega}_1 = -\frac{\partial \overset{(0)}{W}}{\partial z_1} \tag{176a}$$

$$\overset{(0)}{\Omega}_2 = -\frac{\partial \overset{(0)}{W}}{\partial z_2} \tag{176b}$$

$$\overset{(0)}{E}_{11} = \frac{\partial \overset{(0)}{U}_1}{\partial z_1} + \sqrt{12} Z_1 \overset{(0)}{W} \tag{177a}$$

$$\overset{(0)}{E}_{22} = \frac{\partial \overset{(0)}{U}_2}{\partial z_2} + \sqrt{12} Z_2 \overset{(0)}{W} \tag{177b}$$

$$\overset{(0)}{G}_{12} = \frac{\partial \overset{(0)}{U}_1}{\partial z_2} + \frac{\partial \overset{(0)}{U}_2}{\partial z_1} \tag{177c}$$

$$\overset{(0)}{\kappa}_{11} = -\frac{\partial^2 \overset{(0)}{W}}{\partial z_1^2} \tag{178a}$$

$$\overset{(0)}{\kappa}_{22} = -\frac{\partial^2 \overset{(0)}{W}}{\partial z_2^2} \tag{178b}$$

$$\overset{(0)}{\kappa}_{12} = -2\frac{\partial^2 \overset{(0)}{W}}{\partial z_1 \partial z_2} \tag{178c}$$

The corresponding constitutive equations are obtained from equations (76) and (78) and are given by

$$\begin{Bmatrix} \overset{(0)}{E}_{11} \\ \overset{(0)}{E}_{22} \\ \overset{(0)}{G}_{12} \end{Bmatrix} = \pi^2 \begin{bmatrix} \dfrac{1}{\alpha_m^2} & -\nu_m & -\dfrac{\delta_m}{\alpha_m} \\ -\nu_m & \alpha_m^2 & -\alpha_m\gamma_m \\ -\dfrac{\delta_m}{\alpha_m} & -\alpha_m\gamma_m & 2(\mu+\nu_m) \end{bmatrix} \begin{Bmatrix} \overset{(0)}{\mathcal{N}}_{11} \\ \overset{(0)}{\mathcal{N}}_{22} \\ \dfrac{\overset{(0)}{\mathcal{N}}_{12}}{\alpha_b} \end{Bmatrix} + \begin{bmatrix} \mathcal{B}_{11} & \mathcal{B}_{12} & \mathcal{B}_{16} \\ \mathcal{B}_{21} & \mathcal{B}_{22} & \mathcal{B}_{26} \\ \mathcal{B}_{61} & \mathcal{B}_{62} & \mathcal{B}_{66} \end{bmatrix} \begin{Bmatrix} \dfrac{\partial^2 \overset{(0)}{W}}{\partial z_1^2} \\ \dfrac{\partial^2 \overset{(0)}{W}}{\partial z_2^2} \\ 2\dfrac{\partial^2 \overset{(0)}{W}}{\partial z_1 \partial z_2} \end{Bmatrix} \tag{179}$$

and

$$\begin{Bmatrix} \overset{(0)}{\mathcal{M}}_{11} \\ \overset{(0)}{\mathcal{M}}_{22} \\ \overset{(0)}{\mathcal{M}}_{12} \end{Bmatrix} = \pi^2 \begin{bmatrix} \mathcal{B}_{11} & \mathcal{B}_{21} & \mathcal{B}_{61} \\ \mathcal{B}_{12} & \mathcal{B}_{22} & \mathcal{B}_{62} \\ \mathcal{B}_{16} & \mathcal{B}_{26} & \mathcal{B}_{66} \end{bmatrix} \begin{Bmatrix} \overset{(0)}{\mathcal{N}}_{11} \\ \overset{(0)}{\mathcal{N}}_{22} \\ \dfrac{\overset{(0)}{\mathcal{N}}_{12}}{\alpha_b} \end{Bmatrix} - \begin{bmatrix} \mathcal{A}_{11} & \mathcal{A}_{12} & \mathcal{A}_{16} \\ \mathcal{A}_{12} & \mathcal{A}_{22} & \mathcal{A}_{26} \\ \mathcal{A}_{16} & \mathcal{A}_{26} & \mathcal{A}_{66} \end{bmatrix} \begin{Bmatrix} \dfrac{\partial^2 \overset{(0)}{W}}{\partial z_1^2} \\ \dfrac{\partial^2 \overset{(0)}{W}}{\partial z_2^2} \\ 2\dfrac{\partial^2 \overset{(0)}{W}}{\partial z_1 \partial z_2} \end{Bmatrix} \tag{180}$$

where $\overset{(0)}{\mathcal{N}}_{11}$, $\overset{(0)}{\mathcal{N}}_{22}$, and $\overset{(0)}{\mathcal{N}}_{12}$ are membrane stress resultants and $\overset{(0)}{\mathcal{M}}_{11}$, $\overset{(0)}{\mathcal{M}}_{22}$, and $\overset{(0)}{\mathcal{M}}_{12}$ are bending stress resultants associated with each primary equilibrium state. The equilibrium equations governing each primary equilibrium state are obtained from linearization of equations (81), (83), (86), (88), and (93) and are given by

$$\frac{\partial \overset{(0)}{\mathcal{N}}_{11}}{\partial z_1} + \frac{1}{\alpha_b}\frac{\partial \overset{(0)}{\mathcal{N}}_{12}}{\partial z_2} + \tilde{p}_{\mathcal{Q}_1} = 0 \tag{181a}$$

$$\frac{1}{\alpha_b}\frac{\partial \overset{(0)}{\mathcal{N}}_{12}}{\partial z_1} + \frac{\partial \overset{(0)}{\mathcal{N}}_{22}}{\partial z_2} + \tilde{p}_{\mathcal{Q}_2} = 0 \tag{181b}$$

$$\frac{\partial \overset{(0)}{\mathcal{M}}_{11}}{\partial z_1} + \frac{\partial \overset{(0)}{\mathcal{M}}_{12}}{\partial z_2} - \overset{(0)}{\mathcal{Z}}_1 = 0 \tag{181c}$$

$$\frac{\partial \overset{(0)}{\mathcal{M}}_{12}}{\partial z_1} + \frac{\partial \overset{(0)}{\mathcal{M}}_{22}}{\partial z_2} - \overset{(0)}{\mathcal{Z}}_2 = 0 \tag{181d}$$

$$\frac{\partial \overset{(0)}{\mathcal{Z}}_1}{\partial z_1} + \frac{\partial \overset{(0)}{\mathcal{Z}}_2}{\partial z_2} + \tilde{p}_{\mathcal{Q}_3} - \pi^2\sqrt{12}\left(\overset{(0)}{\mathcal{N}}_{11}Z_1 + \overset{(0)}{\mathcal{N}}_{22}Z_2\right) = 0 \tag{181e}$$

where $\overset{(0)}{\mathcal{Z}}_1$ and $\overset{(0)}{\mathcal{Z}}_2$ are transverse shear stress resultants associated with each primary equilibrium state and the surface tractions $\mathcal{Q}_1$, $\mathcal{Q}_2$, and $\mathcal{Q}_3$ have been scaled by the loading parameter so that a

unique solution is associated with each value of $\tilde{p}$.

The boundary conditions associated with each primary equilibrium state are also obtained from linearization of equations (98) and (99), with the applied edge tractions and displacements also scaled by the loading parameter $\tilde{p}$. Thus, the boundary conditions on the edges $z_1 = a_1 / L_1$ and $z_1 = b_1 / L_1$, given by equations (98), become

$$\overset{(0)}{\mathcal{N}}_{11} = \tilde{p}\overline{N}(z_2) \quad \text{or} \quad \overset{(0)}{U}_1 = \tilde{p}\overline{\Delta}_1(z_2) \tag{182a}$$

$$\overset{(0)}{\mathcal{N}}_{12} = \tilde{p}\overline{S}(z_2) \quad \text{or} \quad \overset{(0)}{U}_2 = \tilde{p}\overline{\Delta}_2(z_2) \tag{182b}$$

$$\overset{(0)}{\mathcal{Q}}_1 + \frac{\partial \overset{(0)}{\mathcal{M}}_{12}}{\partial z_2} = \tilde{p}\overline{V}(z_2) \quad \text{or} \quad \overset{(0)}{W} = \tilde{p}\overline{\Delta}_n(z_2) \tag{182c}$$

$$\overset{(0)}{\mathcal{M}}_{11} = \tilde{p}\overline{M}(z_2) \quad \text{or} \quad -\frac{\partial \overset{(0)}{W}}{\partial z_1} = \tilde{p}\overline{\Phi}(z_2) \tag{182d}$$

where $\overset{(0)}{\mathcal{Q}}_1$ is given by equation (181c). On the edges $z_2 = a_2 / L_2$ and $z_2 = b_2 / L_2$, the boundary conditions given by equation (99) become

$$\overset{(0)}{\mathcal{N}}_{22} = \tilde{p}\overline{N}(z_1) \quad \text{or} \quad \overset{(0)}{U}_2 = \tilde{p}\overline{\Delta}_2(z_1) \tag{183a}$$

$$\overset{(0)}{\mathcal{N}}_{12} = \tilde{p}\overline{S}(z_1) \quad \text{or} \quad \overset{(0)}{U}_1 = \tilde{p}\overline{\Delta}_1(z_1) \tag{183b}$$

$$\overset{(0)}{\mathcal{Q}}_2 + \frac{\partial \overset{(0)}{\mathcal{M}}_{12}}{\partial z_1} = \tilde{p}\overline{V}(z_1) \quad \text{or} \quad \overset{(0)}{W} = \tilde{p}\overline{\Delta}_n(z_1) \tag{183c}$$

$$\overset{(0)}{\mathcal{M}}_{22} = \tilde{p}\overline{M}(z_1) \quad \text{or} \quad -\frac{\partial \overset{(0)}{W}}{\partial z_2} = \tilde{p}\overline{\Phi}(z_1) \tag{183d}$$

where $\overset{(0)}{\mathcal{Q}}_2$ is given by equation (181d).

Equations (176) - (183) constitute a family of linear boundary-value problems whose solutions depend on the loading parameter $\tilde{p}$ and the relative magnitudes of the loads. The relative magnitudes of the loads are given by the specific values selected for the surface tractions $\mathcal{g}_1$, $\mathcal{g}_2$, and $\mathcal{g}_3$ and the edge tractions or displacements specified in equations (182) and (183). The family of solutions is represented by

$$\overset{(0)}{U}_1 = \overset{(0)}{U}_1(z_1, z_2, \tilde{p}) \tag{184a}$$

$$\overset{(0)}{U}_2 = \overset{(0)}{U}_2(z_1, z_2, \tilde{p}) \tag{184b}$$

$$\overset{(0)}{W} = \overset{(0)}{W}(z_1, z_2, \tilde{p}) \tag{184c}$$

$$\overset{(0)}{E}_{11} = \overset{(0)}{E}_{11}(z_1, z_2, \tilde{p}) \tag{185a}$$

$$\overset{(0)}{E}_{22} = \overset{(0)}{E}_{22}(z_1, z_2, \tilde{p}) \tag{185b}$$

$$\overset{(0)}{G}_{12} = \overset{(0)}{G}_{12}(z_1, z_2, \tilde{p}) \tag{185c}$$

$$\overset{(0)}{\mathcal{N}}_{11} = \overset{(0)}{\mathcal{N}}_{11}(z_1, z_2, \tilde{p}) \tag{186a}$$

$$\overset{(0)}{\mathcal{N}}_{22} = \overset{(0)}{\mathcal{N}}_{22}(z_1, z_2, \tilde{p}) \tag{186b}$$

$$\overset{(0)}{\mathcal{N}}_{12} = \overset{(0)}{\mathcal{N}}_{12}(z_1, z_2, \tilde{p}) \tag{186c}$$

$$\overset{(0)}{\mathcal{M}}_{11} = \overset{(0)}{\mathcal{M}}_{11}(z_1, z_2, \tilde{p}) \tag{187a}$$

$$\overset{(0)}{\mathcal{M}}_{22} = \overset{(0)}{\mathcal{M}}_{22}(z_1, z_2, \tilde{p}) \tag{187b}$$

$$\overset{(0)}{\mathcal{M}}_{12} = \overset{(0)}{\mathcal{M}}_{12}(z_1, z_2, \tilde{p}) \tag{187c}$$

$$\overset{(0)}{\mathcal{Q}}_1 = \overset{(0)}{\mathcal{Q}}_1(z_1, z_2, \tilde{p}) \tag{188a}$$

$$\overset{(0)}{\mathcal{Q}}_2 = \overset{(0)}{\mathcal{Q}}_2(z_1, z_2, \tilde{p}) \tag{188b}$$

which are generally transcendental functions of the loading parameter $\tilde{p}$.

Equations for Adjacent Equilibrium Paths

The equations governing adjacent equilibrium paths at a bifurcation point of the primary equilibrium path are obtained by substituting equations (175) into the equations for the nonlinear boundary-value problem of the idealized, geometrically perfect shell, and then noting that all

resulting equations for the primary equilibrium path are satisfied identically. In particular, substituting equations (175) into equations (40) and (42) gives

$$\Omega_1 = \overset{(0)}{\Omega}_1 + \varepsilon \overset{(1)}{\Omega}_1 \tag{189a}$$

$$\Omega_2 = \overset{(0)}{\Omega}_2 + \varepsilon \overset{(1)}{\Omega}_2 \tag{189b}$$

and substituting equations (175) into equations (46) and (49) gives

$$E_{11} = \overset{(0)}{E}_{11} + \varepsilon \overset{(1)}{E}_{11} + \mathcal{O}\left(\varepsilon^2\right) \tag{190a}$$

$$E_{22} = \overset{(0)}{E}_{22} + \varepsilon \overset{(1)}{E}_{22} + \mathcal{O}\left(\varepsilon^2\right) \tag{190b}$$

$$G_{12} = \overset{(0)}{G}_{12} + \varepsilon \overset{(1)}{G}_{12} + \mathcal{O}\left(\varepsilon^2\right) \tag{190c}$$

$$\mathcal{K}_{11} = \overset{(0)}{\mathcal{K}}_{11} + \varepsilon \overset{(1)}{\mathcal{K}}_{11} \tag{191a}$$

$$\mathcal{K}_{22} = \overset{(0)}{\mathcal{K}}_{22} + \varepsilon \overset{(1)}{\mathcal{K}}_{22} \tag{191b}$$

$$\mathcal{K}_{12} = \overset{(0)}{\mathcal{K}}_{12} + \varepsilon \overset{(1)}{\mathcal{K}}_{12} \tag{191c}$$

where the symbol $\mathcal{O}\left(\varepsilon^2\right)$ is used to denote terms with magnitudes that are at most second order in the small parameter ε. In these equations,

$$\overset{(1)}{\Omega}_1 \equiv -\frac{\partial \overset{(1)}{W}}{\partial z_1} \tag{192a}$$

$$\overset{(1)}{\Omega}_2 \equiv -\frac{\partial \overset{(1)}{W}}{\partial z_2} \tag{192b}$$

$$\overset{(1)}{E}_{11} \equiv \frac{\partial \overset{(1)}{U}_1}{\partial z_1} + \sqrt{12} Z_1 \overset{(1)}{W} + \frac{\partial \overset{(0)}{W}}{\partial z_1} \frac{\partial \overset{(1)}{W}}{\partial z_1} \tag{193a}$$

$$\overset{(1)}{E}_{22} \equiv \frac{\partial \overset{(1)}{U}_2}{\partial z_2} + \sqrt{12} Z_2 \overset{(1)}{W} + \frac{\partial \overset{(0)}{W}}{\partial z_2} \frac{\partial \overset{(1)}{W}}{\partial z_2} \tag{193b}$$

$$\overset{(1)}{G}_{12} \equiv \frac{\partial \overset{(1)}{U}_1}{\partial z_2} + \frac{\partial \overset{(1)}{U}_2}{\partial z_1} + \frac{\partial \overset{(0)}{W}}{\partial z_1}\frac{\partial \overset{(1)}{W}}{\partial z_2} + \frac{\partial \overset{(0)}{W}}{\partial z_2}\frac{\partial \overset{(1)}{W}}{\partial z_1} \tag{193c}$$

$$\overset{(1)}{\mathcal{K}}_{11} \equiv -\frac{\partial^2 \overset{(1)}{W}}{\partial z_1^2} \tag{194a}$$

$$\overset{(1)}{\mathcal{K}}_{22} \equiv -\frac{\partial^2 \overset{(1)}{W}}{\partial z_2^2} \tag{194b}$$

$$\overset{(1)}{\mathcal{K}}_{12} \equiv -2\,\frac{\partial^2 \overset{(1)}{W}}{\partial z_1 \partial z_2} \tag{194c}$$

Next, substituting equations (175c) and (193) into equations (76) and (78) implies the expansions

$$\mathcal{N}_{11} = \overset{(0)}{\mathcal{N}}_{11} + \varepsilon \overset{(1)}{\mathcal{N}}_{11} + \mathcal{O}\left(\varepsilon^2\right) \tag{195a}$$

$$\mathcal{N}_{22} = \overset{(0)}{\mathcal{N}}_{22} + \varepsilon \overset{(1)}{\mathcal{N}}_{22} + \mathcal{O}\left(\varepsilon^2\right) \tag{195b}$$

$$\mathcal{N}_{12} = \overset{(0)}{\mathcal{N}}_{12} + \varepsilon \overset{(1)}{\mathcal{N}}_{12} + \mathcal{O}\left(\varepsilon^2\right) \tag{195c}$$

$$\mathcal{M}_{11} = \overset{(0)}{\mathcal{M}}_{11} + \varepsilon \overset{(1)}{\mathcal{M}}_{11} + \mathcal{O}\left(\varepsilon^2\right) \tag{195d}$$

$$\mathcal{M}_{22} = \overset{(0)}{\mathcal{M}}_{22} + \varepsilon \overset{(1)}{\mathcal{M}}_{22} + \mathcal{O}\left(\varepsilon^2\right) \tag{195e}$$

$$\mathcal{M}_{12} = \overset{(0)}{\mathcal{M}}_{12} + \varepsilon \overset{(1)}{\mathcal{M}}_{12} + \mathcal{O}\left(\varepsilon^2\right) \tag{195f}$$

and the constitutive equations

$$\begin{Bmatrix} \overset{(1)}{E}_{11} \\ \overset{(1)}{E}_{22} \\ \overset{(1)}{G}_{12} \end{Bmatrix} = \pi^2 \begin{bmatrix} \frac{1}{\alpha_m^2} & -\nu_m & -\frac{\delta_m}{\alpha_m} \\ -\nu_m & \alpha_m^2 & -\alpha_m \gamma_m \\ -\frac{\delta_m}{\alpha_m} & -\alpha_m \gamma_m & 2(\mu + \nu_m) \end{bmatrix} \begin{Bmatrix} \overset{(1)}{\mathcal{N}}_{11} \\ \overset{(1)}{\mathcal{N}}_{22} \\ \frac{\overset{(1)}{\mathcal{N}}_{12}}{\alpha_b} \end{Bmatrix} + \begin{bmatrix} \mathcal{B}_{11} & \mathcal{B}_{12} & \mathcal{B}_{16} \\ \mathcal{B}_{21} & \mathcal{B}_{22} & \mathcal{B}_{26} \\ \mathcal{B}_{61} & \mathcal{B}_{62} & \mathcal{B}_{66} \end{bmatrix} \begin{Bmatrix} \frac{\partial^2 \overset{(1)}{W}}{\partial z_1^2} \\ \frac{\partial^2 \overset{(1)}{W}}{\partial z_2^2} \\ 2\,\frac{\partial^2 \overset{(1)}{W}}{\partial z_1 \partial z_2} \end{Bmatrix} \tag{196}$$

and

$$\begin{Bmatrix} \overset{(1)}{\mathcal{M}}_{11} \\ \overset{(1)}{\mathcal{M}}_{22} \\ \overset{(1)}{\mathcal{M}}_{12} \end{Bmatrix} = \pi^2 \begin{bmatrix} \mathcal{B}_{11} & \mathcal{B}_{21} & \mathcal{B}_{61} \\ \mathcal{B}_{12} & \mathcal{B}_{22} & \mathcal{B}_{62} \\ \mathcal{B}_{16} & \mathcal{B}_{26} & \mathcal{B}_{66} \end{bmatrix} \begin{Bmatrix} \overset{(1)}{\mathcal{N}}_{11} \\ \overset{(1)}{\mathcal{N}}_{22} \\ \dfrac{\overset{(1)}{\mathcal{N}}_{12}}{\alpha_b} \end{Bmatrix} - \begin{bmatrix} \mathcal{A}_{11} & \mathcal{A}_{12} & \mathcal{A}_{16} \\ \mathcal{A}_{12} & \mathcal{A}_{22} & \mathcal{A}_{26} \\ \mathcal{A}_{16} & \mathcal{A}_{26} & \mathcal{A}_{66} \end{bmatrix} \begin{Bmatrix} \dfrac{\partial^2 \overset{(1)}{W}}{\partial z_1^2} \\ \dfrac{\partial^2 \overset{(1)}{W}}{\partial z_2^2} \\ 2\dfrac{\partial^2 \overset{(1)}{W}}{\partial z_1 \partial z_2} \end{Bmatrix} \tag{197}$$

where $\overset{(1)}{\mathcal{N}}_{11}$, $\overset{(1)}{\mathcal{N}}_{22}$, and $\overset{(1)}{\mathcal{N}}_{12}$ are membrane stress resultants and $\overset{(1)}{\mathcal{M}}_{11}$, $\overset{(1)}{\mathcal{M}}_{22}$, and $\overset{(1)}{\mathcal{M}}_{12}$ are bending stress resultants associated with the adjacent equilibrium states. The equilibrium equations governing the adjacent equilibrium states are obtained by substituting equations (175c) and (195) into equations (81), (83), (86), (88), and (94) and then enforcing equations (181) and neglecting terms of second order and higher and nonlinear terms associated with the primary equilibrium states. The resulting equations are given by

$$\frac{\partial \overset{(1)}{\mathcal{N}}_{11}}{\partial z_1} + \frac{1}{\alpha_b}\frac{\partial \overset{(1)}{\mathcal{N}}_{12}}{\partial z_2} = 0 \tag{198a}$$

$$\frac{1}{\alpha_b}\frac{\partial \overset{(1)}{\mathcal{N}}_{12}}{\partial z_1} + \frac{\partial \overset{(1)}{\mathcal{N}}_{22}}{\partial z_2} = 0 \tag{198b}$$

$$\frac{\partial \overset{(1)}{\mathcal{M}}_{11}}{\partial z_1} + \frac{\partial \overset{(1)}{\mathcal{M}}_{12}}{\partial z_2} - \overset{(1)}{\mathcal{Z}}_1 = 0 \tag{198c}$$

$$\frac{\partial \overset{(1)}{\mathcal{M}}_{12}}{\partial z_1} + \frac{\partial \overset{(1)}{\mathcal{M}}_{22}}{\partial z_2} - \overset{(1)}{\mathcal{Z}}_2 = 0 \tag{198d}$$

$$\begin{aligned} &\frac{\partial \overset{(1)}{\mathcal{Z}}_1}{\partial z_1} + \frac{\partial \overset{(1)}{\mathcal{Z}}_2}{\partial z_2} - \pi^2\sqrt{12}\left(\overset{(1)}{\mathcal{N}}_{11}Z_1 + \overset{(1)}{\mathcal{N}}_{22}Z_2\right) \\ &\quad + \pi^2\frac{\partial}{\partial z_1}\left[\overset{(0)}{\mathcal{N}}_{11}\frac{\partial \overset{(1)}{W}}{\partial z_1} + \frac{\overset{(0)}{\mathcal{N}}_{12}}{\alpha_b}\frac{\partial \overset{(1)}{W}}{\partial z_2} + \overset{(1)}{\mathcal{N}}_{11}\frac{\partial \overset{(0)}{W}}{\partial z_1} + \frac{\overset{(1)}{\mathcal{N}}_{12}}{\alpha_b}\frac{\partial \overset{(0)}{W}}{\partial z_2}\right] \\ &\quad + \pi^2\frac{\partial}{\partial z_2}\left[\frac{\overset{(0)}{\mathcal{N}}_{12}}{\alpha_b}\frac{\partial \overset{(1)}{W}}{\partial z_1} + \overset{(0)}{\mathcal{N}}_{22}\frac{\partial \overset{(1)}{W}}{\partial z_2} + \frac{\overset{(1)}{\mathcal{N}}_{12}}{\alpha_b}\frac{\partial \overset{(0)}{W}}{\partial z_1} + \overset{(1)}{\mathcal{N}}_{22}\frac{\partial \overset{(0)}{W}}{\partial z_2}\right] = 0 \end{aligned} \tag{198e}$$

where it is noted that

$$\mathcal{Z}_1 = \overset{(0)}{\mathcal{Z}}_1 + \varepsilon\overset{(1)}{\mathcal{Z}}_1 + \mathcal{O}\left(\varepsilon^2\right) \tag{199a}$$

$$\mathcal{Z}_2 = \overset{(0)}{\mathcal{Z}}_2 + \varepsilon \overset{(1)}{\mathcal{Z}}_2 + \mathcal{O}\left(\varepsilon^2\right) \tag{199b}$$

such that $\overset{(1)}{\mathcal{Z}}_1$ and $\overset{(1)}{\mathcal{Z}}_2$ are transverse shear stress resultants associated with the adjacent equilibrium states. The loading parameter enters the equations for the adjacent equilibrium states through the displacement $\overset{(0)}{W}$ and the membrane stress resultants $\overset{(0)}{\mathcal{N}}_{11}$, $\overset{(0)}{\mathcal{N}}_{22}$, and $\overset{(0)}{\mathcal{N}}_{12}$. To further simplify matters, sometimes it is presumed that the pre-bifurcation displacement $\overset{(0)}{W}$ is mildy varying such that the corresponding pre-bifurcation rotations, given by the derivatives of $\overset{(0)}{W}$ in equation (198e), are negligible. For this case, equation (198e) reduces to

$$\begin{aligned} &\frac{\partial \overset{(1)}{\mathcal{Z}}_1}{\partial Z_1} + \frac{\partial \overset{(1)}{\mathcal{Z}}_2}{\partial Z_2} - \pi^2 \sqrt{12}\left(\overset{(1)}{\mathcal{N}}_{11} Z_1 + \overset{(1)}{\mathcal{N}}_{22} Z_2 \right) \\ &\quad + \pi^2 \frac{\partial}{\partial Z_1}\left[\overset{(0)}{\mathcal{N}}_{11} \frac{\partial \overset{(1)}{W}}{\partial Z_1} + \frac{\overset{(0)}{\mathcal{N}}_{12}}{\alpha_b} \frac{\partial \overset{(1)}{W}}{\partial Z_2} \right] + \pi^2 \frac{\partial}{\partial Z_2}\left[\frac{\overset{(0)}{\mathcal{N}}_{12}}{\alpha_b} \frac{\partial \overset{(1)}{W}}{\partial Z_1} + \overset{(0)}{\mathcal{N}}_{22} \frac{\partial \overset{(1)}{W}}{\partial Z_2} \right] = 0 \end{aligned} \tag{200a}$$

Expanding the derivatives of the bracketed terms in this equation and using equations (198a) and (198b) give the alternate form

$$\begin{aligned} &\frac{\partial \overset{(1)}{\mathcal{Z}}_1}{\partial Z_1} + \frac{\partial \overset{(1)}{\mathcal{Z}}_2}{\partial Z_2} - \pi^2 \sqrt{12}\left(\overset{(1)}{\mathcal{N}}_{11} Z_1 + \overset{(1)}{\mathcal{N}}_{22} Z_2 \right) - \tilde{p}\pi^2 \left[\mathcal{G}_1 \frac{\partial \overset{(1)}{W}}{\partial Z_1} + \mathcal{G}_2 \frac{\partial \overset{(1)}{W}}{\partial Z_2} \right] \\ &\quad + \pi^2 \left[\overset{(0)}{\mathcal{N}}_{11} \frac{\partial^2 \overset{(1)}{W}}{\partial Z_1^2} + \overset{(0)}{\mathcal{N}}_{22} \frac{\partial^2 \overset{(1)}{W}}{\partial Z_2^2} + 2 \frac{\overset{(0)}{\mathcal{N}}_{12}}{\alpha_b} \frac{\partial^2 \overset{(1)}{W}}{\partial Z_1 \partial Z_2} \right] = 0 \end{aligned} \tag{200b}$$

Setting $Z_1 = Z_2 = 0$ in this equation yields the bifurcation equation that is comonly cited for buckling of flat plates.

The boundary conditions associated with the adjacent equilibrium states are also obtained from equations (98) and (99). In particular, substituting equations (175), (195), and (199) into equations (98) and using equations (182), the boundary conditions on the edges $Z_1 = a_1 / L_1$ and $Z_1 = b_1 / L_1$, given by equations (98), become

$$\overset{(1)}{\mathcal{N}}_{11} = 0 \quad \text{or} \quad \overset{(1)}{U}_1 = 0 \tag{201a}$$

$$\overset{(1)}{\mathcal{N}}_{12} = 0 \quad \text{or} \quad \overset{(1)}{U}_2 = 0 \tag{201b}$$

$$\overset{(1)}{\mathcal{Z}}_1 + \frac{\partial \overset{(1)}{\mathcal{M}}_{12}}{\partial z_2} + \pi^2 \overset{(0)}{\mathcal{N}}_{11} \frac{\partial \overset{(1)}{W}}{\partial z_1} + \frac{\pi^2}{\alpha_b} \overset{(0)}{\mathcal{N}}_{12} \frac{\partial \overset{(1)}{W}}{\partial z_2} + \pi^2 \overset{(1)}{\mathcal{N}}_{11} \frac{\partial \overset{(0)}{W}}{\partial z_1} + \frac{\pi^2}{\alpha_b} \overset{(1)}{\mathcal{N}}_{12} \frac{\partial \overset{(0)}{W}}{\partial z_2} = 0 \quad \text{or} \quad \overset{(1)}{W} = 0 \tag{201c}$$

$$\overset{(1)}{\mathcal{M}}_{11} = 0 \quad \text{or} \quad \frac{\partial \overset{(1)}{W}}{\partial z_1} = 0 \tag{201d}$$

where $\overset{(1)}{\mathcal{Z}}_1$ is given by equation (198c). If nonlinear pre-bifurcation rotations $\overset{(0)}{\Omega}_1$ and $\overset{(0)}{\Omega}_2$ are neglected, equation (201c) reduces to

$$\overset{(1)}{\mathcal{Z}}_1 + \frac{\partial \overset{(1)}{\mathcal{M}}_{12}}{\partial z_2} + \pi^2 \overset{(0)}{\mathcal{N}}_{11} \frac{\partial \overset{(1)}{W}}{\partial z_1} + \frac{\pi^2}{\alpha_b} \overset{(0)}{\mathcal{N}}_{12} \frac{\partial \overset{(1)}{W}}{\partial z_2} = 0 \quad \text{or} \quad \overset{(1)}{W} = 0 \tag{201e}$$

Similarly, on the edges $z_2 = a_2 / L_2$ and $z_2 = b_2 / L_2$, the boundary conditions given by equation (99) become

$$\overset{(1)}{\mathcal{N}}_{22} = 0 \quad \text{or} \quad \overset{(1)}{U}_2 = 0 \tag{202a}$$

$$\overset{(1)}{\mathcal{N}}_{12} = 0 \quad \text{or} \quad \overset{(1)}{U}_1 = 0 \tag{202b}$$

$$\overset{(1)}{\mathcal{Z}}_2 + \frac{\partial \overset{(1)}{\mathcal{M}}_{12}}{\partial z_1} + \frac{\pi^2}{\alpha_b} \overset{(0)}{\mathcal{N}}_{12} \frac{\partial \overset{(1)}{W}}{\partial z_1} + \pi^2 \overset{(0)}{\mathcal{N}}_{22} \frac{\partial \overset{(1)}{W}}{\partial z_2} + \frac{\pi^2}{\alpha_b} \overset{(1)}{\mathcal{N}}_{12} \frac{\partial \overset{(0)}{W}}{\partial z_1} + \pi^2 \overset{(1)}{\mathcal{N}}_{22} \frac{\partial \overset{(0)}{W}}{\partial z_2} = 0 \quad \text{or} \quad \overset{(1)}{W} = 0 \tag{202c}$$

$$\overset{(1)}{\mathcal{M}}_{22} = 0 \quad \text{or} \quad \frac{\partial \overset{(1)}{W}}{\partial z_2} = 0 \tag{202d}$$

where $\overset{(1)}{\mathcal{Z}}_2$ is given by equation (198d). If nonlinear pre-bifurcation rotations are neglected, then equation (202c) reduces to

$$\overset{(1)}{\mathcal{Z}}_2 + \frac{\partial \overset{(1)}{\mathcal{M}}_{12}}{\partial z_1} + \frac{\pi^2}{\alpha_b} \overset{(0)}{\mathcal{N}}_{12} \frac{\partial \overset{(1)}{W}}{\partial z_1} + \pi^2 \overset{(0)}{\mathcal{N}}_{22} \frac{\partial \overset{(1)}{W}}{\partial z_2} = 0 \quad \text{or} \quad \overset{(1)}{W} = 0 \tag{202e}$$

Inspection of equations (189)-(202) indicates a system of homogeneous differential equations and homogeneous boundary conditions that depend on the loading parameter $\tilde{p}$ through the displacement $\overset{(0)}{W}$ and the membrane stress resultants $\overset{(0)}{\mathcal{N}}_{11}$, $\overset{(0)}{\mathcal{N}}_{22}$, and $\overset{(0)}{\mathcal{N}}_{12}$, generally in a transcendental manner. Thus, the equations for the adjacent equilibrium states constitute a nonlinear boundary-eigenvalue problem.

Variational Principle for Bifurcation

A variational principle for bifurcation is obtained by noting that equations (198a), (198b), and (198e) represent pointwise summations of internal forces in the three coordinate directions, for the adjacent equilibrium states. Likewise, the traction boundary conditions in equations (201) and (202) represent pointwise summations of internal forces acting at the edges given by constant values of z_1 and z_2, respectively. Thus, a statement of the corresponding virtual work is given by

$$\delta\overset{(1)}{W} = -\int\int_{\mathcal{A}} \delta\overset{(1)}{\mathcal{W}} dz_1 dz_2 + \int_{\frac{a_1}{L_1}}^{\frac{b_1}{L_1}} \left\{ \delta\overset{(1)}{\mathcal{W}}_1^{B} \right\}_{\frac{a_2}{L_2}}^{\frac{b_2}{L_2}} dz_1 + \int_{\frac{a_2}{L_2}}^{\frac{b_2}{L_2}} \left\{ \delta\overset{(1)}{\mathcal{W}}_2^{B} \right\}_{\frac{a_1}{L_1}}^{\frac{b_1}{L_1}} dz_2 \tag{203}$$

where $\mathcal{A}$ is the nondimensional domain given by $\frac{a_1}{L_1} \le z_1 \le \frac{b_1}{L_1}$ and $\frac{a_2}{L_2} \le z_2 \le \frac{b_2}{L_2}$, and

$$\begin{aligned}\delta\overset{(1)}{\mathcal{W}} = &\left[\frac{\partial \overset{(1)}{\mathcal{N}}_{11}}{\partial z_1} + \frac{1}{\alpha_b} \frac{\partial \overset{(1)}{\mathcal{N}}_{12}}{\partial z_2} \right] \delta U_1 + \left[\frac{1}{\alpha_b} \frac{\partial \overset{(1)}{\mathcal{N}}_{12}}{\partial z_1} + \frac{\partial \overset{(1)}{\mathcal{N}}_{22}}{\partial z_2} \right] \delta U_2 + \left[\frac{\partial \overset{(1)}{\mathcal{Z}}_1}{\partial z_1} + \frac{\partial \overset{(1)}{\mathcal{Z}}_2}{\partial z_2} \right. \\ &- \pi^2 \sqrt{12} \left(\overset{(1)}{\mathcal{N}}_{11} Z_1 + \overset{(1)}{\mathcal{N}}_{22} Z_2 \right) + \pi^2 \frac{\partial}{\partial z_1} \left(\overset{(0)}{\mathcal{N}}_{11} \frac{\partial \overset{(1)}{W}}{\partial z_1} + \frac{\overset{(0)}{\mathcal{N}}_{12}}{\alpha_b} \frac{\partial \overset{(1)}{W}}{\partial z_2} + \overset{(1)}{\mathcal{N}}_{11} \frac{\partial \overset{(0)}{W}}{\partial z_1} + \frac{\overset{(1)}{\mathcal{N}}_{12}}{\alpha_b} \frac{\partial \overset{(0)}{W}}{\partial z_2} \right) \\ &\left. + \pi^2 \frac{\partial}{\partial z_2} \left(\frac{\overset{(0)}{\mathcal{N}}_{12}}{\alpha_b} \frac{\partial \overset{(1)}{W}}{\partial z_1} + \overset{(0)}{\mathcal{N}}_{22} \frac{\partial \overset{(1)}{W}}{\partial z_2} + \frac{\overset{(1)}{\mathcal{N}}_{12}}{\alpha_b} \frac{\partial \overset{(0)}{W}}{\partial z_1} + \overset{(1)}{\mathcal{N}}_{22} \frac{\partial \overset{(0)}{W}}{\partial z_2} \right) \right] \delta W\end{aligned} \tag{204a}$$

$$\begin{aligned}\delta\overset{(1)}{\mathcal{W}}_1^{B} = &\overset{(1)}{\mathcal{N}}_{12} \delta U_2 + \overset{(1)}{\mathcal{N}}_{22} \delta U_2 - \overset{(1)}{\mathcal{M}}_{22} \frac{\partial \delta W}{\partial z_2} \\ &+ \left[\overset{(1)}{\mathcal{Z}}_2 + \frac{\partial \overset{(1)}{\mathcal{M}}_{12}}{\partial z_1} + \frac{\pi^2}{\alpha_b} \overset{(0)}{\mathcal{N}}_{12} \frac{\partial \overset{(1)}{W}}{\partial z_1} + \pi^2 \overset{(0)}{\mathcal{N}}_{22} \frac{\partial \overset{(1)}{W}}{\partial z_2} + \frac{\pi^2}{\alpha_b} \overset{(1)}{\mathcal{N}}_{12} \frac{\partial \overset{(0)}{W}}{\partial z_1} + \pi^2 \overset{(1)}{\mathcal{N}}_{22} \frac{\partial \overset{(0)}{W}}{\partial z_2} \right] \delta W\end{aligned} \tag{204b}$$

$$\begin{aligned}\delta\overset{(1)}{\mathcal{W}}_2^{B} = &\overset{(1)}{\mathcal{N}}_{11} \delta U_2 + \overset{(1)}{\mathcal{N}}_{12} \delta U_2 - \overset{(1)}{\mathcal{M}}_{11} \frac{\partial \delta W}{\partial z_1} \\ &+ \left[\overset{(1)}{\mathcal{Z}}_1 + \frac{\partial \overset{(1)}{\mathcal{M}}_{12}}{\partial z_2} + \pi^2 \overset{(0)}{\mathcal{N}}_{11} \frac{\partial \overset{(1)}{W}}{\partial z_1} + \frac{\pi^2}{\alpha_b} \overset{(0)}{\mathcal{N}}_{12} \frac{\partial \overset{(1)}{W}}{\partial z_2} + \pi^2 \overset{(1)}{\mathcal{N}}_{11} \frac{\partial \overset{(0)}{W}}{\partial z_1} + \frac{\pi^2}{\alpha_b} \overset{(1)}{\mathcal{N}}_{12} \frac{\partial \overset{(0)}{W}}{\partial z_2} \right] \delta W\end{aligned} \tag{204c}$$

In equations (204) δU_1, δU_2, and δW are arbitrary nondimensional virtual displacement fields along the z_1, z_2, and ζ directions, respectively. Integrating by parts, by using equations (25) specialized for the nondimensional coordinates (z_1, z_2), gives

$$\iint_A \delta\overset{(1)}{\mathcal{W}} dz_1 dz_2 = -\int\int_A \left[\delta\overset{(1)}{\mathcal{W}}_{int} + \delta\overset{(1)}{\mathcal{W}'}_{int}\right] dz_1 dz_2 + \overset{(1)B}{\mathcal{I}}_1 + \overset{(1)B}{\mathcal{I}}_2 - \left\{\left\{\overset{(1)}{\mathcal{M}}_{12}\,\delta W\right\}_{\frac{a_2}{L_2}}^{\frac{b_2}{L_2}}\right\}_{\frac{a_1}{L_1}}^{\frac{b_1}{L_1}} \tag{205a}$$

where:

$$\delta\overset{(1)}{\mathcal{W}}_{int} =$$

$$\pi^2\overset{(1)}{\mathcal{N}}_{11}\left(\frac{\partial\delta U_1}{\partial z_1} + \sqrt{12}Z_1\delta W + \frac{\partial\overset{(0)}{W}}{\partial z_1}\frac{\partial\delta W}{\partial z_1}\right) + \pi^2\overset{(1)}{\mathcal{N}}_{22}\left(\frac{\partial\delta U_2}{\partial z_2} + \sqrt{12}Z_2\delta W + \frac{\partial\overset{(0)}{W}}{\partial z_2}\frac{\partial\delta W}{\partial z_2}\right) + \tag{205b}$$

$$\pi^2\frac{\overset{(1)}{\mathcal{N}}_{12}}{\alpha_b}\left(\frac{\partial\delta U_1}{\partial z_2} + \frac{\partial\delta U_2}{\partial z_1} + \frac{\partial\overset{(0)}{W}}{\partial z_1}\frac{\partial\delta W}{\partial z_2} + \frac{\partial\overset{(0)}{W}}{\partial z_2}\frac{\partial\delta W}{\partial z_1}\right) - \overset{(1)}{\mathcal{M}}_{11}\frac{\partial^2\delta W}{\partial z_1^2} - 2\overset{(1)}{\mathcal{M}}_{12}\frac{\partial^2\delta W}{\partial z_1\partial z_2} - \overset{(1)}{\mathcal{M}}_{22}\frac{\partial^2\delta W}{\partial z_2^2}$$

$$\delta\overset{(1)}{\mathcal{W}'}_{int} = \pi^2\left[\overset{(0)}{\mathcal{N}}_{11}\left(\frac{\partial\overset{(1)}{W}}{\partial z_1}\frac{\partial\delta W}{\partial z_1}\right) + \frac{\overset{(0)}{\mathcal{N}}_{12}}{\alpha_b}\left(\frac{\partial\overset{(1)}{W}}{\partial z_2}\frac{\partial\delta W}{\partial z_1} + \frac{\partial\overset{(1)}{W}}{\partial z_1}\frac{\partial\delta W}{\partial z_2}\right) + \overset{(0)}{\mathcal{N}}_{22}\left(\frac{\partial\overset{(1)}{W}}{\partial z_2}\frac{\partial\delta W}{\partial z_2}\right)\right] \tag{205c}$$

$$\overset{(1)B}{\mathcal{I}}_1 = \int_{\frac{a_2}{L_2}}^{\frac{b_2}{L_2}}\left\{\pi^2\overset{(1)}{\mathcal{N}}_{11}\,\delta U_1 + \pi^2\frac{\overset{(1)}{\mathcal{N}}_{12}}{\alpha_b}\,\delta U_2 - \overset{(1)}{\mathcal{M}}_{11}\frac{\partial\delta W}{\partial z_1}\right.$$

$$\left. + \left[\overset{(1)}{\mathcal{Z}}_1 + \frac{\partial\overset{(1)}{\mathcal{M}}_{12}}{\partial z_2} + \pi^2\left(\overset{(0)}{\mathcal{N}}_{11}\frac{\partial\overset{(1)}{W}}{\partial z_1} + \frac{\overset{(0)}{\mathcal{N}}_{12}}{\alpha_b}\frac{\partial\overset{(1)}{W}}{\partial z_2} + \overset{(1)}{\mathcal{N}}_{11}\frac{\partial\overset{(0)}{W}}{\partial z_1} + \frac{\overset{(1)}{\mathcal{N}}_{12}}{\alpha_b}\frac{\partial\overset{(0)}{W}}{\partial z_2}\right)\right]\delta W\right\}_{\frac{a_1}{L_1}}^{\frac{b_1}{L_1}} dz_2 \tag{205d}$$

$$\overset{(1)}{\mathcal{I}}{}^{B}_{2} = \int_{\frac{a_1}{L_1}}^{\frac{b_1}{L_1}} \left[\pi^2 \frac{\overset{(1)}{\mathcal{N}}_{12}}{\alpha_b} \delta U_1 + \pi^2 \overset{(1)}{\mathcal{N}}_{22} \delta U_2 - \overset{(1)}{\mathcal{M}}_{22} \frac{\partial \delta W}{\partial z_2} \right.$$

$$\left. + \left\{ \overset{(1)}{\mathcal{Z}}_2 + \frac{\partial \overset{(1)}{\mathcal{M}}_{12}}{\partial z_1} + \pi^2 \left(\frac{\overset{(0)}{\mathcal{N}}_{12}}{\alpha_b} \frac{\partial \overset{(1)}{W}}{\partial z_1} + \overset{(0)}{\mathcal{N}}_{22} \frac{\partial \overset{(1)}{W}}{\partial z_2} + \frac{\overset{(1)}{\mathcal{N}}_{12}}{\alpha_b} \frac{\partial \overset{(0)}{W}}{\partial z_1} + \overset{(1)}{\mathcal{N}}_{22} \frac{\partial \overset{(0)}{W}}{\partial z_2} \right) \right\} \delta W \right]_{\frac{a_2}{L_2}}^{\frac{b_2}{L_2}} dz_1 \tag{205e}$$

The symbol $\left\{ \left\{ \overset{(1)}{\mathcal{M}}_{12} \delta W \right\}_{\frac{a_2}{L_2}}^{\frac{b_2}{L_2}} \right\}_{\frac{a_1}{L_1}}^{\frac{b_1}{L_1}}$ denotes the evalution of $\overset{(1)}{\mathcal{M}}_{12} \delta W$ at discontinuities of the boundary curve $\partial\mathcal{A}$ and are commonly called corner conditions. Next, noting that the boundary conditions given by equations (201) and (202) are homogeneous and enforcing the conditions that the virtual displacements satisfy the kinematic boundary conditions and the kinematic relations given by equations (192)-(194) results in the following form for equation (205a):

$$\int\int_{\mathcal{A}} \left[\delta \overset{(1)}{\mathcal{W}}_{int} + \delta \overset{(1)}{\mathcal{W}'}_{int} \right] dz_1 dz_2 = 0 \tag{206a}$$

with

$$\delta \overset{(1)}{\mathcal{W}}_{int} = \pi^2 \left(\overset{(1)}{\mathcal{N}}_{11} \overset{(1)}{\delta E}_{11} + \frac{\overset{(1)}{\mathcal{N}}_{12}}{\alpha_b} \overset{(1)}{\delta G}_{12} + \overset{(1)}{\mathcal{N}}_{22} \overset{(1)}{\delta E}_{22} \right) + \overset{(1)}{\mathcal{M}}_{11} \overset{(1)}{\delta \mathcal{K}}_{11} + \overset{(1)}{\mathcal{M}}_{12} \overset{(1)}{\delta \mathcal{K}}_{12} + \overset{(1)}{\mathcal{M}}_{22} \overset{(1)}{\delta \mathcal{K}}_{22} \tag{206b}$$

$$\delta \overset{(1)}{\mathcal{W}'}_{int} = \pi^2 \left[\overset{(0)}{\mathcal{N}}_{11} \left(\overset{(1)}{\Omega}_1 \overset{(1)}{\delta \Omega}_1 \right) + \frac{\overset{(0)}{\mathcal{N}}_{12}}{\alpha_b} \left(\overset{(1)}{\Omega}_2 \overset{(1)}{\delta \Omega}_1 + \overset{(1)}{\Omega}_1 \overset{(1)}{\delta \Omega}_2 \right) + \overset{(0)}{\mathcal{N}}_{22} \left(\overset{(1)}{\Omega}_2 \overset{(1)}{\delta \Omega}_2 \right) \right] \tag{206c}$$

where

$$\overset{(1)}{\delta \Omega}_1 \equiv - \frac{\partial \overset{(1)}{\delta W}}{\partial z_1} = \delta \left(\overset{(1)}{\Omega}_1 \right) \tag{207a}$$

$$\overset{(1)}{\delta \Omega}_2 \equiv - \frac{\partial \overset{(1)}{\delta W}}{\partial z_2} = \delta \left(\overset{(1)}{\Omega}_2 \right) \tag{207b}$$

$$\overset{(1)}{\delta E}_{11} \equiv \frac{\partial \overset{(1)}{\delta U}_1}{\partial z_1} + \sqrt{12} Z_1 \overset{(1)}{\delta W} + \frac{\partial \overset{(0)}{W}}{\partial z_1} \frac{\partial \overset{(1)}{\delta W}}{\partial z_1} = \delta\left(\overset{(1)}{E}_{11} \right) \tag{208a}$$

$$\overset{(1)}{\delta E}_{22} \equiv \frac{\partial \overset{(1)}{\delta U}_2}{\partial z_2} + \sqrt{12} Z_2 \overset{(1)}{\delta W} + \frac{\partial \overset{(0)}{W}}{\partial z_2} \frac{\partial \overset{(1)}{\delta W}}{\partial z_2} = \delta\left(\overset{(1)}{E}_{22} \right) \tag{208b}$$

$$\overset{(1)}{\delta G}_{12} \equiv \frac{\partial \overset{(1)}{\delta U}_1}{\partial z_2} + \frac{\partial \overset{(1)}{\delta U}_2}{\partial z_1} + \frac{\partial \overset{(0)}{W}}{\partial z_1} \frac{\partial \overset{(1)}{\delta W}}{\partial z_2} + \frac{\partial \overset{(0)}{W}}{\partial z_2} \frac{\partial \overset{(1)}{\delta W}}{\partial z_1} = \delta\left(\overset{(1)}{G}_{12} \right) \tag{208c}$$

$$\overset{(1)}{\delta \varkappa}_{11} \equiv - \frac{\partial^2 \overset{(1)}{\delta W}}{\partial z_1^2} = \delta\left(\overset{(1)}{\varkappa}_{11} \right) \tag{209a}$$

$$\overset{(1)}{\delta \varkappa}_{22} \equiv - \frac{\partial^2 \overset{(1)}{\delta W}}{\partial z_2^2} = \delta\left(\overset{(1)}{\varkappa}_{22} \right) \tag{209b}$$

$$\overset{(1)}{\delta \varkappa}_{12} \equiv - 2 \frac{\partial^2 \overset{(1)}{\delta W}}{\partial z_1 \partial z_2} = \delta\left(\overset{(1)}{\varkappa}_{12} \right) \tag{209c}$$

where δ denotes the variational operator of the Calculus of Variations. A convenient matrix form of this variational statement is given by

$$\iint_{\mathcal{A}} \left[\pi^2 \left\{ \overset{(1)}{n} \right\}^{\mathbf{T}} \left\{ \overset{(1)}{\delta E} \right\} + \left\{ \overset{(1)}{m} \right\}^{\mathbf{T}} \left\{ \overset{(1)}{\delta \varkappa} \right\} + \pi^2 \left\{ \overset{(1)}{\Omega} \right\}^{\mathbf{T}} \left[\overset{(0)}{n} \right] \left\{ \overset{(1)}{\delta \Omega} \right\} \right] dz_1 dz_2 = 0 \tag{210}$$

where

$$\left\{ \overset{(1)}{n} \right\}^{\mathbf{T}} = \left[\overset{(1)}{n}_{11} \quad \overset{(1)}{n}_{22} \quad \frac{\overset{(1)}{n}_{12}}{\alpha_b} \right] \tag{211a}$$

$$\left\{ \overset{(1)}{m} \right\}^{\mathbf{T}} = \left[\overset{(1)}{m}_{11} \quad \overset{(1)}{m}_{22} \quad \overset{(1)}{m}_{12} \right] \tag{211b}$$

$$\left[\overset{(0)}{\mathcal{N}}\right] = \begin{bmatrix} \overset{(0)}{\mathcal{N}}_{11} & \dfrac{\overset{(0)}{\mathcal{N}}_{12}}{\alpha_b} \\ \dfrac{\overset{(0)}{\mathcal{N}}_{12}}{\alpha_b} & \overset{(0)}{\mathcal{N}}_{22} \end{bmatrix} = \left[\overset{(0)}{\mathcal{N}}(\tilde{p})\right] \tag{211c}$$

$$\left\{\overset{(0)}{\Omega}\right\}^T = \left[\overset{(0)}{\Omega}_1 \;\; \overset{(0)}{\Omega}_2\right] = \left\{\overset{(0)}{\Omega}(\tilde{p})\right\}^T \tag{212a}$$

$$\left\{\overset{(1)}{\Omega}\right\}^T = \left[\overset{(1)}{\Omega}_1 \;\; \overset{(1)}{\Omega}_2\right] \tag{212b}$$

$$\left\{\delta\overset{(1)}{\Omega}\right\}^T = \left[\delta\overset{(1)}{\Omega}_1 \;\; \delta\overset{(1)}{\Omega}_2\right] \tag{212c}$$

$$\left\{\overset{(1)}{E}\right\}^T = \left[\overset{(1)}{E}_{11} \;\; \overset{(1)}{E}_{22} \;\; \overset{(1)}{G}_{12}\right] \tag{213a}$$

$$\left\{\delta\overset{(1)}{E}\right\}^T = \left[\delta\overset{(1)}{E}_{11} \;\; \delta\overset{(1)}{E}_{22} \;\; \delta\overset{(1)}{G}_{12}\right] \tag{213b}$$

$$\left\{\overset{(1)}{\mathcal{K}}\right\}^T = \left[\overset{(1)}{\mathcal{K}}_{11} \;\; \overset{(1)}{\mathcal{K}}_{22} \;\; \overset{(1)}{\mathcal{K}}_{12}\right] \tag{213c}$$

$$\left\{\delta\overset{(1)}{\mathcal{K}}\right\}^T = \left[\delta\overset{(1)}{\mathcal{K}}_{11} \;\; \delta\overset{(1)}{\mathcal{K}}_{22} \;\; \delta\overset{(1)}{\mathcal{K}}_{12}\right] \tag{213d}$$

Nondimensional Stress-Function Formulation for Bifurcation

Like for the nonlinear boundary-value problem described previously herein, the stress-function formulation of the Donnell-Mushtari-Vlasov bifurcation equations is also used to facilitiate solution of practical problems by reducing the number of unknown functions to two. These two unknowns for this case are the normal displacement $\overset{(1)}{W}(z_1, z_2)$ and a corresponding stress function $\overset{(1)}{\mathcal{F}}(z_1, z_2)$, and the procedure for obtaining the corresponding equations is the same as that previously described herein for the nonlinear boundary-value problem. Subsequently, the reduction of the boundary-eigenvalue problem to two coupled partial differential equations is presented, along with the corresponding boundary conditions. Then, the corresponding expressions for the virtual work and complementary virtual work, are presented that are useful for

for solving boundary-value problems by direct variational methods.

Following the definitions given by equations (115), let $\overset{(1)}{\mathcal{F}} = \overset{(1)}{\mathcal{F}}(z_1, z_2)$ denote the stress function defined by

$$\pi^2 \overset{(1)}{\mathcal{N}}_{11} = \frac{\partial^2 \overset{(1)}{\mathcal{F}}}{\partial z_2^2} \tag{214a}$$

$$\pi^2 \overset{(1)}{\mathcal{N}}_{22} = \frac{\partial^2 \overset{(1)}{\mathcal{F}}}{\partial z_1^2} \tag{214b}$$

$$\frac{\pi^2}{\alpha_b} \overset{(1)}{\mathcal{N}}_{12} = - \frac{\partial^2 \overset{(1)}{\mathcal{F}}}{\partial z_1 \partial z_2} \tag{214c}$$

such that equations (198a) and (198b) are satisfied identically and

$$\mathcal{F} = \overset{(0)}{\mathcal{F}} + \varepsilon \overset{(1)}{\mathcal{F}} + \mathcal{O}(\varepsilon^2) \tag{214d}$$

Using equations (181), (198a) - (198d), and (214), the transverse equilibrium equation given by equation (198e) becomes

$$\begin{aligned} &\frac{\partial^2 \overset{(1)}{\mathcal{M}}_{11}}{\partial z_1^2} + 2 \frac{\partial^2 \overset{(1)}{\mathcal{M}}_{12}}{\partial z_1 \partial z_2} + \frac{\partial^2 \overset{(1)}{\mathcal{M}}_{22}}{\partial z_2^2} - \sqrt{12} \left(\frac{\partial^2 \overset{(1)}{\mathcal{F}}}{\partial z_2^2} Z_1 + \frac{\partial^2 \overset{(1)}{\mathcal{F}}}{\partial z_1^2} Z_2 \right) - \tilde{p} \pi^2 \left[g_1 \frac{\partial \overset{(1)}{W}}{\partial z_1} + g_2 \frac{\partial \overset{(1)}{W}}{\partial z_2} \right] \\ &\qquad + \mathcal{L}\left(\overset{(1)}{\mathcal{F}}, \overset{(0)}{W} \right) + \pi^2 \overset{(0)}{\mathcal{N}}_{11}(\tilde{p}) \frac{\partial^2 \overset{(1)}{W}}{\partial z_1^2} + \frac{2\pi^2}{\alpha_b} \overset{(0)}{\mathcal{N}}_{12}(\tilde{p}) \frac{\partial^2 \overset{(1)}{W}}{\partial z_1 \partial z_2} + \pi^2 \overset{(0)}{\mathcal{N}}_{22}(\tilde{p}) \frac{\partial^2 \overset{(1)}{W}}{\partial z_2^2} = 0 \end{aligned} \tag{215}$$

where

$$\mathcal{L}\left(\overset{(1)}{\mathcal{F}}, \overset{(0)}{W} \right) = \frac{\partial^2 \overset{(1)}{\mathcal{F}}}{\partial z_2^2} \frac{\partial^2 \overset{(0)}{W}}{\partial z_1^2} + \frac{\partial^2 \overset{(1)}{\mathcal{F}}}{\partial z_1^2} \frac{\partial^2 \overset{(0)}{W}}{\partial z_2^2} - 2 \frac{\partial^2 \overset{(1)}{\mathcal{F}}}{\partial z_1 \partial z_2} \frac{\partial^2 \overset{(0)}{W}}{\partial z_1 \partial z_2} \tag{216}$$

Next, substituting equations (214) into equations (197), and then substituting the result into equation (215) yields the nondimensional stress-function form of transverse equilibrium equation given by

$$\begin{aligned} &\mathcal{D}_b\left(\overset{(1)}{W} \right) + \sqrt{12} \mathcal{D}_c\left(\overset{(1)}{\mathcal{F}} \right) - \mathcal{D}_\varepsilon\left(\overset{(1)}{\mathcal{F}} \right) - \mathcal{L}\left(\overset{(1)}{\mathcal{F}}, \overset{(0)}{W}(\tilde{p}) \right) + \tilde{p} \pi^2 \left[g_1 \frac{\partial \overset{(1)}{W}}{\partial z_1} + g_2 \frac{\partial \overset{(1)}{W}}{\partial z_2} \right] \\ &\qquad - \pi^2 \left[\overset{(0)}{\mathcal{N}}_{11}(\tilde{p}) \frac{\partial^2 \overset{(1)}{W}}{\partial z_1^2} + \frac{2}{\alpha_b} \overset{(0)}{\mathcal{N}}_{12}(\tilde{p}) \frac{\partial^2 \overset{(1)}{W}}{\partial z_1 \partial z_2} + \overset{(0)}{\mathcal{N}}_{22}(\tilde{p}) \frac{\partial^2 \overset{(1)}{W}}{\partial z_2^2} \right] = 0 \end{aligned} \tag{217}$$

where

$$\mathcal{D}_b\left(\overset{(1)}{W}\right) = \mathcal{A}_{11}\frac{\partial^4 \overset{(1)}{W}}{\partial z_1^4} + 4\mathcal{A}_{16}\frac{\partial^4 \overset{(1)}{W}}{\partial z_1^3 \partial z_2} + 2\left(\mathcal{A}_{12} + 2\mathcal{A}_{66}\right)\frac{\partial^4 \overset{(1)}{W}}{\partial z_1^2 \partial z_2^2} + 4\mathcal{A}_{26}\frac{\partial^4 \overset{(1)}{W}}{\partial z_1 \partial z_2^3} + \mathcal{A}_{22}\frac{\partial^4 \overset{(1)}{W}}{\partial z_2^4} \tag{218a}$$

$$\mathcal{D}_c\left(\overset{(1)}{\mathcal{F}}\right) = Z_1\frac{\partial^2 \overset{(1)}{\mathcal{F}}}{\partial z_2^2} + Z_2\frac{\partial^2 \overset{(1)}{\mathcal{F}}}{\partial z_1^2} \tag{218b}$$

$$\begin{aligned}\mathcal{D}_{\mathcal{B}}\left(\overset{(1)}{\mathcal{F}}\right) = {} & \mathcal{B}_{21}\frac{\partial^4 \overset{(1)}{\mathcal{F}}}{\partial z_1^4} + \left(2\mathcal{B}_{26} - \mathcal{B}_{61}\right)\frac{\partial^4 \overset{(1)}{\mathcal{F}}}{\partial z_1^3 \partial z_2} + \left(\mathcal{B}_{11} + \mathcal{B}_{22} - 2\mathcal{B}_{66}\right)\frac{\partial^4 \overset{(1)}{\mathcal{F}}}{\partial z_1^2 \partial z_2^2} \\ & + \left(2\mathcal{B}_{16} - \mathcal{B}_{62}\right)\frac{\partial^4 \overset{(1)}{\mathcal{F}}}{\partial z_1 \partial z_2^3} + \mathcal{B}_{12}\frac{\partial^4 \overset{(1)}{\mathcal{F}}}{\partial z_2^4}\end{aligned} \tag{218c}$$

The nondimensional compatibility equation needed is obtained by substituting equations (175c) and (190) into equation (105), and then retaining only terms that are first order in the small parameter ε. The resulting equation is given by

$$\frac{\partial^2 \overset{(1)}{E}_{11}}{\partial z_2^2} + \frac{\partial^2 \overset{(1)}{E}_{22}}{\partial z_1^2} - \frac{\partial^2 \overset{(1)}{G}_{12}}{\partial z_1 \partial z_2} = \sqrt{12}\,\mathcal{D}_c\left(\overset{(1)}{W}\right) + \mathcal{L}\left(\overset{(0)}{W}(\tilde{p}), \overset{(1)}{W}\right) \tag{219}$$

Next, substituting equations (214) into equations (196), and then substituting the result into equation (219) yields the nondimensional stress-function form of the compatibility equation as

$$\mathcal{D}_m\left(\overset{(1)}{\mathcal{F}}\right) + \mathcal{D}_{\mathcal{B}}\left(\overset{(1)}{W}\right) - \sqrt{12}\,\mathcal{D}_c\left(\overset{(1)}{W}\right) = \mathcal{L}\left(\overset{(0)}{W}(\tilde{p}), \overset{(1)}{W}\right) \tag{220}$$

where

$$\mathcal{D}_m\left(\overset{(1)}{\mathcal{F}}\right) \equiv \alpha_m^2\frac{\partial^4 \overset{(1)}{\mathcal{F}}}{\partial z_1^4} + 2\alpha_m\gamma_m\frac{\partial^4 \overset{(1)}{\mathcal{F}}}{\partial z_1^3 \partial z_2} + 2\mu\frac{\partial^4 \overset{(1)}{\mathcal{F}}}{\partial z_1^2 \partial z_2^2} + 2\frac{\delta_m}{\alpha_m}\frac{\partial^4 \overset{(1)}{\mathcal{F}}}{\partial z_1 \partial z_2^3} + \frac{1}{\alpha_m^2}\frac{\partial^4 \overset{(1)}{\mathcal{F}}}{\partial z_2^4} \tag{221a}$$

$$\mathcal{L}\left(\overset{(0)}{W}(\tilde{p}), \overset{(1)}{W}\right) = \frac{\partial^2 \overset{(0)}{W}}{\partial z_2^2}\frac{\partial^2 \overset{(1)}{W}}{\partial z_1^2} + \frac{\partial^2 \overset{(0)}{W}}{\partial z_1^2}\frac{\partial^2 \overset{(1)}{W}}{\partial z_2^2} - 2\frac{\partial^2 \overset{(0)}{W}}{\partial z_1 \partial z_2}\frac{\partial^2 \overset{(1)}{W}}{\partial z_1 \partial z_2} \tag{221b}$$

The boundary conditions associated with the adjacent equilibrium states are obtained by using equations (197), (198c), (198d), and (214) with equations (201) and (202). The boundary conditions on the edges $z_1 = a_1 / L_1$ and $z_1 = b_1 / L_1$, given by equations (201), become

$$\frac{\partial^2 \overset{(1)}{\mathcal{F}}}{\partial z_2^2} = 0 \quad \text{or} \quad \overset{(1)}{U}_1 = 0 \tag{222a}$$

$$\frac{\partial^{2}\mathcal{F}^{(1)}}{\partial z_1 \partial z_2} = 0 \quad \text{or} \quad \overset{(1)}{U}_2 = 0 \tag{222b}$$

$$\mathcal{B}_{21}\frac{\partial^{3}\mathcal{F}^{(1)}}{\partial z_1^{3}} + \left(2\mathcal{B}_{26} - \mathcal{B}_{61}\right)\frac{\partial^{3}\mathcal{F}^{(1)}}{\partial z_1^{2}\partial z_2} + \left(\mathcal{B}_{11} - 2\mathcal{B}_{66}\right)\frac{\partial^{3}\mathcal{F}^{(1)}}{\partial z_1 \partial z_2^{2}} + 2\mathcal{B}_{16}\frac{\partial^{3}\mathcal{F}^{(1)}}{\partial z_2^{3}} - \mathcal{A}_{11}\frac{\partial^{3}\overset{(1)}{W}}{\partial z_1^{3}} - 4\mathcal{A}_{16}\frac{\partial^{3}\overset{(1)}{W}}{\partial z_1^{2}\partial z_2}$$
$$- \left(\mathcal{A}_{12} + 4\mathcal{A}_{66}\right)\frac{\partial^{3}\overset{(1)}{W}}{\partial z_1 \partial z_2^{2}} - 2\mathcal{A}_{26}\frac{\partial^{3}\overset{(1)}{W}}{\partial z_2^{3}} + \pi^{2}\overset{(0)}{\mathcal{N}}_{11}\frac{\partial \overset{(1)}{W}}{\partial z_1} + \frac{\pi^{2}}{\alpha_b}\overset{(0)}{\mathcal{N}}_{12}\frac{\partial \overset{(1)}{W}}{\partial z_2} + \frac{\partial^{2}\mathcal{F}^{(1)}}{\partial z_2^{2}}\frac{\partial \overset{(0)}{W}}{\partial z_1} - \frac{\partial^{2}\mathcal{F}^{(1)}}{\partial z_1 \partial z_2}\frac{\partial \overset{(0)}{W}}{\partial z_2} = 0$$

$$\text{or} \quad \overset{(1)}{W} = 0 \tag{222c}$$

$$\mathcal{B}_{11}\frac{\partial^{2}\mathcal{F}^{(1)}}{\partial z_2^{2}} + \mathcal{B}_{21}\frac{\partial^{2}\mathcal{F}^{(1)}}{\partial z_1^{2}} - \mathcal{B}_{61}\frac{\partial^{2}\mathcal{F}^{(1)}}{\partial z_1 \partial z_2} - \mathcal{A}_{11}\frac{\partial^{2}\overset{(1)}{W}}{\partial z_1^{2}} - \mathcal{A}_{12}\frac{\partial^{2}\overset{(1)}{W}}{\partial z_2^{2}} - 2\mathcal{A}_{16}\frac{\partial^{2}\overset{(1)}{W}}{\partial z_1 \partial z_2} = 0 \quad \text{or} \quad \frac{\partial \overset{(1)}{W}}{\partial z_1} = 0 \tag{222d}$$

Similarly, on the edges $z_2 = a_2 / L_2$ and $z_2 = b_2 / L_2$, the boundary conditions given by equation (202) become

$$\frac{\partial^{2}\mathcal{F}^{(1)}}{\partial z_1^{2}} = 0 \quad \text{or} \quad \overset{(1)}{U}_2 = 0 \tag{223a}$$

$$\frac{\partial^{2}\mathcal{F}^{(1)}}{\partial z_1 \partial z_2} = 0 \quad \text{or} \quad \overset{(1)}{U}_1 = 0 \tag{223b}$$

$$2\mathcal{B}_{26}\frac{\partial^{3}\mathcal{F}^{(1)}}{\partial z_1^{3}} + \left(\mathcal{B}_{22} - 2\mathcal{B}_{66}\right)\frac{\partial^{3}\mathcal{F}^{(1)}}{\partial z_1^{2}\partial z_2} + \left(2\mathcal{B}_{16} - \mathcal{B}_{62}\right)\frac{\partial^{3}\mathcal{F}^{(1)}}{\partial z_1 \partial z_2^{2}} + \mathcal{B}_{12}\frac{\partial^{3}\mathcal{F}^{(1)}}{\partial z_2^{3}} - 2\mathcal{A}_{16}\frac{\partial^{3}\overset{(1)}{W}}{\partial z_1^{3}} - \mathcal{A}_{22}\frac{\partial^{3}\overset{(1)}{W}}{\partial z_2^{3}}$$
$$- \left(\mathcal{A}_{12} + 4\mathcal{A}_{66}\right)\frac{\partial^{3}\overset{(1)}{W}}{\partial z_1^{2}\partial z_2} - 4\mathcal{A}_{26}\frac{\partial^{3}\overset{(1)}{W}}{\partial z_1 \partial z_2^{2}} + \frac{\pi^{2}}{\alpha_b}\overset{(0)}{\mathcal{N}}_{12}\frac{\partial \overset{(1)}{W}}{\partial z_1} + \pi^{2}\overset{(0)}{\mathcal{N}}_{22}\frac{\partial \overset{(1)}{W}}{\partial z_2} + \frac{\partial^{2}\mathcal{F}^{(1)}}{\partial z_1^{2}}\frac{\partial \overset{(0)}{W}}{\partial z_2} - \frac{\partial^{2}\mathcal{F}^{(1)}}{\partial z_1 \partial z_2}\frac{\partial \overset{(0)}{W}}{\partial z_1} = 0$$

$$\text{or} \quad \overset{(1)}{W} = 0 \tag{223c}$$

$$\mathcal{B}_{12}\frac{\partial^{2}\mathcal{F}^{(1)}}{\partial z_2^{2}} + \mathcal{B}_{22}\frac{\partial^{2}\mathcal{F}^{(1)}}{\partial z_1^{2}} - \mathcal{B}_{62}\frac{\partial^{2}\mathcal{F}^{(1)}}{\partial z_1 \partial z_2} - \mathcal{A}_{12}\frac{\partial^{2}\overset{(1)}{W}}{\partial z_1^{2}} - \mathcal{A}_{22}\frac{\partial^{2}\overset{(1)}{W}}{\partial z_2^{2}} - 2\mathcal{A}_{26}\frac{\partial^{2}\overset{(1)}{W}}{\partial z_1 \partial z_2} = 0 \quad \text{or} \quad \frac{\partial \overset{(1)}{W}}{\partial z_2} = 0 \tag{223d}$$

In these equations, the tangential displacements must be expressed in terms of the normal displacement and the stress function. Expressions for the tangential displacements $\overset{(1)}{U}_1$ and $\overset{(1)}{U}_2$ are obtained from the nondimensional strain-displacement relation, equations (193); that is

$$\frac{\partial \overset{(1)}{U}_1}{\partial z_1} = \overset{(1)}{E}_{11} - \sqrt{12} Z_1 \overset{(1)}{W} - \frac{\partial \overset{(0)}{W}}{\partial z_1} \frac{\partial \overset{(1)}{W}}{\partial z_1} \tag{224a}$$

$$\frac{\partial \overset{(1)}{U}_2}{\partial z_2} = \overset{(1)}{E}_{22} - \sqrt{12} Z_2 \overset{(1)}{W} - \frac{\partial \overset{(0)}{W}}{\partial z_2} \frac{\partial \overset{(1)}{W}}{\partial z_2} \tag{224b}$$

$$\frac{\partial \overset{(1)}{U}_1}{\partial z_2} + \frac{\partial \overset{(1)}{U}_2}{\partial z_1} = \overset{(1)}{G}_{12} - \frac{\partial \overset{(0)}{W}}{\partial z_1} \frac{\partial \overset{(1)}{W}}{\partial z_2} - \frac{\partial \overset{(0)}{W}}{\partial z_2} \frac{\partial \overset{(1)}{W}}{\partial z_1} \tag{224c}$$

Substituting equations (214) into equation (196) and the result into these three expressions gives

$$\begin{aligned} \frac{\partial \overset{(1)}{U}_1}{\partial z_1} = {} & \frac{1}{\alpha_m^2} \frac{\partial^2 \overset{(1)}{\mathcal{F}}}{\partial z_2^2} - \nu_m \frac{\partial^2 \overset{(1)}{\mathcal{F}}}{\partial z_1^2} + \frac{\delta_m}{\alpha_m} \frac{\partial^2 \overset{(1)}{\mathcal{F}}}{\partial z_1 \partial z_2} \\ & + \mathcal{B}_{11} \frac{\partial^2 \overset{(1)}{W}}{\partial z_1^2} + \mathcal{B}_{12} \frac{\partial^2 \overset{(1)}{W}}{\partial z_2^2} + 2\mathcal{B}_{16} \frac{\partial^2 \overset{(1)}{W}}{\partial z_1 \partial z_2} - \sqrt{12} Z_1 \overset{(1)}{W} - \frac{\partial \overset{(0)}{W}}{\partial z_1} \frac{\partial \overset{(1)}{W}}{\partial z_1} \end{aligned} \tag{225a}$$

$$\begin{aligned} \frac{\partial \overset{(1)}{U}_2}{\partial z_2} = {} & - \nu_m \frac{\partial^2 \overset{(1)}{\mathcal{F}}}{\partial z_2^2} + \alpha_m^2 \frac{\partial^2 \overset{(1)}{\mathcal{F}}}{\partial z_1^2} + \alpha_m \gamma_m \frac{\partial^2 \overset{(1)}{\mathcal{F}}}{\partial z_1 \partial z_2} \\ & + \mathcal{B}_{21} \frac{\partial^2 \overset{(1)}{W}}{\partial z_1^2} + \mathcal{B}_{22} \frac{\partial^2 \overset{(1)}{W}}{\partial z_2^2} + 2\mathcal{B}_{26} \frac{\partial^2 \overset{(1)}{W}}{\partial z_1 \partial z_2} - \sqrt{12} Z_2 \overset{(1)}{W} - \frac{\partial \overset{(0)}{W}}{\partial z_2} \frac{\partial \overset{(1)}{W}}{\partial z_2} \end{aligned} \tag{225b}$$

$$\begin{aligned} \frac{\partial \overset{(1)}{U}_1}{\partial z_2} + \frac{\partial \overset{(1)}{U}_2}{\partial z_1} = {} & - \frac{\delta_m}{\alpha_m} \frac{\partial^2 \overset{(1)}{\mathcal{F}}}{\partial z_2^2} - \alpha_m \gamma_m \frac{\partial^2 \overset{(1)}{\mathcal{F}}}{\partial z_1^2} - 2\left(\mu + \nu_m\right) \frac{\partial^2 \overset{(1)}{\mathcal{F}}}{\partial z_1 \partial z_2} + \\ & \mathcal{B}_{61} \frac{\partial^2 \overset{(1)}{W}}{\partial z_1^2} + \mathcal{B}_{62} \frac{\partial^2 \overset{(1)}{W}}{\partial z_2^2} + 2\mathcal{B}_{66} \frac{\partial^2 \overset{(1)}{W}}{\partial z_1 \partial z_2} - \frac{\partial \overset{(0)}{W}}{\partial z_1} \frac{\partial \overset{(1)}{W}}{\partial z_2} - \frac{\partial \overset{(0)}{W}}{\partial z_2} \frac{\partial \overset{(1)}{W}}{\partial z_1} \end{aligned} \tag{225c}$$

The nondimensional displacements are represented in terms of $\overset{(1)}{\mathcal{F}}$ and $\overset{(1)}{W}$, to within a rigid-body motion, by the integrals of these three equations.

Virtual Work in terms of $\overset{(1)}{W}$ and $\overset{(1)}{\mathcal{F}}$

Equations (217) and (220) are the nondimensional forms of the equations governing pointwise equilibrium normal to the tangent plane and compatibility, respectively. For some problems, it is more useful to use a stress-function formulation of the variational principle given by equation (210) instead of equation (217). First, by using equations (214), equation (211a) is written as

$$\pi^2\left\{\overset{(1)}{\mathcal{N}}\right\} = \left\{\partial\overset{(1)}{\mathcal{F}}\right\} \equiv \left[\frac{\partial^2\overset{(1)}{\mathcal{F}}}{\partial z_2^2} \quad \frac{\partial^2\overset{(1)}{\mathcal{F}}}{\partial z_1^2} \quad -\frac{\partial^2\overset{(1)}{\mathcal{F}}}{\partial z_1 \partial z_2}\right]^{\mathbf{T}} \tag{226a}$$

such that

$$\delta\left\{\partial\overset{(1)}{\mathcal{F}}\right\} = \left\{\partial\delta\overset{(1)}{\mathcal{F}}\right\} \equiv \left[\frac{\partial^2\delta\overset{(1)}{\mathcal{F}}}{\partial z_2^2} \quad \frac{\partial^2\delta\overset{(1)}{\mathcal{F}}}{\partial z_1^2} \quad -\frac{\partial^2\delta\overset{(1)}{\mathcal{F}}}{\partial z_1 \partial z_2}\right]^{\mathbf{T}} \tag{226b}$$

Similarly, by using equations (194), (207)-(209), and (214), equations (196) and (197) yield

$$\left\{\delta\overset{(1)}{\mathrm{E}}\right\} = \left[\mathcal{a}\right]\left\{\partial\delta\overset{(1)}{\mathcal{F}}\right\} - \left[\mathcal{B}\right]\left\{\delta\overset{(1)}{\mathcal{K}}\right\} \tag{227}$$

and

$$\left\{\overset{(1)}{\mathcal{M}}\right\} = \left[\mathcal{B}\right]^{\mathbf{T}}\left\{\partial\overset{(1)}{\mathcal{F}}\right\} + \left[\mathcal{d}\right]\left\{\overset{(1)}{\mathcal{K}}\right\} \tag{228}$$

where $\left[\mathcal{a}\right]$, $\left[\mathcal{B}\right]$, and $\left[\mathcal{d}\right]$ are defined by equations (154a), (139b), and (139c), respectively. Noting that equation (206b) can be expressed as

$$\delta\overset{(1)}{\mathcal{W}}_{\mathrm{int}} = \left\{\partial\overset{(1)}{\mathcal{F}}\right\}^{\mathbf{T}}\left\{\delta\overset{(1)}{\mathrm{E}}\right\} + \left\{\overset{(1)}{\mathcal{M}}\right\}^{\mathbf{T}}\left\{\delta\overset{(1)}{\mathcal{K}}\right\} \tag{229}$$

it follows that

$$\delta\overset{(1)}{\mathcal{W}}_{\mathrm{int}} = \left\{\partial\overset{(1)}{\mathcal{F}}\right\}^{\mathbf{T}}\left[\mathcal{a}\right]\left\{\partial\delta\overset{(1)}{\mathcal{F}}\right\} - \left\{\partial\overset{(1)}{\mathcal{F}}\right\}^{\mathbf{T}}\left[\mathcal{B}\right]\left\{\delta\overset{(1)}{\mathcal{K}}\right\} \tag{230}$$

The variational principle specified by equation (206a) is given in terms of the stress function $\overset{(1)}{\mathcal{F}}$ and normal displacement $\overset{(1)}{\mathrm{W}}$ by using equation (230) and

$$\delta\overset{(1)}{\mathcal{W}}'_{\mathrm{int}} = \pi^2\left\{\overset{(1)}{\Omega}\right\}^{\mathbf{T}}\left[\overset{(0)}{\mathcal{N}}\right]\left\{\delta\overset{(1)}{\Omega}\right\} \tag{231}$$

The boundary-eigenvalue problem is then posed with the resulting variational principle, the compatibility equation given by equation (220), and the appropriate boundary conditions. The variational principle enforces equilibrium in the direction normal to the shell reference surface.

Complementary Virtual Work in terms of $\overset{(1)}{W}$ and $\overset{(1)}{\mathcal{F}}$

In lieu of using compatibilty equation (220), a variational principle is obtained from the complementary virtual work given by

$$\int\int_{\mathcal{A}} \delta\overset{(1)}{\mathcal{W}}{}^{*}_{\text{int}} dz_1 dz_2 + \delta\overset{(1)}{\mathcal{W}}{}^{*\,B} = 0 \tag{232a}$$

with

$$\begin{aligned}\delta\overset{(1)}{\mathcal{W}}{}^{*}_{\text{int}} = &\left[\overset{(1)}{E}_{11} - \frac{\partial \overset{(1)}{U}_1}{\partial z_1} - \sqrt{12} Z_1 \overset{(1)}{W} - \frac{\partial \overset{(0)}{W}}{\partial z_1}\frac{\partial \overset{(1)}{W}}{\partial z_1}\right]\pi^2 \delta\mathcal{N}^{*}_{11} \\ &+ \left[\overset{(1)}{E}_{22} - \frac{\partial \overset{(1)}{U}_2}{\partial z_2} - \sqrt{12} Z_2 \overset{(1)}{W} - \frac{\partial \overset{(0)}{W}}{\partial z_2}\frac{\partial \overset{(1)}{W}}{\partial z_2}\right]\pi^2 \delta\mathcal{N}^{*}_{22} \\ &+ \left[\overset{(1)}{G}_{12} - \frac{\partial \overset{(1)}{U}_1}{\partial z_2} - \frac{\partial \overset{(1)}{U}_2}{\partial z_1} - \frac{\partial \overset{(0)}{W}}{\partial z_1}\frac{\partial \overset{(1)}{W}}{\partial z_2} - \frac{\partial \overset{(0)}{W}}{\partial z_2}\frac{\partial \overset{(1)}{W}}{\partial z_1}\right]\frac{\pi^2}{\alpha_b}\delta\mathcal{N}^{*}_{12}\end{aligned} \tag{232b}$$

$$\delta\overset{(1)}{\mathcal{W}}{}^{*\,B} = \pi^2 \int_{\frac{a_1}{L_1}}^{\frac{b_1}{L_1}} \left\{\overset{(1)}{U}_1 \frac{\delta\mathcal{N}^{*}_{12}}{\alpha_b} + \overset{(1)}{U}_2 \delta\mathcal{N}^{*}_{22}\right\}_{\frac{a_2}{L_2}}^{\frac{b_2}{L_2}} dz_1 + \pi^2 \int_{\frac{a_2}{L_2}}^{\frac{b_2}{L_2}} \left\{\overset{(1)}{U}_1 \delta\mathcal{N}^{*}_{11} + \overset{(1)}{U}_2 \frac{\delta\mathcal{N}^{*}_{12}}{\alpha_b}\right\}_{\frac{a_1}{L_1}}^{\frac{b_1}{L_1}} dz_2 \tag{232c}$$

and where $\pi^2\delta\mathcal{N}^{*}_{11}$, $\pi^2\delta\mathcal{N}^{*}_{22}$, and $\frac{\pi^2}{\alpha_b}\delta\mathcal{N}^{*}_{12}$ are statically admissible virtual stress resultants associated with the corresponding incompatible tangential strains defined by equations (193). Equation (232c) represents the virtual work that occurs when the tangential displacements fail to satisfy the geometric boundary conditions specified by equations (201a,b) and (202a,b). If the geometric constraints are forced to be satisfied and the strains are forced to be compatible, pointwise, then the resulting work must be zero, as stated by equation (232a). Integrating equation (232b) by parts, by using equations (25) specialized for the nondimensional coordinates (z_1, z_2), gives

$$\int\int_{\mathcal{A}} \delta\overset{(1)}{\mathcal{W}}{}^{*}_{\text{int}}\, dz_1 dz_2 = \int\int_{\mathcal{A}} \left(\left[\overset{(1)}{E}_{11} - \sqrt{12} Z_1 \overset{(1)}{W} - \frac{\partial \overset{(0)}{W}}{\partial z_1} \frac{\partial \overset{(1)}{W}}{\partial z_1} \right] \pi^2 \delta\mathcal{N}^{*}_{11} \right.$$

$$+ \left[\overset{(1)}{E}_{22} - \sqrt{12} Z_2 \overset{(1)}{W} - \frac{\partial \overset{(0)}{W}}{\partial z_2} \frac{\partial \overset{(1)}{W}}{\partial z_2} \right] \pi^2 \delta\mathcal{N}^{*}_{22} + \left. \left[\overset{(1)}{G}_{12} - \frac{\partial \overset{(0)}{W}}{\partial z_1} \frac{\partial \overset{(1)}{W}}{\partial z_2} - \frac{\partial \overset{(0)}{W}}{\partial z_2} \frac{\partial \overset{(1)}{W}}{\partial z_1} \right] \frac{\pi^2}{\alpha_b} \delta\mathcal{N}^{*}_{12} \right) dz_1 dz_2$$

$$+ \int\int_{\mathcal{A}} \left(\left[\pi^2 \frac{\partial \delta\mathcal{N}^{*}_{11}}{\partial z_1} + \frac{\pi^2}{\alpha_b} \frac{\partial \delta\mathcal{N}^{*}_{12}}{\partial z_2} \right] \overset{(1)}{U}_1 + \left[\frac{\pi^2}{\alpha_b} \frac{\partial \delta\mathcal{N}^{*}_{12}}{\partial z_1} + \pi^2 \frac{\partial \delta\mathcal{N}^{*}_{22}}{\partial z_2} \right] \overset{(1)}{U}_2 \right) dz_1 dz_2 \tag{233}$$

$$- \pi^2 \int_{\frac{a_2}{L_2}}^{\frac{b_2}{L_2}} \left\{ \overset{(1)}{U}_1 \delta\mathcal{N}^{*}_{11} + \overset{(1)}{U}_2 \frac{\delta\mathcal{N}^{*}_{12}}{\alpha_b} \right\}_{\frac{a_1}{L_1}}^{\frac{b_1}{L_1}} dz_2 - \pi^2 \int_{\frac{a_1}{L_1}}^{\frac{b_1}{L_1}} \left\{ \overset{(1)}{U}_1 \frac{\delta\mathcal{N}^{*}_{12}}{\alpha_b} + \overset{(1)}{U}_2 \delta\mathcal{N}^{*}_{22} \right\}_{\frac{a_2}{L_2}}^{\frac{b_2}{L_2}} dz_1$$

The virtual stress resultants are required to be statically admissible; that is they satisfy equilibrium equations (198a,b) and the force boundary conditions in equations (201a,b) and (202a,b). This requirement yields $\delta\mathcal{N}^{*}_{11} \to \delta\overset{(1)}{\mathcal{N}}_{11}$, $\delta\mathcal{N}^{*}_{22} \to \delta\overset{(1)}{\mathcal{N}}_{22}$, and $\delta\mathcal{N}^{*}_{11} \to \delta\overset{(1)}{\mathcal{N}}_{11}$. In addition, the boundary integrals in equations (232c) and (233) cancel. Thus, equation (232a) reduces to

$$\int\int_{\mathcal{A}} \delta\overset{(1)}{\mathcal{W}}{}^{*}_{\text{int}}\, dz_1 dz_2 = \int\int_{A} \left(\left[\overset{(1)}{E}_{11} - \sqrt{12} Z_1 \overset{(1)}{W} - \frac{\partial \overset{(0)}{W}}{\partial z_1} \frac{\partial \overset{(1)}{W}}{\partial z_1} \right] \frac{\partial^2 \overset{(1)}{\delta\mathcal{F}}}{\partial z_2^2} \right.$$

$$+ \left. \left[\overset{(1)}{E}_{22} - \sqrt{12} Z_2 \overset{(1)}{W} - \frac{\partial \overset{(0)}{W}}{\partial z_2} \frac{\partial \overset{(1)}{W}}{\partial z_2} \right] \frac{\partial^2 \overset{(1)}{\delta\mathcal{F}}}{\partial z_1^2} - \left[\overset{(1)}{G}_{12} - \frac{\partial \overset{(0)}{W}}{\partial z_1} \frac{\partial \overset{(1)}{W}}{\partial z_2} - \frac{\partial \overset{(0)}{W}}{\partial z_2} \frac{\partial \overset{(1)}{W}}{\partial z_1} \right] \frac{\partial^2 \overset{(1)}{\delta\mathcal{F}}}{\partial z_1 \partial z_2} \right) dz_1 dz_2 = 0 \tag{234}$$

where the eqauations

$$\pi^2 \delta\overset{(1)}{\mathcal{N}}_{11} = \frac{\partial^2 \overset{(1)}{\delta\mathcal{F}}}{\partial z_2^2} \tag{235a}$$

$$\pi^2 \delta\overset{(1)}{\mathcal{N}}_{22} = \frac{\partial^2 \overset{(1)}{\delta\mathcal{F}}}{\partial z_1^2} \tag{235b}$$

$$\frac{\pi^2}{\alpha_b} \delta\overset{(1)}{\mathcal{N}}_{12} = - \frac{\partial^2 \overset{(1)}{\delta\mathcal{F}}}{\partial z_1 \partial z_2} \tag{235c}$$

have been used. Equation (234) is an integral statement of compatibility of the tangential strains

associated with adjacent equilibrium states. Further integration by parts of equation (234) yields

$$\int\int_{\mathcal{A}} \delta \overset{(1)}{\mathcal{W}}{}^{*}_{\text{int}} dz_1 dz_2 =$$

$$\int\int_{A} \left[\frac{\partial^2 \overset{(1)}{E}_{11}}{\partial z_2^2} + \frac{\partial^2 \overset{(1)}{E}_{22}}{\partial z_1^2} - \frac{\partial^2 \overset{(1)}{G}_{12}}{\partial z_1 \partial z_2} - \sqrt{12}\mathcal{D}_c\left(\overset{(1)}{W}\right) - \mathcal{L}\left(\overset{(0)}{W}(\tilde{p}), \overset{(1)}{W}\right) \right] \delta \overset{(1)}{\mathcal{F}}\, dz_1 dz_2 \qquad (236)$$

+ boundary terms

where the integrand is the compatibility equation given by equation (219).

A convenient matrix representation of equation (234) is given by

$$\int\int_{A} \left(\left\{ \overset{(1)}{E} \right\}^{T} - \sqrt{12} \overset{(1)}{W} \left[Z_1 \;\; Z_2 \;\; 0 \right] - \left\{ \overset{(1)}{\Omega} \right\}^{T} \left[\overset{(0)}{\Omega} \right] \right) \left\{ \partial \delta \overset{(1)}{\mathcal{F}} \right\} dz_1 dz_2 = 0 \qquad (237)$$

where $\left\{ \overset{(1)}{\Omega} \right\}$ is defined by equation (212b) and (192), and

$$\left[\overset{(0)}{\Omega} \right] \equiv \begin{bmatrix} -\frac{\partial \overset{(0)}{W}}{\partial z_1} & 0 & -\frac{\partial \overset{(0)}{W}}{\partial z_2} \\ 0 & -\frac{\partial \overset{(0)}{W}}{\partial z_2} & -\frac{\partial \overset{(0)}{W}}{\partial z_1} \end{bmatrix} \qquad (238)$$

Using constitutive equation (196), the integrand of equation (237) is expressed as

$$\begin{aligned} &\left[\left\{ \overset{(1)}{E} \right\}^{T} - \sqrt{12} \overset{(1)}{W} \left[Z_1 \;\; Z_2 \;\; 0 \right] - \left\{ \overset{(1)}{\Omega} \right\}^{T} \left[\overset{(0)}{\Omega} \right] \right] \left\{ \partial \delta \overset{(1)}{\mathcal{F}} \right\} \\ &\quad = \left[\left\{ \partial \overset{(1)}{\mathcal{F}} \right\}^{T} \left[a \right] - \left\{ \overset{(1)}{\kappa} \right\}^{T} \left[\mathcal{B} \right]^{T} - \sqrt{12} \overset{(1)}{W} \left[Z_1 \;\; Z_2 \;\; 0 \right] - \left\{ \overset{(1)}{\Omega} \right\}^{T} \left[\overset{(0)}{\Omega} \right] \right] \left\{ \partial \delta \overset{(1)}{\mathcal{F}} \right\} \end{aligned} \qquad (239)$$

Values of the Nondimensional Parameters

An extensive collection of tables and figures is presented in this section that shows the effects of lamina material properties and stacking sequence on the fundamental nondimensional parameters, and in some cases, their associated coefficients. In particular, results are presented for the nine lamina material systems given in Table 1 and for several stacking sequences. The fiber orientation angle θ of an arbitrary lamina is depicted in figure 3. This angle is defined as the angle between the line tangent to the ξ_1-coordinate curve and the line tangent to the fiber at a given point (ξ_1, ξ_2, ζ) of a shell. The stacking sequences considered include balanced symmetric angle-ply laminates, balanced antisymmetric angle-ply laminates, symmetric quasi-isotropic laminates, antisymmetric quasi-isotropic laminates, and unsymmetric quasi-isotropic laminates. Results are also given for unbalanced, unsymmetric laminates composed of perpendicular plies aligned with the two surface coordinates and a single family of angle plies. For every laminate considered, the total thickness h is calculated based on the number of plies and a ply thickness of 0.005 in.

Results for Angle-Ply Laminates

Results showing the effects of the fiber orientation angle θ on the values of the nondimensional parameters, or their associated coefficients, for $[(+\theta/-\theta)_m]_S$ and $[(-\theta/+\theta)_m]_S$ symmetric laminates and for $(+\theta/-\theta)_m$ and $(-\theta/+\theta)_m$ antisymmetric laminates are presented in Tables 2-14 and figures 4-20. The results shown in the figures were computed for one-degree increments of θ. In each of figures 4-14, nine curves are shown that correspond to the nine material system given in Table 1, and the results indicate that the P-100/3502 laminates generally possess the most extreme values of the nondimensional parameters, or their associated coefficients. In contrast, the effect of fiber angle is generally the most benign for the boron-aluminum laminates. As a consequence of the extreme values exhibited, results for laminates made of the P-100/3502 material are presented in Tables 11-14, and curves are shown in figures 15-20 that correspond to different values of the stacking sequence number m.

Results showing the effect of the fiber orientation angle θ on the values of the flexural orthotropy parameter β are shown in figure 4 and Table 2 for the symmetric and antisymmetric angle-ply laminates. Each of these laminates has the same value of β for a given material system, regardless of the number of plies ($m = 1, 2, \ldots$). For all laminates, the larger values of β occur in the range $30 \text{ degrees} \le \theta \le 60 \text{ degrees}$, with the maximum at $\theta = 45$ degrees. For all the results, $0.250 \le \beta \le 2.76$.

Values of the orthotropy coefficients $(a_{22}/a_{11})^{1/4}$ and $(D_{11}/D_{22})^{1/4}$ that appear in the nondimensional parameters α_m and α_b, respectively, are given in Table 3 and shown in figure 5 as a function of the fiber angle θ. For these particular laminates, both coefficients have the same value for a given material system and a given value of θ. In addition, these values are independent of the number of laminate plies. The results presented in figure 5 show monotonic reductions in the values of the coefficients with increasing values of θ. Moreover, the larger values of the coefficients for each laminate occurs for $\theta < 45$ degrees and the smaller values for $\theta > 45$ degrees. All values of these coefficients are between 0.342 and 2.93.

The effects of material system and fiber orientation on the values for the generalized Poisson's ratios ν_m and ν_b are given in Table 4 and shown in figure 6. For these symmetric and antisymmetric angle-ply laminates, the Poisson's ratios possess identical values for a given material system and fiber angle, and these values are independent of the number of plies. Figure 6 indicates that all Poisson's ratios are positive valued and the largest value is less than 0.9. For all laminates, the larger values occur in the range 30 degrees $\leq \theta \leq$ 60 degrees, with the maximum at θ = 45 degrees.

Results showing the effect of the fiber orientation angle θ on the values of the membrane orthotropy parameter μ are shown in figure 7 and Table 5 for the symmetric and antisymmetric angle-ply laminates. Each of these laminates also has the same value of μ for a given material system, regardless of the number of plies. For all laminates, the larger values of μ occur in the ranges $\theta < 10$ degrees and $\theta > 80$ degrees, and the smallest occur in the range 30 degrees $\leq \theta \leq$ 60 degrees, with the minimum at θ = 45 degrees. Altogether, $-1 < \mu < 5.5$.

Values of the coefficient $\frac{h}{\sqrt{12}[a_{11}a_{22}D_{11}D_{22}]^{\frac{1}{4}}}$ that appears in the nondimensional Batdorf-Stein parameters Z_1 and Z_2 are given in Table 6 and shown in figure 8 as a function of the fiber angle θ. Each of these laminates also has the same value of this coefficient for a given material system and fiber angle, regardless of the number of plies. All values of the coefficient are between 0.4 and 1.0, with the smaller values in the range 30 degrees $\leq \theta \leq$ 60 degrees.

The effects of material system and fiber orientation on the values of the flexural anisotropy parameters γ_b and δ_b for $(+\theta/-\theta)_S$ and $(-\theta/+\theta)_S$ four-ply symmetric laminates are given in Tables 7 and 8, respectively, and shown in figure 9-10, respectively. The values of these two parameters are between -0.015 and 0.7 for the $(+\theta/-\theta)_S$ laminates, and between -0.7 and 0.015 for the $(-\theta/+\theta)_S$ laminates. Although it is not shown herein for all material systems considered, the magnitudes of these parameters diminish in the $[(+\theta/-\theta)_m]_S$ and $[(-\theta/+\theta)_m]_S$ symmetric laminates as the number of plies increases. For the $(+\theta/-\theta)_m$ and $(-\theta/+\theta)_m$ antisymmetric laminates, γ_b and δ_b are identically equal to zero for all values of θ and m. A parametric plot of γ_b and δ_b is presented in figure 11 for the $(+\theta/-\theta)_S$ and $(-\theta/+\theta)_S$ symmetric laminates, where θ is the parameter. Each curve in this figure is traversed counterclockwise as θ increases from 0 to 90 degrees, and each curve is symmetric about a line passing through the points of the curves that correspond to θ = 45 degrees. Moreover, each curve begins and ends at the origin where θ = 0 and 90 degrees, consistent with a lack of flexural anisotropy. The unfilled circular symbols correspond to sequential values of θ in 15-degree increments. The difference in shape of the parametric curves indicates that the lamina material properties have a moderate effect on the relative proportions of the two anisotropy parameters, with respect to the fiber angle.

Values of the only nonzero load-path eccentricity parameters, e_{16} and e_{26}, are given for the $(+\theta/-\theta)$ and $(-\theta/+\theta)$ two-ply antisymmetric laminates in Tables 9 and 10, respectively, and are shown in figures 12 and 13, respectively, as a function of the fiber angle θ. The corresponding parametric plot, with θ as the parameter, is shown in figure 14. Each parametric curve in this figure is also traversed counterclockwise as θ increase from 0 to 90 degrees, and each curve is

also symmetric about a line passing through the points of the curves that correspond to $\theta = 45$ degrees. The unfilled circular symbols in this figure also correspond to sequential values of θ in 15-degree increments. The values of these two parameters are between -0.015 and 1.78 for the $(-\theta/+\theta)$ laminates, and between -1.78 and 0.015 for the $[+\theta/-\theta]$ laminates. The difference in shape of the parametric curves shown in figure 14 indicates that the lamina material properties has a moderate effect on the relative proportions of the two load-path eccentricity parameters, with respect to the fiber angle. For the symmetric angle-ply laminates, all load-path eccentricity parameters are identically equal to zero.

The combined effects of fiber orientation and number of plies on the values of the flexural anisotropy parameters γ_b and δ_b are given in Tables 11 and 12, respectively, and shown in figures 15-16, respectively, for $[(+\theta/-\theta)_m]_S$ and $[(-\theta/+\theta)_m]_S$ symmetric laminates made of the P-100/3502 material. The corresponding parametric plot, with θ as the parameter, is shown in figure 17. Each parametric curve in this figure is also traversed counterclockwise as θ increases from 0 to 90 degrees, and each curve is also symmetric about a line passing through the points of the curves that correspond to $\theta = 45$ degrees. In going from four to twenty-four plies, the maximum magnitude of these anisotropy parameters is reduced by 83%. Likewise, in going from four to forty-eight plies, the maximum magnitude of these anisotropy parameters is reduced by 92%. The similar shape of the parametric curves indicates that the number of plies has a relatively small effect on the relative proportions of the two anisotropy parameters, with respect to the fiber angle.

The combined effects of fiber orientation and number of plies on the values of the load-path eccentricity parameters e_{16} and e_{26} are given in Tables 13 and 14, respectively, and shown in figure 18-19, respectively, for the $(+\theta/-\theta)_m$ and $(-\theta/+\theta)_m$ antisymmetric laminates made of the P-100/3502 material. The corresponding parametric plot, with θ as the parameter, is shown in figure 20. Each parametric curve in this figure is also traversed counterclockwise as θ increase from 0 to 90 degrees, and each curve is also symmetric about a line passing through the points of the curves that correspond to $\theta = 45$ degrees. In going from two to twenty-four plies, the maximum magnitude of these anisotropy parameters is reduced by 92%. Likewise, in going from two to forty-eight plies, the maximum magnitude of these anisotropy parameters is reduced by 96%. The similar shape of the parametric curves for these parameters also indicates that the number of plies has no significant effect on their relative proportions, with respect to the fiber angle.

Results for Quasi-Isotropic Laminates

Results showing the effects of the number of plies, and their order, on the values of the nondimensional parameters, and associated coefficients, for quasi-isotropic laminates made of the nine lamina material systems are presented in Tables 15-45. Additionally, the results for the P-100/3502 laminates are shown figures 21-30. In particular, results are presented in these Tables and figures for $[(\pm 45/0/90)_m]_S$ and $[(0/90/\pm 45)_m]_S$ symmetric laminates, $[(\pm 45/0/90)_m]_A$ and $[(0/90/\pm 45)_m]_A$ antisymmetric laminates (antisymmetry is indicated by the subscript A in the stacking sequence notation herein), and $(\pm 45/0/90)_m$ and $(0/90/\pm 45)_m$ unsymmetric laminates, for sequential integer values of m from 1 to 8. Likewise, three or four curves that connect symbols are shown in figures 21-30. In most of the figures, the dashed and solid blue curves correspond to

results for the $[(\pm 45/0/90)_m]_S$ and $[(\pm 45/0/90)_m]_A$ laminates and the $[(0/90/\pm 45)_m]_S$ and $[(0/90/\pm 45)_m]_A$ laminates, respectively. The dashed and solid gray curves correspond to results for the $(\pm 45/0/90)_m$ laminates and the $(0/90/\pm 45)_m$ laminates, respectively. For each of these laminates, $(a_{22}/a_{11})^{1/4} = 1$ and $\mu = 1$, regardless of the lamina material system and number of plies. Similarly, the values of the generalized membrane Poisson's ratio ν_m are independent of the number of plies. The variation of ν_m with material system is presented in Table 15 and ranges from 0.272 to 0.325.

The effects of lamina material properties and number of plies on the coefficient $(D_{11}/D_{22})^{1/4}$ that appears in the nondimensional parameter α_b are presented in Tables 16-19. Specifically, the values given in Table 16 are for the $[(\pm 45/0/90)_m]_S$ and $[(\pm 45/0/90)_m]_A$ laminates, the values in Table 17 are for the $[(0/90/\pm 45)_m]_S$ and $[(0/90/\pm 45)_m]_A$ laminates, the values in Table 18 are for the $(\pm 45/0/90)_m$ laminates, and the values in Table 19 are for the $(0/90/\pm 45)_m$ laminates. The results for each of these laminates made of the P-100/3502 material are shown in figure 21. The results in Tables 16 and 17 for the symmetric and antisymmetric laminates, and in Table 19 for the $(0/90/\pm 45)_m$ unsymmetric laminates, indicate that the values for $(D_{11}/D_{22})^{1/4}$ approach unity, the value for a homogeneous isotropic material, from above as the number of plies increases, regardless of the lamina material system, as shown in figure 21 for the corresponding P-100/3502 laminates. However, the results in Table 18 and figure 21 for the $(\pm 45/0/90)_m$ unsymmetric laminates show convergence from below to unity as the number of plies increases. Altogether, these results are bounded by the values $(D_{11}/D_{22})^{1/4} = 0.772$ and 1.30.

Results that show the effects of lamina material properties and number of plies on the nondimensional parameter β are presented in Table 20 for the $[(\pm 45/0/90)_m]_S$ and $[(\pm 45/0/90)_m]_A$ laminates, in Table 21 for the $[(0/90/\pm 45)_m]_S$ and $[(0/90/\pm 45)_m]_A$ laminates, and in Table 22 for the $(\pm 45/0/90)_m$ and $(0/90/\pm 45)_m$ laminates. The results for each of these laminates made of the P-100/3502 material are shown in figure 22. The results in Table 20 for the $[(\pm 45/0/90)_m]_S$ and $[(\pm 45/0/90)_m]_A$ laminates, and in Table 22 for both families of unsymmetric laminates, indicate that the values for β approach unity, the value for a homogeneous isotropic material, from above as the number of plies increases, regardless of the lamina material system. This trend is shown in figure 22 for the corresponding P-100/3502 laminates. However, the results in Table 21 and figure 22 for the $[(0/90/\pm 45)_m]_S$ and $[(0/90/\pm 45)_m]_A$ laminates show convergence from below to unity as the number of plies increases. Altogether, $0.266 \le \beta \le 2.22$, and the unsymmetric laminates exhibit significantly faster convergence to unity than the other laminates with increasing number of plies. This convergence characteristic is explained by noting the basic unit forming each stacking sequence is repeated more for the unsymmetric laminates, for a given number of plies, thus approaching the homogeneity of an isotropic material faster.

Results that show the effects of lamina material properties and number of plies on the generalized Poisson's ratio ν_b are presented in Table 23 for the $[(\pm 45/0/90)_m]_S$ and $[(\pm 45/0/90)_m]_A$ laminates, in Table 24 for the $[(0/90/\pm 45)_m]_S$ and $[(0/90/\pm 45)_m]_A$ laminates, and in Table 25 for the $(\pm 45/0/90)_m$ and $(0/90/\pm 45)_m$ laminates. The results for each of these laminates made of the P-100/3502 material are shown in figure 23. The results in Table 23 for the $[(\pm 45/0/90)_m]_S$ and $[(\pm 45/0/90)_m]_A$ laminates, and in Table 25 for both families of unsymmetric laminates, indicate that the values for ν_b approach the corresponding value of ν_m given in Table 15, from above as the

number of plies increases, regardless of the lamina material system. This trend is shown in figure 23 for the corresponding P-100/3502 laminates. In contrast, the results in Table 24 and figure 23 for the $[(0/90/\pm45)_m]_S$ and $[(0/90/\pm45)_m]_A$ laminates show convergence from below to the corresponding value of ν_m as the number of plies increases. Altogether, $0.091 \le \nu_b \le 0.716$, and the unsymmetric laminates exhibit significantly faster convergence than the other laminates with increasing number of plies.

The effects of lamina material properties and number of plies on the flexural anisotropy parameters γ_b and δ_b are presented in Tables 26 and 30 for the $[(\pm45/0/90)_m]_S$ laminates, respectively; in Tables 27 and 31 for the $[(0/90/\pm45)_m]_S$ laminates, respectively; in Tables 28 and 32 for the $(\pm45/0/90)_m$ laminates, respectively; and in Tables 29 and 33 for the $(0/90/\pm45)_m$ laminates, respectively. Values of γ_b and δ_b for each of these laminates made of the P-100/3502 material are shown in figures 24 and 25, respectively. In contrast to the previous figures, results for the $[(\pm45/0/90)_m]_S$ and $[(0/90/\pm45)_m]_S$ symmetric laminates are indicated in these two figures by dashed and solid black lines, respectively. The values of γ_b and δ_b for the $[(\pm45/0/90)_m]_A$ and $[(0/90/\pm45)_m]_A$ antisymmetric laminates are equal to zero and are indicated in the two figures by the solid blue line. Unlike the previous corresponding results, the results in Tables 26-33, and figures 24 and 25, indicate convergence to a value of zero, the value for a homogeneous isotropic material, from above for the $[(\pm45/0/90)_m]_S$, $[(0/90/\pm45)_m]_S$, and $(\pm45/0/90)_m$ laminates and from below for the $(0/90/\pm45)_m$ laminates. Altogether, $-0.209 \le \gamma_b \le 0.351$, $-0.351 \le \delta_b \le 0.253$, and the unsymmetric laminates exhibit significantly faster convergence than the other laminates with increasing number of plies.

Values of the coefficient $\frac{h}{\sqrt{12}[a_{11}a_{22}D_{11}D_{22}]^{\frac{1}{4}}}$ that appears in the nondimensional Batdorf-Stein parameters Z_1 and Z_2 are given in Table 34 for the $[(\pm45/0/90)_m]_S$ and $[(\pm45/0/90)_m]_A$ laminates, in Table 35 for the $[(0/90/\pm45)_m]_S$ and $[(0/90/\pm45)_m]_A$ laminates, and in Table 36 for the $(\pm45/0/90)_m$ and $(0/90/\pm45)_m$ laminates. The results for each of these laminates made of the P-100/3502 material are shown in figure 26. The results in Tables 34 and 36 indicate that the values for the coefficient for each lamina material system approach the corresponding value of $\sqrt{1-\nu_m^2}$, where ν_m is given in Table 15, from above as the number of plies increases. This trend is shown in figure 26 for the corresponding P-100/3502 laminates. In contrast, the results in Table 35 and figure 26 for the $[(0/90/\pm45)_m]_S$ and $[(0/90/\pm45)_m]_A$ laminates show convergence from below to the corresponding value of $\sqrt{1-\nu_m^2}$ as the number of plies increases. For all cases considered, the values for $\frac{h}{\sqrt{12}[a_{11}a_{22}D_{11}D_{22}]^{\frac{1}{4}}}$ are between 0.875 and 1.09, and the unsymmetric laminates exhibit significantly faster convergence than the other laminates with increasing number of plies.

Values of the load-path eccentricity parameter e_{11} are given for the $(\pm45/0/90)_m$ and $(0/90/\pm45)_m$ laminates in Tables 37 and 38, respectively, and are shown in figure 27 as a function of the number of plies for the laminates made of the P-100/3502 material. The values of this parameter for the symmetric and antisymmetric quasi-isotropic laminates are equal to zero, and are indicated in figure 27 by the solid blue line. These results indicate that the values of e_{11} are negative and approach zero from below with increasing number of plies for all the laminates except the (±45/

$0/90)_m$ laminates made from the Boron-Aluminum and the Boron-epoxy materials. These two exceptions approach zero from above with increasing number of plies. Moreover, the values of ε_{11} for the $(0/90/\pm45)_m$ laminates are significantly larger than the values for the corresponding $(\pm45/0/90)_m$ laminates, and exhibit a slower convergence rate. This difference in convergence rates is illustrated in figure 27 for the laminates made of the P-100/3502 material.

Values of the load-path eccentricity parameters ε_{12} and ε_{66} are given for the $(\pm45/0/90)_m$ and $(0/90/\pm45)_m$ laminates in Tables 39 and 40, respectively, and are shown in figure 28 as a function of the number of plies for the laminates made of the P-100/3502 material. The values of these two parameters for the symmetric and antisymmetric quasi-isotropic laminates are equal to zero, and are indicated in figure 28 by the solid blue line. These results indicate that the values of ε_{12} and ε_{66} are negative and approach zero from below with increasing number of plies for all the $(\pm45/0/90)_m$ laminates. However, the values of ε_{12} and ε_{66} for the $(0/90/\pm45)_m$ laminates are positive and approach zero from above with increasing number of plies. Moreover, the values of the parameters for a given $(\pm45/0/90)_m$ laminate are the negative of the corresponding $(0/90/\pm45)_m$ laminate. Thus, both laminate constructions exhibit the same convergence rate as illustrated in figure 28 for the laminates made of the P-100/3502 material.

The effects of lamina material properties and number of plies on the load-path eccentricity parameters ε_{16} and ε_{26} are given for the $[(\pm45/0/90)_m]_A$ and $[(0/90/\pm45)_m]_A$ antisymmetric laminates in Tables 41 and 42, respectively, and for the $(\pm45/0/90)_m$ and $(0/90/\pm45)_m$ unsymmetric laminates in Table 43. The corresponding results are shown in figure 29 as a function of the number of plies for the laminates made of the P-100/3502 material. These results indicate that the values of ε_{16} and ε_{26} are equal and negative and approach zero from below with increasing number of plies for all the laminates. In addition, all the laminate families exhibit nearly the same convergence rate, as depicted in figure 29. The values of the parameters for the corresponding symmetric laminates are identically equal to zero and are depicted in figure 29 by the black solid line.

Values of the load-path eccentricity parameter ε_{22} are given for the $(\pm45/0/90)_m$ and $(0/90/\pm45)_m$ laminates in Tables 44 and 45, respectively, and are shown in figure 30 as a function of the number of plies for the laminates made of the P-100/3502 material. The values of this parameter for the symmetric and antisymmetric quasi-isotropic laminates are equal to zero, and are indicated in figure 30 by the solid blue line. These results indicate that the values of ε_{22} are positive and approach zero from above with increasing number of plies for all the laminates except the $(\pm45/0/90)_m$ laminates made from the Boron-Aluminum and the Boron-epoxy materials. These two exceptions approach zero from above with increasing number of plies. Moreover, the values of ε_{22} for the $(0/90/\pm45)_m$ laminates are significantly smaller than the values for the corresponding $(\pm45/0/90)_m$ laminates, and exhibit a faster convergence rate, as is illustrated in figure 30 for the laminates made of the P-100/3502 material.

Results for Unbalanced, Unsymmetric Laminates

Results showing the effects of the fiber orientation angle θ on the values of the nondimensional parameters, and associated coefficients, for $(+\theta/0/90)_m$ and $(-\theta/0/90)_m$ laminates are presented in Tables 46-72 and figures 31-62. In each of figures 31-49, nine curves are shown for one-degree increments of θ that correspond to the nine material systems given in Table 1, and the results also indicate that the P-100/3502 laminates generally possess the most extreme values of the nondimensional parameters, or their associated coefficients. As seen for the angle-ply and quasi-isotropic laminates examined herein, the effect of fiber angle is generally the most benign for the boron-aluminum laminates. As a consequence, results for laminates made of the P-100/3502 material are presented in Tables 62-72, and curves are shown in figures 50-62 that correspond to different values of the stacking sequence number m.

Values of the nondimensional flexural orthotropy parameter β for the $(+\theta/0/90)_m$ and $(-\theta/0/90)_m$ laminates vary with the number of plies forming a given laminate. The effects of the fiber orientation angle θ on the values of β are shown in figure 31 and given in Table 46 for the (+θ/0/90) and (-θ/0/90) three-ply laminates. For all three-ply laminates, the larger values of β generally occur in the range 40 degrees ≤ θ ≤ 65 degrees, with the maximums between θ = 50 and 55 degrees. Overall, $0.064 \le \beta \le 1.23$ for the three-ply laminates.

Values of the orthotropy coefficients $(D_{11}/D_{22})^{1/4}$ and $(a_{22}/a_{11})^{1/4}$ that appear in the nondimensional parameters α_b and α_m, respectively, are given in Tables 47 and 48, respectively, and shown in figures 32 and 33, respectively, as a function of the fiber angle θ. For these families of unbalanced and unsymmetric laminates, the two coefficients generally have different values for a given material system and a given value of θ, unlike the symmetric angle-ply laminates examined herein. In addition, the values of $(a_{22}/a_{11})^{1/4}$ are independent of the number of laminate plies, whereas the values of $(D_{11}/D_{22})^{1/4}$ depend on the number of plies. Thus, the results presented in figure 32 are for (+θ/0/90) and (-θ/0/90) three-ply laminates. The general trend shown in figures 32 and 33 is a monotonic reduction in the values of the coefficients with increasing values of θ. Moreover, the coefficient $(D_{11}/D_{22})^{1/4}$ exhibits the the most pronounced reductions with increasing values of θ. Altogether, $0.478 \le (D_{11}/D_{22})^{1/4} \le 1.02$ for the three-ply laminates and $0.845 \le (a_{22}/a_{11})^{1/4} \le 1.18$ for these laminates with any number of plies.

The effects of material system and fiber orientation on the values of the generalized Poisson's ratios ν_m and ν_b are given in Tables 49 and 50, respectively, and shown in figures 34 and 35, respectively. For these families of unbalanced and unsymmetric laminates, the two coefficients also generally have different values for a given material system and a given value of θ. In addition, the values for ν_m are independent of the number of laminate plies, whereas the values of ν_b depend on the number of plies. Thus, the results presented in figure 35 are for (+θ/0/90) and (-θ/0/90) three-ply laminates. The results given for these parameters indicate that all Poisson's ratios are positive valued and the largest value is less than 0.4. For all laminates, the larger values of both Poisson's ratios occur in the range $40 \le \theta \le 65$ degrees. Moreover, the results indicate $0.008 \le \nu_b \le 0.385$ for the three-ply laminates and $0.009 \le \nu_m \le 0.242$ for these laminates with any number of plies.

Results showing the effect of the fiber orientation angle θ on the values of the membrane orthotropy parameter μ are shown in figure 36 and given in Table 51 for the two families of unbalanced, unsymmetric laminates. Each of these laminates also has the same value of μ for a given material system, regardless of the number of plies. For all laminates, the larger values of μ occur in the ranges $\theta < 10$ degrees and $\theta > 80$ degrees, and the smallest occur in the range 30 degrees $\leq \theta \leq$ 60 degrees, with the minimum at $\theta = 45$ degrees. Altogether, $1.23 < \mu < 16.9$.

The effects of material system and fiber orientation on the values for the membrane anisotropy parameters γ_m and δ_m for the $(+\theta/0/90)_m$ and $(-\theta/0/90)_m$ laminates (m = 1, 2, ...) are given in Tables 52 and 53, respectively, and shown in figure 37 and 38, respectively. The values of these two parameters are between -0.048 and 2.06 for the $(+\theta/0/90)_m$ laminates, and between -2.06 and 0.048 for the $(-\theta/0/90)_m$ laminates. The largest magnitudes of γ_m and δ_m occur for $\theta >$ 65 and $\theta <$ 25 degrees, respectively. A parametric plot of γ_m and δ_m is presented in figure 39 for the $(+\theta/0/90)_m$ laminates, where θ is the parameter. Each curve in this figure is traversed clockwise as θ increases from 0 to 90 degrees, and each curve is symmetric about a line passing through the points of the curves that correspond to $\theta = 45$ degrees. The unfilled circular symbols correspond to sequential values of θ in 15-degree increments. The difference in shape of the parametric curves indicates that the lamina material properties have a moderate effect on the relative proportions of the two anisotropy parameters, with respect to the fiber angle.

The values of the flexural anisotropy parameters γ_b and δ_b for $(+\theta/0/90)_m$ and $(-\theta/0/90)_m$ laminates generally vary with the number of plies, for a given material system and fiber angle θ. To gain insight into the nature of these parameters, the effects of material system and fiber orientation on the values of the flexural anisotropy parameters γ_b and δ_b for the $(+\theta/0/90)$ and $(-\theta/0/90)$ three-ply laminates are given in Tables 54 and 55, respectively, and shown in figures 40 and 41, respectively. The values of γ_b are between -0.008 and 0.499 for the $(+\theta/0/90)$ laminates, and between -0.499 and 0.008 for the $(-\theta/0/90)$ laminates. The corresponding magnitudes of δ_b are generally smaller than the corresponding magnitudes of γ_b. In particular, the values of δ_b are between -0.007 and 0.349 for the $(+\theta/0/90)$ laminates, and between -0.349 and 0.007 for the $(-\theta/0/90)$ laminates. In addition, the larger magnitudes of γ_b and δ_b occur in the ranges $40 < \theta <$ 50 degrees and $55 < \theta <$ 65 degrees, respectively. A parametric plot of γ_b and δ_b is presented in figure 42 for the $(+\theta/0/90)$ three-ply laminates, where θ is the parameter. Each curve in this figure is traversed counterclockwise as θ increases from 0 to 90 degrees, and each curve is not symmetric about a line passing through the points of the curves that correspond to $\theta = 45$ degrees. The unfilled circular symbols correspond to sequential values of θ in 15-degree increments. The difference in shape of the parametric curves indicates that the lamina material properties have only a moderate effect on the relative proportions of the two anisotropy parameters, with respect to the fiber angle.

Values of the coefficient $\frac{h}{\sqrt{12}[a_{11}a_{22}D_{11}D_{22}]^{\frac{1}{4}}}$ that appears in the nondimensional Batdorf-Stein parameters Z_1 and Z_2 are given in Table 56 and shown in figure 43 as a function of the fiber angle θ for the $(+\theta/0/90)$ and $(-\theta/0/90)$ three-ply laminates. Unlike the symmetric and antisymmetric angle-ply laminates examined herein, the value of this parameter for the $(+\theta/0/90)_m$ and $(-\theta/0/90)_m$ laminates depends on the number of plies, for a given material system and fiber angle. All values of this coefficient for the three-ply laminates are between 0.911 and 1.48, with the smaller values

in the range $10 < \theta < 25$ degrees.

The $(+\theta/0/90)_m$ and $(-\theta/0/90)_m$ laminates exhibit all six load-path eccentricity parameters, which vary with the number of plies for a given material system and fiber angle θ. Values of e_{11} are presented in Table 57 and shown in figure 44 for the corresponding three-ply laminates. All values of this parameter are between -0.715 and 0, and the magnitudes diminish as θ increases. Corresponding values of e_{12} and e_{66} are presented in Table 58 and shown in figure 45 for the three-ply laminates. For this case, the values of both parameters are identical and are between -0.272 and 0. The largest magnitudes occur for values of $30 < \theta < 60$ degrees. The effects of material system and fiber angle on e_{22} are presented in Table 59 and shown in figure 46 for the three-ply laminates. These results indicate a monotonic reduction in e_{22} as θ increases. In addition, $0 \le e_{22} \le 0.928$.

Values of the load-path eccentricity parameters, e_{16} and e_{26}, are given for the three-ply laminates in Tables 60 and 61, respectively, and shown in figures 47 and 48, respectively, as a function of the fiber angle θ. These results indicate that the values of these two parameters are nonpositive and, for the most part, negative for the $(+\theta/0/90)$ laminates. In contrast, the values of these two parameters are nonnegative and, for the most part, positive for the $(-\theta/0/90)$ laminates. In addition, the magnitude of e_{26} is generally larger than the corresponding magnitude of e_{16} for values of $\theta > 45$ degrees, and vice versa. In particular, $0.316 \le |e_{16}| \le 0$ and $0.395 \le |e_{26}| \le 0$. The corresponding parametric plot, with θ as the parameter, is shown in figure 49 for the $(+\theta/0/90)$ laminates. Each parametric curve in this figure is also traversed counterclockwise as θ increases from 0 to 90 degrees, and the unfilled circular symbols correspond to sequential values of θ in 15-degree increments. Examination of this figure indicates that the curves are generally not symmetric about a line passing through the points of the curves that correspond to $\theta = 45$ degrees. The amount of asymmetry is also influenced slightly by the lamina material properties.

The combined effects of fiber orientation and number of plies on the values of the parameter coefficient $(D_{11}/D_{22})^{1/4}$ for $(+\theta/0/90)_m$ and $(-\theta/0/90)_m$ laminates made of the P-100/3502 material are indicated in Table 62 and shown in figure 50. These results indicate a monotonic reduction in the value of $(D_{11}/D_{22})^{1/4}$ as θ increases and a coalescence of the curves as the number of plies increases. Associated with this coalescence of the curves is an increase in the value of the coefficient and a reduction in the variation of the values as the fiber angle varies. Similar results are presented in Table 63 and figure 51 for the flexural orthotropy parameter β, and in Table 64 and figure 52 for the generalized Poisson's ratio ν_b. The results for these two parameters also show a coalescence of the curves as the number of plies increases, but the magnitudes of each parameter generally decreases as the number of plies increases. Moreover, the curves coalesce to a curve that is symmetric about the line given by $\theta = 45$ degrees.

The combined effects of fiber orientation and number of plies on the values of the flexural anisotropy parameters γ_b and δ_b are given in Tables 65 and 66, respectively, and shown in figures 53 and 54 respectively, for $(+\theta/0/90)_m$ and $(-\theta/0/90)_m$ laminates made of the P-100/3502 material. The corresponding parametric plot, with θ as the parameter, is shown in figure 55. Each parametric curve in this figure is also traversed counterclockwise as θ increases from 0 to 90

degrees, and the curves for laminates with $m \leq 3$ are generally not symmetric about a line passing through the points of the curves that correspond to $\theta = 45$ degrees. However, the parametric curves coalesce to a curve that exhibits symmetry about the line corresponding to $\theta = 45$ degrees as the number of plies increases. In going from three to twenty-four plies, the curves shown in these figures coalesce and the maximum magnitude of γ_b and δ_b are reduced by 55% and 36%, respectively.

Values of the coefficient $\frac{h}{\sqrt{12}[a_{11}a_{22}D_{11}D_{22}]^{\frac{1}{4}}}$ are given in Table 67 and shown in figure 56 as a function of the fiber angle θ and number of plies for the $(+\theta/0/90)_m$ and $(-\theta/0/90)_m$ laminates made of the P-100/3502 material. These results indicate substantial reductions in the values of this coefficient as the number of plies increases for $\theta > 35$ degrees. In going from three to twenty-four plies, the maximum magnitude is reduced by approximately 32%.

The effects of fiber orientation and number of plies on the values of the load-path eccentricity parameters e_{11} and e_{22} are given in Tables 68 and 69, respectively, and shown in figures 57 and 58, respectively, for the $(+\theta/0/90)_m$ and $(-\theta/0/90)_m$ laminates made of the P-100/3502 material. The values of e_{11} are nonpositive and negative for the most part, the values of e_{22} are nonnegative and positive for the most part. The curves shown in each figure coalesce to a single curve with substantially smaller magnitudes as the number of plies increases. In going from three to twenty-four plies, the maximum magnitudes of e_{11} and e_{22} are reduced by approximately 89% and 85%, respectively. Similar results for the load-path eccentricity parameters e_{12} and e_{66} are given in Table 70 and shown in figure 59. For this case the values of these two parameters are identical and are nonpositive and negative for the most part. The curves shown in figure 59 also coalesce as the number of plies increases, with a reduction in the maximum magnitude of approximately 90%.

Values of the load-path eccentricity parameters e_{16} and e_{26} are given in Tables 71 and 72, respectively, and shown in figure 60 and 61, respectively, for the $(+\theta/0/90)_m$ and $(-\theta/0/90)_m$ laminates made of the P-100/3502 material as a function of fiber orientation and number of plies. The corresponding parametric plot for the $(+\theta/0/90)_m$ laminates, with θ as the parameter, is shown in figure 62. Each parametric curve in this figure is also traversed counterclockwise as θ increases from 0 to 90 degrees. In going from three to twenty-four plies, the maximum magnitude of e_{16} and e_{26} are reduced by approximately 90% and the parametric curves coalesce to a curve that is symmetric about a line corresponding to $\theta = 45$ degrees.

Concluding Remarks

A comprehensive development of nondimensional parameters and equations for nonlinear and bifurcations analyses of quasi-shallow shells, based on the Donnell-Mushtari-Vlasov theory for thin anisotropic shells, has been presented. A complete set of field equations for geometrically imperfect shells that includes kinematic equations, isothermal constitutive equations for generally laminated shells, equilibrium equations, boundary conditions, the compatibility equation, and the

virtual work has been presented in terms of lines-of-curvature coordinates. A systematic nondimensionalization of these equations has been developed, several new nondimensional parameters have been defined, and a comprehensive stress-function formulation has been presented that includes variational principles for equilibrium and compatibility. Bifurcation analysis was also applied to the nondimensional nonlinear field equations and a comprehensive set of bifurcation equations have been given that include the effects of pre-bifurcation rotations, which are commonly neglected. These bifurcation equations also include a stress-function formulation with variational principles for equilibrium and compatibility of the adjacent equilibrium states.

An extensive collection of tables and figures has been presented that show the effects of lamina material properties and stacking sequence on the nondimensional parameters. In particular, results are presented for nine lamina material systems and several stacking sequences. These stacking sequences include balanced symmetric angle-ply laminates, balanced antisymmetric angle-ply laminates, symmetric quasi-isotropic laminates, antisymmetric quasi-isotropic laminates, and unsymmetric quasi-isotropic laminates. Results are also given for unbalanced, unsymmetric laminates composed of perpendicular unidirectional plies aligned with the shell surface coordinate curves and angle plies. For each laminate configuration, the numerical range of each nondimensional parameter, or the associated coefficient, has been given. These numerical values provide reasonable estimates to boundaries of the nondimensional design space for a wide range of practical laminates and highly tailored laminates. Overall, the analysis and results should be of great interest to researchers developing structural design technology.

References

1. Seydel, E.: *Wrinkling of Reinforced Plates Subjected to Shear Stresses*. NACA TM 602, 1931.

2. Seydel, E.: Über das Ausbeulen von rechteckigen, isotropic oder orthogonal-anisotropen Platten bei Schubbeanspruchung. *Ingenieur-Archiv*, vol. 4, 1933, pp. 169-191.

3. Huber, M. T.: Die Theorie der Kreuzweise bewehrten Eisenbeton-Platte nebst Anwendungen auf mehrere bautechnisch wichtige Aufgaben uiber rechteckige Platten. *Bauingenieur*, vol. 4, 1923, pp. 354-360 and 392-395.

4. Heck, O. S.; and Ebner, H.: *Methods and Formulas for Calculating the Strength of Plate and Shell Constructions as used in Aiplane Design*. NACA TM 785, 1936.

5. Cozzone, F. P.; and Melcon, M. A.: Nondimensional Buckling Curves - Their Development and Application. *Journal of the Aeronautical Sciences*, vol. 13, no. 10, 1946, pp. 511-517.

6. Batdorf, S. B.: *A Simplified Method of Elastic-Stability Analysis for Thin Cylindrical Shells, I - Donnell's Equation*. NACA TN 1341, 1947.

7. Batdorf, S. B.: *A Simplified Method of Elastic-Stability Analysis for Thin Cylindrical Shells, II - Modified Equilibrium Equation*. NACA TN 1342, 1947.

8. Batdorf, S. B.; Schildcrout, M.; and Stein, M.: *Critical Stress of Thin-Walled Cylinders in Axial Compression*. NACA TN 1343, 1947.

9. Batdorf, S. B.; Schildcrout, M.; and Stein, M.: *Critical Stress of Thin-Walled Cylinders in Torsion*. NACA TN 1344, 1947.

10. Batdorf, S. B.: *A Simplified Method of Elastic-Stability Analysis for Thin Cylindrical Shells*. NACA Rep. 874, 1947.

11. Thielemann, W. F.: *Contribution to the Problem of Buckling of Orthotropic Plates, with Special Reference to Plywood*. NACA TM 1263, 1950.

12. Wittrick, W. H.: Correlation Between some Stability Problems for Orthotropic and Isotropic Plates under Bi-Axial and Uni-Axial Direct Stress. *The Aeronautical Quarterly*, vol. 4, August, 1952, pp. 83-92.

13. Shuleshko, P.: A Reduction Method for Buckling Problems of Orthotropic Plates. *The Aeronautical Quarterly*, vol. 8, May, 1957, pp. 145-156.

14. Thielemann, W. F.: New Developments in the Nonlinear Theories of the Buckling of Thin Cylindrical Shells. *Aeronautics and Astronautics*, N. J. Hoff and W. G. Vincenti, eds., Pergamon Press, 1960.

15. Geier, B.: Beullasten versteifter Kreiszylinderschalen. Jahrbuch 1965 der WGLR, Friedr. Vieweg, and Sohn GmbH, 1965, pp. 440-447.

16. Seggelke, P.; and Geier, B.: Das Beulverhalten versteifter Zylinderschalen. Zeitschrift für Flugwissenschaften, vol. 15, no. 12, 1967, pp. 477-490.

17. Brukva, N. F.: Stability of Rectangular Orthotropic Plates. *Prikladnaya Mekhanika*, vol. 4, no. 3, 1968, pp. 77-85.

18. Khot, N. S.: *On the Influence of Initial Geometric Imperfections on the Buckling and Postbuckling Behavior of Fiber-Reinforced Cylindrical Shells Under Uniform Axial Compression*. Report AFFDL-TR-68-136, Air Force Flight Dynamics Laboratory, October, 1968.

19. Khot, N. S.: Buckling and Postbuckling Behavior of Composite Cylindrical Shells Under Axial Compression. AIAA Journal, vol. 8, no. 2, 1970, pp 229-235.

20. Khot, N. S.; and Venkayya, V. B.: *Effect of Fiber Orientation on Initial Postbuckling Behavior and Imperfection Sensitivity of Composite Cylindrical Shells*. Report AFFDL-TR-70-125, Air Force Flight Dynamics Laboratory, December, 1970.

21. Johns, D. J.: *Shear Buckling of Isotropic and Orthotropic Plates - A Review*. Report R & M No. 3677, Aeronautical Research Council, United Kingdom, 1971.

22. Housner, J. M.; and Stein, M.: *Numerical Analysis and Parametric Studies of the Buckling of Composite Orthotropic Compression and Shear Panels*. NASA TN D-7996, 1975.

23. Wiggenraad, J. F. M.: *The Influence of Bending-Torsional Coupling on the Buckling Load of General Orthotropic, Midplane Symmetric and Elastic Plates*. Report NLR TR 77126 U, National Aerospace Laboratory, The Netherlands, 1977.

24. Oyibo, G. A.: The Use of Affine Transformations in the Analysis of Stability and Vibrations of Orthotropic Plates. Ph.D. Dissertation, Rensselaer Polytechnic Institute, 1981.

25. Fogg, L.: Stability Analysis of Laminated Materials. *State of the Art Design and Analysis of Advanced Composite Materials*, Lockheed California Co., Sessions I and II, 1982.

26. Brunelle, E. J.; and Oyibo, G. A.: Generic Buckling Curves for Specially Orthotropic Rectangular Plates. *AIAA Journal*, vol. 21, no. 8, 1983, pp. 1150-1156.

27. Oyibo, G. A.: Flutter of Orthotropic Panels in Supersonic Flow Using Affine Transformations. *AIAA Journal*, vol. 21, no. 2, 1983, pp. 283-289.

28. Oyibo, G. A.: Unified Panel Flutter Theory with Viscous Damping Effects. *AIAA Journal*, vol. 21, no. 5, 1983, pp. 767-768.

29. Oyibo, G. A.: Unified Aeroelastic Flutter Theory for Very Low Aspect Ratio Panels. *AIAA Journal*, vol. 21, no. 11, 1983, pp. 1581-1587.

30. Stein, M.: Postbuckling of Orthotropic Composite Plates Loaded in Compression. *AIAA Journal*, vol. 21, no. 12, 1983, pp. 1729-1735.

31. Nemeth, M. P.: Buckling Behavior of Orthotropic Composite Plates with Centrally-Located Cutouts. Ph.D. Dissertation, Virginia Polytechnic Institute and State University, 1983.

32. Oyibo, G. A.; and Berman, J.: Influence of Warpage on Composite Aeroelastic Theories. *Proceedings of the AIAA/ASME/ASCE/AHS 26th Structures, Structural Dynamics and Materials Conference*, 1985. AIAA Paper No. 85-0710-CP.

33. Nemeth, M. P.: Importance of Anisotropic Bending Stiffness on buckling of Symmetrically Laminated Composite Plates Loaded in Compression. *Proceedings of the AIAA/ASME/ASCE/AHS 26th Structures, Structural Dynamics and Materials Conference*, 1985. AIAA Paper No. 85-0673-CP.

34. Nemeth, M. P.: Importance of Anisotropy on Buckling of Compression-Loaded Symmetric Composite Plates. *AIAA Journal*, vol. 24, no. 11, 1986, pp. 1831-1835.

35. Nemeth, M. P.: *Buckling Behavior of Long Symmetrically Laminated Plates Subjected to Combined Loadings*. NASA TP 3195, 1992.

36. Nemeth, M. P.: Buckling of Symmetrically Laminated Plates with Compression, Shear, and In-Plane Bending. AIAA Journal, vol. 30, no. 12, 1992, pp. 2959-2965.

37. Nemeth, M. P.: *Buckling Behavior of Long Anisotropic Plates Subjected to Combined Loads*. NASA TP 3568, 1995.

38. Nemeth, M. P.: *Buckling Behavior of Long Symmetrically Laminated Plates Subjected to Shear and Linearly Varying Axial Edge Loads*. NASA TP 3659, 1997.

39. Nemeth, M. P.: Buckling Behavior of Long Anisotropic Plates Subjected to Restrained Thermal Expansion and Mechanical Loads. *Journal of Thermal Stresses*, vol. 23, 2000, pp. 873-916.

40. Nemeth, M. P.: *Buckling Behavior of Long Anisotropic Plates Subjected to Fully Restrained Thermal Expansion*. NASA/TP-2003-212131, 2003.

41. Nemeth, M. P.: *Buckling Behavior of Long Anisotropic Plates Subjected to Elastically Restrained Thermal Expansion and Contraction*. NASA/TP-2004-213512, 2004.

42. Nemeth, M. P.: Buckling of Long Compression-Loaded Anisotropic Plates Restrained Against Inplane Lateral and Shear Deformations. *Thin-Walled Structures*, vol. 42, 2004, pp. 639-685.

43. Stein, M.: Postbuckling of Long Orthotropic Composite Plates Under Combined Loading. *AIAA Journal*, vol. 23, no. 8, 1985, pp. 1267-1272.

44. Stein, M.: Analytical Results for Post-Buckling Behaviour of Plates in Compression and in Shear. *Aspects of the Analysis of Plate Structures, A Volume in Honour of W. H. Wittrick*. D. J. Dawe, R. W. Horsington, A. G. Kamtekar, and G. H. Little, eds., Clarendon Press, 1985, pp. 205-223.

45. Brunelle, E. J.: The Fundamental Constants of Orthotropic Affine Slab/Plate Equations. *AIAA Journal*, vol. 23, no. 12, 1985, pp. 1957-1961.

46. Brunelle, E. J.: Eigenvalue Similarity Rules for Symmetric Cross-Ply Laminated Plates. *AIAA Journal*, vol. 24, no. 1, 1986, pp. 151-154.

46. Brunelle, E. J.: Generic Karman-Rostovstev Plate Equations in an Affine Space. *AIAA Journal*, vol. 24, no. 3, 1986, pp. 472-478.

48. Oyibo, G. A.; and Brunelle, E. J.: Vibrations of Circular Orthotropic Plates in Affine Space. *AIAA Journal*, vol. 23, no. 2, 1985, pp. 296-300.

49. Yang, I. H.; and Liu, C. R.: Buckling and Bending Behaviour of Initially Stressed Specially Orthotropic Thick Plates. *International Journal of Mechanical Sciences*, vol. 29, no. 12, 1987, pp. 779-791.

50. Yang, I. H.; and Shieh, J. A.: Vibrations of Initially Stressed Thick, Rectangular Orthotropic Plates. *Journal of Sound and Vibration*, vol. 119, no. 3, 1987, pp. 545-558.

51. Yang, I. H.; and Shieh, J. A.: Vibrational Behavior of an Initially Stressed Orthotropic Circular Mindlin Plate. *Journal of Sound and Vibration*, vol. 123, no. 1, 1988, pp. 145-156.

52. Yang, I. H.; and Shieh, J. A.: Generic Thermal Buckling of Initially Stressed Antisymmetric Cross-Ply Thick Laminates. *International Journal of Solids and Structures*, vol. 24, no. 10, 1988, pp. 1059-1070.

53. Kuo, W. S.; and Yang, I. H.: On the Global Large Deflection and Postbuckling of Symmetric Angle-Ply Laminated Plates. *Engineering Fracture Mechanics*, vol. 30, no. 6, 1988, pp. 801-810.

54. Kuo, W. S.; and Yang, I. H.: Generic Nonlinear Behavior of Antisymmetric Angle-Ply Laminated Plates. *International Journal of Mechanical Sciences*, vol. 31, no. 2, 1989, pp. 131-143.

55. Yang, I. H.: Generic Buckling and Bending Behavior of Initially Stressed Antisymmetric Cross-Ply Thick Laminates. *Journal of Composite Materials*, vol. 23, July, 1989, pp. 651-672.

56. Yang, I. H.: Bending, Buckling, and Vibration of Antisymmetrically Laminated Angle-Ply Rectangular Simply Supported Plates. *Aeronautical Journal*, vol. 93, no. 927, 1989, pp. 265-271.

57. Brunelle, E. J.; and Shin, K. S.: Postbuckling Behavior of Affine Form of Specially Orthotropic Plates Using Perturbation Method. *12th Annual ETCE ASME Meeting - Composite Materials Symposium*, 1989, pp. 175-189.

58. Brunelle, E. J.; and Shin, K. S.: Postbuckling Behavior of Affine Form of Specially Orthotropic Plates. *12th Annual Canadian Congress of Applied Mechanics - Mechanics of Solids and Structures Symposium*, 1989.

59. Brunelle, E. J.; and Shin, K. S.: Postbuckling Behavior of Affine Form of Specially Orthotropic Plates with Simply Supported-Free Edge. *Proceedings of the 1989 ASME International Computers in Engineering Conference and Exposition*, 1989, pp. 259-266.

60. Nemeth, M. P.: *Nondimensional Parameters and Equations for Buckling of Symmetrically Laminated Thin Elastic Shallow Shells*. NASA TM 104060, 1991.

61. Nemeth, M. P.: Nondimensional Parameters and Equations for Buckling of Anisotropic Shallow Shells. *Journal of Applied Mechanics*, vol. 61, no. 9, 1994, pp. 664-669.

62. Radloff, H. D.; Hyer, M. W.; and Nemeth, M. P.: The Buckling Response of Symmetrically Laminated Composite Plates Having a Trapezoidal Planform Area. NASA CR-196975, 1994.

63. Lee, Y.-S.; and Yang, M.-S.: Behaviour of Antisymmetric Angle-Ply Laminated Plates Using the Affine Transformation. *Computers & Structures*, vol. 61, no. 2, 1996, pp. 375-383.

64. Nemeth, M. P.; and Smeltzer, S. S., III: *Bending Boundary Layers in Laminated-Composite Circular Cylindrical Shells*. NASA/TP-2000-210549, 2000.

65. Hilburger, M. W.; Rose, C. A.; and Starnes, J. H., Jr.: Nonlinear Analysis and Scaling Laws for Noncircular Composite Structures Subjected to Combined Loads. *Proceedings of the AIAA/ASME/ASCE/AHS/ASC 42nd Structures, Structural Dynamics and Materials Conference*, 2001, AIAA Paper No. 2001-1335.

66. Weaver, P. M.; Driesen, J. R.; and Roberts, P.: The Effects of Flexural/Twist Anisotropy on the Compression Buckling of Quasi-Isotropic Laminated Cylindrical Shells. *Composite Structures*, vol. 55, 2002, pp. 195-204.

67. Weaver, P. M.; Driesen, J. R.; and Roberts, P.: Anisotropic Effects in the Compression Buckling of Laminated Composite Cylindrical Shells. *Composites Science and Technology*, vol. 62, 2002, pp. 91-105.

68. Weaver, P. M.: The Effect of Extension/Twist Anisotropy on Compression Buckling in Cylindrical Shells. *Composites: Part B*, vol. 34, 2003, pp. 251-260.

69. Diaconu, C.; and Weaver, P. M.: Approximate Solution and Optimum Design of Compression-Loaded, Postbuckled Laminated Composite Plates. *AIAA Journal*, vol. 43, no. 4, 2005, pp. 906-914.

70. Weaver, P. M.: Design Formulae for Buckling of Biaxially Loaded Laminated Rectangular Plate with Flexural/Twist Anisotropy. *Proceedings of the AIAA/ASME/ASCE/AHS/ASC 46th Structures, Structural Dynamics and Materials Conference*, 2005, AIAA Paper No. 2005-2105.

71. Wong, K. F. W.; and Weaver, P. M.: Approximate Solution for the Compression Buckling of Fully Anisotropic Cylindrical Shells. *AIAA Journal*, vol. 43, no. 12, 2005, pp. 2639-2645.

72. Diaconu, C.; and Weaver, P. M.: Postbuckling of Long Unsymmetrically Laminated Composite Plates Under Axial Compression. *International Journal of Solids and Structures*, vol. 43, 2006, pp. 6978-6997.

73. Weaver, P. M.: Physical Insight into the Buckling Phenomena of Composite Structures. *Proceedings of the AIAA/ASME/ASCE/AHS/ASC 47th Structures, Structural Dynamics and Materials Conference*, 2006, AIAA Paper No. 2006-2031.

74. Weaver, P. M.: Approximate Analysis for Buckling of Compression Loaded Long Rectangular Plates with Flexural/Twist Anisotropy. *Proceedings of the Royal Society A*, vol. 462, 2006, pp. 59-73.

75. Weaver, P. M.: Anisotropic Elastic Tailoring in Laminated Composite Plates and Shells. *Buckling and Postbuckling of Structures-Experimental, Analytical and Numerical Studies*, B. G. Falzon and M. H. Aliabadi, eds., Imperial College Press, 2008, pp. 177-224.

76. Weaver, P. M.; and Nemeth, M. P.: Bounds on Flexural Properties and Buckling Response for Symmetrically Laminated Composite Plates. *Journal of Engineering Mechanics*, vol. 133, no. 11, 2007, pp. 1178-1191.

77. Weaver, P. M.; and Nemeth, M. P.: Improved Design Formulas for Buckling of Orthotropic Plates Under Combined Loading. *AIAA Journal*, vol. 46, no. 9, 2008, pp. 2391-2396.

78. Mittelstedt, C.; and Beerhorst, M.: Closed-Form Buckling Analysis of Compressively Loaded Composite Plates Braced by Omega-Stringers. *Composite Structures*, vol. 88, 2009, pp. 424-435.

79. Nemeth, M. P; and Mikulas, M. M., Jr.: *Simple Formulas and Results for Buckling-Resistance and Stiffness Design of Compression-Loaded Laminated-Composite Cylinders*. NASA/TP-2009-215778, 2009.

80. Brush, D. O.; and Almroth, B.: *Buckling of Bars, Plates, and Shells*. McGraw-Hill, 1975.

81. Sanders, J. L., Jr.: Nonlinear Theories for Thin Shells. *Quarterly Journal of Applied Mathematics*, vol. 21, no. 1, 1963, pp. 21-36.

82. Novozhilov, V. V.: *Thin Shell Theory*. Second ed., Wolters-Noordhoff, 1970.

83. Donnell, L. H.: *Beams, Plates, and Shells*. McGraw-Hill Book Co., 1976.

84. Novozhilov, V. V.: *Foundations of the Nonlinear Theory of Elasticity*. Dover Publications,, Inc., 1999.

85. Jones, R. M.: *Mechanics of Composite Materials*. Second ed., Taylor & Francis, 1999.

86. Washizu, K.: *Variational Methods in Elasticity and Plasticity*. Third ed., Pergamon Press, 1982.

87. Reddy, J. N.: *Energy Principles and Variational Methods in Applied Mechanics*. Second ed., John Wiley & Sons, Inc., 2002.

88. Wempner, G.: *Mechanics of Solids With Applications to Thin Bodies*. Sijthoff and Noordhoff, 1981.

89. Zhang, Y. and Matthews, F. L.: Large Deflection Behavior of Simply Supported Laminated Panels Under In-Plane Loading. *Journal of Applied Mechanics*, vol. 52, no. 9, 1985, pp. 553-558.

Table 1. Lamina Properties

Lamina property*	Material Systems								
	Boron-Al	S-glass-epoxy	Kevlar 49-epoxy	IM7/ 5260	AS4/ 3502	AS4/ 3501-6	Boron-epoxy	IM7/ PETI-5	P-100/ 3502
E_L, Msi	33	7.5	11.02	22.1	18.5	20.01	29.58	20.35	53.5
E_T, Msi	21	1.7	0.8	1.457	1.64	1.30	2.68	1.16	0.73
ν_{LT}	0.23	0.25	0.34	0.258	0.30	0.30	0.23	0.29	0.31
G_{LT}, Msi	7.0	0.80	0.33	0.860	0.87	1.03	0.81	0.61	0.76

* The symbols L and T denote the longitudinal fiber and transverse matrix directions of a specially orthotropic lamina, respectively.

Table 2. Values of $\beta = \frac{D_{12} + 2D_{66}}{\sqrt{D_{11}D_{22}}}$ for $[(+\theta/-\theta)_m]_S$, $[(-\theta/+\theta)_m]_S$, $(+\theta/-\theta)_m$, and $(-\theta/+\theta)_m$ laminates (m = 1, 2, ...)

θ, deg	Material Systems								
	Boron/Al	S-glass/ Epoxy	Kevlar49/ Epoxy	IM7/5260	AS4/3502	AS4/ 3501-6	Boron- epoxy	IM7/ PETI-5	P-100/ 3502
0	.697	.561	.312	.368	.403	.478	.250	.319	.279
5	.715	.596	.390	.447	.469	.551	.324	.406	.460
10	.768	.699	.617	.674	.661	.757	.539	.659	.954
15	.851	.860	.966	1.02	.954	1.06	.880	1.04	1.57
20	.957	1.06	1.38	1.41	1.30	1.40	1.30	1.47	2.09
25	1.08	1.28	1.77	1.77	1.64	1.72	1.72	1.86	2.42
30	1.19	1.48	2.09	2.06	1.92	1.96	2.08	2.16	2.60
35	1.29	1.65	2.30	2.26	2.12	2.13	2.33	2.36	2.70
40	1.36	1.75	2.42	2.36	2.24	2.23	2.47	2.46	2.74
45	1.38	1.79	2.46	2.40	2.28	2.26	2.51	2.50	2.76
50	1.36	1.75	2.42	2.36	2.24	2.23	2.47	2.46	2.74
55	1.29	1.65	2.30	2.26	2.12	2.13	2.33	2.36	2.70
60	1.19	1.48	2.09	2.06	1.92	1.96	2.78	2.16	2.60
65	1.08	1.28	1.77	1.77	1.64	1.72	1.72	1.86	2.42
70	.957	1.06	1.38	1.41	1.30	1.40	1.30	1.47	2.09
75	.851	.860	.966	1.02	.954	1.06	.880	1.04	1.57
80	.768	.699	.617	.674	.661	.757	.539	.659	.954
85	.715	.596	.390	.447	.469	.551	.324	.406	.460
90	.697	.561	.312	.368	.403	.478	.250	.319	.279

Table 3. Values of $\left(\frac{a_{22}}{a_{11}}\right)^{\frac{1}{4}}$ and $\left(\frac{D_{11}}{D_{22}}\right)^{\frac{1}{4}}$ for $[(+\theta/-\theta)_m]_S$, $[(-\theta/+\theta)_m]_S$, $(+\theta/-\theta)_m$, and $(-\theta/+\theta)_m$ laminates (m = 1, 2, ...)

θ, deg	Material Systems								
	Boron/Al	S-glass/ Epoxy	Kevlar49/ Epoxy	IM7/5260	AS4/3502	AS4/ 3501-6	Boron- epoxy	IM7/ PETI-5	P-100/ 3502
0	1.12	1.45	1.93	1.97	1.83	1.98	1.82	2.05	2.93
5	1.12	1.44	1.92	1.96	1.82	1.97	1.82	2.04	2.90
10	1.11	1.43	1.89	1.93	1.80	1.92	1.80	2.00	2.79
15	1.11	1.40	1.83	1.86	1.74	1.85	1.76	1.93	2.56
20	1.10	1.36	1.74	1.75	1.65	1.73	1.68	1.81	2.24
25	1.08	1.30	1.61	1.61	1.54	1.59	1.57	1.66	1.92
30	1.07	1.24	1.45	1.45	1.41	1.43	1.43	1.48	1.63
35	1.05	1.16	1.29	1.29	1.26	1.28	1.28	1.31	1.38
40	1.02	1.08	1.14	1.14	1.13	1.13	1.14	1.15	1.17
45	1.00	1.00	1.00	1.00	1.00	1.00	1.00	1.00	1.00
50	.977	.927	.878	.879	.888	.883	.881	.873	.852
55	.957	.863	.774	.775	.791	.782	.780	.765	.725
60	.939	.809	.689	.688	.712	.697	.698	.675	.615
65	.924	.767	.623	.620	.650	.629	.637	.604	.522
70	.912	.736	.576	.570	.604	.577	.595	.552	.446
75	.903	.714	.546	.538	.575	.542	.570	.519	.391
80	.898	.700	.529	.519	.557	.520	.556	.500	.359
85	.894	.692	.521	.509	.548	.508	.550	.491	.345
90	.893	.690	.519	.507	.546	.505	.549	.489	.342

Table 4. Values of $\nu_m = \frac{-a_{12}}{\sqrt{a_{11}a_{22}}}$ and $\nu_b = \frac{D_{12}}{\sqrt{D_{11}D_{22}}}$ for $[(+\theta/-\theta)_m]_S$, $[(-\theta/+\theta)_m]_S$, $(+\theta/-\theta)_m$, and $(-\theta/+\theta)_m$ laminates (m = 1, 2, ...)

θ, deg	Material Systems								
	Boron/Al	S-glass/ Epoxy	Kevlar49/ Epoxy	IM7/5260	AS4/3502	AS4/ 3501-6	Boron- epoxy	IM7/ PETI-5	P-100/ 3502
0	.183	.119	.092	.066	.089	.076	.069	.069	.036
5	.189	.131	.118	.092	.111	.101	.094	.098	.097
10	.206	.164	.193	.168	.175	.170	.165	.182	.263
15	.233	.217	.309	.282	.272	.272	.278	.309	.475
20	.267	.283	.447	.414	.388	.388	.418	.453	.654
25	.305	.354	.578	.538	.503	.497	.559	.586	.770
30	.342	.421	.684	.636	.598	.583	.678	.688	.836
35	.374	.475	.756	.703	.666	.642	.761	.755	.872
40	.396	.510	.796	.741	.706	.676	.809	.791	.889
45	.403	.522	.809	.753	.719	.687	.824	.803	.895
50	.396	.510	.796	.741	.706	.676	.809	.791	.889
55	.374	.475	.756	.703	.666	.642	.761	.755	.872
60	.342	.421	.684	.636	.598	.583	.678	.688	.836
65	.305	.354	.578	.538	.503	.497	.559	.586	.770
70	.267	.283	.447	.414	.388	.388	.418	.453	.654
75	.233	.217	.309	.282	.272	.272	.278	.309	.475
80	.206	.164	.193	.168	.175	.170	.165	.182	.263
85	.189	.131	.118	.092	.111	.101	.094	.098	.097
90	.183	.119	.092	.066	.089	.076	.069	.069	.036

Table 5. Values of $\mu = \frac{2a_{12} + a_{66}}{2\sqrt{a_{11}a_{22}}}$ for $[(+\theta/-\theta)_m]_S$, $[(-\theta/+\theta)_m]_S$, $(+\theta/-\theta)_m$, and $(-\theta/+\theta)_m$ laminates (m = 1, 2, ...)

θ, deg	Material Systems								
	Boron/Al	S-glass/ Epoxy	Kevlar49/ Epoxy	IM7/5260	AS4/3502	AS4/ 3501-6	Boron- epoxy	IM7/ PETI-5	P-100/ 3502
0	1.70	2.11	4.41	3.23	3.08	2.40	5.43	3.91	4.08
5	1.64	1.98	3.50	2.71	2.65	2.10	4.22	3.12	2.63
10	1.50	1.65	2.08	1.75	1.82	1.48	2.43	1.85	1.09
15	1.30	1.26	1.07	.973	1.09	.902	1.25	.931	.230
20	1.08	.898	.413	.420	.543	.450	.518	.328	-.255
25	.873	.592	-.021	.037	.154	.122	.031	-.072	-.522
30	.697	.355	-.304	-.219	-.114	-.104	-.292	-.331	-.665
35	.564	.186	-.478	-.378	-.285	-.247	-.493	-.486	-.740
40	.481	.086	-.570	-.463	-.379	-.326	-.601	-.567	-.777
45	.453	.053	-.599	-.490	-.409	-.351	-.635	-.593	-.788
50	.481	.086	-.570	-.463	-.379	-.326	-.601	-.567	-.777
55	.564	.186	-.478	-.378	-.285	-.247	-.493	-.486	-.740
60	.697	.355	-.304	-.219	-.114	-.104	-.292	-.331	-.665
65	.873	.592	-.021	.037	.154	.122	.031	-.072	-.522
70	1.08	.898	.413	.420	.543	.450	.518	.328	-.255
75	1.30	1.26	1.07	.973	1.09	.902	1.25	.931	.230
80	1.50	1.65	2.08	1.75	1.82	1.48	2.43	1.85	1.09
85	1.64	1.98	3.50	2.71	2.65	2.10	4.22	3.12	2.63
90	1.70	2.11	4.41	3.23	3.08	2.40	5.43	3.91	4.08

Table 6. Values of $\frac{h}{\sqrt{12}(a_{11}a_{22}D_{11}D_{22})^{1/4}}$ for $[(+\theta/-\theta)_m]_S$, $[(-\theta/+\theta)_m]_S$, $(+\theta/-\theta)_m$, and $(-\theta/+\theta)_m$ laminates (m = 1, 2, ...)

θ, deg	Material Systems								
	Boron/Al	S-glass/ Epoxy	Kevlar49/ Epoxy	IM7/5260	AS4/3502	AS4/ 3501-6	Boron- epoxy	IM7/ PETI-5	P-100/ 3502
0	.983	.993	.996	.998	.996	.997	.998	.998	.999
5	.982	.991	.993	.996	.994	.995	.996	.995	.995
10	.979	.986	.981	.986	.985	.985	.986	.983	.965
15	.973	.976	.951	.960	.962	.962	.960	.951	.880
20	.964	.959	.895	.911	.922	.921	.908	.891	.757
25	.952	.935	.816	.843	.865	.868	.829	.810	.638
30	.940	.907	.730	.771	.801	.813	.735	.726	.549
35	.927	.880	.655	.711	.746	.767	.648	.656	.490
40	.918	.860	.606	.672	.708	.737	.588	.612	.457
45	.915	.853	.588	.658	.695	.726	.566	.596	.446
50	.918	.860	.606	.672	.708	.737	.588	.612	.457
55	.927	.880	.655	.711	.746	.767	.648	.656	.490
60	.940	.907	.730	.771	.801	.813	.735	.726	.549
65	.952	.935	.816	.843	.865	.868	.829	.810	.638
70	.964	.959	.895	.911	.922	.921	.908	.891	.757
75	.973	.976	.951	.960	.962	.962	.960	.951	.880
80	.979	.986	.981	.986	.985	.985	.986	.983	.965
85	.982	.991	.993	.996	.994	.995	.996	.995	.995
90	.983	.993	.996	.998	.996	.997	.998	.998	.999

Table 7. Values of $\gamma_b = \frac{D_{16}}{\left(D_{11}^3 D_{22}\right)^{1/4}}$ for $(+\theta/-\theta)_S$ laminates and $-\gamma_b$ for $(-\theta/+\theta)_S$ laminates

θ, deg	Material Systems								
	Boron/Al	S-glass/ Epoxy	Kevlar49/ Epoxy	IM7/5260	AS4/3502	AS4/ 3501-6	Boron- epoxy	IM7/ PETI-5	P-100/ 3502
0	0	0	0	0	0	0	0	0	0
5	.032	.069	.115	.116	.105	.113	.110	.123	.184
10	.063	.136	.228	.230	.208	.222	.219	.243	.356
15	.090	.199	.333	.335	.303	.322	.322	.355	.496
20	.112	.255	.425	.424	.386	.405	.414	.449	.589
25	.127	.300	.496	.493	.452	.469	.488	.519	.642
30	.133	.332	.543	.538	.497	.512	.538	.565	.670
35	.131	.348	.568	.562	.522	.536	.564	.589	.683
40	.119	.347	.574	.569	.527	.544	.567	.595	.688
45	.099	.329	.561	.558	.515	.536	.549	.585	.686
50	.075	.295	.528	.530	.483	.512	.509	.557	.676
55	.049	.248	.474	.482	.431	.471	.443	.510	.657
60	.025	.193	.394	.410	.358	.410	.352	.437	.621
65	.006	.137	.293	.317	.269	.330	.243	.338	.557
70	-.007	.088	.186	.213	.177	.238	.136	.225	.449
75	-.012	.049	.094	.119	.098	.149	.055	.122	.296
80	-.012	.024	.035	.053	.044	.079	.010	.051	.140
85	-.007	.009	.009	.018	.015	.032	-.003	.015	.042
90	0	0	0	0	0	0	0	0	0

Table 8. Values of $\delta_b = \frac{D_{26}}{\left(D_{11}D_{22}^3\right)^{1/4}}$ for $(+\theta/-\theta)_S$ laminates and $-\delta_b$ for $(-\theta/+\theta)_S$ laminates

θ, deg	Material Systems								
	Boron/Al	S-glass/ Epoxy	Kevlar49/ Epoxy	IM7/5260	AS4/3502	AS4/ 3501-6	Boron- epoxy	IM7/ PETI-5	P-100/ 3502
0	0	0	0	0	0	0	0	0	0
5	-.007	.009	.009	.018	.015	.032	-.003	.015	.042
10	-.012	.024	.035	.053	.044	.079	.010	.051	.140
15	-.012	.049	.094	.119	.098	.149	.055	.122	.296
20	-.007	.088	.186	.213	.177	.238	.136	.225	.449
25	.006	.137	.293	.317	.269	.330	.243	.338	.557
30	.025	.193	.394	.410	.358	.410	.352	.437	.621
35	.049	.248	.474	.482	.431	.471	.443	.510	.657
40	.075	.295	.528	.530	.483	.512	.509	.557	.676
45	.099	.329	.561	.558	.515	.536	.549	.585	.686
50	.119	.347	.574	.569	.527	.544	.567	.595	.688
55	.131	.348	.568	.562	.522	.536	.564	.589	.683
60	.133	.332	.543	.538	.497	.512	.538	.565	.670
65	.127	.300	.496	.493	.452	.469	.488	.519	.642
70	.112	.255	.425	.424	.386	.405	.414	.449	.589
75	.090	.199	.333	.335	.303	.322	.322	.355	.496
80	.063	.136	.228	.230	.208	.222	.219	.243	.356
85	.032	.069	.115	.116	.105	.113	.110	.123	.184
90	0	0	0	0	0	0	0	0	0

Table 9. Values of $e_{16} = B_{16}\left(\frac{a_{11}^2}{D_{11}D_{22}}\right)^{1/4}$ for $(-\theta/+\theta)$ laminates and $-e_{16}$ for $(+\theta/-\theta)$ laminates

θ, deg	Material Systems								
	Boron/Al	S-glass/ Epoxy	Kevlar49/ Epoxy	IM7/5260	AS4/3502	AS4/ 3501-6	Boron- epoxy	IM7/ PETI-5	P-100/ 3502
0	0	0	0	0	0	0	0	0	0
5	.038	.081	.134	.135	.122	.131	.128	.143	.213
10	.074	.160	.268	.269	.243	.260	.256	.286	.426
15	.107	.236	.405	.403	.364	.386	.387	.430	.650
20	.134	.307	.549	.538	.484	.508	.527	.581	.898
25	.154	.371	.702	.675	.604	.624	.680	.740	1.16
30	.164	.423	.860	.805	.716	.727	.845	.899	1.41
35	.163	.457	1.00	.914	.808	.807	1.00	1.04	1.61
40	.149	.466	1.09	.978	.860	.852	1.12	1.12	1.74
45	.125	.446	1.10	.980	.855	.852	1.12	1.13	1.77
50	.094	.397	1.01	.912	.787	.803	1.00	1.05	1.71
55	.060	.326	.835	.783	.667	.710	.789	.897	1.55
60	.030	.246	.624	.614	.515	.583	.552	.694	1.31
65	.007	.170	.415	.434	.359	.439	.338	.482	1.01
70	-.008	.105	.240	.270	.222	.298	.173	.292	.686
75	-.014	.058	.115	.144	.118	.179	.066	.148	.388
80	-.014	.028	.042	.063	.052	.092	.012	.059	.167
85	-.008	.011	.010	.020	.018	.037	-.004	.017	.049
90	0	0	0	0	0	0	0	0	0

Table 10. Values of $e_{26} = B_{26}\left(\frac{a_{22}^2}{D_{11}D_{22}}\right)^{1/4}$ for (-θ/+θ) laminates and $-e_{26}$ for (+θ/-θ) laminates

θ, deg	Material Systems								
	Boron/Al	S-glass/ Epoxy	Kevlar49/ Epoxy	IM7/5260	AS4/3502	AS4/ 3501-6	Boron- epoxy	IM7/ PETI-5	P-100/ 3502
0	0	0	0	0	0	0	0	0	0
5	-.008	.011	.010	.020	.018	.037	-.004	.017	.049
10	-.014	.028	.042	.063	.052	.092	.012	.059	.167
15	-.014	.058	.115	.144	.118	.179	.066	.148	.388
20	-.008	.105	.240	.270	.222	.298	.173	.292	.686
25	.007	.170	.415	.434	.359	.439	.338	.482	1.01
30	.030	.246	.624	.614	.515	.583	.552	.694	1.31
35	.060	.326	.835	.783	.667	.710	.789	.897	1.55
40	.094	.397	1.01	.912	.787	.803	1.00	1.05	1.71
45	.125	.446	1.10	.980	.855	.852	1.12	1.13	1.77
50	.149	.466	1.09	.978	.860	.852	1.12	1.12	1.74
55	.163	.457	1.00	.914	.808	.807	1.00	1.04	1.61
60	.164	.423	.860	.805	.716	.727	.845	.899	1.41
65	.154	.371	.702	.675	.604	.624	.680	.740	1.16
70	.134	.307	.549	.538	.484	.508	.527	.581	.898
75	.107	.236	.405	.403	.364	.386	.387	.430	.650
80	.074	.160	.268	.269	.243	.260	.256	.286	.426
85	.038	.081	.134	.135	.122	.131	.128	.143	.213
90	0	0	0	0	0	0	0	0	0

Table 11. Values of $\gamma_b = \frac{D_{16}}{\left(D_{11}^3 D_{22}\right)^{1/4}}$ for $[(+\theta/-\theta)_m]_S$ and $-\gamma_b$ for $[(-\theta/+\theta)_m]_S$ P-100/3502 laminates

θ, deg	Stacking sequence number, m						
	m = 1	m = 2	m = 3	m = 4	m = 5	m = 6	m = 12
0	0	0	0	0	0	0	0
5	.184	.092	.061	.046	.037	.031	.015
10	.356	.178	.119	.089	.071	.059	.030
15	.496	.248	.165	.124	.099	.083	.041
20	.589	.294	.196	.147	.118	.098	.049
25	.642	.321	.214	.160	.128	.107	.053
30	.670	.335	.223	.167	.134	.112	.056
35	.683	.342	.228	.171	.137	.114	.057
40	.688	.344	.229	.172	.138	.115	.057
45	.686	.343	.229	.171	.137	.114	.057
50	.676	.338	.225	.169	.135	.113	.056
55	.657	.328	.219	.164	.131	.109	.055
60	.621	.310	.207	.155	.124	.103	.052
65	.557	.278	.186	.139	.111	.093	.046
70	.449	.225	.150	.112	.090	.075	.037
75	.296	.148	.099	.074	.059	.049	.025
80	.140	.070	.047	.035	.028	.023	.012
85	.042	.021	.014	.011	.008	.007	.004
90	0	0	0	0	0	0	0

Table 12. Values of $\delta_b = \frac{D_{26}}{\left(D_{11}D_{22}^3\right)^{1/4}}$ for $[(+\theta/-\theta)_m]_S$ and $-\delta_b$ for $[(-\theta/+\theta)_m]_S$ P-100/3502 laminates

θ, deg	Stacking sequence number, m						
	m = 1	m = 2	m = 3	m = 4	m = 5	m = 6	m = 12
0	0	0	0	0	0	0	0
5	.042	.021	.014	.011	.008	.007	.004
10	.140	.070	.047	.035	.028	.023	.012
15	.296	.148	.099	.074	.059	.049	.025
20	.449	.225	.150	.112	.090	.075	.037
25	.557	.278	.186	.139	.111	.093	.046
30	.621	.310	.207	.155	.124	.103	.052
35	.657	.328	.219	.164	.131	.109	.055
40	.676	.338	.225	.169	.135	.113	.056
45	.686	.343	.229	.171	.137	.114	.057
50	.688	.344	.229	.172	.138	.115	.057
55	.683	.342	.228	.171	.137	.114	.057
60	.670	.335	.223	.167	.134	.112	.056
65	.642	.321	.214	.160	.128	.107	.053
70	.589	.294	.196	.147	.118	.098	.049
75	.496	.248	.165	.124	.099	.083	.041
80	.356	.178	.119	.089	.071	.059	.030
85	.184	.092	.061	.046	.037	.031	.015
90	0	0	0	0	0	0	0

Table 13. Values of $e_{16} = B_{16}\left(\frac{a_{11}^2}{D_{11}D_{22}}\right)^{1/4}$ for $(-\theta/+\theta)_m$ and $-e_{16}$ for $(+\theta/-\theta)_m]_S$ P-100/3502 laminates

θ, deg	Stacking sequence number, m							
	m = 1	m = 2	m = 3	m = 4	m = 5	m = 6	m = 12	m = 24
0	0	0	0	0	0	0	0	0
5	.213	.107	.071	.053	.043	.036	.018	.009
10	.426	.213	.142	.106	.085	.071	.035	.018
15	.650	.325	.217	.163	.130	.108	.054	.027
20	.898	.449	.299	.225	.180	.150	.075	.037
25	1.16	.581	.387	.290	.232	.194	.097	.048
30	1.41	.705	.470	.352	.282	.235	.117	.059
35	1.61	.806	.537	.403	.322	.269	.134	.067
40	1.74	.869	.580	.435	.348	.290	.145	.072
45	1.77	.887	.591	.443	.355	.296	.148	.074
50	1.71	.854	.570	.427	.342	.285	.142	.071
55	1.55	.774	.516	.387	.310	.258	.129	.065
60	1.31	.653	.435	.327	.261	.218	.109	.054
65	1.01	.504	.336	.252	.201	.168	.084	.042
70	.686	.343	.229	.171	.137	.114	.057	.029
75	.388	.194	.129	.097	.078	.065	.032	.016
80	.167	.084	.056	.042	.033	.028	.014	.007
85	.049	.024	.016	.012	.010	.008	.004	.002
90	0	0	0	0	0	0	0	0

Table 14. Values of $e_{26} = B_{26}\left(\frac{a_{22}^2}{D_{11}D_{22}}\right)^{1/4}$ for $(-\theta/+\theta)_m$ and $-e_{26}$ for $(+\theta/-\theta)_m]_S$ P-100/3502 laminates

θ, deg	Stacking sequence number, m							
	m = 1	m = 2	m = 3	m = 4	m = 5	m = 6	m = 12	m = 24
0	0	0	0	0	0	0	0	0
5	.049	.024	.016	.012	.010	.008	.004	.002
10	.167	.084	.056	.042	.033	.028	.014	.007
15	.388	.194	.129	.097	.078	.065	.032	.016
20	.686	.343	.229	.171	.137	.114	.057	.029
25	1.01	.504	.336	.252	.201	.168	.084	.042
30	1.31	.653	.435	.327	.261	.218	.109	.054
35	1.55	.774	.516	.387	.310	.258	.129	.065
40	1.71	.854	.570	.427	.342	.285	.142	.071
45	1.77	.887	.591	.443	.355	.296	.148	.074
50	1.74	.869	.580	.435	.348	.290	.145	.072
55	1.61	.806	.537	.403	.322	.269	.134	.067
60	1.41	.705	.470	.352	.282	.235	.117	.059
65	1.16	.581	.387	.290	.232	.194	.097	.048
70	.898	.449	.299	.225	.180	.150	.075	.037
75	.650	.325	.217	.163	.130	.108	.054	.027
80	.426	.213	.142	.106	.085	.071	.035	.018
85	.213	.107	.071	.053	.043	.036	.018	.009
90	0	0	0	0	0	0	0	0

Table 15. Values of $\nu_m = \frac{-a_{12}}{\sqrt{a_{11}a_{22}}}$ for $[(\pm45/0/90)_m]_S$, $[(\pm45/0/90)_m]_A$, $[(0/90/\pm45)_m]_S$, $[(0/90/\pm45)_m]_A$, $(\pm45/0/90)_m$, and $(0/90/\pm45)_m$ laminates (m = 1, 2, ...)

Material Systems								
Boron/Al	S-glass/ Epoxy	Kevlar49/ Epoxy	IM7/5260	AS4/3502	AS4/ 3501-6	Boron-epoxy	IM7/ PETI-5	P-100/ 3502
.281	.272	.325	.299	.303	.284	.323	.312	.316

Table 16. Values of $\left(\frac{D_{11}}{D_{22}}\right)^{\frac{1}{4}}$ for $[(\pm 45/0/90)_m]_S$ and $[(\pm 45/0/90)_m]_A$ laminates

m	Material Systems								
	Boron/Al	S-glass/ Epoxy	Kevlar49/ Epoxy	IM7/5260	AS4/3502	AS4/ 3501-6	Boron- epoxy	IM7/ PETI-5	P-100/ 3502
1	1.01	1.04	1.07	1.07	1.06	1.06	1.07	1.07	1.08
2	1.01	1.03	1.04	1.04	1.04	1.04	1.04	1.05	1.05
3	1.01	1.02	1.03	1.03	1.03	1.03	1.03	1.03	1.04
4	1.01	1.02	1.02	1.02	1.02	1.02	1.02	1.03	1.03
5	1.00	1.01	1.02	1.02	1.02	1.02	1.02	1.02	1.02
6	1.00	1.01	1.02	1.02	1.02	1.02	1.02	1.02	1.02
7	1.00	1.01	1.01	1.01	1.01	1.01	1.01	1.02	1.02
8	1.00	1.01	1.01	1.01	1.01	1.01	1.01	1.01	1.01

Table 17. Values of $\left(\frac{D_{11}}{D_{22}}\right)^{\frac{1}{4}}$ for $[(0/90/\pm 45)_m]_S$ and $[(0/90/\pm 45)_m]_A$ laminates

m	Material Systems								
	Boron/Al	S-glass/ Epoxy	Kevlar49/ Epoxy	IM7/5260	AS4/3502	AS4/ 3501-6	Boron- epoxy	IM7/ PETI-5	P-100/ 3502
1	1.03	1.10	1.14	1.14	1.14	1.14	1.14	1.15	1.16
2	1.01	1.04	1.06	1.06	1.06	1.06	1.06	1.06	1.07
3	1.01	1.03	1.04	1.04	1.04	1.04	1.04	1.04	1.04
4	1.01	1.02	1.03	1.03	1.03	1.03	1.03	1.03	1.03
5	1.01	1.02	1.02	1.02	1.02	1.02	1.02	1.02	1.03
6	1.00	1.01	1.02	1.02	1.02	1.02	1.02	1.02	1.02
7	1.00	1.01	1.02	1.02	1.02	1.02	1.02	1.02	1.02
8	1.00	1.01	1.01	1.01	1.01	1.01	1.01	1.01	1.02

Table 18. Values of $\left(\frac{D_{11}}{D_{22}}\right)^{\frac{1}{4}}$ for $(\pm 45/0/90)_m$ unsymmetric laminates

m	Material Systems								
	Boron/Al	S-glass/ Epoxy	Kevlar49/ Epoxy	IM7/5260	AS4/3502	AS4/ 3501-6	Boron- epoxy	IM7/ PETI-5	P-100/ 3502
1	.956	.868	.804	.802	.814	.805	.810	.797	.772
2	.989	.966	.950	.949	.952	.950	.951	.948	.942
3	.995	.985	.977	.977	.979	.978	.978	.977	.974
4	.997	.991	.987	.987	.988	.987	.988	.987	.985
5	.998	.995	.992	.992	.992	.992	.992	.992	.991
6	.999	.996	.994	.994	.995	.994	.994	.994	.993
7	.999	.997	.996	.996	.996	.996	.996	.996	.995
8	.999	.998	.997	.997	.997	.997	.997	.997	.996

Table 19. Values of $\left(\frac{D_{11}}{D_{22}}\right)^{\frac{1}{4}}$ for $(0/90/\pm45)_m$ unsymmetric laminates

m	Material Systems								
	Boron/Al	S-glass/ Epoxy	Kevlar49/ Epoxy	IM7/5260	AS4/3502	AS4/ 3501-6	Boron- epoxy	IM7/ PETI-5	P-100/ 3502
1	1.05	1.15	1.24	1.25	1.23	1.24	1.24	1.26	1.30
2	1.01	1.04	1.05	1.05	1.05	1.05	1.05	1.06	1.06
3	1.01	1.02	1.02	1.02	1.02	1.02	1.02	1.02	1.03
4	1.00	1.01	1.01	1.01	1.01	1.01	1.01	1.01	1.02
5	1.00	1.01	1.01	1.01	1.01	1.01	1.01	1.01	1.01
6	1.00	1.00	1.01	1.01	1.01	1.01	1.01	1.01	1.01
7	1.00	1.00	1.00	1.00	1.00	1.00	1.00	1.00	1.01
8	1.00	1.00	1.00	1.00	1.00	1.00	1.00	1.00	1.00

Table 20. Values of $\beta = \frac{D_{12} + 2D_{66}}{\sqrt{D_{11}D_{22}}}$ for $[(\pm45/0/90)_m]_S$ and $[(\pm45/0/90)_m]_A$ laminates

m	Material Systems								
	Boron/Al	S-glass/ Epoxy	Kevlar49/ Epoxy	IM7/5260	AS4/3502	AS4/ 3501-6	Boron- epoxy	IM7/ PETI-5	P-100/ 3502
1	1.28	1.57	2.02	1.98	1.90	1.89	2.05	2.04	2.22
2	1.14	1.27	1.45	1.44	1.40	1.40	1.46	1.46	1.53
3	1.09	1.17	1.29	1.28	1.26	1.26	1.30	1.30	1.33
4	1.07	1.13	1.21	1.21	1.19	1.19	1.22	1.22	1.25
5	1.05	1.10	1.17	1.16	1.15	1.15	1.17	1.17	1.19
6	1.04	1.08	1.14	1.13	1.13	1.12	1.14	1.14	1.16
7	1.04	1.07	1.12	1.12	1.11	1.11	1.12	1.12	1.14
8	1.03	1.06	1.10	1.10	1.09	1.10	1.11	1.11	1.12

Table 21. Values of $\beta = \frac{D_{12} + 2D_{66}}{\sqrt{D_{11}D_{22}}}$ for $[(0/90\pm45)_m]_S$ and $[(0/90/\pm45)_m]_A$ laminates

m	Material Systems								
	Boron/Al	S-glass/ Epoxy	Kevlar49/ Epoxy	IM7/5260	AS4/3502	AS4/ 3501-6	Boron- epoxy	IM7/ PETI-5	P-100/ 3502
1	.757	.571	.344	.362	.398	.406	.327	.334	.266
2	.874	.770	.640	.651	.671	.676	.631	.634	.594
3	.915	.843	.752	.759	.774	.777	.745	.747	.719
4	.936	.881	.810	.816	.827	.830	.805	.807	.785
5	.949	.904	.847	.851	.861	.862	.842	.844	.826
6	.957	.920	.871	.875	.883	.885	.868	.869	.854
7	.963	.931	.889	.892	.899	.901	.886	.887	.874
8	.968	.939	.903	.906	.912	.913	.900	.901	.889

Table 22. Values of $\beta = \frac{D_{12} + 2D_{66}}{\sqrt{D_{11}D_{22}}}$ for $(\pm 45/0/90)_m$ and $(0/90/\pm 45)_m$ unsymmetric laminates

m	Material Systems								
	Boron/Al	S-glass/ Epoxy	Kevlar49/ Epoxy	IM7/5260	AS4/3502	AS4/ 3501-6	Boron- epoxy	IM7/ PETI-5	P-100/ 3502
1	1.00	1.04	1.10	1.10	1.09	1.10	1.09	1.11	1.14
2	1.00	1.00	1.01	1.01	1.01	1.01	1.01	1.01	1.01
3	1.00	1.00	1.00	1.00	1.00	1.00	1.00	1.00	1.00
4	1.00	1.00	1.00	1.00	1.00	1.00	1.00	1.00	1.00
5	1.00	1.00	1.00	1.00	1.00	1.00	1.00	1.00	1.00
6	1.00	1.00	1.00	1.00	1.00	1.00	1.00	1.00	1.00
7	1.00	1.00	1.00	1.00	1.00	1.00	1.00	1.00	1.00
8	1.00	1.00	1.00	1.00	1.00	1.00	1.00	1.00	1.00

Table 23. Values of $\nu_b = \frac{D_{12}}{\sqrt{D_{11}D_{22}}}$ for $[(\pm 45/0/90)_m]_S$ and $[(\pm 45/0/90)_m]_A$ laminates

m	Material Systems								
	Boron/Al	S-glass/ Epoxy	Kevlar49/ Epoxy	IM7/5260	AS4/3502	AS4/ 3501-6	Boron- epoxy	IM7/ PETI-5	P-100/ 3502
1	.371	.452	.663	.617	.596	.569	.672	.654	.716
2	.325	.356	.475	.440	.434	.412	.477	.463	.489
3	.310	.327	.421	.390	.387	.366	.422	.409	.426
4	.303	.313	.396	.366	.365	.345	.396	.383	.397
5	.298	.304	.381	.352	.352	.332	.380	.368	.380
6	.296	.299	.371	.343	.344	.324	.371	.358	.369
7	.293	.295	.365	.336	.338	.318	,364	.352	.361
8	.292	.292	.360	.332	.333	.314	.358	.346	.355

Table 24. Values of $\nu_b = \frac{D_{12}}{\sqrt{D_{11}D_{22}}}$ for $[(0/90/\pm 45)_m]_S$ and $[(0/90/\pm 45)_m]_A$ laminates

m	Material Systems								
	Boron/Al	S-glass/ Epoxy	Kevlar49/ Epoxy	IM7/5260	AS4/3502	AS4/ 3501-6	Boron- epoxy	IM7/ PETI-5	P-100/ 3502
1	.203	.135	.108	.091	.106	.092	.100	.093	.074
2	.241	.199	.206	.185	.196	.180	.201	.192	.183
3	.254	.222	.243	.221	.229	.212	.239	.229	.224
4	.261	.234	.263	.239	.247	.229	.259	.249	.245
5	.265	.241	.275	.251	.257	.240	.271	.261	.259
6	.268	.246	.283	.259	.265	.247	.280	.269	.268
7	.270	.250	.289	.264	.270	.252	.286	.275	.275
8	.271	.253	.293	.268	.274	.256	.290	.279	.280

Table 25. Values of $\nu_b = \frac{D_{12}}{\sqrt{D_{11}D_{22}}}$ for $(\pm 45/0/90)_m$ and $(0/90/\pm 45)_m$ unsymmetric laminates

m	Material Systems								
	Boron/Al	S-glass/ Epoxy	Kevlar49/ Epoxy	IM7/5260	AS4/3502	AS4/ 3501-6	Boron- epoxy	IM7/ PETI-5	P-100/ 3502
1	.283	.283	.357	.329	.329	.311	.353	.345	.360
2	.281	.273	.327	.301	.304	.286	.325	.314	.319
3	.281	.272	.326	.299	.303	.284	.324	.312	.317
4	.281	.272	.326	.299	.303	.284	.323	.312	.316
5	.281	.272	.325	.299	.303	.284	.323	.312	.316
6	.281	.272	.325	.299	.303	.284	.323	.312	.316
7	.281	.272	.325	.299	.303	.284	.323	.312	.316
8	.281	.272	.325	.299	.303	.284	.323	.312	.316

Table 26. Values of $\gamma_b = \frac{D_{16}}{\left(D_{11}^3 D_{22}\right)^{1/4}}$ for $[(\pm 45/0/90)_m]_S$ laminates

m	Material Systems								
	Boron/Al	S-glass/ Epoxy	Kevlar49/ Epoxy	IM7/5260	AS4/3502	AS4/ 3501-6	Boron- epoxy	IM7/ PETI-5	P-100/ 3502
1	.036	.114	.182	.182	.170	.176	.178	.189	.217
2	.015	.045	.069	.069	.065	.067	.067	.071	.080
3	.009	.027	.042	.042	.039	.041	.040	.043	.048
4	.006	.020	.030	.030	.028	.029	.029	.031	.035
5	.005	.015	.023	.023	.022	.023	.022	.024	.027
6	.004	.013	.019	.019	.018	.019	.018	.020	.022
7	.003	.011	.016	.016	.015	.016	.016	.017	.019
8	.003	.009	.014	.014	.013	.014	.013	.014	.016

Table 27. Values of $\gamma_b = \frac{D_{16}}{\left(D_{11}^3 D_{22}\right)^{1/4}}$ for $[(0/90/\pm 45)_m]_S$ laminates

m	Material Systems								
	Boron/Al	S-glass/ Epoxy	Kevlar49/ Epoxy	IM7/5260	AS4/3502	AS4/ 3501-6	Boron- epoxy	IM7/ PETI-5	P-100/ 3502
1	.010	.028	.039	.039	.038	.039	.038	.040	.044
2	.008	.023	.033	.034	.032	.033	.032	.034	.038
3	.006	.018	.026	.026	.025	.026	.025	.027	.030
4	.005	.014	.021	.021	.020	.021	.020	.022	.024
5	.004	.012	.017	.018	.017	.017	.017	.018	.020
6	.003	.010	.015	.015	.014	.015	.014	.015	.017
7	.003	.009	.013	.013	.012	.013	.013	.014	.015
8	.003	.008	.012	.012	.011	.012	.011	.012	.013

Table 28. Values of $\gamma_b = \frac{D_{16}}{\left(D_{11}^3 D_{22}\right)^{1/4}}$ for $(\pm 45/0/90)_m$ unsymmetric laminates

m	Material Systems								
	Boron/Al	S-glass/ Epoxy	Kevlar49/ Epoxy	IM7/5260	AS4/3502	AS4/ 3501-6	Boron- epoxy	IM7/ PETI-5	P-100/ 3502
1	.048	.165	.280	.283	.260	.277	.268	.295	.351
2	.011	.036	.054	.055	.051	.054	.053	.056	.064
3	.005	.016	.023	.024	.022	.023	.023	.024	.027
4	.003	.009	.013	.013	.012	.013	.013	.013	.015
5	.002	.006	.008	.008	.008	.008	.008	.009	.010
6	.001	.004	.006	.006	.005	.006	.006	.006	.007
7	.001	.003	.004	.004	.004	.004	.004	.004	.005
8	.001	.002	.003	.003	.003	.003	.003	.003	.004

Table 29. Values of $\gamma_b = \frac{D_{16}}{\left(D_{11}^3 D_{22}\right)^{1/4}}$ for $(0/90/\pm 45)_m$ unsymmetric laminates

m	Material Systems								
	Boron/Al	S-glass/ Epoxy	Kevlar49/ Epoxy	IM7/5260	AS4/3502	AS4/ 3501-6	Boron- epoxy	IM7/ PETI-5	P-100/ 3502
1	-.043	-.124	-.181	-.182	-.172	-.180	-.176	-.187	-.209
2	-.011	-.033	-.049	-.049	-.047	-.049	-.048	-.051	-.056
3	-.005	-.015	-.022	-.022	-.021	-.022	-.022	-.023	-.026
4	-.003	-.009	-.013	-.013	-.012	-.013	-.012	-.013	-.015
5	-.002	-.005	-.008	-.008	-.008	-.008	-.008	-.008	-.009
6	-.001	-.004	-.006	-.006	-.005	-.006	-.006	-.006	-.007
7	-.001	-.003	-.004	-.004	-.004	-.004	-.004	-.004	-.005
8	-.001	-.002	-.003	-.003	-.003	-.003	-.003	-.003	-.004

Table 30. Values of $\delta_b = \frac{D_{26}}{\left(D_{11} D_{22}^3\right)^{1/4}}$ for $[(\pm 45/0/90)_m]_S$ laminates

m	Material Systems								
	Boron/Al	S-glass/ Epoxy	Kevlar49/ Epoxy	IM7/5260	AS4/3502	AS4/ 3501-6	Boron- epoxy	IM7/ PETI-5	P-100/ 3502
1	.037	.123	.207	.207	.191	.200	.202	.216	.253
2	.015	.047	.075	.075	.070	.073	.073	.078	.089
3	.009	.028	.044	.044	.042	.044	.043	.046	.052
4	.007	.020	.031	.031	.029	.031	.030	.032	.037
5	.005	.016	.024	.024	.023	.024	.023	.025	.028
6	.004	.013	.020	.020	.018	.019	.019	.020	.023
7	.004	.011	.016	.017	.016	.016	.016	.017	.019
8	.003	.009	.014	.014	.013	.014	.014	.015	.017

Table 31. Values of $\delta_b = \frac{D_{26}}{\left(D_{11}D_{22}^3\right)^{1/4}}$ for $[(0/90/\pm45)_m]_S$ laminates

m	Material Systems								
	Boron/Al	S-glass/ Epoxy	Kevlar49/ Epoxy	IM7/5260	AS4/3502	AS4/ 3501-6	Boron- epoxy	IM7/ PETI-5	P-100/ 3502
1	.011	.034	.050	.051	.048	.051	.048	.052	.059
2	.008	.025	.037	.038	.036	.037	.036	.039	.043
3	.006	.019	.028	.028	.027	.028	.027	.029	.032
4	.005	.015	.022	.022	.021	.022	.021	.023	.025
5	.004	.012	.018	.018	.017	.018	.018	.019	.021
6	.003	.010	.015	.016	.015	.015	.015	.016	.018
7	.003	.009	.013	.014	.013	.013	.013	.014	.016
8	.003	.008	.012	.012	.011	.012	.012	.012	.014

Table 32. Values of $\delta_b = \frac{D_{26}}{\left(D_{11}D_{22}^3\right)^{1/4}}$ for $(\pm45/0/90)_m$ unsymmetric laminates

m	Material Systems								
	Boron/Al	S-glass/ Epoxy	Kevlar49/ Epoxy	IM7/5260	AS4/3502	AS4/ 3501-6	Boron- epoxy	IM7/ PETI-5	P-100/ 3502
1	.043	.124	.181	.182	.172	.180	.176	.187	.209
2	.011	.033	.049	.049	.047	.049	.048	.051	.056
3	.005	.015	.022	.022	.021	.022	.022	.023	.026
4	.003	.009	.013	.013	.012	.013	.012	.013	.015
5	.002	.005	.008	.008	.008	.008	.008	.008	.009
6	.001	.004	.006	.006	.005	.006	.006	.006	.007
7	.001	.003	.004	.004	.004	.004	.004	.004	.005
8	.001	.002	.003	.003	.003	.003	.003	.003	.004

Table 33. Values of $\delta_b = \frac{D_{26}}{\left(D_{11}D_{22}^3\right)^{1/4}}$ for $(0/90/\pm45)_m$ unsymmetric laminates

m	Material Systems								
	Boron/Al	S-glass/ Epoxy	Kevlar49/ Epoxy	IM7/5260	AS4/3502	AS4/ 3501-6	Boron- epoxy	IM7/ PETI-5	P-100/ 3502
1	-.048	-.165	-.280	-.283	-.260	-.277	-.268	-.295	-.351
2	-.011	-.036	-.054	-.055	-.051	-.054	-.053	-.056	-.064
3	-.005	-.016	-.023	-.024	-.022	-.023	-.023	-.024	-.027
4	-.003	-.009	-.013	-.013	-.012	-.013	-.013	-.013	-.015
5	-.002	-.006	-.008	-.008	-.008	-.008	-.008	-.009	-.010
6	-.001	-.004	-.006	-.006	-.005	-.006	-.006	-.006	-.007
7	-.001	-.003	-.004	-.004	-.004	-.004	-.004	-.004	-.005
8	-.001	-.002	-.003	-.003	-.003	-.003	-.003	-.003	-.004

Table 34. Values of $\frac{h}{\sqrt{12}(a_{11}a_{22}D_{11}D_{22})^{1/4}}$ for $[(\pm 45/0/90)_m]_S$ and $[(\pm 45/0/90)_m]_A$ laminates

m	Material Systems								
	Boron/Al	S-glass/ Epoxy	Kevlar49/ Epoxy	IM7/5260	AS4/3502	AS4/ 3501-6	Boron- epoxy	IM7/ PETI-5	P-100/ 3502
1	.993	1.03	1.06	1.07	1.06	1.06	1.07	1.07	1.09
2	.976	.994	.999	1.01	1.00	1.01	1.00	1.01	1.01
3	.970	.983	.980	.988	.984	.990	.981	.985	.988
4	.968	.978	.971	.979	.976	.982	.972	.976	.978
5	.966	.975	.965	.974	.971	.977	.967	.970	.972
6	.965	.972	.962	.970	.968	.974	.963	.967	.968
7	.964	.971	.960	.968	.966	.971	.961	.964	.965
8	.964	.970	.958	.966	.964	.970	.959	.963	.963

Table 35. Values of $\frac{h}{\sqrt{12}(a_{11}a_{22}D_{11}D_{22})^{1/4}}$ for $[(0/90/\pm 45)_m]_S$ and $[(0/90/\pm 45)_m]_A$ laminates

m	Material Systems								
	Boron/Al	S-glass/ Epoxy	Kevlar49/ Epoxy	IM7/5260	AS4/3502	AS4/ 3501-6	Boron- epoxy	IM7/ PETI-5	P-100/ 3502
1	.931	.916	.878	.889	.891	.898	.875	.882	.875
2	.944	.935	.905	.914	.915	.922	.904	.908	.903
3	.949	.944	.917	.926	.927	.933	.917	.921	.916
4	.952	.948	.923	.933	.933	.939	.923	.927	.924
5	.953	.951	.928	.937	.937	.942	.928	.932	.928
6	.954	.953	.930	.939	.939	.945	.931	.935	.931
7	.955	.954	.933	.941	.941	.947	.933	.937	.934
8	.956	.955	.934	.943	.943	.948	.934	.938	.936

Table 36. Values of $\frac{h}{\sqrt{12}(a_{11}a_{22}D_{11}D_{22})^{1/4}}$ for $(\pm 45/0/90)_m$ and $(0/90/\pm 45)_m$ unsymmetric laminates

m	Material Systems								
	Boron/Al	S-glass/ Epoxy	Kevlar49/ Epoxy	IM7/5260	AS4/3502	AS4/ 3501-6	Boron- epoxy	IM7/ PETI-5	P-100/ 3502
1	.962	.981	.990	1.00	.993	1.00	.988	.999	1.01
2	.960	.963	.948	.957	.955	.961	.949	.953	.952
3	.960	.963	.946	.955	.953	.959	.947	.951	.949
4	.960	.962	.946	.954	.953	.959	.946	.950	.949
5	.960	.962	.946	.954	.953	.959	.946	.950	.949
6	.960	.962	.946	.954	.953	.959	.946	.950	.949
7	.960	.962	.946	.954	.953	.959	.946	.950	.949
8	.960	.962	.946	.954	.953	.959	.946	.950	.949

Table 37. Values of $e_{11} = B_{11}\left(\frac{a_{11}}{D_{11}}\right)^{1/2}$ for $(\pm 45/0/90)_m$ unsymmetric laminates

m	Material Systems								
	Boron/Al	S-glass/ Epoxy	Kevlar49/ Epoxy	IM7/5260	AS4/3502	AS4/ 3501-6	Boron- epoxy	IM7/ PETI-5	P-100/ 3502
1	.025	-.020	-.008	-.020	-.021	-.039	.011	-.014	-.015
2	.012	-.009	-.003	-.008	-.009	-.016	.004	-.006	-.006
3	.008	-.006	-.002	-.005	-.006	-.010	.003	-.004	-.004
4	.006	-.004	-.002	-.004	-.004	-.008	.002	-.003	-.003
5	.005	-.003	-.001	-.003	-.003	-.006	.002	-.002	-.002
6	.004	-.003	-.001	-.003	-.003	-.005	.001	-.002	-.002
7	.003	-.002	-.001	-.002	-.002	-.004	.001	-.002	-.002
8	.003	-.002	-.001	-.002	-.002	-.004	.001	-.001	-.001

Table 38. Values of $e_{11} = B_{11}\left(\frac{a_{11}}{D_{11}}\right)^{1/2}$ for $(0/90/\pm 45)_m$ unsymmetric laminates

m	Material Systems								
	Boron/Al	S-glass/ Epoxy	Kevlar49/ Epoxy	IM7/5260	AS4/3502	AS4/ 3501-6	Boron- epoxy	IM7/ PETI-5	P-100/ 3502
1	-.127	-.277	-.417	-.408	-.387	-.389	-.418	-.424	-.468
2	-.066	-.151	-.236	-.231	-.218	-.220	-.236	-.241	-.269
3	-.044	-.103	-.162	-.158	-.149	-.150	-.161	-.165	-.185
4	-.033	-.078	-.122	-.120	-.113	-.114	-.122	-.125	-.140
5	-.027	-.062	-.098	-.096	-.091	-.092	-.098	-.100	-.113
6	-.022	-.052	-.082	-.080	-.076	-.076	-.082	-.084	-.094
7	-.019	-.045	-.070	-.069	-.065	-.066	-.070	-.072	-.081
8	-.017	-.039	-.062	-.060	-.057	-.057	-.062	-.063	-.071

Table 39. Values of $e_{12} = B_{12}\left(\frac{a_{11}a_{22}}{D_{11}D_{22}}\right)^{1/4}$ and $e_{66} = B_{66}\left(\frac{a_{11}a_{22}}{D_{11}D_{22}}\right)^{1/4}$ for $(\pm 45/0/90)_m$ unsymmetric laminates

m	Material Systems								
	Boron/Al	S-glass/ Epoxy	Kevlar49/ Epoxy	IM7/5260	AS4/3502	AS4/ 3501-6	Boron- epoxy	IM7/ PETI-5	P-100/ 3502
1	-.079	-.151	-.256	-.246	-.229	-.226	-.262	-.261	-.297
2	-.039	-.074	-.123	-.118	-.110	-.108	-.126	-.124	-.140
3	-.026	-.049	-.082	-.078	-.073	-.072	-.084	-.083	-.093
4	-.020	-.037	-.061	-.059	-.055	-.054	-.063	-.062	-.070
5	-.016	-.030	-.049	-.047	-.044	-.043	-.050	-.050	-.056
6	-.013	-.025	-.041	-.039	-.037	-.036	-.042	-.041	-.046
7	-.011	-.021	-.035	-.034	-.031	-.031	-.036	-.035	-.040
8	-.010	-.018	-.031	-.029	-.028	-.027	-.031	-.031	-.035

Table 40. Values of $\epsilon_{12} = B_{12}\left(\frac{a_{11}a_{22}}{D_{11}D_{22}}\right)^{1/4}$ and $\epsilon_{66} = B_{66}\left(\frac{a_{11}a_{22}}{D_{11}D_{22}}\right)^{1/4}$ for $(0/90/\pm45)_m$ unsymmetric laminates

m	Material Systems								
	Boron/Al	S-glass/ Epoxy	Kevlar49/ Epoxy	IM7/5260	AS4/3502	AS4/ 3501-6	Boron- epoxy	IM7/ PETI-5	P-100/ 3502
1	.079	.151	.256	.246	.229	.226	.262	.261	.297
2	.039	.074	.123	.118	.110	.108	.126	.124	.140
3	.026	.049	.082	.078	.073	.072	.084	.083	.093
4	.020	.037	.061	.059	.055	.054	.063	.062	.070
5	.016	.030	.049	.047	.044	.043	.050	.050	.056
6	.013	.025	.041	.039	.037	.036	.042	.041	.046
7	.011	.021	.035	.034	.031	.031	.036	.035	.040
8	.010	.018	.031	.029	.028	.027	.031	.031	.035

Table 41. Values of $\epsilon_{16} = B_{16}\left(\frac{a_{11}^2}{D_{11}D_{22}}\right)^{1/4}$ and $\epsilon_{26} = B_{26}\left(\frac{a_{22}^2}{D_{11}D_{22}}\right)^{1/4}$ for $[(\pm45/0/90)_m]_A$ laminates

m	Material Systems								
	Boron/Al	S-glass/ Epoxy	Kevlar49/ Epoxy	IM7/5260	AS4/3502	AS4/ 3501-6	Boron- epoxy	IM7/ PETI-5	P-100/ 3502
1	-.014	-.044	-.070	-.070	-.066	-.068	-.068	-.073	-.083
2	-.007	-.021	-.033	-.033	-.031	-.032	-.032	-.034	-.039
3	-.005	-.014	-.022	-.022	-.020	-.021	-.021	-.022	-.025
4	-.003	-.010	-.016	-.016	-.015	-.016	-.016	-.017	-.019
5	-.003	-.008	-.013	-.013	-.012	-.013	-.012	-.013	-.015
6	-.002	-.007	-.011	-.011	-.010	-.010	-.010	-.011	-.012
7	-.002	-.006	-.009	-.009	-.009	-.009	-.009	-.009	-.011
8	-.002	-.005	-.008	-.008	-.007	-.008	-.008	-.008	-.009

Table 42. Values of $\epsilon_{16} = B_{16}\left(\frac{a_{11}^2}{D_{11}D_{22}}\right)^{1/4}$ and $\epsilon_{26} = B_{26}\left(\frac{a_{22}^2}{D_{11}D_{22}}\right)^{1/4}$ for $[(0/90/\pm45)_m]_A$ laminates

m	Material Systems								
	Boron/Al	S-glass/ Epoxy	Kevlar49/ Epoxy	IM7/5260	AS4/3502	AS4/ 3501-6	Boron- epoxy	IM7/ PETI-5	P-100/ 3502
1	-.013	-.039	-.058	-.058	-.055	-.058	-.056	-.060	-.067
2	-.007	-.020	-.030	-.030	-.028	-.030	-.029	-.031	-.034
3	-.004	-.013	-.020	-.020	-.019	-.020	-.020	-.021	-.023
4	-.003	-.010	-.015	-.015	-.014	-.015	-.015	-.016	-.018
5	-.003	-.008	-.012	-.012	-.012	-.012	-.012	-.013	-.014
6	-.002	-.007	-.010	-.010	-.010	-.010	-.010	-.011	-.012
7	-.002	-.006	-.009	-.009	-.008	-.009	-.009	-.009	-.010
8	-.002	-.005	-.008	-.008	-.007	-.008	-.008	-.008	-.009

Table 43. Values of $\epsilon_{16} = B_{16}\left(\frac{a_{11}^2}{D_{11}D_{22}}\right)^{1/4}$ and $\epsilon_{26} = B_{26}\left(\frac{a_{22}^2}{D_{11}D_{22}}\right)^{1/4}$ for $(\pm 45/0/90)_m$ and $(0/90/\pm 45)_m$ unsymmetric laminates

m	Material Systems								
	Boron/Al	S-glass/ Epoxy	Kevlar49/ Epoxy	IM7/5260	AS4/3502	AS4/ 3501-6	Boron- epoxy	IM7/ PETI-5	P-100/ 3502
1	-.027	-.084	-.131	-.131	-.123	-.129	-.127	-.136	-.155
2	-.014	-.041	-.063	-.063	-.059	-.062	-.061	-.065	-.073
3	-.009	-.028	-.042	-.042	-.039	-.041	-.041	-.043	-.048
4	-.007	-.021	-.031	-.031	-.030	-.031	-.030	-.032	-.036
5	-.005	-.017	-.025	-.025	-.024	-.025	-.024	-.026	-.029
6	-.005	-.014	-.021	-.021	-.020	-.020	-.020	-.022	-.024
7	-.004	-.012	-.018	-.018	-.017	-.018	-.017	-.018	-.021
8	-.003	-.010	-.016	-.016	-.015	-.015	-.015	-.016	-.018

Table 44. Values of $\epsilon_{22} = B_{22}\left(\frac{a_{22}}{D_{22}}\right)^{1/2}$ for $(\pm 45/0/90)_m$ unsymmetric laminates

m	Material Systems								
	Boron/Al	S-glass/ Epoxy	Kevlar49/ Epoxy	IM7/5260	AS4/3502	AS4/ 3501-6	Boron- epoxy	IM7/ PETI-5	P-100/ 3502
1	.127	.277	.417	.408	.387	.389	.418	.424	.468
2	.066	.151	.236	.231	.218	.220	.236	.241	.269
3	.044	.103	.162	.158	.149	.150	.161	.165	.185
4	.033	.078	.122	.120	.113	.114	.122	.125	.140
5	.027	.062	.098	.096	.091	.092	.098	.100	.113
6	.022	.052	.082	.080	.076	.076	.082	.084	.094
7	.019	.045	.070	.069	.065	.066	.070	.072	.081
8	.017	.039	.062	.060	.057	.057	.062	.063	.071

Table 45. Values of $\epsilon_{22} = B_{22}\left(\frac{a_{22}}{D_{22}}\right)^{1/2}$ for $(0/90/\pm 45)_m$ unsymmetric laminates

m	Material Systems								
	Boron/Al	S-glass/ Epoxy	Kevlar49/ Epoxy	IM7/5260	AS4/3502	AS4/ 3501-6	Boron- epoxy	IM7/ PETI-5	P-100/ 3502
1	-.025	.020	.008	.020	.021	.039	-.011	.014	.015
2	-.012	.009	.003	.008	.009	.016	-.004	.006	.006
3	-.008	.006	.002	.005	.006	.010	-.003	.004	.004
4	-.006	.004	.002	.004	.004	.008	-.002	.003	.003
5	-.005	.003	.001	.003	.003	.006	-.002	.002	.002
6	-.004	.003	.001	.003	.003	.005	-.001	.002	.002
7	-.003	.002	.001	.002	.002	.004	-.001	.002	.002
8	-.003	.002	.001	.002	.002	.004	-.001	.001	.001

Table 46. Values of $\beta = \frac{D_{12} + 2D_{66}}{\sqrt{D_{11}D_{22}}}$ for (+θ/0/90) and (-θ/0/90) three-ply laminates

θ, deg	Material Systems								
	Boron/Al	S-glass/ Epoxy	Kevlar49/ Epoxy	IM7/5260	AS4/3502	AS4/ 3501-6	Boron- epoxy	IM7/ PETI-5	P-100/ 3502
0	.680	.435	.157	.177	.220	.229	.138	.144	.064
5	.689	.450	.176	.196	.239	.247	.158	.164	.085
10	.713	.491	.234	.253	.293	.300	.216	.222	.147
15	.752	.556	.326	.343	.379	.386	.310	.315	.247
20	.801	.641	.447	.462	.492	.498	.433	.438	.380
25	.855	.736	.589	.601	.624	.629	.578	.582	.537
30	.907	.834	.740	.748	.763	.768	.731	.736	.708
35	.951	.923	.886	.891	.896	.902	.879	.886	.877
40	.981	.992	1.01	1.01	1.09	1.02	1.00	1.02	1.03
45	.993	1.03	1.10	1.10	1.09	1.10	1.09	1.11	1.15
50	.985	1.04	1.13	1.14	1.11	1.14	1.11	1.15	1.22
55	.959	1.01	1.10	1.12	1.09	1.12	1.08	1.13	1.23
60	.918	.941	1.01	1.03	1.01	1.05	.973	1.04	1.15
65	.868	.856	.868	.896	.878	.932	.821	.896	.994
70	.815	.762	.695	.730	.728	.784	.645	.717	.776
75	.767	.672	.525	.564	.579	.634	.475	.537	.538
80	.728	.600	.384	.425	.457	.506	.337	.387	.332
85	.703	.552	.293	.335	.376	.422	.248	.290	.196
90	.695	.536	.262	.303	.349	.393	.217	.256	.148

Table 47. Values of $\left(\frac{D_{11}}{D_{22}}\right)^{\frac{1}{4}}$ for (+θ/0/90) and (-θ/0/90) three-ply laminates

θ, deg	Material Systems								
	Boron/Al	S-glass/ Epoxy	Kevlar49/ Epoxy	IM7/5260	AS4/3502	AS4/ 3501-6	Boron- epoxy	IM7/ PETI-5	P-100/ 3502
0	1.00	1.01	1.02	1.02	1.02	1.02	1.02	1.02	1.02
5	1.00	1.01	1.01	1.01	1.01	1.01	1.01	1.01	1.02
10	1.00	1.00	1.00	1.00	1.00	1.00	1.00	1.00	1.00
15	.997	.991	.988	.987	.988	.987	.988	.987	.986
20	.991	.975	.965	.965	.966	.965	.966	.964	.960
25	.984	.955	.936	.935	.938	.935	.938	.933	.927
30	.976	.931	.900	.899	.904	.900	.903	.897	.886
35	.967	.903	.859	.858	.866	.860	.863	.854	.838
40	.957	.874	.815	.813	.824	.816	.820	.808	.785
45	.948	.845	.769	.767	.781	.770	.776	.760	.730
50	.938	.817	.724	.722	.739	.726	.733	.713	.674
55	.929	.791	.684	.680	.701	.685	.695	.670	.622
60	.922	.769	.649	.645	.668	.649	.663	.633	.576
65	.915	.751	.622	.616	.642	.620	.638	.604	.538
70	.910	.738	.602	.596	.623	.598	.621	.583	.511
75	.906	.728	.589	.582	.610	.583	.609	.569	.493
80	.903	.721	.582	.574	.602	.573	.603	.561	.484
85	.901	.717	.578	.569	.598	.568	.600	.557	.479
90	.901	.716	.577	.568	.597	.567	.599	.556	.478

Table 48. Values of $\left(\frac{a_{22}}{a_{11}}\right)^{\frac{1}{4}}$ for $(+\theta/0/90)_m$ and $(-\theta/0/90)_m$ laminates (m = 1, 2, ...)

θ, deg	Material Systems								
	Boron/Al	S-glass/ Epoxy	Kevlar49/ Epoxy	IM7/5260	AS4/3502	AS4/ 3501-6	Boron- epoxy	IM7/ PETI-5	P-100/ 3502
0	1.04	1.11	1.16	1.16	1.15	1.16	1.15	1.17	1.18
5	1.04	1.11	1.15	1.15	1.15	1.16	1.14	1.15	1.16
10	1.04	1.10	1.12	1.13	1.13	1.14	1.11	1.13	1.12
15	1.03	1.09	1.09	1.10	1.10	1.11	1.09	1.10	1.08
20	1.03	1.07	1.07	1.08	1.08	1.09	1.06	1.07	1.05
25	1.02	1.06	1.05	1.06	1.06	1.07	1.04	1.05	1.03
30	1.02	1.04	1.03	1.04	1.04	1.05	1.03	1.03	1.02
35	1.01	1.03	1.02	1.03	1.03	1.03	1.02	1.02	1.01
40	1.01	1.01	1.01	1.01	1.01	1.01	1.01	1.01	1.01
45	1.00	1.00	1.00	1.00	1.00	1.00	1.00	1.00	1.00
50	.994	.986	.990	.988	.988	.986	.992	.990	.994
55	.989	.973	.980	.976	.975	.971	.983	.979	.987
60	.983	.959	.968	.962	.960	.955	.972	.967	.978
65	.978	.945	.954	.946	.944	.938	.959	.952	.967
70	.974	.931	.936	.927	.926	.919	.942	.934	.951
75	.969	.919	.915	.906	.906	.899	.921	.912	.928
80	.966	.908	.891	.884	.887	.880	.897	.887	.897
85	.964	.901	.871	.867	.872	.865	.876	.866	.862
90	.964	.899	.862	.860	.866	.860	.867	.858	.845

Table 49. Values of $\nu_m = \frac{-a_{12}}{\sqrt{a_{11}a_{22}}}$ for $(+\theta/0/90)_m$ and $(-\theta/0/90)_m$ laminates (m = 1, 2, ...)

θ, deg	Material Systems								
	Boron/Al	S-glass/ Epoxy	Kevlar49/ Epoxy	IM7/5260	AS4/3502	AS4/ 3501-6	Boron- epoxy	IM7/ PETI-5	P-100/ 3502
0	.179	.095	.048	.033	.051	.038	.040	.033	.009
5	.182	.097	.053	.037	.055	.041	.046	.037	.012
10	.188	.106	.064	.046	.064	.048	.059	.046	.017
15	.197	.117	.076	.057	.076	.058	.074	.057	.022
20	.207	.130	.086	.067	.087	.067	.086	.066	.025
25	.218	.143	.095	.075	.097	.076	.095	.073	.028
30	.228	.153	.100	.081	.105	.082	.101	.078	.029
35	.235	.161	.104	.085	.110	.086	.106	.082	.030
40	.240	.166	.106	.088	.113	.089	.108	.084	.030
45	.242	.168	.107	.088	.114	.090	.109	.084	.030
50	.240	.166	.106	.088	.113	.089	.108	.084	.030
55	.235	.161	.104	.085	.110	.086	.106	.082	.030
60	.228	.153	.100	.081	.105	.082	.101	.078	.029
65	.218	.143	.095	.075	.097	.076	.095	.073	.028
70	.207	.130	.086	.067	.087	.067	.086	.066	.025
75	.197	.117	.076	.057	.076	.058	.074	.057	.022
80	.188	.106	.064	.046	.064	.048	.059	.046	.017
85	.182	.097	.053	.037	.055	.041	.046	.037	.012
90	.179	.095	.048	.033	.051	.038	.040	.033	.009

Table 50. Values of $\nu_b = \frac{D_{12}}{\sqrt{D_{11}D_{22}}}$ for (+θ/0/90) and (-θ/0/90) three-ply laminates

θ, deg	Material Systems								
	Boron/Al	S-glass/ Epoxy	Kevlar49/ Epoxy	IM7/5260	AS4/3502	AS4/ 3501-6	Boron- epoxy	IM7/ PETI-5	P-100/ 3502
0	.179	.092	.046	.032	.049	.037	.038	.031	.008
5	.182	.097	.052	.038	.055	.042	.045	.038	.015
10	.190	.110	.071	.056	.072	.060	.064	.057	.036
15	.202	.131	.102	.086	.101	.087	.095	.087	.069
20	.218	.158	.142	.124	.137	.123	.136	.128	.112
25	.235	.188	.189	.169	.180	.165	.184	.175	.164
30	.251	.219	.239	.217	.225	.209	.234	.225	.220
35	.266	.246	.287	.262	.268	.251	.283	.274	.275
40	.275	.268	.328	.301	.304	.286	.324	.315	.325
45	.279	.279	.357	.328	.328	.311	.351	.345	.363
50	.276	.280	.368	.338	.336	.320	.359	.357	.385
55	.268	.268	.358	.329	.325	.312	.346	.349	.385
60	.255	.247	.327	.299	.296	.286	.312	.318	.357
65	.238	.218	.279	.252	.253	.244	.261	.269	.303
70	.222	.187	.221	.196	.203	.194	.202	.209	.229
75	.206	.158	.164	.141	.154	.143	.146	.149	.149
80	.194	.134	.118	.095	.113	.100	.100	.099	.080
85	.186	.119	.087	.065	.086	.073	.070	.067	.035
90	.183	.114	.077	.055	.077	.063	.060	.055	.019

Table 51. Values of $\mu = \frac{2a_{12} + a_{66}}{2\sqrt{a_{11}a_{22}}}$ for $(+\theta/0/90)_m$ and $(-\theta/0/90)_m$ laminates (m = 1, 2, ...)

θ, deg	Material Systems								
	Boron/Al	S-glass/ Epoxy	Kevlar49/ Epoxy	IM7/5260	AS4/3502	AS4/ 3501-6	Boron- epoxy	IM7/ PETI-5	P-100/ 3502
0	1.75	2.73	8.58	6.54	5.54	4.93	9.56	8.42	16.9
5	1.73	2.68	8.06	6.24	5.32	4.76	8.91	7.92	14.9
10	1.68	2.55	6.84	5.49	4.78	4.33	7.42	6.74	11.2
15	1.61	2.36	5.51	4.61	4.10	3.78	5.85	5.44	7.98
20	1.52	2.15	4.38	3.81	3.46	3.24	4.57	4.34	5.80
25	1.43	1.95	3.53	3.17	2.93	2.79	3.63	3.52	4.41
30	1.36	1.78	2.94	2.70	2.53	2.44	2.99	2.94	3.53
35	1.28	1.65	2.56	2.39	2.25	2.20	2.58	2.57	3.00
40	1.24	1.57	2.35	2.21	2.09	2.06	2.35	2.36	2.72
45	1.23	1.54	2.28	2.15	2.04	2.01	2.28	2.29	2.63
50	1.24	1.57	2.35	2.21	2.09	2.06	2.35	2.36	2.72
55	1.28	1.65	2.56	2.39	2.25	2.20	2.58	2.57	3.00
60	1.35	1.78	2.94	2.70	2.53	2.44	2.99	2.94	3.53
65	1.43	1.95	3.53	3.17	2.93	2.79	3.63	3.52	4.41
70	1.52	2.15	4.38	3.81	3.46	3.24	4.57	4.34	5.80
75	1.60	2.36	5.51	4.61	4.10	3.78	5.85	5.44	7.98
80	1.68	2.55	6.84	5.49	4.78	4.33	7.42	6.74	11.2
85	1.73	2.68	8.06	6.24	5.32	4.76	8.91	7.92	14.9
90	1.75	2.73	8.58	6.54	5.54	4.93	9.56	8.42	16.9

Table 52. Values of $\gamma_m = \frac{-a_{26}}{\left(a_{11}a_{22}^3\right)^{1/4}}$ for $(+\theta/0/90)_m$ and $-\gamma_m$ for $(-\theta/0/90)_m$ laminates (m = 1, 2, ...)

θ, deg	Material Systems								
	Boron/Al	S-glass/ Epoxy	Kevlar49/ Epoxy	IM7/5260	AS4/3502	AS4/ 3501-6	Boron- epoxy	IM7/ PETI-5	P-100/ 3502
0	0	0	0	0	0	0	0	0	0
5	-.022	-.004	-.019	.008	.001	.023	-.045	.001	.036
10	-.039	.000	-.010	.032	.016	.054	-.052	.023	.094
15	-.048	.014	.033	.077	.053	.100	-.012	.073	.173
20	-.046	.043	.105	.142	.110	.159	.062	.146	.265
25	-.034	.084	.196	.223	.184	.231	.157	.235	.366
30	-.011	.137	.298	.315	.270	.312	.265	.336	.474
35	.019	.197	.410	.415	.365	.401	.382	.444	.590
40	.055	.263	.530	.522	.467	.495	.507	.560	.716
45	.092	.329	.657	.635	.573	.593	.640	.684	.855
50	.128	.393	.792	.752	.682	.692	.781	.815	1.01
55	.158	.448	.933	.871	.790	.788	.931	.953	1.19
60	.180	.489	1.08	.986	.890	.874	1.09	1.09	1.39
65	.188	.506	1.21	1.09	.969	.936	1.24	1.23	1.62
70	.181	.490	1.32	1.14	1.00	.954	1.36	1.33	1.86
75	.156	.432	1.33	1.11	.957	.894	1.41	1.34	2.06
80	.116	.326	1.17	.934	.782	.719	1.26	1.17	2.05
85	.061	.176	.716	.550	.451	.409	.786	.715	1.45
90	0	0	0	0	0	0	0	0	0

Table 53. Values of $\delta_m = \frac{-a_{16}}{\left(a_{11}^3a_{22}\right)^{1/4}}$ for $(+\theta/0/90)_m$ and $-\delta_m$ for $(-\theta/0/90)_m$ laminates (m = 1, 2, ...)

θ, deg	Material Systems								
	Boron/Al	S-glass/ Epoxy	Kevlar49/ Epoxy	IM7/5260	AS4/3502	AS4/ 3501-6	Boron- epoxy	IM7/ PETI-5	P-100/ 3502
0	0	0	0	0	0	0	0	0	0
5	.061	.176	.716	.550	.451	.409	.786	.715	1.45
10	.116	.326	1.17	.934	.782	.719	1.26	1.17	2.05
15	.156	.432	1.33	1.11	.957	.894	1.41	1.34	2.06
20	.181	.490	1.32	1.14	1.00	.954	1.36	1.33	1.86
25	.188	.506	1.21	1.09	.969	.936	1.24	1.23	1.62
30	.180	.489	1.08	.986	.890	.874	1.09	1.09	1.39
35	.158	.448	.933	.871	.790	.788	.931	.953	1.19
40	.128	.393	.792	.752	.682	.692	.781	.815	1.011
45	.092	.329	.657	.635	.573	.593	.640	.684	.855
50	.055	.263	.530	.522	.467	.495	.507	.560	.716
55	.019	.197	.410	.415	.365	.401	.382	.444	.590
60	-.011	.137	.298	.315	.270	.312	.265	.336	.474
65	-.034	.084	.196	.223	.184	.231	.157	.235	.366
70	-.046	.043	.105	.142	.110	.159	.062	.146	.265
75	-.048	.014	.033	.077	.053	.100	-.012	.073	.173
80	-.039	.000	-.010	.032	.016	.054	-.052	.023	.094
85	-.022	-.004	-.019	.008	.001	.023	-.045	.001	.036
90	0	0	0	0	0	0	0	0	0

Table 54. Values of $\gamma_b = \frac{D_{16}}{\left(D_{11}^3 D_{22}\right)^{1/4}}$ for (+θ/0/90) and $-\gamma_b$ for (-θ/0/90) three-ply laminates

θ, deg	Material Systems								
	Boron/Al	S-glass/ Epoxy	Kevlar49/ Epoxy	IM7/5260	AS4/3502	AS4/ 3501-6	Boron- epoxy	IM7/ PETI-5	P-100/ 3502
0	0	0	0	0	0	0	0	0	0
5	.022	.049	.070	.070	.067	.068	.070	.072	.079
10	.043	.097	.139	.139	.132	.134	.138	.143	.156
15	.061	.141	.205	.204	.193	.198	.203	.210	.231
20	.075	.179	.265	.264	.250	.256	.262	.272	.301
25	.084	.209	.318	.316	.298	.307	.313	.327	.365
30	.087	.230	.359	.359	.336	.348	.353	.372	.420
35	.083	.239	.387	.387	.360	.376	.378	.403	.463
40	.075	.236	.398	.400	.368	.389	.384	.417	.491
45	.062	.220	.388	.392	.357	.384	.369	.411	.499
50	.046	.193	.356	.364	.327	.359	.332	.382	.484
55	.030	.158	.303	.314	.279	.316	.274	.331	.441
60	.015	.120	.235	.249	.218	.257	.204	.262	.369
65	.004	.083	.162	.177	.154	.191	.132	.185	.275
70	-.004	.052	.096	.110	.096	.127	.071	.113	.175
75	-.008	.029	.047	.059	.051	.075	.028	.057	.092
80	-.007	.014	.017	.026	.023	.038	.005	.023	.037
85	-.004	.005	.004	.008	.008	.015	-.002	.007	.010
90	0	0	0	0	0	0	0	0	0

Table 55. Values of $\delta_b = \frac{D_{26}}{\left(D_{11} D_{22}^3\right)^{1/4}}$ for (+θ/0/90) and $-\delta_b$ for (-θ/0/90) three-ply laminates

θ, deg	Material Systems								
	Boron/Al	S-glass/ Epoxy	Kevlar49/ Epoxy	IM7/5260	AS4/3502	AS4/ 3501-6	Boron- epoxy	IM7/ PETI-5	P-100/ 3502
0	0	0	0	0	0	0	0	0	0
5	-.004	.003	.001	.003	.003	.005	-.001	.002	.002
10	-.007	.008	.006	.009	.009	.013	.002	.007	.008
15	-.007	.017	.017	.020	.020	.026	.011	.019	.020
20	-.004	.032	.036	.040	.039	.047	.028	.039	.042
25	.003	.051	.064	.068	.066	.075	.056	.068	.074
30	.013	.076	.100	.105	.100	.110	.092	.105	.116
35	.027	.104	.143	.147	.140	.149	.135	.149	.164
40	.041	.132	.187	.190	.180	.190	.180	.194	.216
45	.055	.157	.229	.231	.218	.228	.222	.237	.266
50	.067	.176	.263	.263	.248	.257	.257	.272	.308
55	.076	.186	.283	.283	.265	.275	.277	.294	.338
60	.079	.186	.287	.287	.267	.278	.281	.298	.349
65	.077	.175	.272	.272	.253	.263	.266	.284	.337
70	.069	.153	.240	.240	.222	.232	.234	.250	.301
75	.057	.123	.192	.193	.178	.187	.187	.201	.244
80	.040	.086	.134	.134	.124	.130	.130	.140	.171
85	.021	.044	.069	.069	.064	.067	.067	.072	.088
90	0	0	0	0	0	0	0	0	0

Table 56. Values of $\frac{h}{\sqrt{12}(a_{11}a_{22}D_{11}D_{22})^{1/4}}$ for (+θ/0/90) and (-θ/0/90) three-ply laminates

θ, deg	Material Systems								
	Boron/Al	S-glass/ Epoxy	Kevlar49/ Epoxy	IM7/5260	AS4/3502	AS4/ 3501-6	Boron- epoxy	IM7/ PETI-5	P-100/ 3502
0	.982	.984	.978	.978	.979	.977	.980	.977	.973
5	.982	.984	.971	.973	.975	.974	.972	.970	.957
10	.982	.982	.957	.962	.967	.967	.957	.956	.929
15	.981	.980	.945	.953	.960	.960	.945	.944	.913
20	.980	.979	.942	.950	.957	.958	.942	.941	.911
25	.980	.981	.947	.955	.961	.962	.949	.947	.921
30	.980	.986	.961	.967	.971	.972	.963	.961	.941
35	.981	.994	.980	.986	.987	.989	.983	.981	.968
40	.982	1.00	1.01	1.01	1.01	1.01	1.01	1.01	1.00
45	.983	1.01	1.03	1.04	1.03	1.04	1.03	1.04	1.04
50	.984	1.03	1.06	1.07	1.06	1.07	1.06	1.07	1.09
55	.985	1.04	1.09	1.10	1.09	1.10	1.09	1.11	1.15
60	.986	1.05	1.12	1.14	1.11	1.14	1.11	1.14	1.20
65	.988	1.06	1.15	1.17	1.14	1.17	1.13	1.17	1.25
70	.989	1.07	1.18	1.20	1.16	1.20	1.15	1.20	1.30
75	.990	1.08	1.20	1.22	1.19	1.23	1.17	1.23	1.35
80	.992	1.09	1.23	1.25	1.21	1.26	1.19	1.26	1.40
85	.993	1.09	1.25	1.27	1.23	1.27	1.22	1.29	1.45
90	.993	1.09	1.26	1.28	1.23	1.28	1.23	1.30	1.48

Table 57. Values of $\epsilon_{11} = B_{11}\left(\frac{a_{11}}{D_{11}}\right)^{1/2}$ for (+θ/0/90) and (-θ/0/90) three-ply laminates

θ, deg	Material Systems								
	Boron/Al	S-glass/ Epoxy	Kevlar49/ Epoxy	IM7/5260	AS4/3502	AS4/ 3501-6	Boron- epoxy	IM7/ PETI-5	P-100/ 3502
0	-.167	-.438	-.578	-.584	-.562	-.585	-.560	-.594	-.640
5	-.165	-.436	-.584	-.588	-.564	-.588	-.566	-.600	-.660
10	-.158	-.429	-.596	-.596	-.568	-.591	-.578	-.613	-.697
15	-.146	-.417	-.599	-.598	-.565	-.590	-.580	-.618	-.715
20	-.130	-.397	-.587	-.586	-.552	-.578	-.565	-.608	-.706
25	-.111	-.369	-.557	-.558	-.524	-.553	-.532	-.578	-.673
30	-.090	-.332	-.510	-.515	-.481	-.513	-.483	-.533	-.621
35	-.068	-.289	-.450	-.458	-.427	-.461	-.421	-.473	-.555
40	-.047	-.241	-.381	-.392	-.364	-.400	-.350	-.404	-.479
45	-.028	-.191	-.308	-.321	-.296	-.332	-.276	-.329	-.397
50	-.013	-.144	-.233	-.248	-.227	-.262	-.203	-.253	-.313
55	-.002	-.101	-.164	-.178	-.162	-.194	-.136	-.181	-.231
60	.004	-.065	-.104	-.117	-.106	-.133	-.081	-.118	-.156
65	.007	-.039	-.059	-.069	-.062	-.083	-.041	-.068	-.093
70	.007	-.020	-.028	-.035	-.032	-.046	-.016	-.034	-.047
75	.005	-.009	-.011	-.015	-.014	-.022	-.004	-.014	-.019
80	.002	-.003	-.003	-.005	-.005	-.008	.000	-.004	-.006
85	.001	-.001	.000	-.001	-.001	-.002	.000	-.001	-.001
90	0	0	0	0	0	0	0	0	0

Table 58. Values of $e_{12} = B_{12}\left(\frac{a_{11}a_{22}}{D_{11}D_{22}}\right)^{1/4}$ and $e_{66} = B_{66}\left(\frac{a_{11}a_{22}}{D_{11}D_{22}}\right)^{1/4}$ for (+θ/0/90) and (-θ/0/90) three-ply laminates

θ, deg	Material Systems								
	Boron/Al	S-glass/ Epoxy	Kevlar49/ Epoxy	IM7/5260	AS4/3502	AS4/ 3501-6	Boron- epoxy	IM7/ PETI-5	P-100/ 3502
0	0	0	0	0	0	0	0	0	0
5	-.002	-.003	-.005	-.005	-.005	-.005	-.005	-.005	-.006
10	-.007	-.013	-.020	-.020	-.019	-.018	-.021	-.021	-.023
15	-.016	-.029	-.045	-.044	-.041	-.041	-.046	-.046	-.052
20	-.027	-.049	-.078	-.075	-.070	-.070	-.080	-.079	-.090
25	-.039	-.071	-.115	-.111	-.104	-.103	-.118	-.117	-.134
30	-.050	-.093	-.153	-.148	-.138	-.136	-.156	-.156	-.178
35	-.060	-.112	-.186	-.180	-.168	-.166	-.190	-.190	-.218
40	-.066	-.125	-.212	-.205	-.190	-.188	-.216	-.216	-.249
45	-.068	-.131	-.225	-.218	-.201	-.200	-.229	-.231	-.268
50	-.066	-.128	-.224	-.217	-.200	-.199	-.228	-.230	-.272
55	-.060	-.117	-.208	-.201	-.185	-.185	-.211	-.215	-.258
60	-.050	-.099	-.179	-.173	-.158	-.159	-.180	-.185	-.227
65	-.039	-.076	-.140	-.136	-.123	-.125	-.140	-.145	-.182
70	-.027	-.053	-.097	-.095	-.086	-.087	-.097	-.101	-.129
75	-.016	-.032	-.057	-.056	-.051	-.052	-.057	-.060	-.077
80	-.007	-.015	-.026	-.026	-.023	-.024	-.026	-.027	-.035
85	-.002	-.004	-.007	-.006	-.006	-.006	-.006	-.007	-.009
90	0	0	0	0	0	0	0	0	0

Table 59. Values of $e_{22} = B_{22}\left(\frac{a_{22}}{D_{22}}\right)^{1/2}$ for (+θ/0/90) and (-θ/0/90) three-ply laminates

θ, deg	Material Systems								
	Boron/Al	S-glass/ Epoxy	Kevlar49/ Epoxy	IM7/5260	AS4/3502	AS4/ 3501-6	Boron- epoxy	IM7/ PETI-5	P-100/ 3502
0	.181	.555	.803	.816	.772	.818	.768	.834	.928
5	.182	.554	.803	.815	.771	.816	.768	.833	.928
10	.184	.552	.801	.812	.769	.812	.769	.831	.925
15	.187	.547	.796	.805	.762	.802	.766	.825	.918
20	.189	.537	.784	.790	.748	.783	.758	.811	.902
25	.190	.519	.761	.764	.724	.754	.739	.786	.874
30	.188	.493	.724	.725	.686	.712	.707	.746	.831
35	.181	.457	.673	.671	.635	.655	.659	.692	.770
40	.170	.412	.606	.602	.570	.585	.597	.622	.693
45	.155	.358	.528	.522	.495	.505	.522	.541	.603
50	.135	.300	.442	.435	.412	.419	.438	.452	.505
55	.112	.240	.352	.346	.328	.332	.351	.360	.403
60	.088	.181	.266	.260	.246	.248	.266	.271	.305
65	.064	.128	.186	.182	.172	.173	.187	.190	.214
70	.043	.083	.118	.115	.109	.110	.119	.120	.137
75	.025	.046	.065	.063	.060	.060	.066	.066	.075
80	.011	.020	.028	.027	.026	.026	.028	.028	.031
85	.003	.005	.007	.007	.006	.006	.007	.007	.007
90	0	0	0	0	0	0	0	0	0

Table 60. Values of $e_{16} = B_{16}\left(\frac{a_{11}^2}{D_{11}D_{22}}\right)^{1/4}$ for (+θ/0/90) and $-e_{16}$ for (-θ/0/90) three-ply laminates

θ, deg	Material Systems								
	Boron/Al	S-glass/ Epoxy	Kevlar49/ Epoxy	IM7/5260	AS4/3502	AS4/ 3501-6	Boron- epoxy	IM7/ PETI-5	P-100/ 3502
0	0	0	0	0	0	0	0	0	0
5	-.018	-.036	-.051	-.051	-.048	-.049	-.051	-.052	-.057
10	-.034	-.072	-.104	-.102	-.097	-.098	-.104	-.106	-.121
15	-.048	-.105	-.156	-.153	-.144	-.146	-.156	-.160	-.185
20	-.059	-.133	-.203	-.199	-.187	-.189	-.203	-.208	-.241
25	-.066	-.154	-.239	-.234	-.220	-.224	-.237	-.246	-.284
30	-.068	-.166	-.261	-.257	-.240	-.246	-.257	-.268	-.309
35	-.065	-.169	-.266	-.263	-.246	-.254	-.261	-.275	-.316
40	-.058	-.162	-.255	-.254	-.238	-.247	-.248	-.265	-.306
45	-.047	-.146	-.231	-.232	-.216	-.228	-.222	-.240	-.279
50	-.035	-.124	-.196	-.199	-.185	-.198	-.185	-.205	-.240
55	-.023	-.099	-.154	-.159	-.147	-.161	-.143	-.163	-.194
60	-.011	-.073	-.112	-.117	-.109	-.123	-.100	-.120	-.145
65	-.003	-.050	-.073	-.079	-.073	-.086	-.062	-.080	-.098
70	.003	-.031	-.042	-.047	-.044	-.055	-.032	-.047	-.058
75	.006	-.017	-.020	-.025	-.023	-.031	-.013	-.023	-.029
80	.006	-.008	-.007	-.011	-.010	-.016	-.002	-.009	-.011
85	.003	-.003	-.002	-.003	-.003	-.006	.001	-.003	-.003
90	0	0	0	0	0	0	0	0	0

Table 61. Values of $e_{26} = B_{26}\left(\frac{a_{22}^2}{D_{11}D_{22}}\right)^{1/4}$ for (+θ/0/90) and $-e_{26}$ for (-θ/0/90) three-ply laminates

θ, deg	Material Systems								
	Boron/Al	S-glass/ Epoxy	Kevlar49/ Epoxy	IM7/5260	AS4/3502	AS4/ 3501-6	Boron- epoxy	IM7/ PETI-5	P-100/ 3502
0	0	0	0	0	0	0	0	0	0
5	.003	-.003	-.001	-.003	-.003	-.005	.001	-.002	-.002
10	.005	-.007	-.006	-.008	-.008	-.012	-.002	-.007	-.008
15	.006	-.016	-.016	-.019	-.019	-.025	-.010	-.018	-.020
20	.003	-.028	-.034	-.038	-.036	-.044	-.027	-.036	-.040
25	-.003	-.046	-.060	-.065	-.062	-.071	-.052	-.064	-.072
30	-.011	-.069	-.096	-.100	-.095	-.105	-.087	-.101	-.113
35	-.023	-.095	-.138	-.142	-.134	-.145	-.129	-.145	-.164
40	-.035	-.122	-.185	-.187	-.176	-.187	-.176	-.193	-.221
45	-.047	-.146	-.231	-.232	-.216	-.228	-.222	-.240	-.279
50	-.058	-.166	-.270	-.269	-.250	-.262	-.262	-.282	-.333
55	-.065	-.176	-.297	-.294	-.271	-.283	-.288	-.310	-.374
60	-.068	-.177	-.305	-.301	-.275	-.288	-.297	-.319	-.395
65	-.066	-.166	-.290	-.286	-.261	-.272	-.283	-.305	-.386
70	-.060	-.145	-.254	-.250	-.227	-.237	-.247	-.266	-.345
75	-.049	-.115	-.199	-.196	-.178	-.187	-.194	-.209	-.273
80	-.035	-.079	-.133	-.133	-.121	-.127	-.130	-.140	-.182
85	-.018	-.040	-.066	-.066	-.061	-.064	-.064	-.069	-.087
90	0	0	0	0	0	0	0	0	0

Table 62. Values of $\left(\frac{D_{11}}{D_{22}}\right)^{\frac{1}{4}}$ for $(+\theta/0/90)_m$ and $(-\theta/0/90)_m$ P-100/3502 laminates

θ, deg	Stacking sequence number, m							
	m = 1	m = 2	m = 3	m = 4	m = 5	m = 6	m = 7	m = 8
0	1.02	1.14	1.16	1.17	1.18	1.18	1.18	1.18
5	1.02	1.14	1.16	1.17	1.17	1.18	1.18	1.18
10	1.00	1.13	1.15	1.16	1.17	1.17	1.17	1.17
15	.986	1.11	1.14	1.15	1.16	1.16	1.16	1.16
20	.960	1.10	1.12	1.13	1.14	1.14	1.14	1.14
25	.927	1.07	1.10	1.11	1.12	1.12	1.12	1.12
30	.886	1.04	1.07	1.08	1.09	1.09	1.09	1.09
35	.838	1.01	1.04	1.05	1.06	1.06	1.06	1.06
40	.785	.973	1.007	1.02	1.02	1.03	1.03	1.03
45	.730	.936	.972	.984	.990	.993	.995	.996
50	.674	.901	.938	.951	.957	.960	.962	.963
55	.622	.869	.907	.920	.927	.930	.932	.933
60	.576	.842	.881	.894	.900	.904	.906	.907
65	.538	.820	.859	.872	.879	.882	.884	.885
70	.511	.802	.842	.855	.862	.865	.867	.868
75	.493	.790	.829	.843	.849	.853	.855	.856
80	.484	.782	.821	.835	.841	.844	.846	.847
85	.479	.777	.816	.830	.836	.839	.841	.842
90	.478	.776	.815	.828	.834	.838	.840	.841

Table 63. Values of $\beta = \frac{D_{12} + 2D_{66}}{\sqrt{D_{11}D_{22}}}$ for $(+\theta/0/90)_m$ and $(-\theta/0/90)_m$ P-100/3502 laminates

θ, deg	Stacking sequence number, m							
	m = 1	m = 2	m = 3	m = 4	m = 5	m = 6	m = 7	m = 8
0	.064	.066	.067	.068	.068	.068	.068	.068
5	.085	.083	.083	.083	.083	.083	.083	.083
10	.147	.131	.129	.128	.128	.128	.128	.128
15	.247	.208	.202	.200	.199	.198	.198	.198
20	.380	.306	.294	.290	.289	.288	.287	.287
25	.537	.415	.397	.391	.388	.387	.386	.385
30	.708	.524	.498	.489	.485	.483	.482	.481
35	.877	.618	.584	.572	.567	.565	.563	.562
40	1.03	.684	.642	.629	.623	.619	.617	.616
45	1.15	.713	.665	.650	.643	.639	.637	.635
50	1.22	.698	.648	.632	.624	.620	.618	.617
55	1.23	.642	.593	.577	.570	.567	.564	.563
60	1.15	.553	.509	.495	.489	.486	.484	.482
65	.994	.444	.408	.397	.392	.389	.388	.387
70	.776	.330	.304	.295	.292	.290	.289	.288
75	.538	.226	.209	.204	.201	.200	.199	.199
80	.332	.144	.134	.131	.130	.129	.129	.128
85	.196	.091	.086	.085	.084	.084	.084	.084
90	.148	.073	.070	.069	.069	.068	.068	.068

Table 64. Values of $\nu_b = \frac{D_{12}}{\sqrt{D_{11}D_{22}}}$ for $(+\theta/0/90)_m$ and $(-\theta/0/90)_m$ P-100/3502 laminates

θ, deg	Stacking sequence number, m							
	m = 1	m = 2	m = 3	m = 4	m = 5	m = 6	m = 7	m = 8
0	.008	.009	.009	.009	.009	.009	.009	.009
5	.015	.014	.014	.014	.014	.014	.014	.014
10	.036	.030	.029	.029	.029	.029	.029	.029
15	.069	.055	.053	.052	.052	.052	.052	.052
20	.112	.088	.084	.082	.082	.081	.081	.081
25	.164	.124	.118	.116	.115	.114	.114	.114
30	.220	.160	.151	.148	.147	.146	.146	.145
35	.275	.191	.179	.175	.174	.173	.172	.172
40	.325	.212	.199	.194	.192	.191	.190	.190
45	.363	.222	.206	.201	.199	.197	.197	.196
50	.385	.217	.200	.195	.193	.191	.191	.190
55	.385	.198	.182	.177	.175	.174	.173	.172
60	.357	.168	.154	.150	.148	.147	.146	.146
65	.303	.132	.121	.117	.116	.115	.114	.114
70	.229	.095	.086	.084	.083	.082	.082	.081
75	.149	.060	.055	.053	.053	.052	.052	.052
80	.080	.033	.030	.029	.029	.029	.029	.029
85	.035	.015	.014	.014	.014	.014	.014	.014
90	.019	.009	.009	.009	.009	.009	.009	.009

Table 65. Values of $\gamma_b = \frac{D_{16}}{\left(D_{11}^3 D_{22}\right)^{1/4}}$ for $(+\theta/0/90)_m$ and $-\gamma_b$ for $(-\theta/0/90)_m$ P-100/3502 laminates

θ, deg	Stacking sequence number, m							
	m = 1	m = 2	m = 3	m = 4	m = 5	m = 6	m = 7	m = 8
0	0	0	0	0	0	0	0	0
5	.079	.056	.052	.051	.050	.050	.050	.050
10	.156	.109	.102	.099	.098	.098	.097	.097
15	.231	.159	.148	.144	.142	.141	.141	.140
20	.301	.201	.186	.181	.179	.178	.177	.177
25	.365	.234	.216	.210	.207	.206	.205	.204
30	.420	.256	.234	.227	.224	.222	.221	.221
35	.463	.263	.239	.232	.228	.226	.225	.224
40	.491	.256	.231	.223	.219	.217	.216	.215
45	.499	.235	.210	.202	.198	.196	.195	.195
50	.484	.201	.178	.171	.168	.166	.165	.165
55	.441	.160	.141	.135	.132	.131	.130	.129
60	.369	.117	.102	.098	.096	.095	.094	.094
65	.275	.077	.067	.064	.063	.062	.061	.061
70	.175	.045	.039	.037	.036	.036	.036	.035
75	.092	.022	.019	.018	.018	.018	.018	.017
80	.037	.009	.008	.007	.007	.007	.007	.007
85	.010	.002	.002	.002	.002	.002	.002	.002
90	0	0	0	0	0	0	0	0

Table 66. Values of $\delta_b = \frac{D_{26}}{\left(D_{11}D_{22}^3\right)^{1/4}}$ for $(+\theta/0/90)_m$ and $-\delta_b$ for $(-\theta/0/90)_m$ P-100/3502 laminates

θ, deg	Stacking sequence number, m							
	m = 1	m = 2	m = 3	m = 4	m = 5	m = 6	m = 7	m = 8
0	0	0	0	0	0	0	0	0
5	.002	.002	.002	.002	.002	.002	.002	.002
10	.008	.007	.007	.007	.007	.007	.007	.007
15	.020	.018	.018	.017	.017	.017	.017	.017
20	.042	.037	.036	.035	.035	.035	.035	.035
25	.074	.063	.062	.061	.061	.061	.061	.061
30	.116	.097	.094	.093	.093	.093	.093	.093
35	.164	.135	.131	.130	.129	.128	.128	.128
40	.216	.173	.167	.165	.164	.164	.163	.163
45	.266	.206	.198	.195	.194	.194	.193	.193
50	.308	.229	.220	.217	.215	.215	.214	.214
55	.338	.240	.230	.226	.225	.224	.223	.223
60	.349	.237	.226	.223	.221	.220	.220	.219
65	.337	.220	.210	.206	.205	.204	.204	.203
70	.301	.191	.182	.179	.178	.177	.176	.176
75	.244	.152	.144	.142	.141	.140	.140	.140
80	.171	.105	.100	.098	.098	.097	.097	.097
85	.088	.054	.051	.050	.050	.050	.050	.050
90	0	0	0	0	0	0	0	0

Table 67. Values of $\frac{h}{\sqrt{12}(a_{11}a_{22}D_{11}D_{22})^{1/4}}$ for $(+\theta/0/90)_m$ and $(-\theta/0/90)_m$ P-100/3502 laminates

θ, deg	Stacking sequence number, m							
	m = 1	m = 2	m = 3	m = 4	m = 5	m = 6	m = 7	m = 8
0	.973	.989	.995	.997	.998	.999	.999	.999
5	.957	.971	.977	.979	.980	.981	.981	.981
10	.929	.940	.944	.946	.947	.948	.948	.948
15	.913	.917	.921	.922	.923	.924	.924	.924
20	.911	.906	.909	.910	.911	.911	.911	.911
25	.921	.904	.905	.906	.907	.907	.907	.907
30	.941	.908	.907	.907	.907	.907	.907	.907
35	.968	.913	.910	.909	.909	.909	.909	.909
40	1.00	.919	.913	.912	.911	.911	.911	.911
45	1.04	.924	.916	.914	.913	.912	.912	.912
50	1.09	.928	.917	.914	.913	.912	.911	.911
55	1.15	.931	.917	.913	.911	.911	.910	.910
60	1.20	.933	.917	.912	.910	.909	.909	.908
65	1.25	.936	.918	.913	.911	.910	.909	.909
70	1.30	.942	.923	.918	.916	.914	.914	.913
75	1.35	.956	.937	.931	.929	.927	.927	.926
80	1.40	.982	.962	.956	.953	.952	.951	.951
85	1.45	1.02	.995	.989	.986	.985	.984	.984
90	1.48	1.04	1.01	1.01	1.00	1.00	1.00	1.00

Table 68. Values of $\epsilon_{11} = B_{11}\left(\frac{a_{11}}{D_{11}}\right)^{1/2}$ for $(+\theta/0/90)_m$ and $(-\theta/0/90)_m$ P-100/3502 laminates

θ, deg	Stacking sequence number, m							
	m = 1	m = 2	m = 3	m = 4	m = 5	m = 6	m = 7	m = 8
0	-.640	-.291	-.191	-.142	-.114	-.095	-.081	-.071
5	-.660	-.299	-.196	-.147	-.117	-.097	-.083	-.073
10	-.697	-.314	-.206	-.153	-.122	-.102	-.087	-.076
15	-.715	-.318	-.208	-.155	-.124	-.103	-.088	-.077
20	-.706	-.308	-.201	-.150	-.119	-.099	-.085	-.074
25	-.673	-.286	-.186	-.138	-.110	-.092	-.078	-.069
30	-.621	-.254	-.165	-.122	-.097	-.081	-.069	-.061
35	-.555	-.217	-.140	-.104	-.083	-.069	-.059	-.051
40	-.479	-.177	-.113	-.084	-.067	-.055	-.047	-.041
45	-.397	-.137	-.087	-.064	-.051	-.043	-.036	-.032
50	-.313	-.100	-.063	-.046	-.037	-.031	-.026	-.023
55	-.231	-.067	-.042	-.031	-.025	-.020	-.018	-.015
60	-.156	-.041	-.026	-.019	-.015	-.013	-.011	-.009
65	-.093	-.023	-.014	-.010	-.008	-.007	-.006	-.005
70	-.047	-.011	-.007	-.005	-.004	-.003	-.003	-.002
75	-.019	-.004	-.003	-.002	-.002	-.001	-.001	-.001
80	-.006	-.001	-.001	-.001	.000	.000	.000	.000
85	-.001	.000	.000	.000	.000	.000	.000	.000
90	0	0	0	0	0	0	0	0

Table 69. Values of $\epsilon_{22} = B_{22}\left(\frac{a_{22}}{D_{22}}\right)^{1/2}$ for $(+\theta/0/90)_m$ and $(-\theta/0/90)_m$ P-100/3502 laminates

θ, deg	Stacking sequence number, m							
	m = 1	m = 2	m = 3	m = 4	m = 5	m = 6	m = 7	m = 8
0	.928	.527	.361	.274	.220	.184	.158	.138
5	.928	.527	.361	.273	.220	.184	.158	.138
10	.925	.525	.360	.273	.219	.183	.157	.138
15	.918	.521	.357	.270	.217	.182	.156	.137
20	.902	.512	.351	.266	.214	.179	.153	.134
25	.874	.496	.340	.258	.207	.173	.149	.130
30	.831	.472	.323	.245	.197	.164	.141	.124
35	.770	.437	.300	.227	.183	.153	.131	.115
40	.693	.394	.270	.204	.164	.137	.118	.103
45	.603	.343	.235	.178	.143	.120	.103	.090
50	.505	.287	.197	.149	.120	.100	.086	.075
55	.403	.229	.157	.119	.096	.080	.069	.060
60	.305	.173	.119	.090	.072	.060	.052	.045
65	.214	.122	.084	.063	.051	.043	.037	.032
70	.137	.078	.053	.040	.032	.027	.023	.020
75	.075	.042	.029	.022	.018	.015	.013	.011
80	.031	.018	.012	.009	.007	.006	.005	.005
85	.007	.004	.003	.002	.002	.001	.001	.001
90	0	0	0	0	0	0	0	0

Table 70. Values of $e_{12} = B_{12}\left(\frac{a_{11}a_{22}}{D_{11}D_{22}}\right)^{1/4}$ and $e_{66} = B_{66}\left(\frac{a_{11}a_{22}}{D_{11}D_{22}}\right)^{1/4}$ for $(+\theta/0/90)_m$ and $(-\theta/0/90)_m$ P-100/3502 laminates

θ, deg	Stacking sequence number, m							
	m = 1	m = 2	m = 3	m = 4	m = 5	m = 6	m = 7	m = 8
0	0	0	0	0	0	0	0	0
5	-.006	-.003	-.002	-.001	-.001	-.001	-.001	-.001
10	-.023	-.012	-.008	-.006	-.005	-.004	-.003	-.003
15	-.052	-.026	-.018	-.013	-.011	-.009	-.008	-.007
20	-.090	-.045	-.030	-.023	-.018	-.015	-.013	-.011
25	-.134	-.066	-.044	-.033	-.026	-.022	-.019	-.016
30	-.178	-.086	-.057	-.043	-.034	-.029	-.024	-.021
35	-.218	-.103	-.068	-.051	-.041	-.034	-.029	-.026
40	-.249	-.114	-.076	-.057	-.045	-.038	-.032	-.028
45	-.268	-.119	-.078	-.059	-.047	-.039	-.033	-.029
50	-.272	-.116	-.076	-.057	-.045	-.038	-.032	-.028
55	-.258	-.105	-.069	-.051	-.041	-.034	-.029	-.026
60	-.227	-.088	-.058	-.043	-.034	-.029	-.025	-.021
65	-.182	-.068	-.044	-.033	-.026	-.022	-.019	-.016
70	-.129	-.047	-.031	-.023	-.018	-.015	-.013	-.011
75	-.077	-.027	-.018	-.013	-.011	-.009	-.008	-.007
80	-.035	-.012	-.008	-.006	-.005	-.004	-.003	-.003
85	-.009	-.003	-.002	-.001	-.001	-.001	-.001	-.001
90	0	0	0	0	0	0	0	0

Table 71. Values of $e_{16} = B_{16}\left(\frac{a_{11}^2}{D_{11}D_{22}}\right)^{1/4}$ for $(+\theta/0/90)_m$ and $-e_{16}$ for $(-\theta/0/90)_m$ P-100/3502 laminates

θ, deg	Stacking sequence number, m							
	m = 1	m = 2	m = 3	m = 4	m = 5	m = 6	m = 7	m = 8
0	0	0	0	0	0	0	0	0
5	-.057	-.029	-.020	-.015	-.012	-.010	-.008	-.007
10	-.121	-.061	-.041	-.031	-.025	-.021	-.018	-.015
15	-.185	-.093	-.062	-.047	-.037	-.031	-.027	-.023
20	-.241	-.120	-.080	-.060	-.048	-.040	-.035	-.030
25	-.284	-.139	-.093	-.070	-.056	-.047	-.040	-.035
30	-.309	-.149	-.099	-.075	-.060	-.050	-.043	-.037
35	-.316	-.149	-.099	-.074	-.059	-.050	-.042	-.037
40	-.306	-.140	-.093	-.069	-.056	-.046	-.040	-.035
45	-.279	-.124	-.082	-.061	-.049	-.041	-.035	-.030
50	-.240	-.102	-.067	-.050	-.040	-.033	-.029	-.025
55	-.194	-.079	-.052	-.039	-.031	-.026	-.022	-.019
60	-.145	-.056	-.037	-.027	-.022	-.018	-.016	-.014
65	-.098	-.036	-.024	-.018	-.014	-.012	-.010	-.009
70	-.058	-.021	-.014	-.010	-.008	-.007	-.006	-.005
75	-.029	-.010	-.007	-.005	-.004	-.003	-.003	-.002
80	-.011	-.004	-.003	-.002	-.002	-.001	-.001	-.001
85	-.003	-.001	-.001	-.001	.000	.000	.000	.000
90	0	0	0	0	0	0	0	0

Table 72. Values of $e_{26} = B_{26}\left(\frac{a_{22}^2}{D_{11}D_{22}}\right)^{1/4}$ for $(+\theta/0/90)_m$ and $-e_{26}$ for $(-\theta/0/90)_m$ P-100/3502 laminates

θ, deg	Stacking sequence number, m							
	m = 1	m = 2	m = 3	m = 4	m = 5	m = 6	m = 7	m = 8
0	0	0	0	0	0	0	0	0
5	-.002	-.001	-.001	-.001	.000	.000	.000	.000
10	-.008	-.004	-.003	-.002	-.002	-.001	-.001	-.001
15	-.020	-.010	-.007	-.005	-.004	-.003	-.003	-.002
20	-.040	-.020	-.013	-.010	-.008	-.007	-.006	-.005
25	-.072	-.035	-.023	-.018	-.014	-.012	-.010	-.009
30	-.113	-.055	-.036	-.027	-.022	-.018	-.016	-.014
35	-.164	-.077	-.051	-.039	-.031	-.026	-.022	-.019
40	-.221	-.101	-.067	-.050	-.040	-.033	-.029	-.025
45	-.279	-.124	-.082	-.061	-.049	-.041	-.035	-.030
50	-.333	-.141	-.093	-.070	-.056	-.046	-.040	-.035
55	-.374	-.152	-.100	-.075	-.060	-.050	-.042	-.037
60	-.395	-.153	-.101	-.075	-.060	-.050	-.043	-.037
65	-.386	-.144	-.094	-.070	-.056	-.047	-.040	-.035
70	-.345	-.125	-.082	-.061	-.049	-.040	-.035	-.030
75	-.273	-.097	-.063	-.047	-.038	-.031	-.027	-.023
80	-.182	-.064	-.042	-.031	-.025	-.021	-.018	-.015
85	-.087	-.031	-.020	-.015	-.012	-.010	-.008	-.007
90	0	0	0	0	0	0	0	0

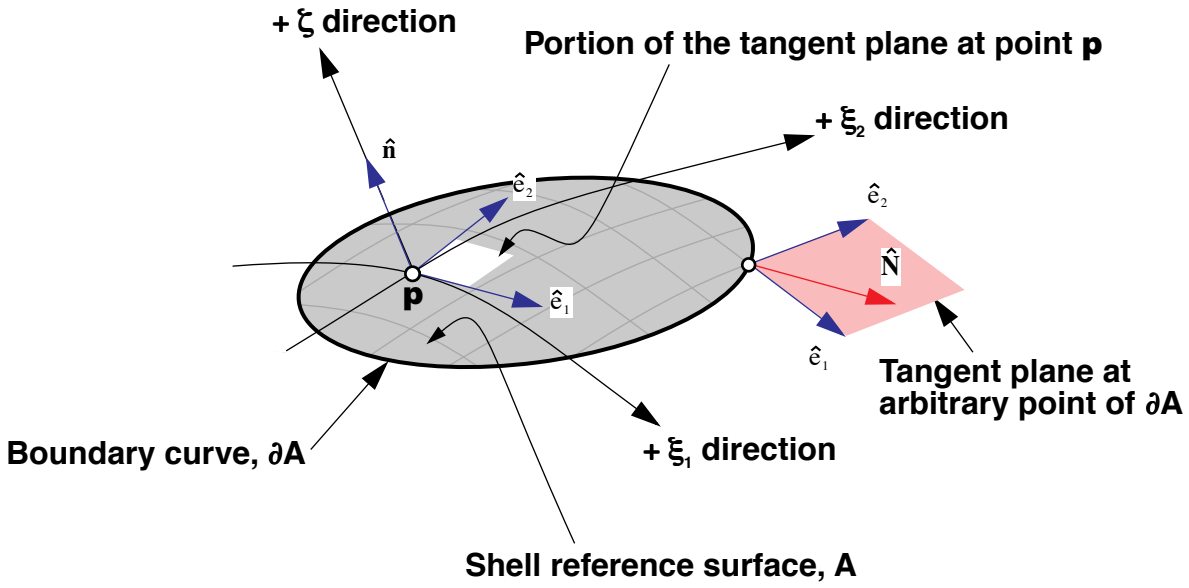

Figure 1. Coordinate system and unit-magnitude base-vector fields for points of undeformed shell.

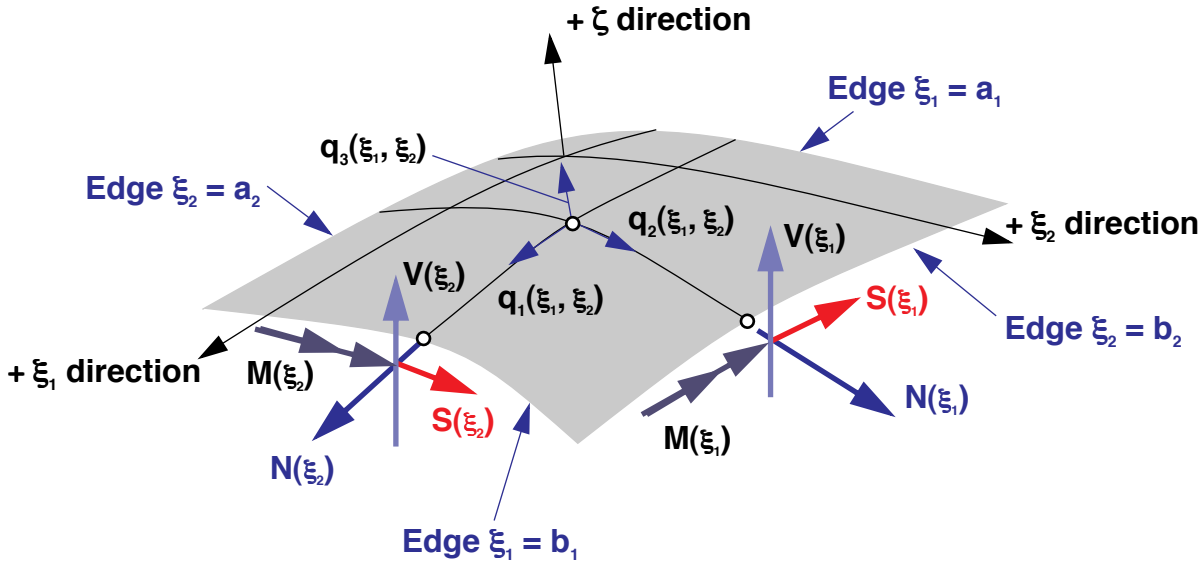

Figure 2. Sign convention for applied loads.

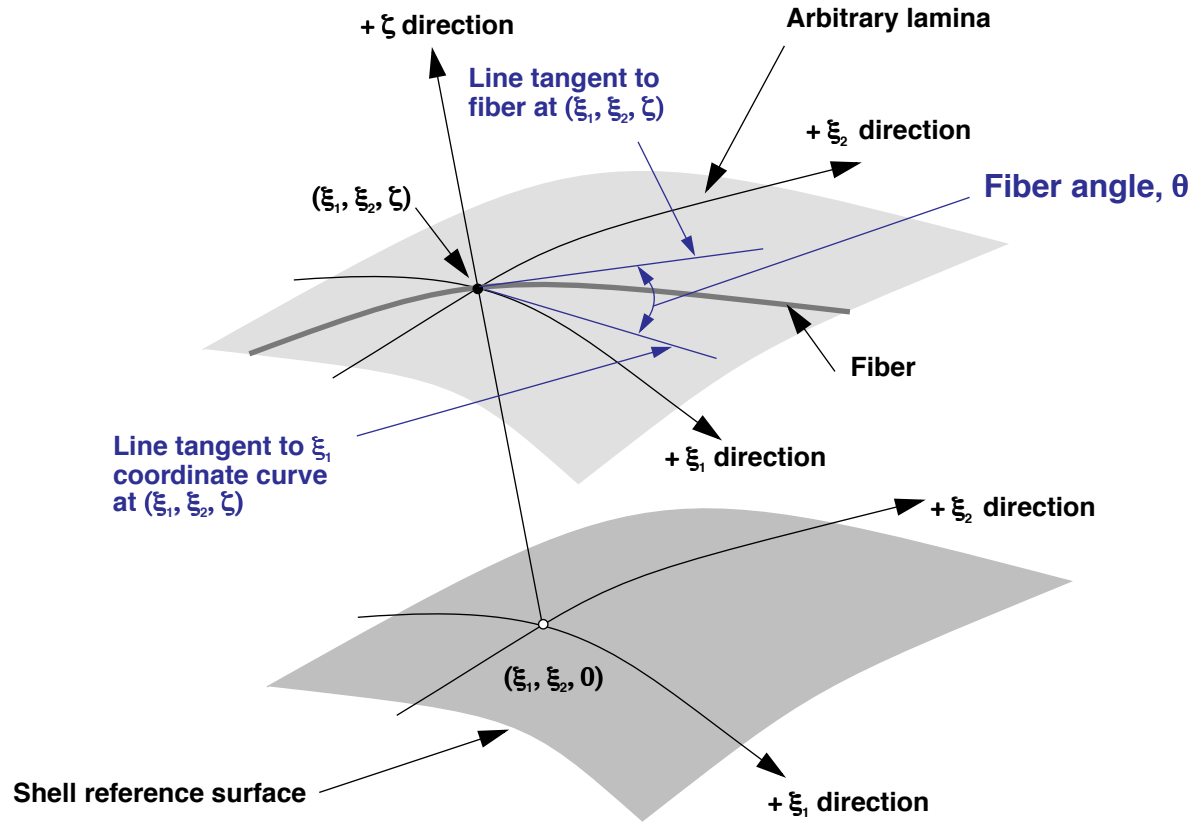

Figure 3. Fiber orientation of an arbitrary lamina.

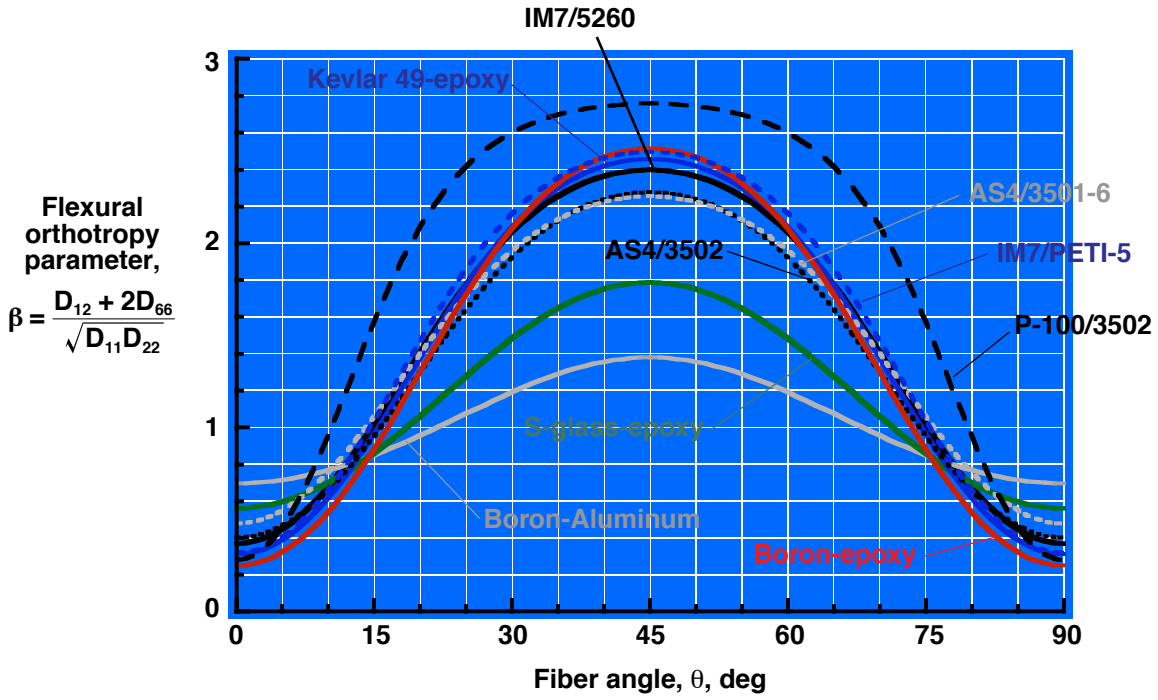

Figure 4. Effects of lamina material properties on nondimensional flexural orthotropy parameter β for $[(+\theta/-\theta)_m]_S$, $[(-\theta/+\theta)_m]_S$, $(+\theta/-\theta)_m$, and $(-\theta/+\theta)_m$ angle-ply laminates (m = 1, 2, ...).

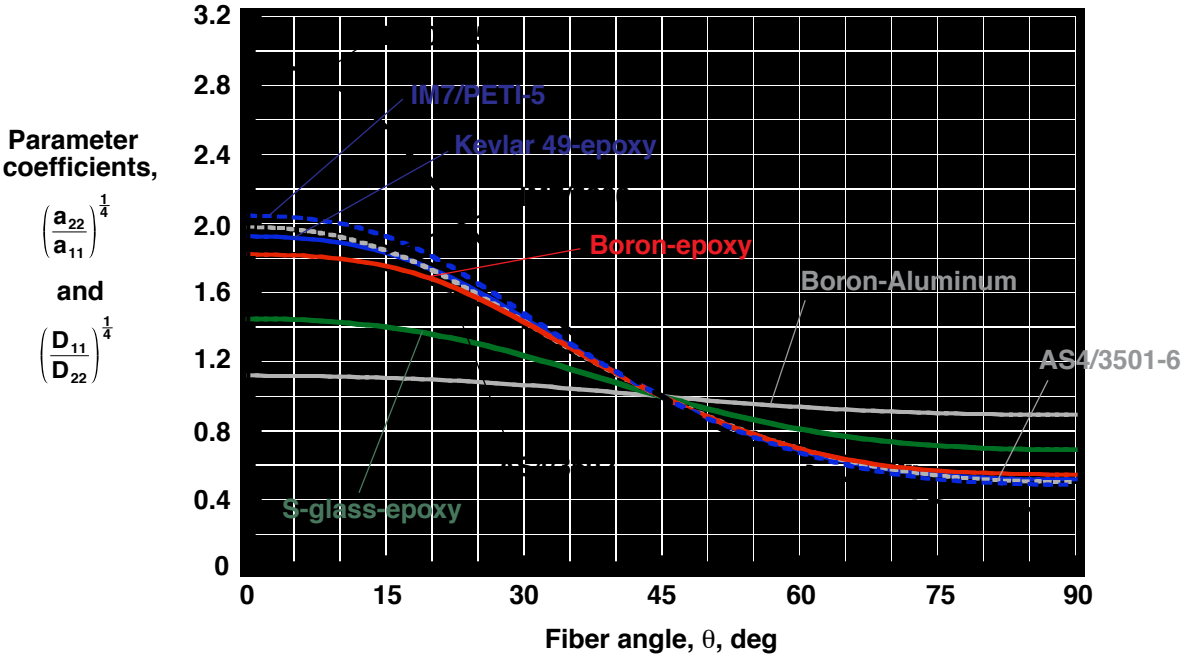

Figure 5. Effects of lamina material properties on parameter coefficients in equations (52a) and (55) for $[(+\theta/-\theta)_m]_S$, $[(-\theta/+\theta)_m]_S$, $(+\theta/-\theta)_m$, and $(-\theta/+\theta)_m$ angle-ply laminates (m = 1, 2, ...).

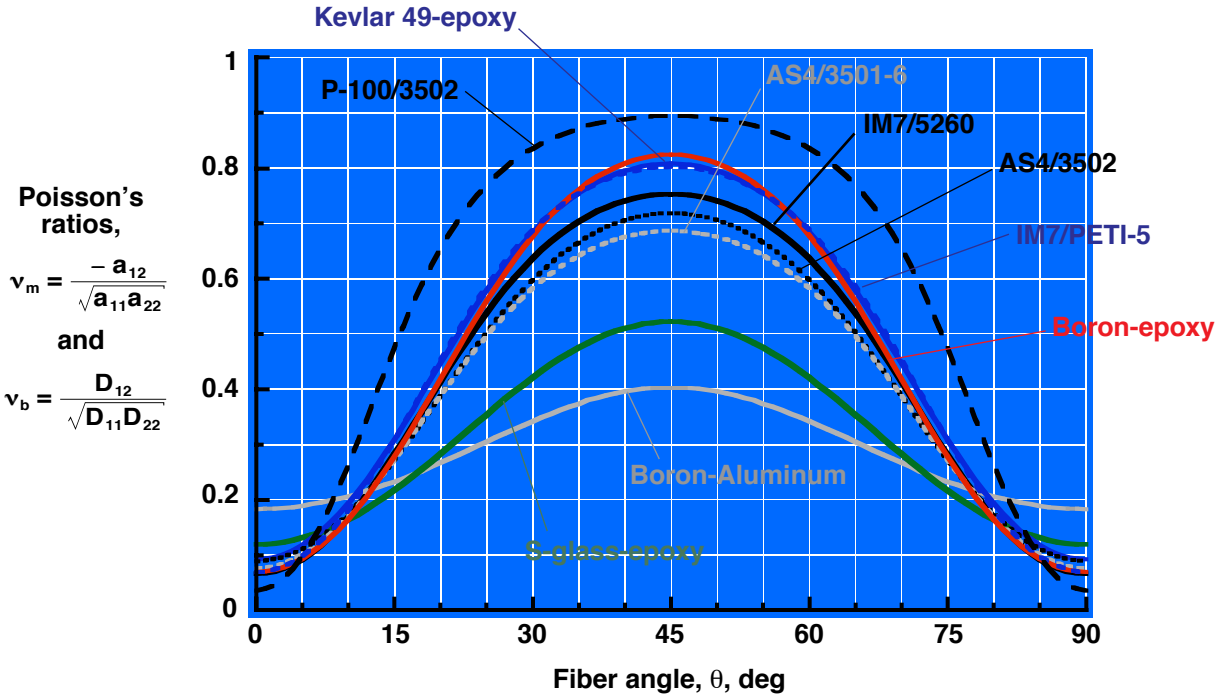

Figure 6. Effects of lamina material properties on Poisson's ratios defined by equations (52e) and (59d) for $[(+\theta/-\theta)_m]_S$, $[(-\theta/+\theta)_m]_S$, $(+\theta/-\theta)_m$, and $(-\theta/+\theta)_m$ angle-ply laminates (m = 1, 2, ...).

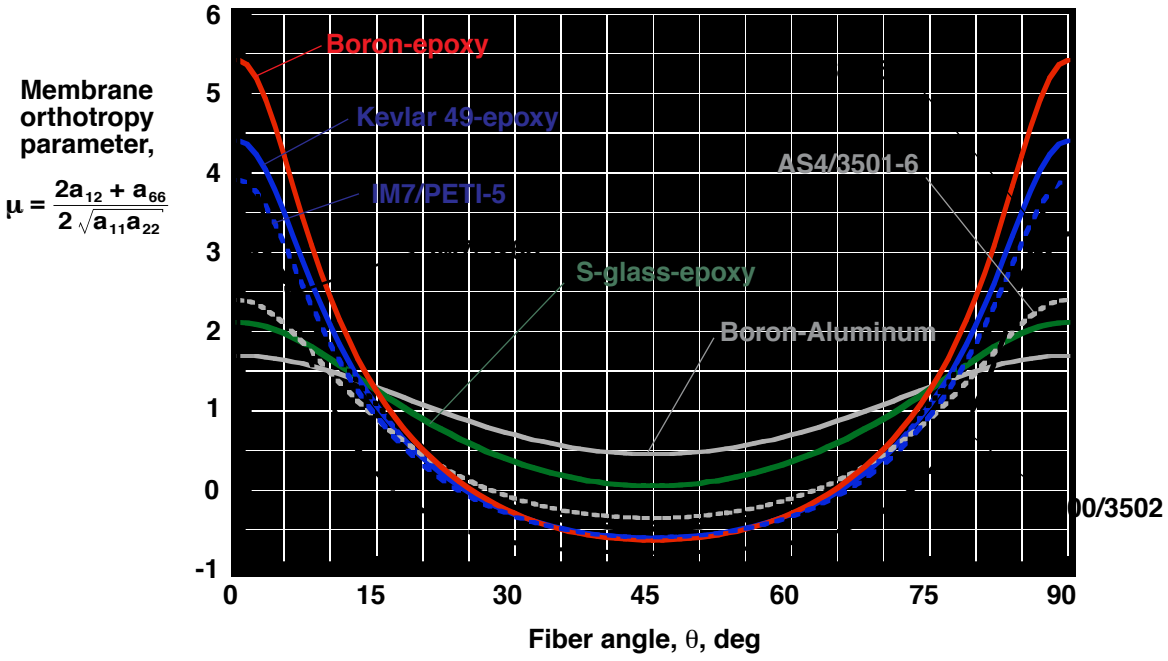

Figure 7. Effects of lamina material properties on nondimensional membrane orthotropy parameter μ for $[(+\theta/-\theta)_m]_S$, $[(-\theta/+\theta)_m]_S$, $(+\theta/-\theta)_m$, and $(-\theta/+\theta)_m$ angle-ply laminates (m = 1, 2, ...).

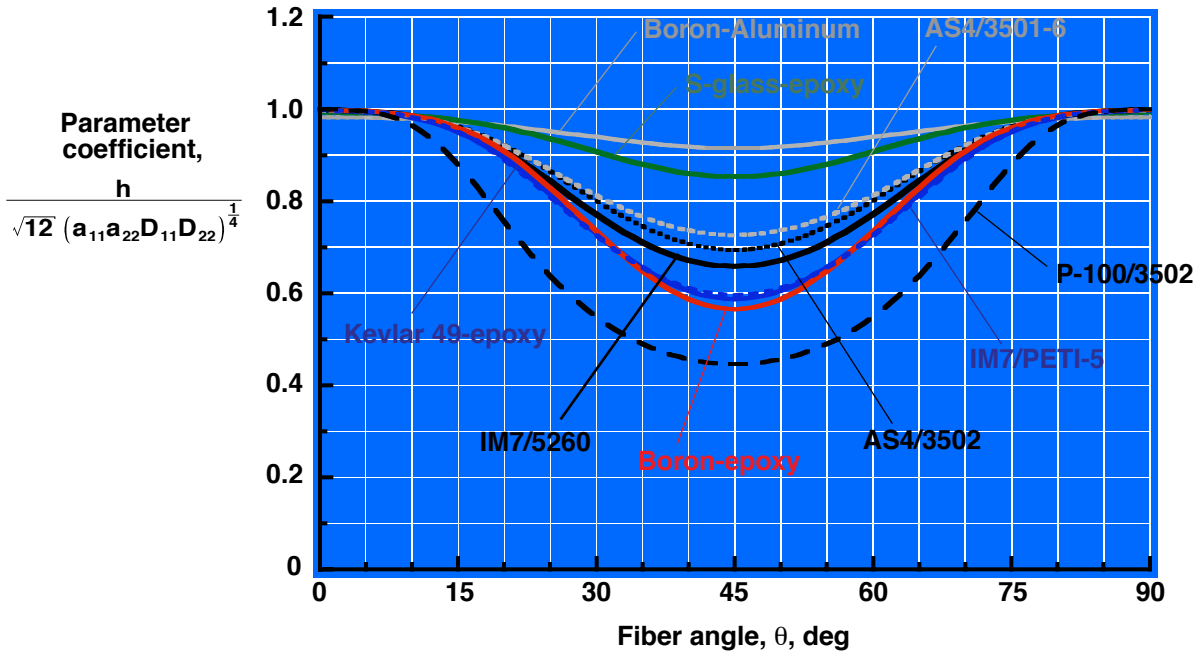

Figure 8. Effects of lamina material properties on Batdorf-Stein-parameter coefficient in equations (45) and (48) for $[(+\theta/-\theta)_m]_S$, $[(-\theta/+\theta)_m]_S$, $(+\theta/-\theta)_m$, and $(-\theta/+\theta)_m$ angle-ply laminates (m = 1, 2, ...).

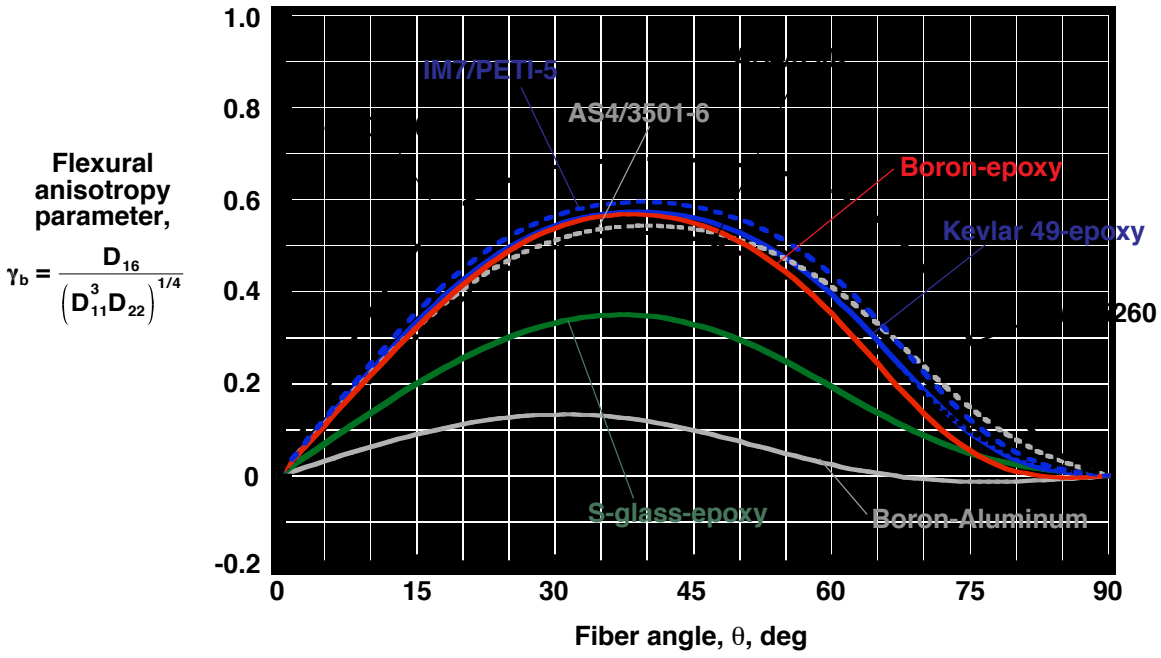

Figure 9. Effects of lamina material properties on nondimensional flexural anisotropy parameters γ_b for $[(+\theta/-\theta)_m]_S$ laminates and $-\gamma_b$ for $[(-\theta/+\theta)_m]_S$ laminates.

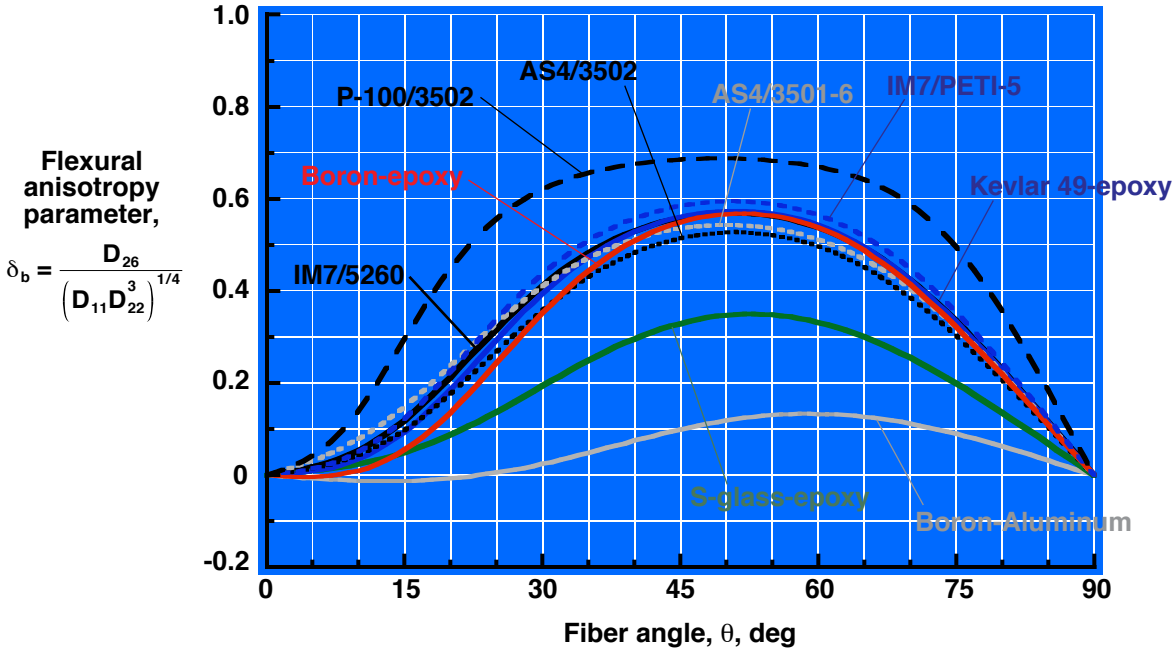

Figure 10. Effects of lamina material properties on nondimensional flexural anisotropy parameters δ_b for $[(+\theta/-\theta)_m]_S$ laminates and $-\delta_b$ for $[(-\theta/+\theta)_m]_S$ laminates.

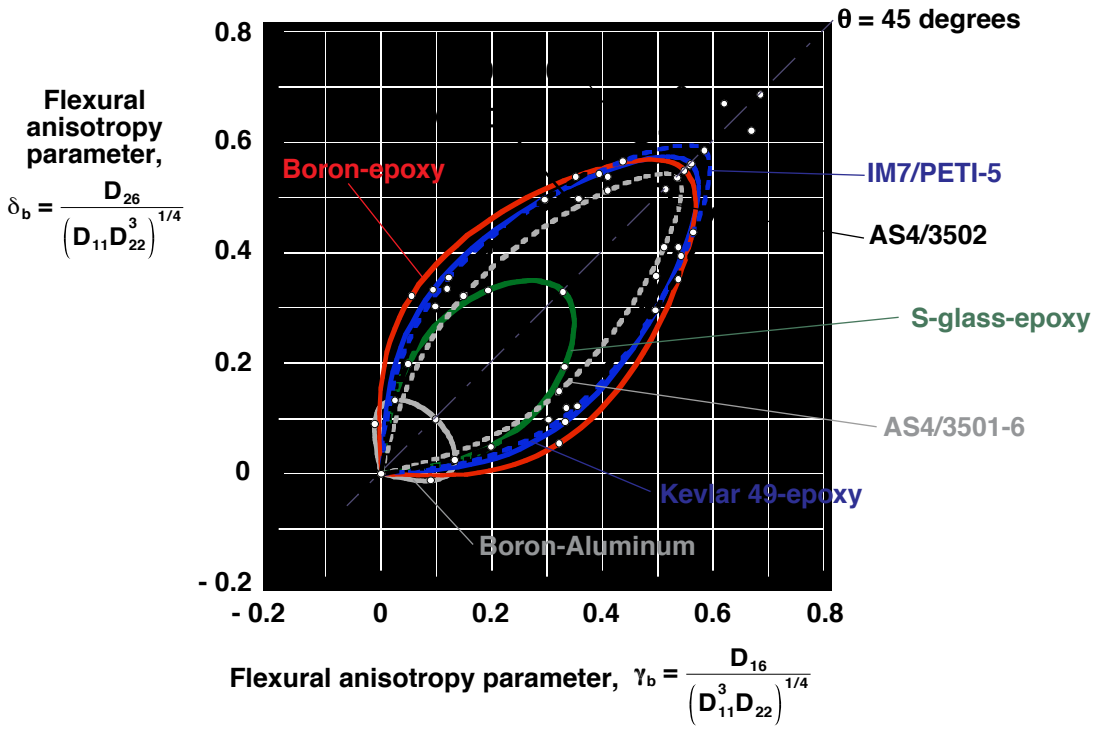

Figure 11. Effects of lamina material properties on flexural anisotropy parameters γ_b and δ_b for $[(+\theta/-\theta)_m]_S$ and $-\gamma_b$ and $-\delta_b$ for $[(-\theta/+\theta)_m]_S$ symmetric angle-ply laminates, respectively (m = 1).

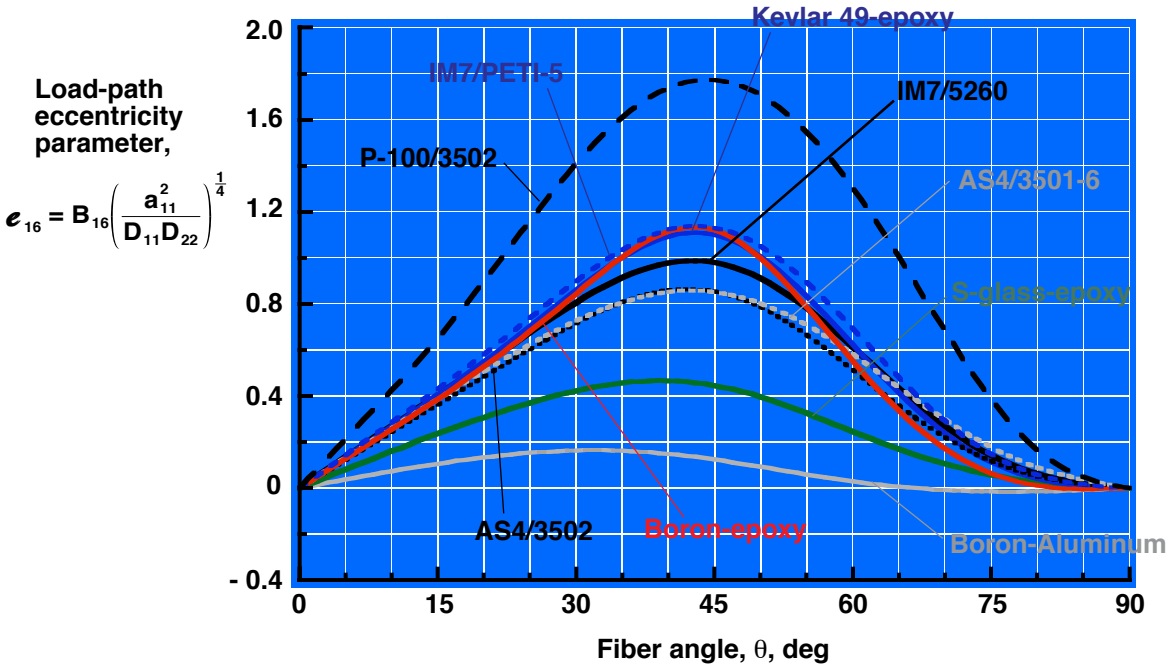

Figure 12. Effects of lamina material properties on nondimensional load-path eccentricity parameters $-e_{16}$ and $+e_{16}$ defined by equation (75b) for $(+\theta/-\theta)_m$ and $(-\theta/+\theta)_m$ antisymmetric angle-ply laminates, respectively (m = 1).

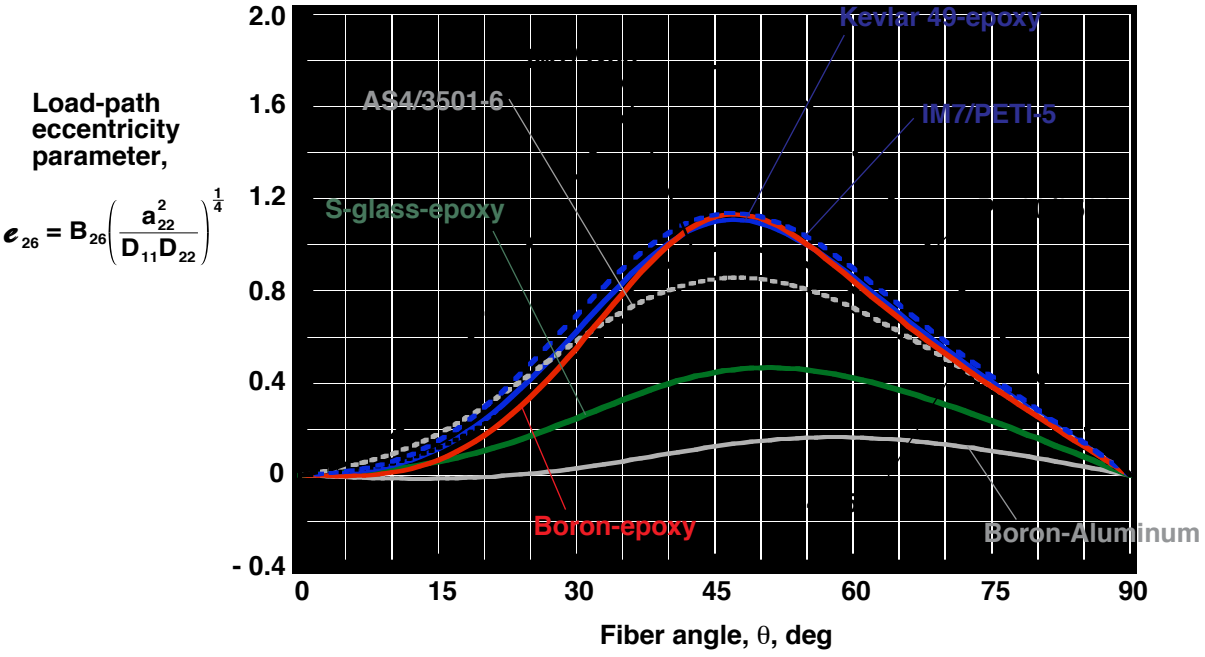

Figure 13. Effects of lamina material properties on nondimensional load-path eccentricity parameters $-e_{26}$ and $+e_{26}$ defined by equation (75f) for $(+\theta/-\theta)_m$ and $(-\theta/+\theta)_m$ antisymmetric angle-ply laminates, respectively (m = 1).

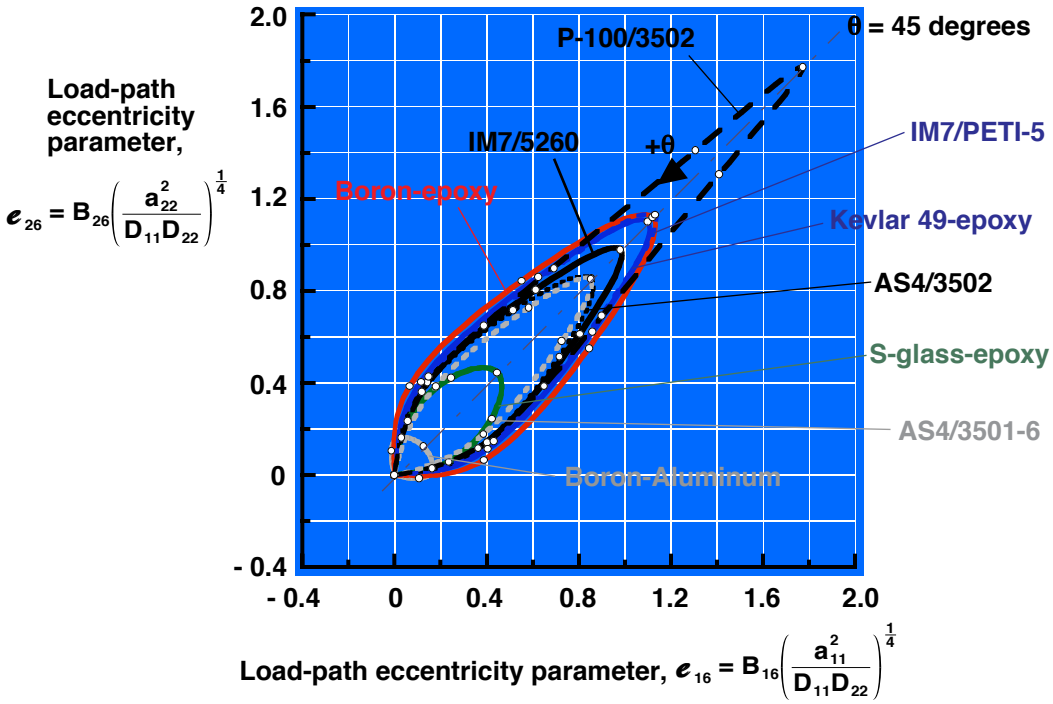

Figure 14. Effects of lamina material properties on nondimensional load-path eccentricity parameters e_{16} and e_{26} defined by equation (75) for $(-\theta/+\theta)_m$ and $-e_{16}$ and $-e_{26}$ for $(+\theta/-\theta)_m$ antisymmetric angle-ply laminates, respectively (m = 1).

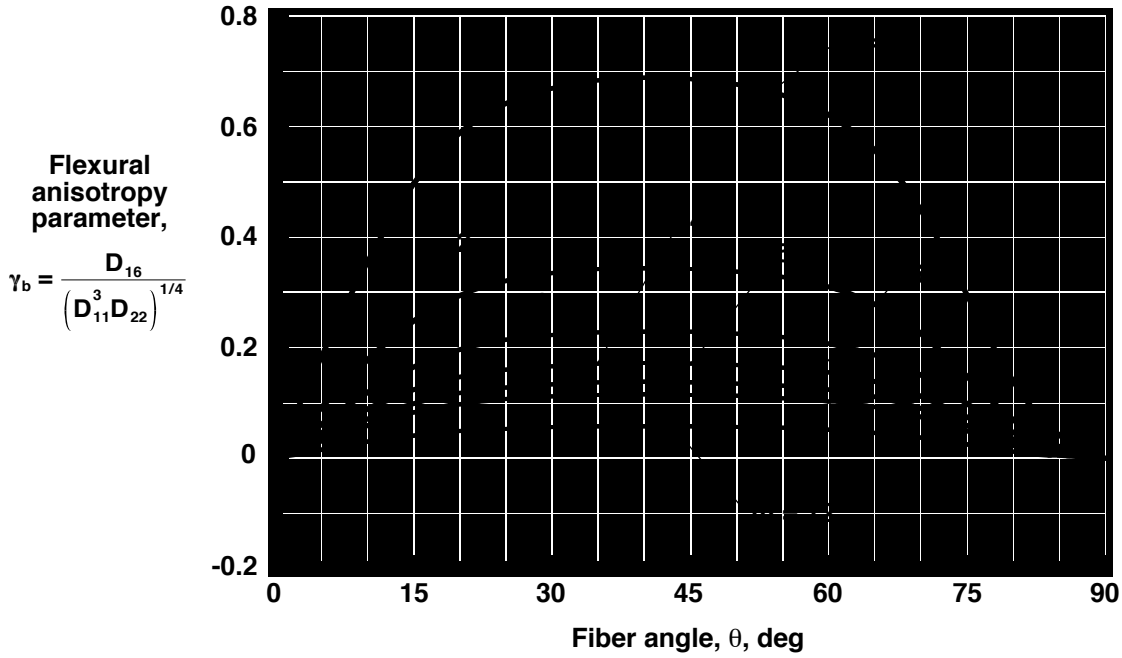

Figure 15. Effects of number of plies on flexural anisotropy parameters γ_b for $[(+\theta/-\theta)_m]_S$ and $-\gamma_b$ for $[(-\theta/+\theta)_m]_S$ P-100/3502 symmetric angle-ply laminates.

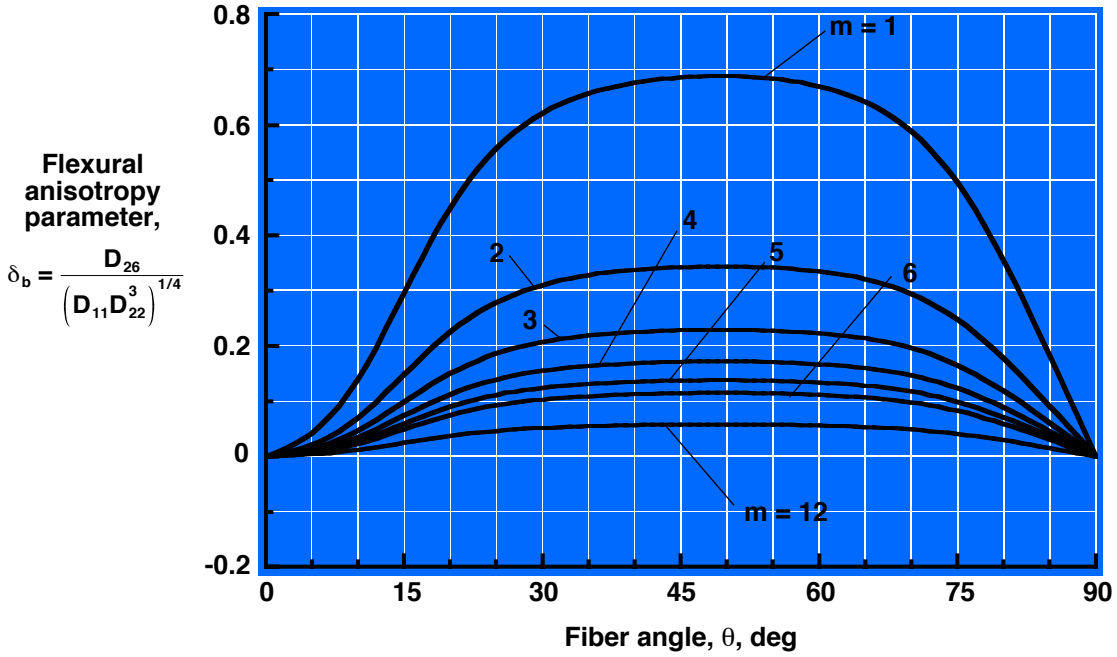

Figure 16. Effects of number of plies on flexural anisotropy parameters δ_b for $[(+\theta/-\theta)_m]_S$ and $-\delta_b$ for $[(-\theta/+\theta)_m]_S$ P-100/3502 symmetric angle-ply laminates.

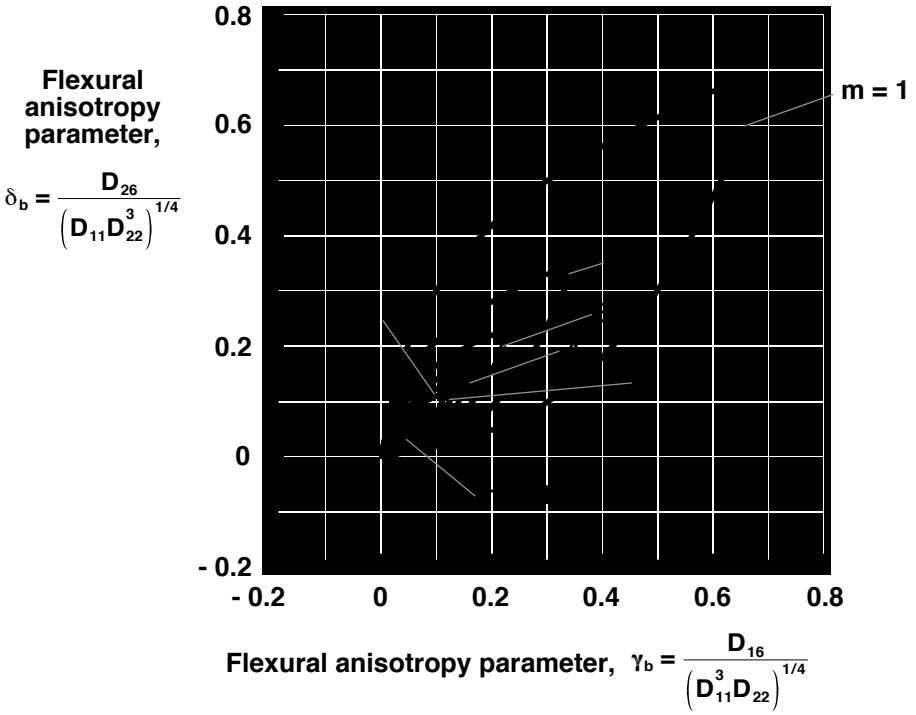

Figure 17. Effects of lamina material properties on flexural anisotropy parameters γ_b and δ_b for $[(+\theta/-\theta)_m]_S$ and $-\gamma_b$ and $-\delta_b$ for $[(-\theta/+\theta)_m]_S$ P-100/3502 symmetric angle-ply laminates, respectively (m = 1).

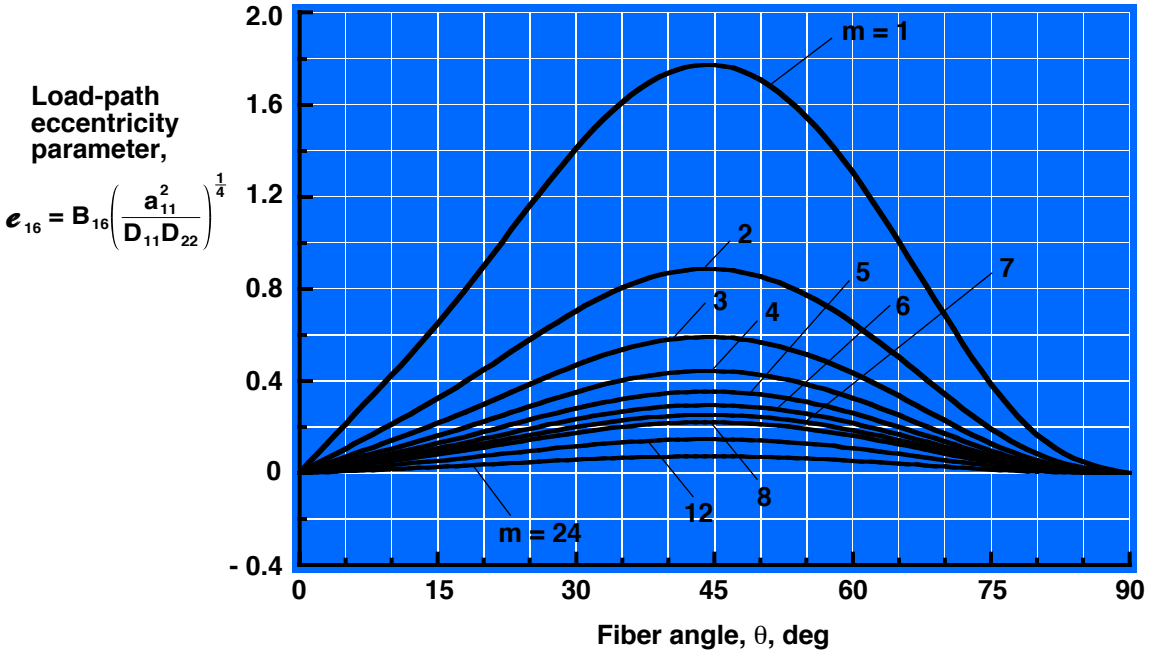

Figure 18. Effects of number of plies on nondimensional load-path eccentricity parameters $-e_{16}$ and $+e_{16}$ defined by equation (75e) for $(+\theta/-\theta)_m$ and $(-\theta/+\theta)_m$ P-100/3502 antisymmetric angle-ply laminates, respectively.

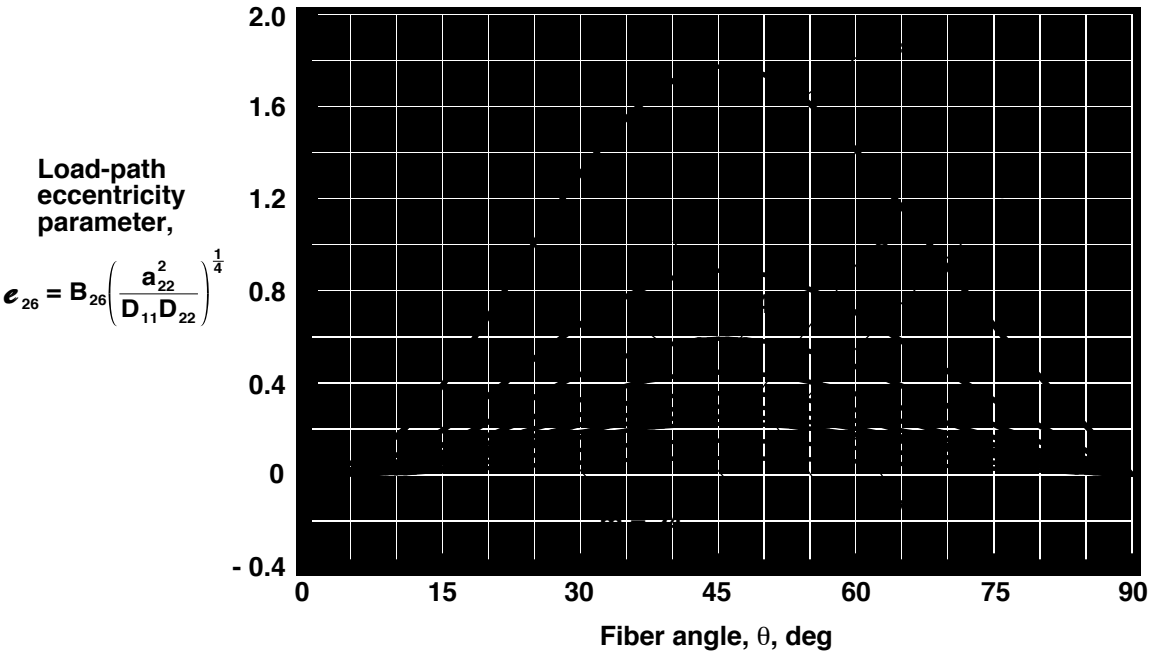

Figure 19. Effects of number of plies on nondimensional load-path eccentricity parameters $-e_{26}$ and $+e_{26}$ defined by equation (75f) for $(+\theta/-\theta)_m$ and $(-\theta/+\theta)_m$ P-100/3502 antisymmetric angle-ply laminates, respectively.

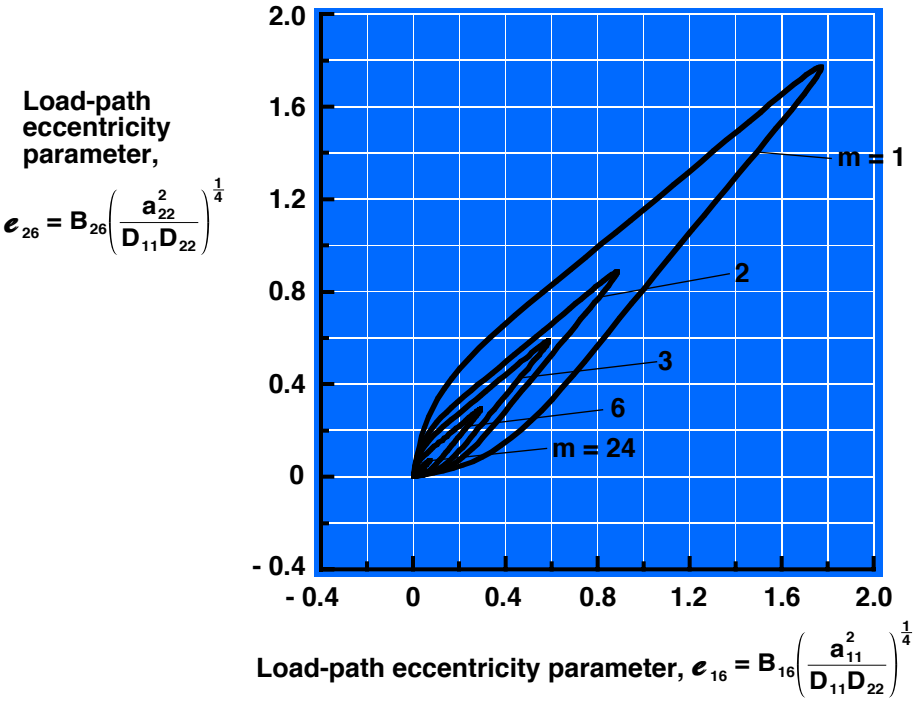

Figure 20. Effects of number of plies on nondimensional load-path eccentricity parameters e_{16} and e_{26} defined by equation (75) for $(-\theta/+\theta)_m$ P100/3502 antisymmetric angle-ply laminates.

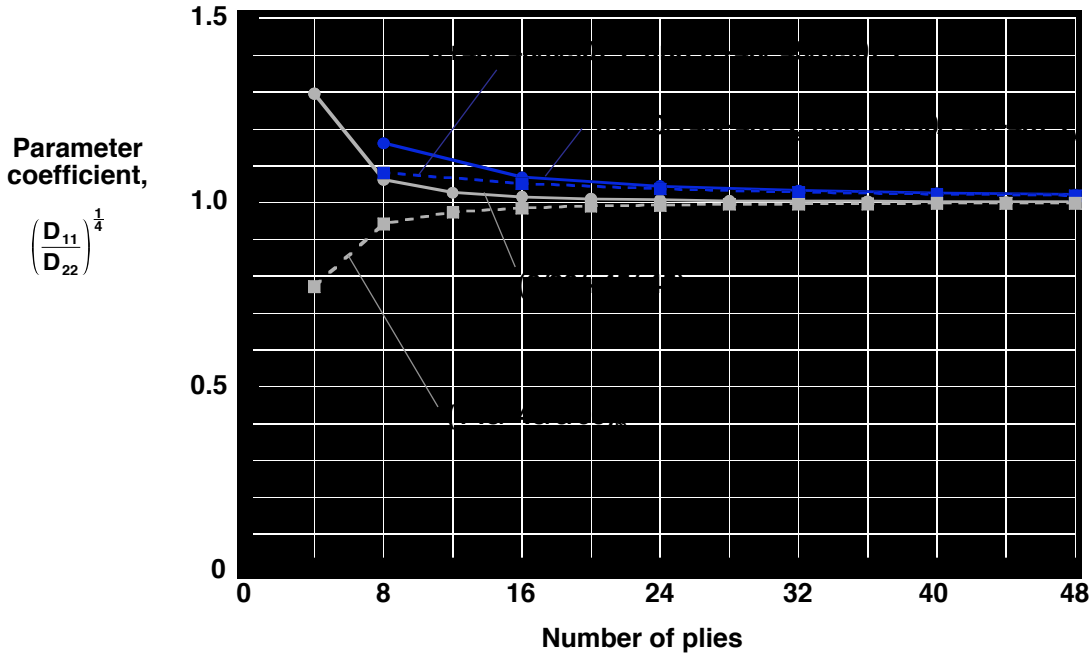

Figure 21. Effects of number of plies on parameter coefficients in equation (55) for P-100/3502 quasi-isotropic laminates.

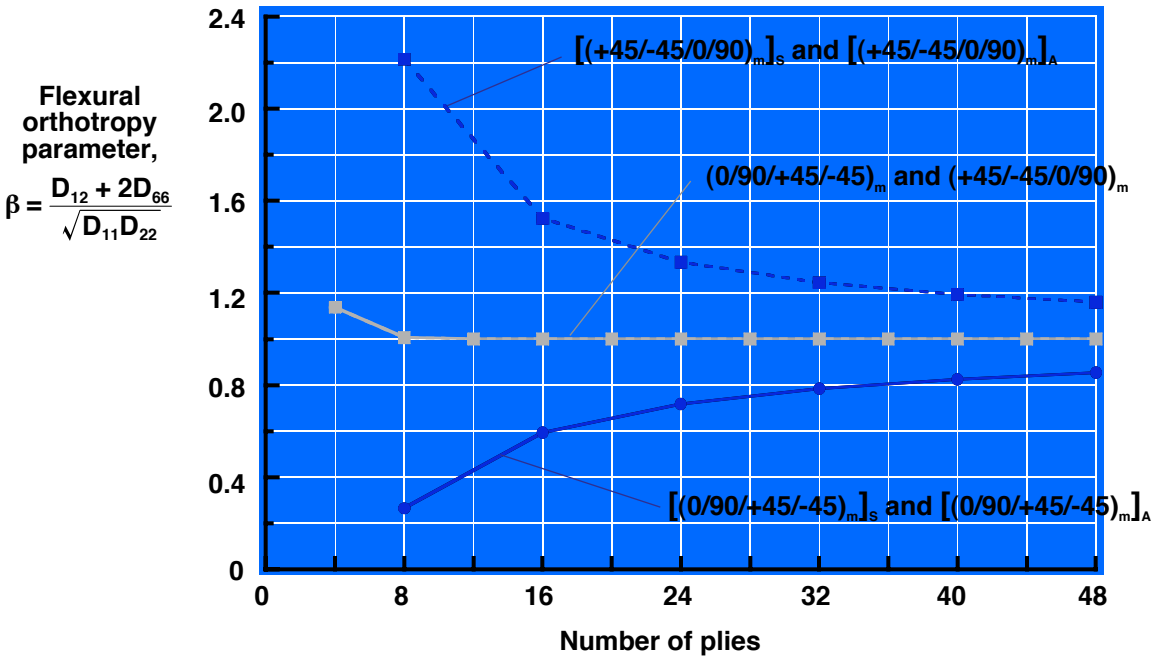

Figure 22. Effects of number of plies on the nondimensional flexural orthotropy parameter β for P-100/3502 quasi-isotropic laminates.

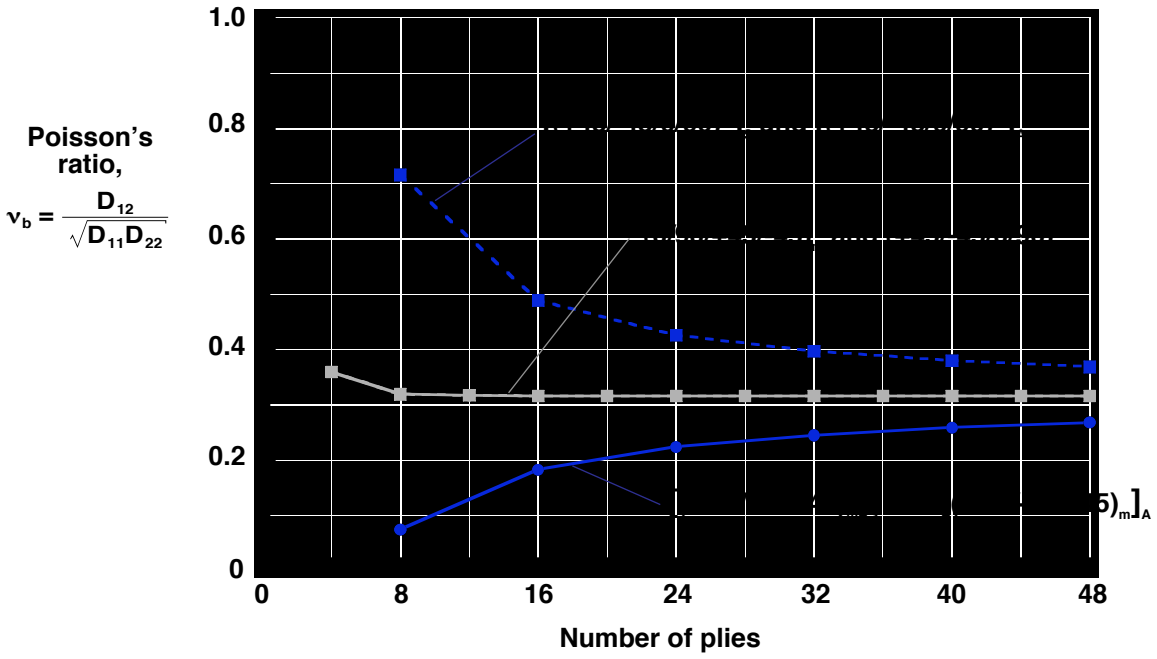

Figure 23. Effects of number of plies on the nondimensional Poisson's ratio ν_b for P-100/3502 quasi-isotropic laminates.

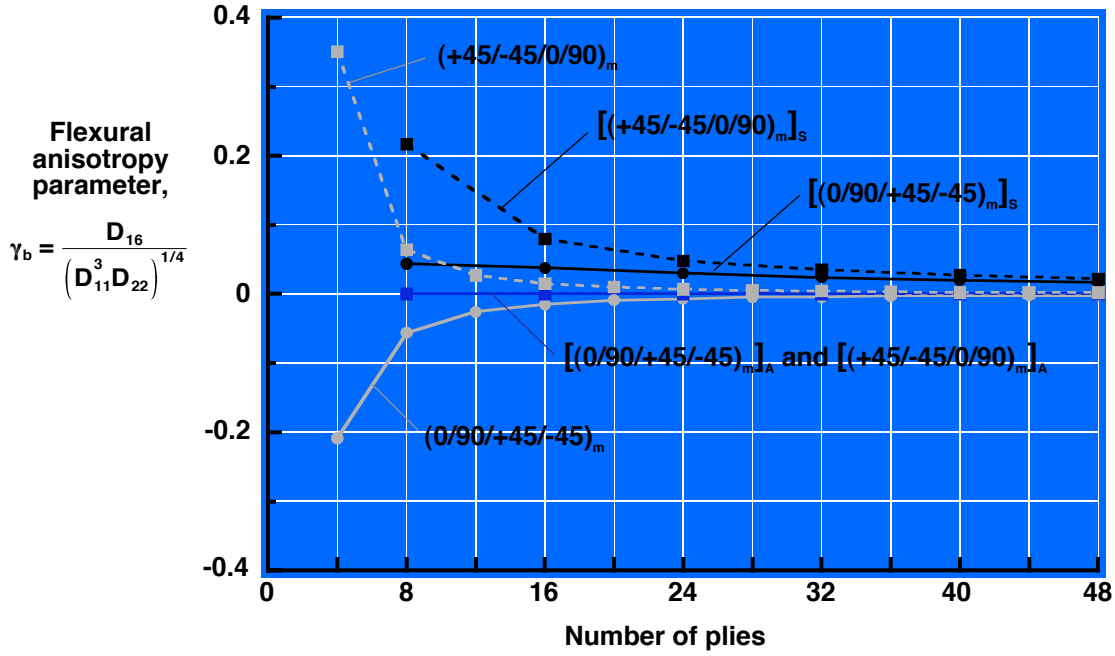

Figure 24. Effects of number of plies on the nondimensional flexural anisotropy parameter γ_b for P-100/3502 quasi-isotropic laminates.

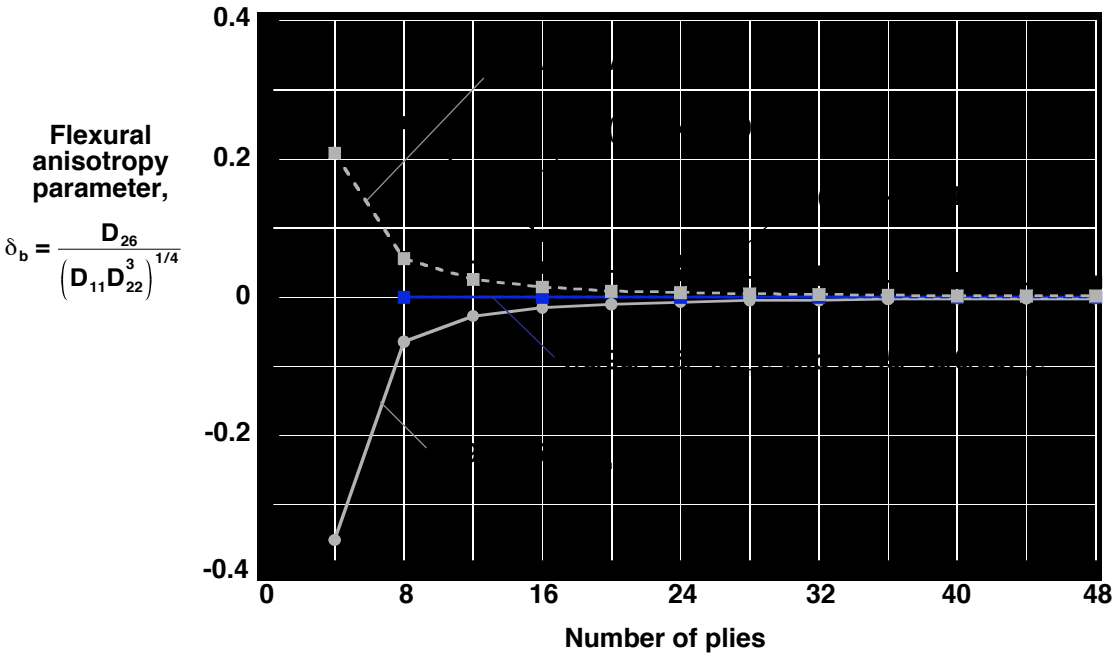

Figure 25. Effects of number of plies on the nondimensional flexural anisotropy parameter δ_b for P-100/3502 quasi-isotropic laminates.

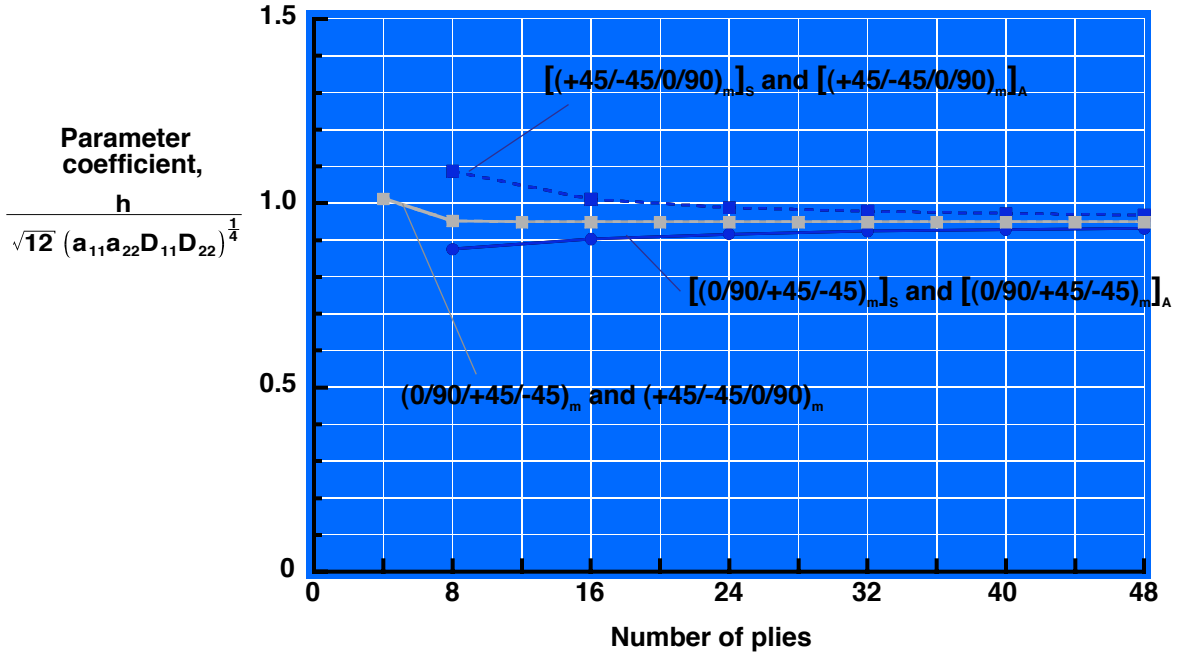

Figure 26. Effects of number of plies on Batdorf-Stein-parameter coefficients in equations (45) and (48) for P-100/3502 quasi-isotropic laminates.

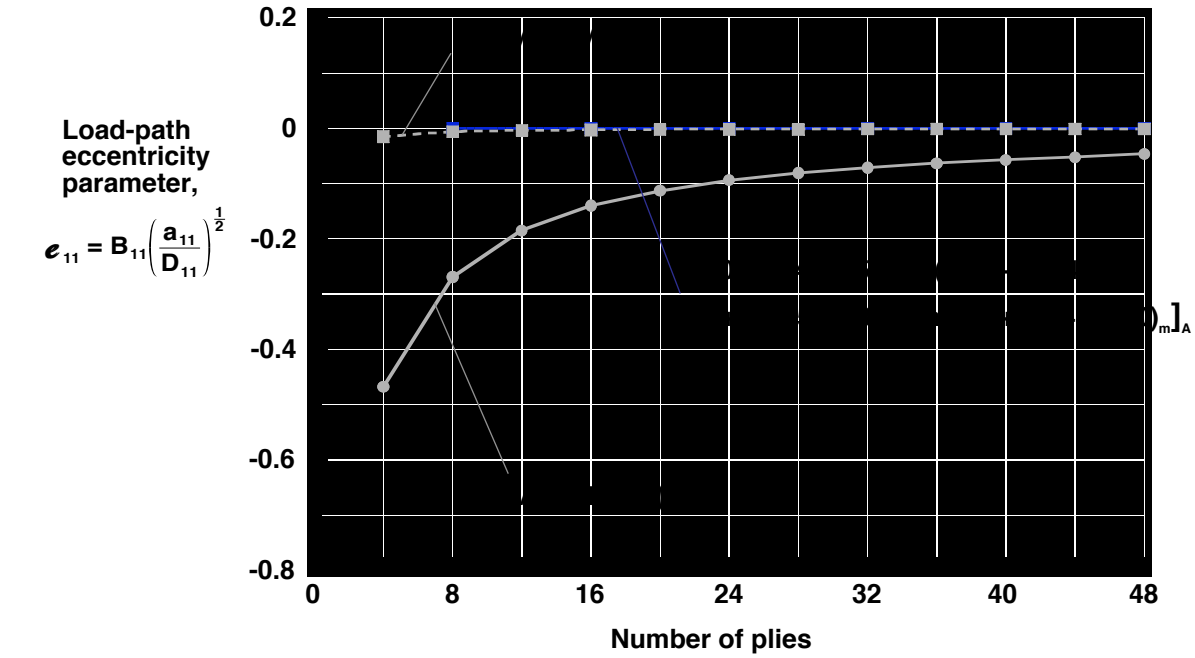

Figure 27. Effects of number of plies on nondimensional load-path eccentricity parameter e_{11} defined by equations (75b) for P-100/3502 quasi-isotropic laminates.

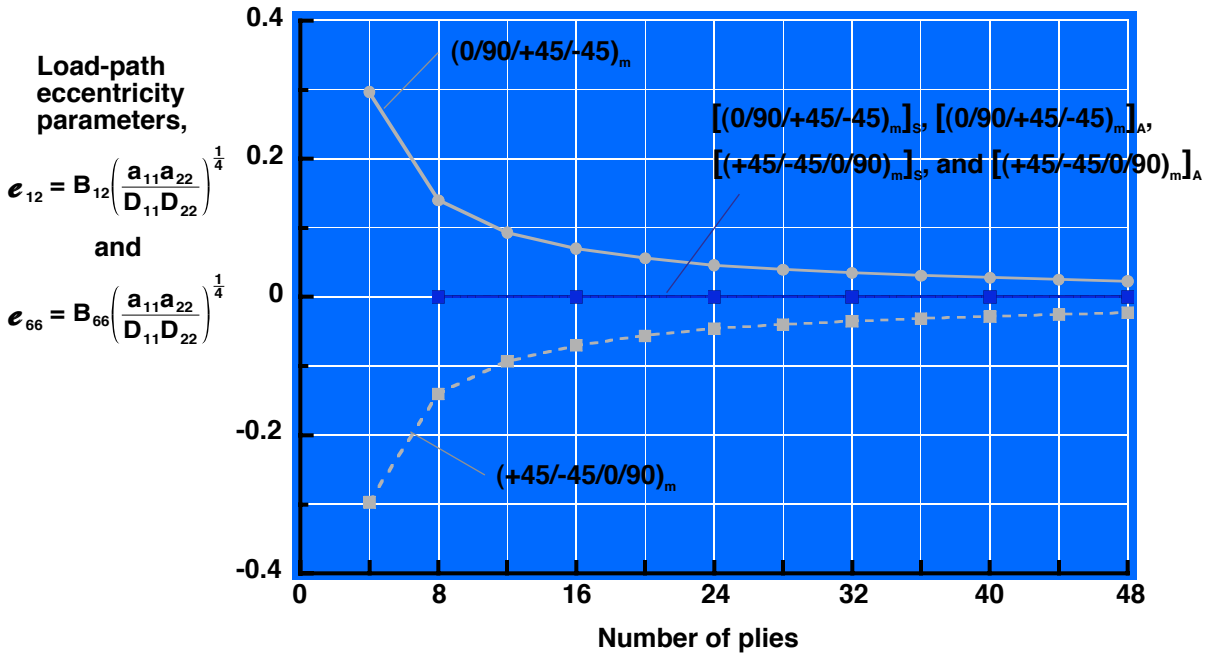

Figure 28. Effects of number of plies on nondimensional load-path eccentricity parameters ϵ_{12} and ϵ_{66} defined by equations (75) for P-100/3502 quasi-isotropic laminates.

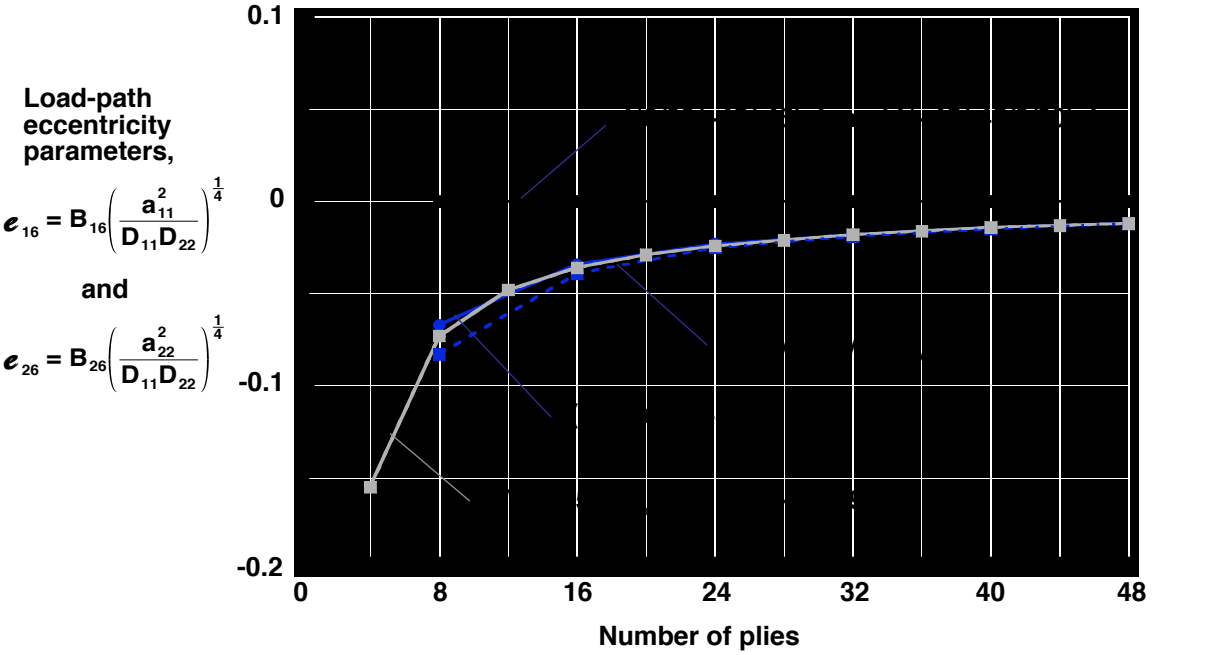

Figure 29. Effects of number of plies on nondimensional load-path eccentricity parameters ϵ_{16} and ϵ_{26} defined by equations (75) for P-100/3502 quasi-isotropic laminates.

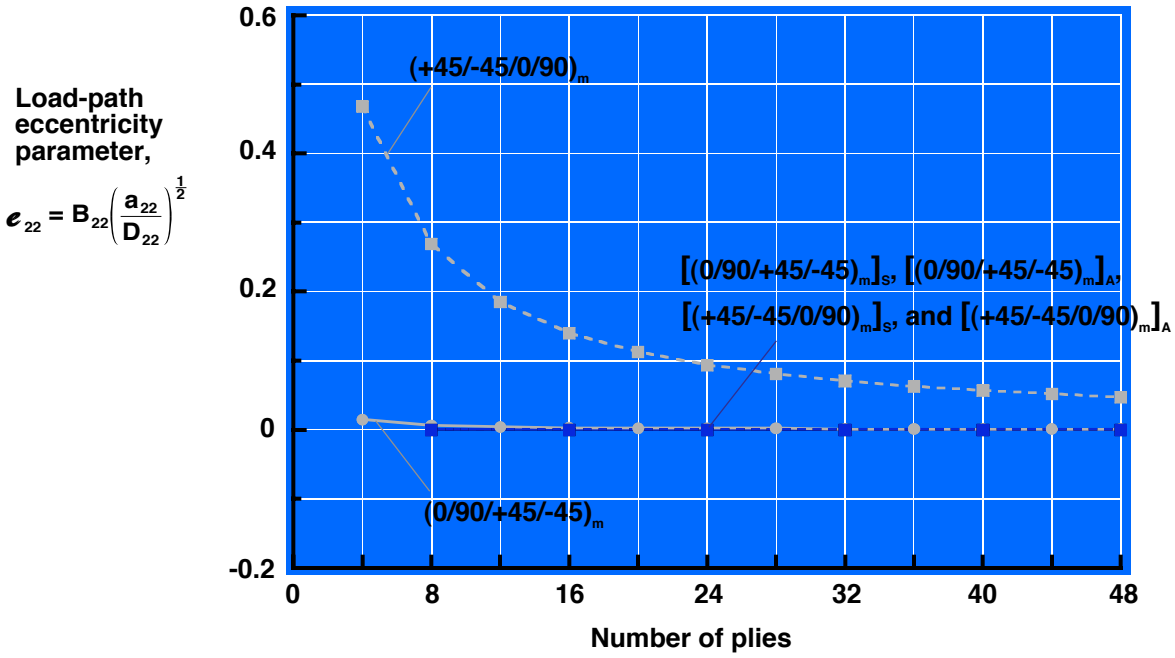

Figure 30. Effects of number of plies on nondimensional load-path eccentricity parameter e_{22} defined by equations (75d) for P-100/3502 quasi-isotropic laminates.

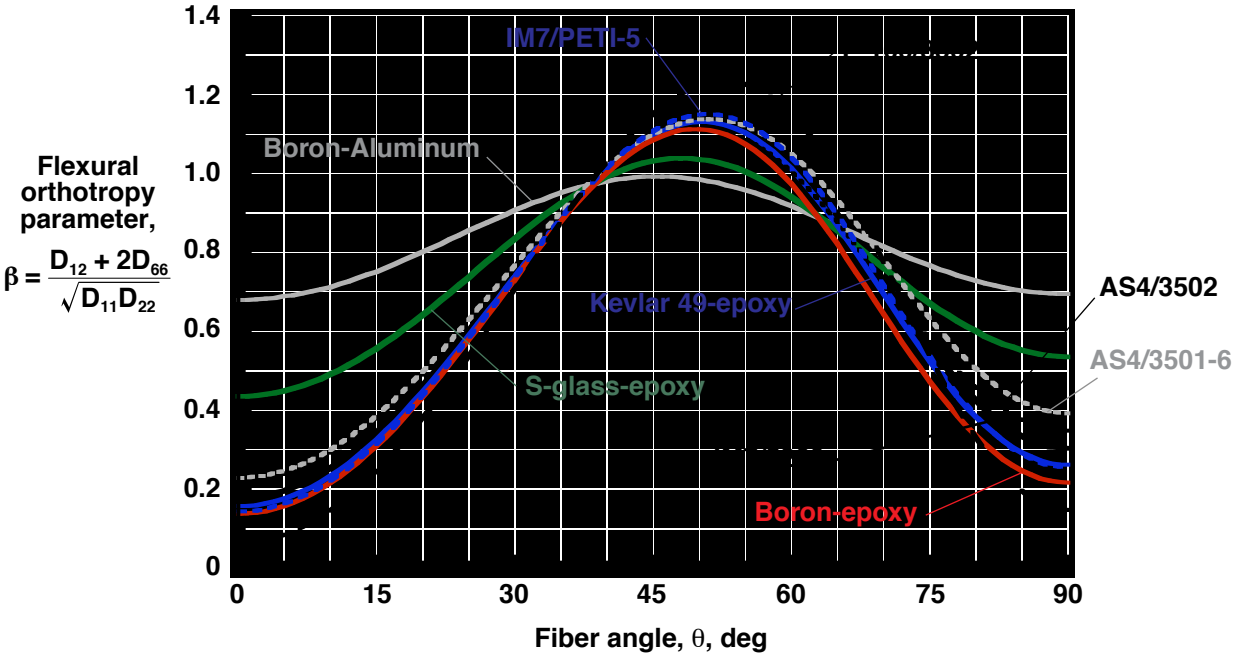

Figure 31. Effects of lamina material properties on nondimensional flexural orthotropy parameter β for (+θ /0/90) and (-θ /0/90) unbalanced, unsymmetric three-ply laminates.

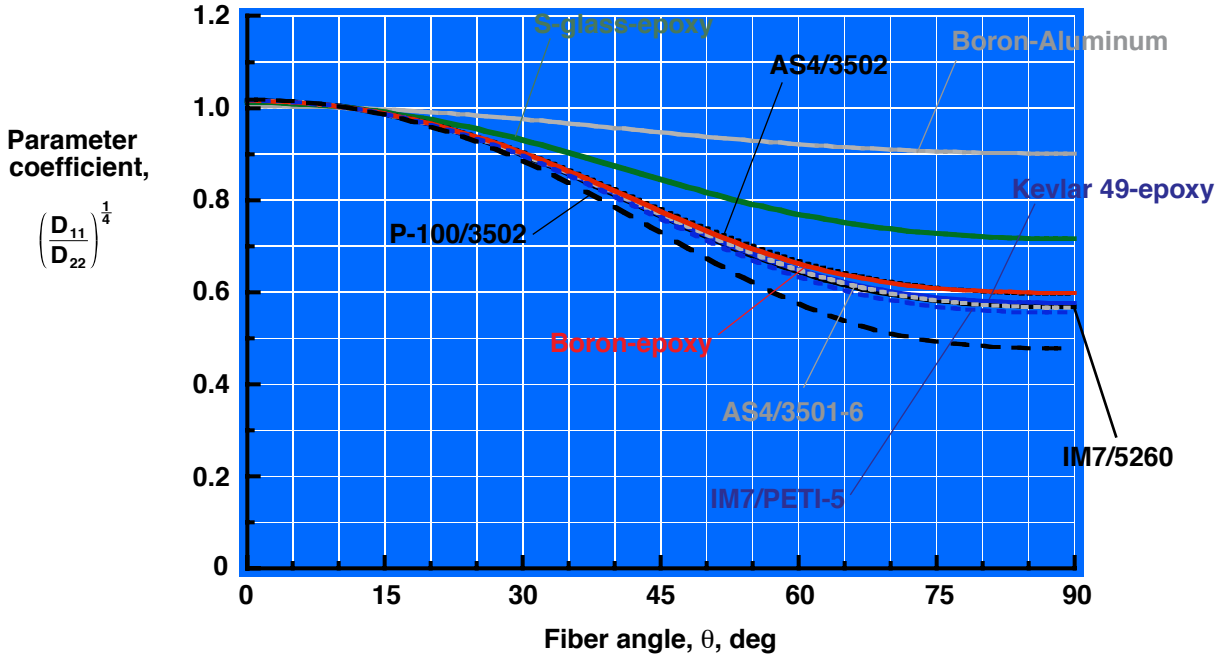

Figure 32. Effects of lamina material properties on parameter coefficient in equation (55) for (+θ /0/90) and (-θ /0/90) unbalanced, unsymmetric three-ply laminates.

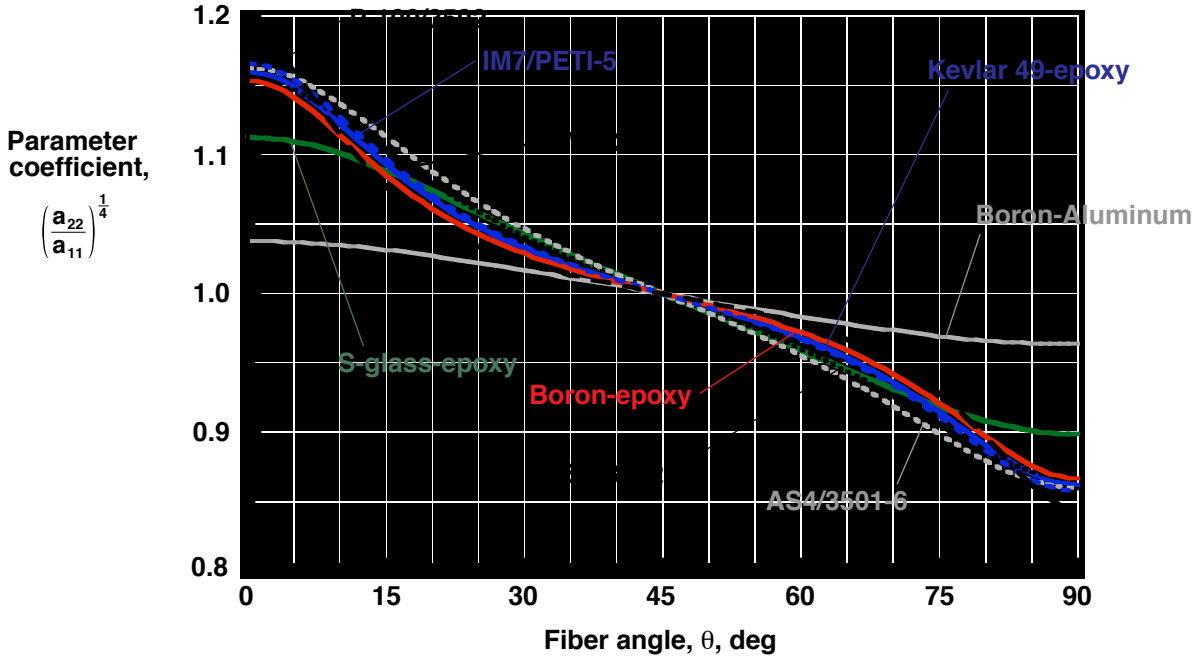

Figure 33. Effects of lamina material properties on parameter coefficient in equation (52a) $(+\theta\ /0/90)_m$ and $(-\theta\ /0/90)_m$ unbalanced, unsymmetric laminates (m = 1, 2, ...).

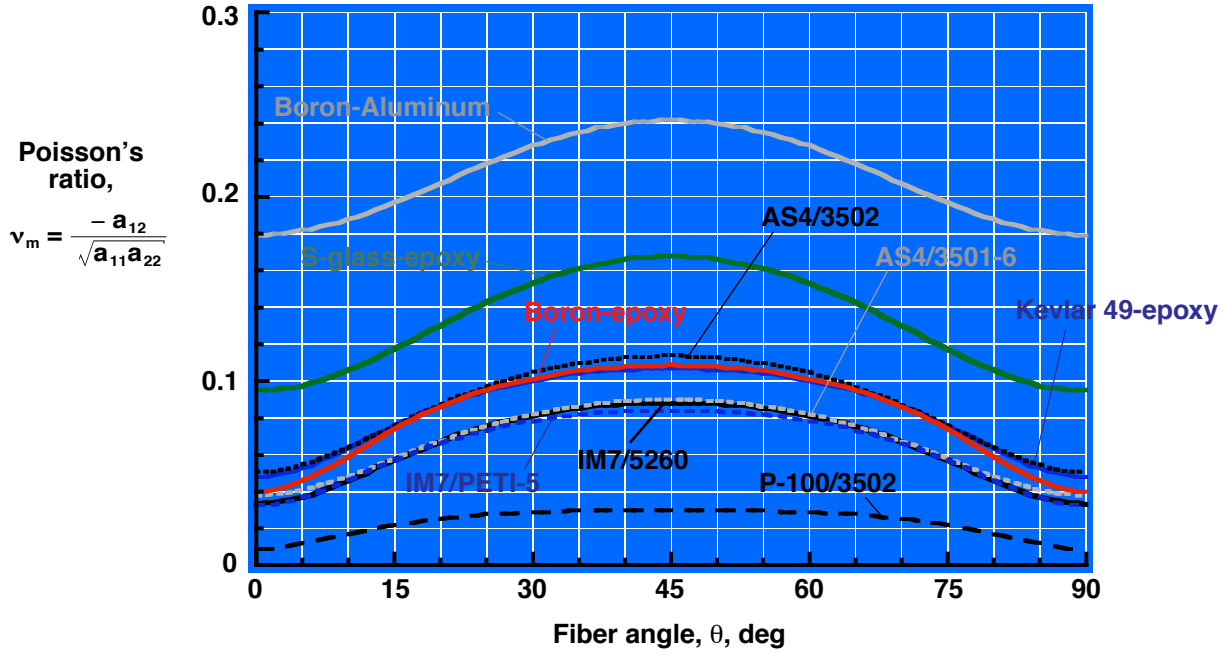

Figure 34. Effects of lamina material properties on Poisson's ratio defined by equation (52e) for $(+\theta\ /0/90)_m$ and $(-\theta\ /0/90)_m$ unbalanced, unsymmetric laminates (m = 1, 2, ...).

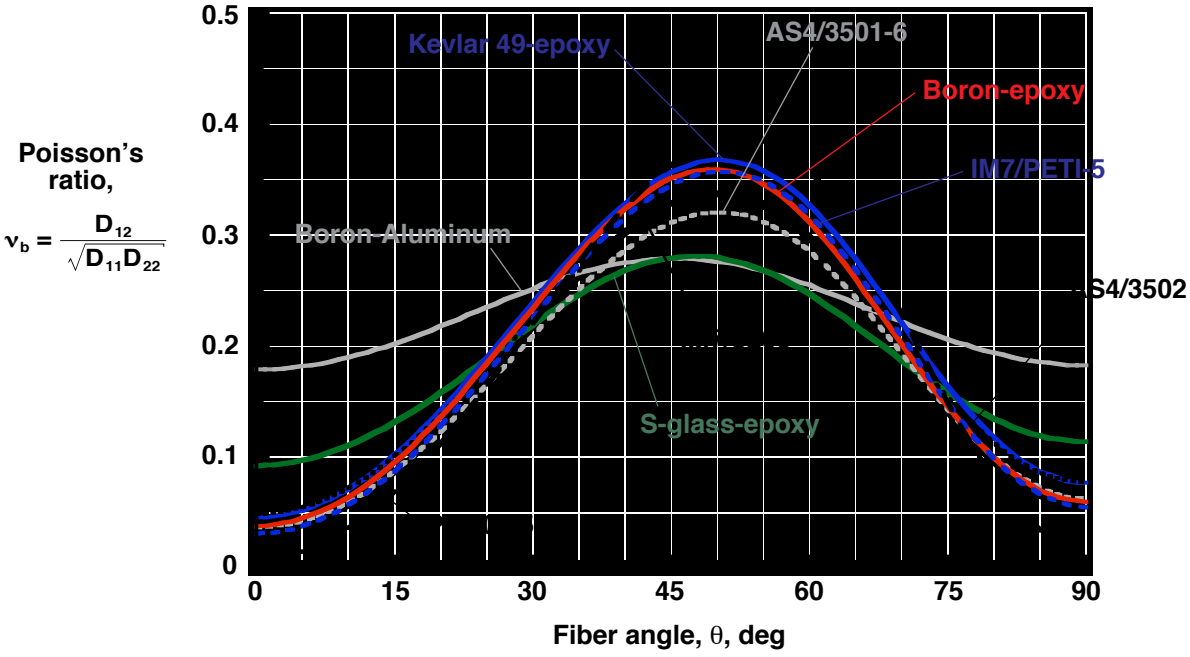

Figure 35. Effects of lamina material properties on Poisson's ratio defined by equation (59d) for $(+\theta\ /0/90)$ and $(-\theta\ /0/90)$ unbalanced, unsymmetric three-ply laminates.

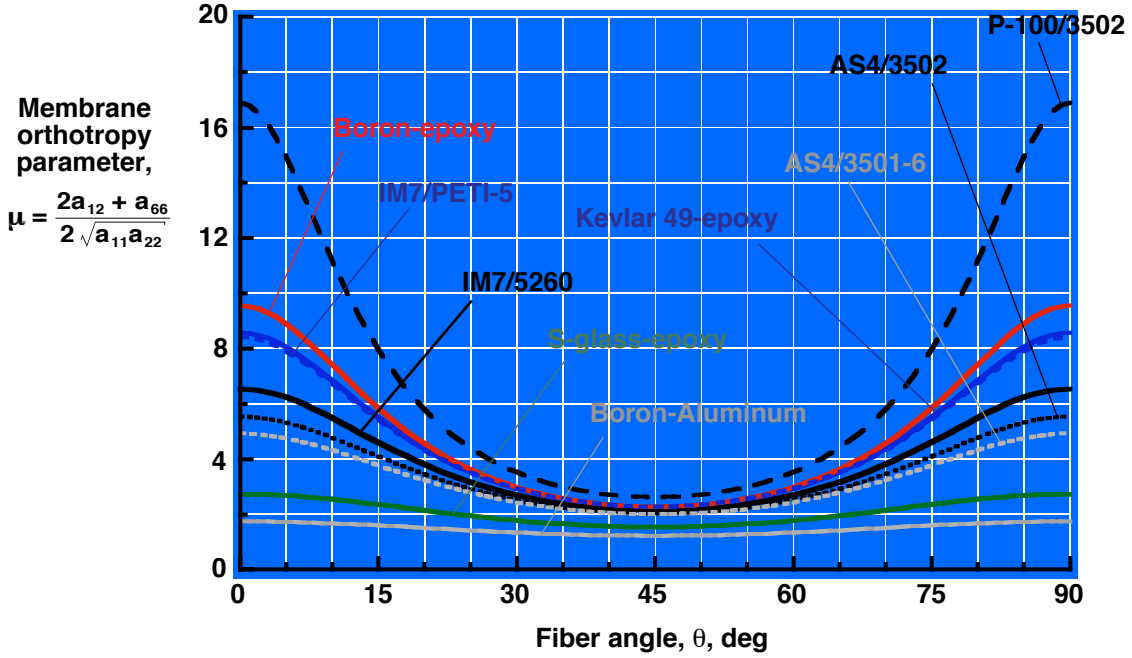

Figure 36. Effects of lamina material properties on nondimensional membrane orthotropy parameter μ for $(+\theta\ /0/90)_m$ and $(-\theta\ /0/90)_m$ unbalanced, unsymmetric laminates (m = 1, 2, ...).

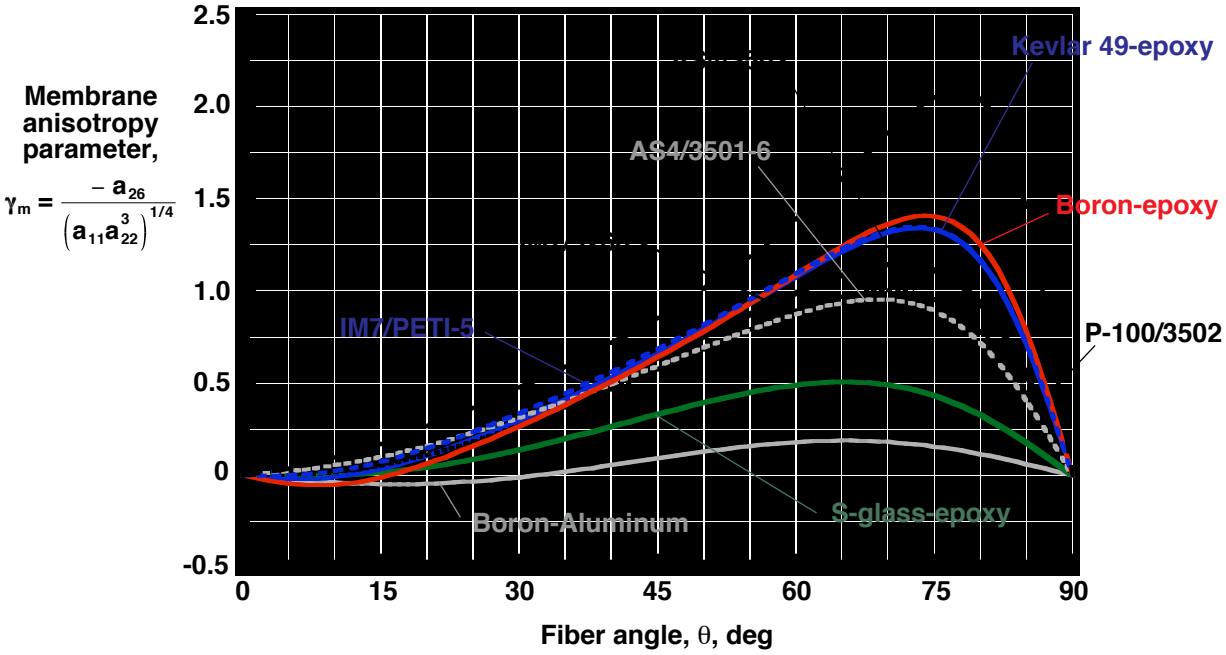

Figure 37. Effects of lamina material properties on nondimensional membrane anisotropy parameters γ_m and $-\gamma_m$ for $(+\theta\ /0/90)_m$ and $(-\theta\ /0/90)_m$ unbalanced, unsymmetric laminates, respectively (m = 1, 2, ...).

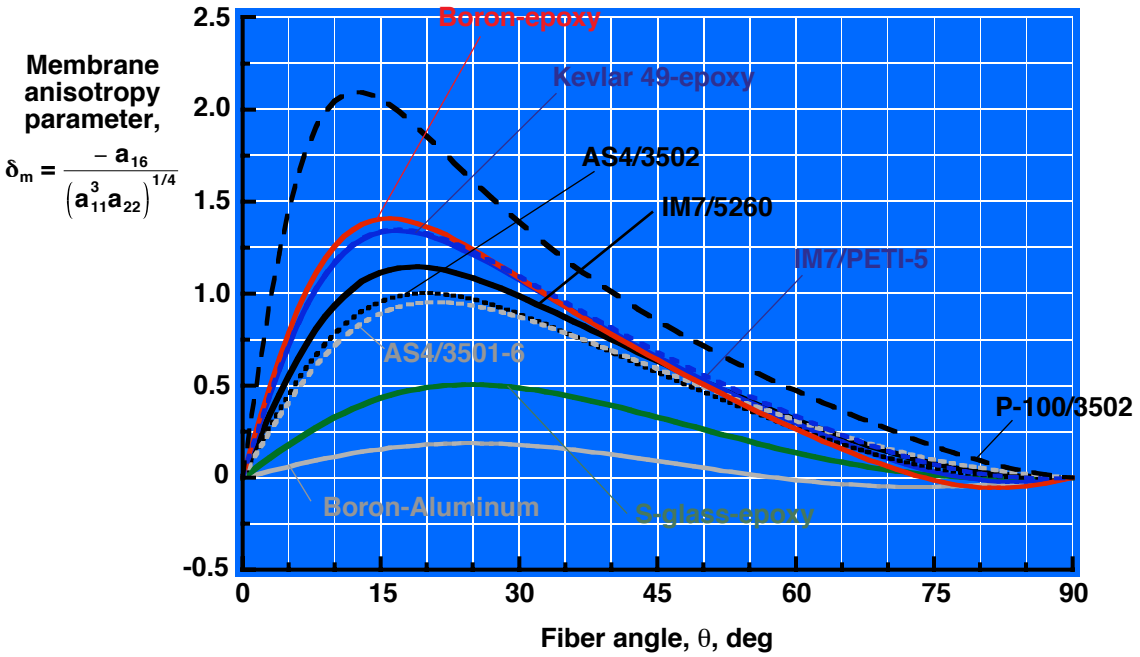

Figure 38. Effects of lamina material properties on nondimensional membrane anisotropy parameters δ_m and $-\delta_m$ for $(+\theta\ /0/90)_m$ and $(-\theta\ /0/90)_m$ unbalanced, unsymmetric laminates, respectively (m = 1, 2, ...).

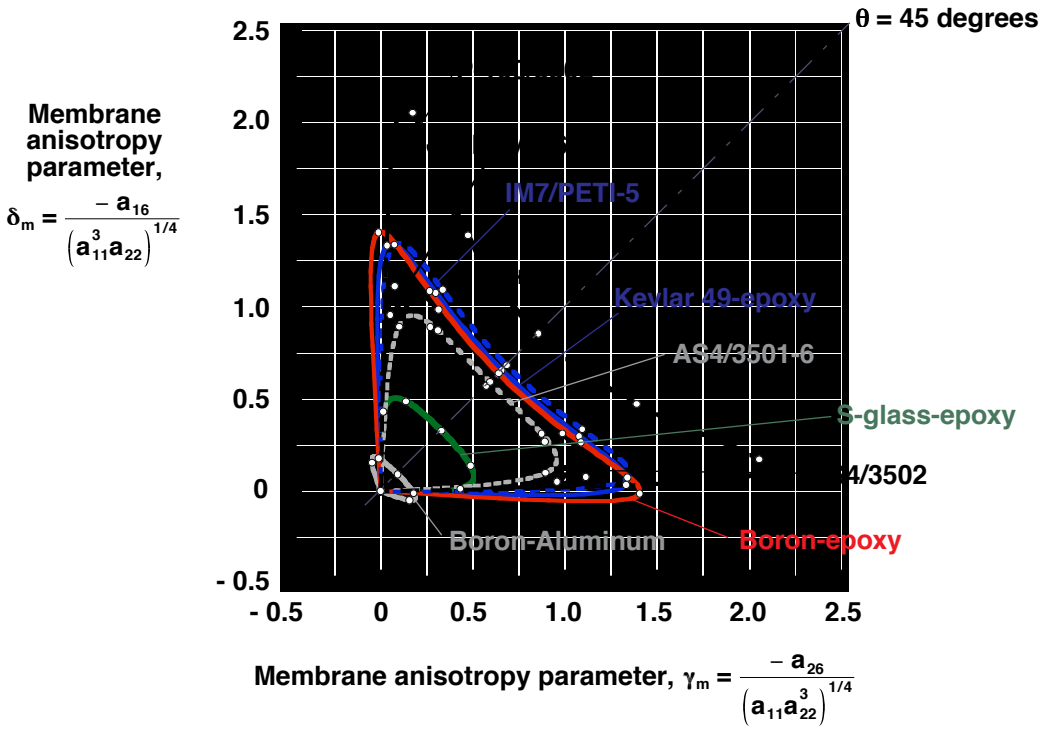

Figure 39. Effects of lamina material properties on membrane anisotropy parameters γ_m and δ_m for $(+\theta\ /0/90)_m$ unbalanced, unsymmetric laminates (m = 1, 2, ...).

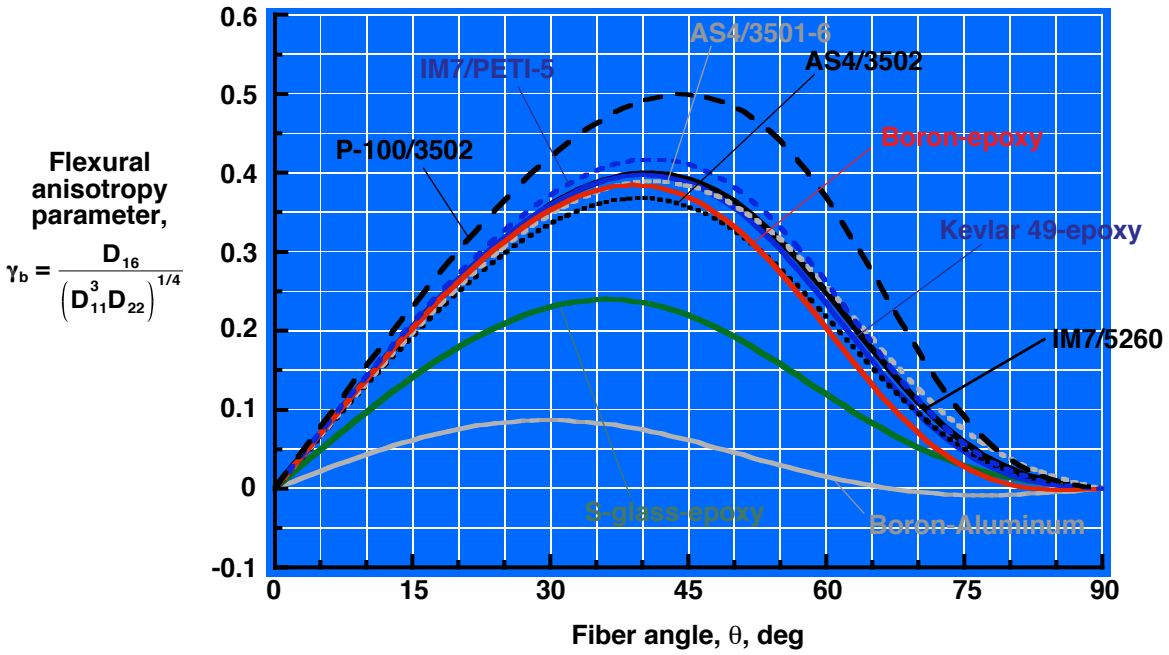

Figure 40. Effects of lamina material properties on nondimensional flexural anisotropy parameters γ_b and $-\gamma_b$ for $(+\theta\ /0/90)_m$ and $(-\theta\ /0/90)_m$ unbalanced, unsymmetric laminates, respectively (m = 1).

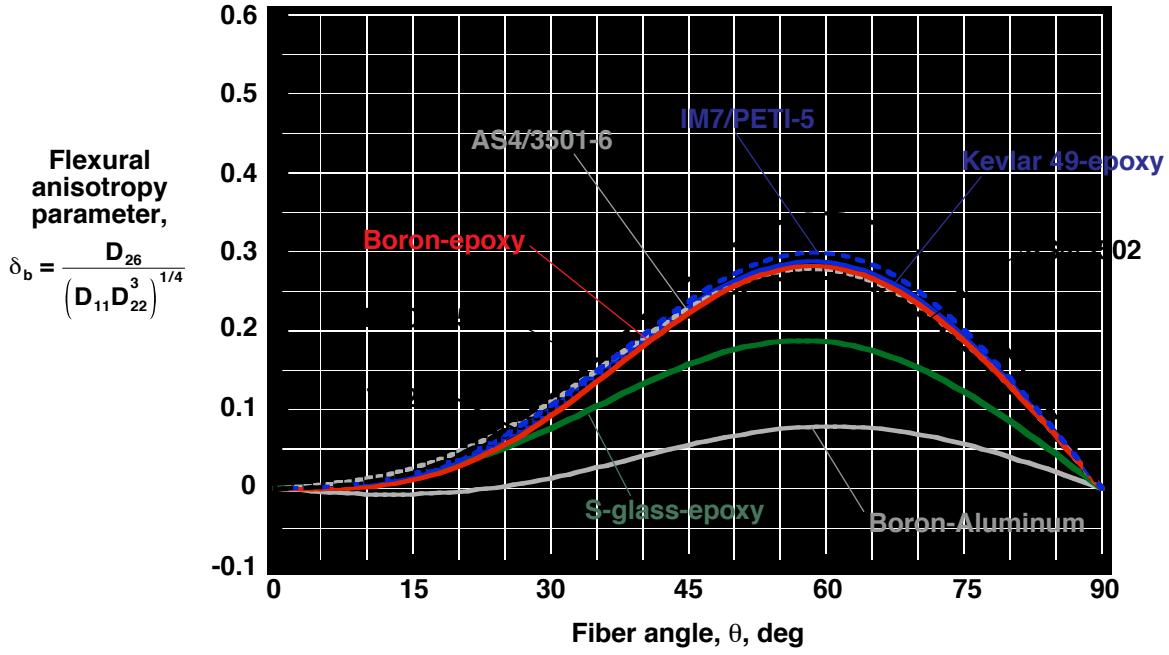

Figur 41. Effects of lamina material properties on nondimensional flexural anisotropy parameters δ_b and $-\delta_b$ for $(+\theta\ /0/90)_m$ and $(-\theta\ /0/90)_m$ unbalanced, unsymmetric laminates, respectively (m = 1).

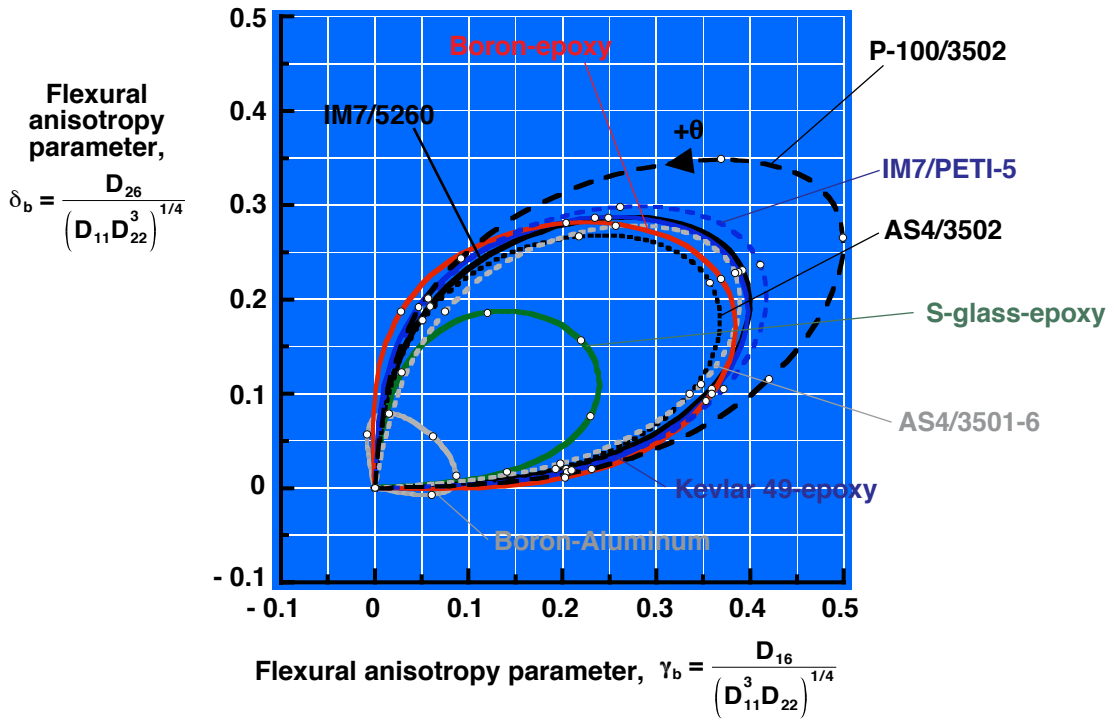

Figure 42. Effects of lamina material properties on flexural anisotropy parameters γ_b and δ_b for $(+\theta/0/90)_m$ unbalanced, unsymmetric laminates (m = 1).

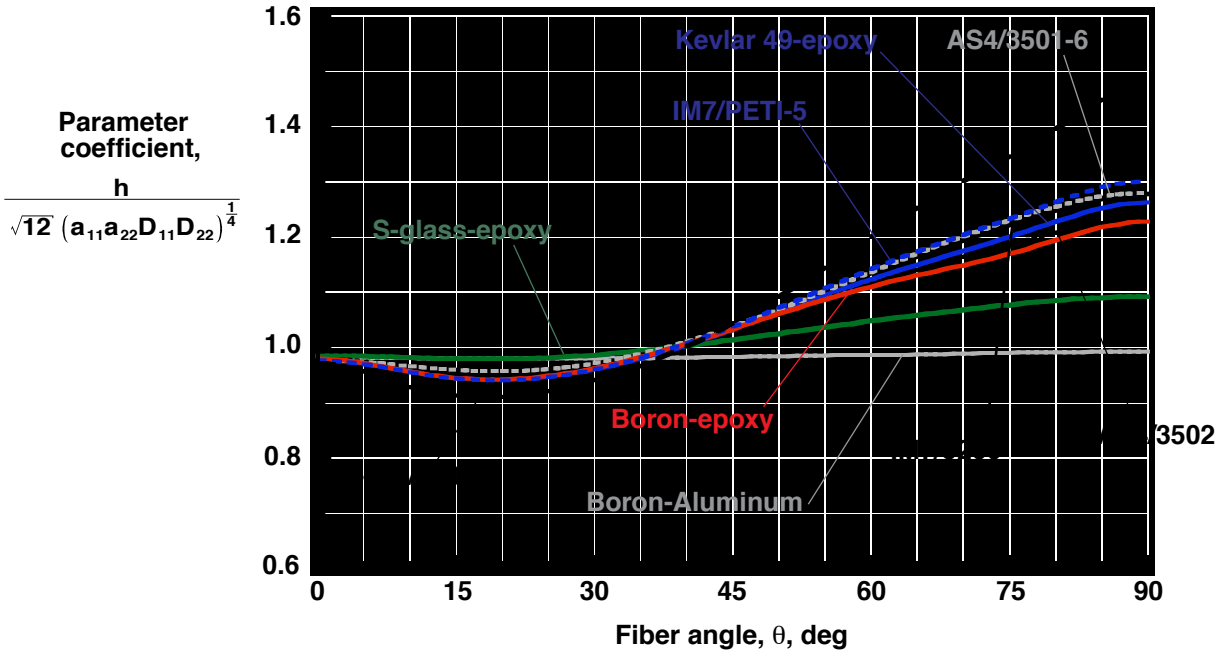

Figure 43. Effects of lamina material properties on Batdorf-Stein-parameter coefficients in equations (45) and (48) for $(+\theta/0/90)_m$ and $(-\theta/0/90)_m$ unbalanced, unsymmetric laminates (m = 1).

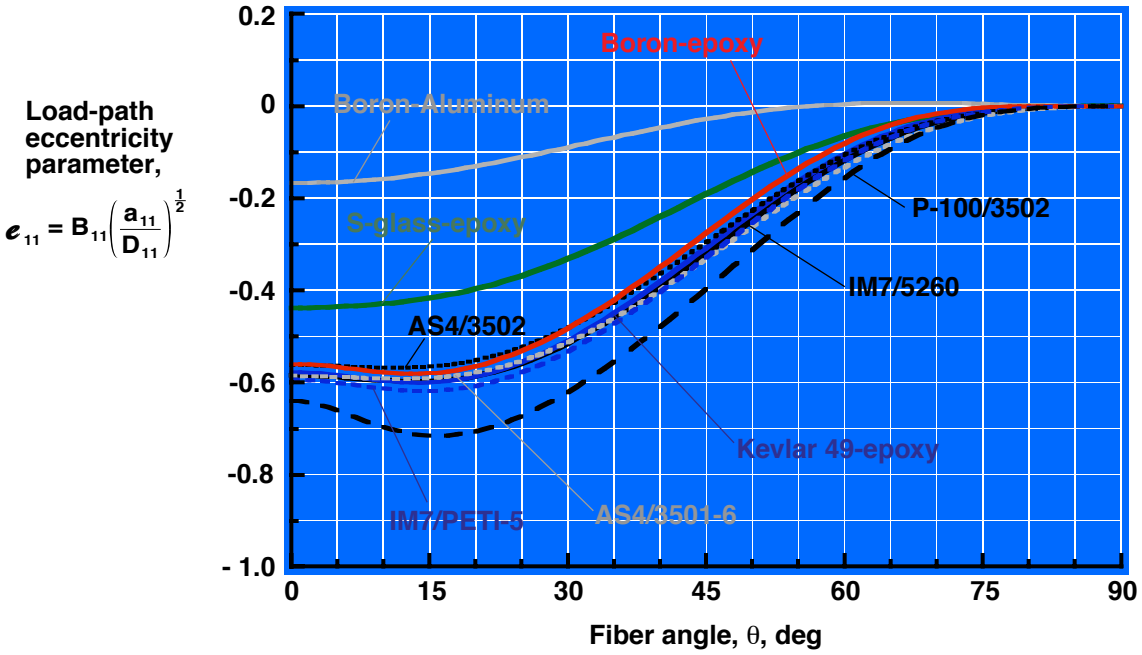

Figure 44. Effects of lamina material properties on nondimensional load-path eccentricity parameter e_{11} defined by equation (75b) for $(+\theta\ /0/90)_m$ and $(-\theta\ /0/90)_m$ unbalanced, unsymmetric laminates, respectively (m = 1).

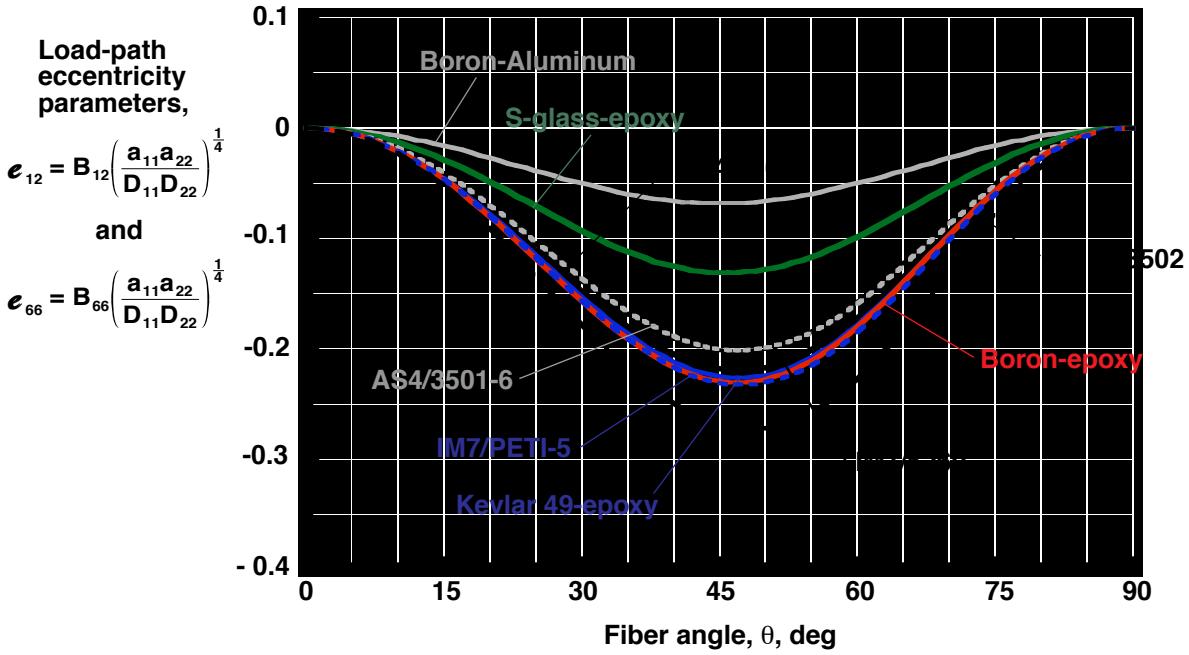

Figure 45. Effects of lamina material properties on nondimensional load-path eccentricity parameters e_{12} and e_{66} defined by equations (75) for $(+\theta\ /0/90)_m$ and $(-\theta\ /0/90)_m$ unbalanced, unsymmetric laminates, respectively (m = 1).

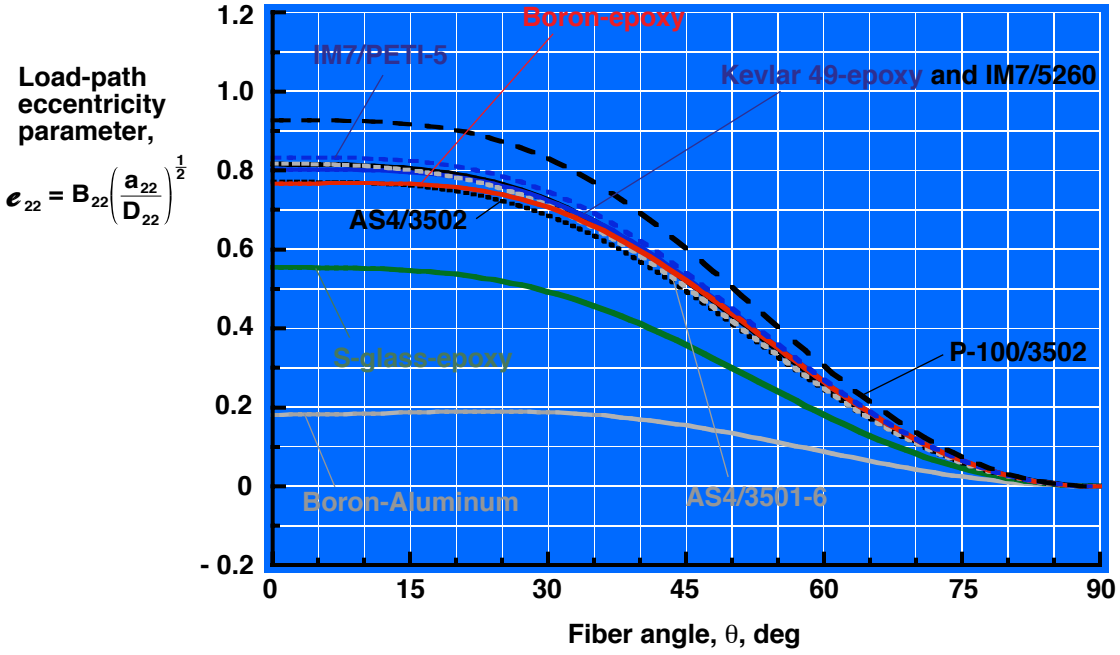

Figure 46. Effects of lamina material properties on nondimensional load-path eccentricity parameter e_{22} defined by equation (75d) for $(+\theta/0/90)_m$ and $(-\theta/0/90)_m$ unbalanced, unsymmetric laminates, respectively (m = 1).

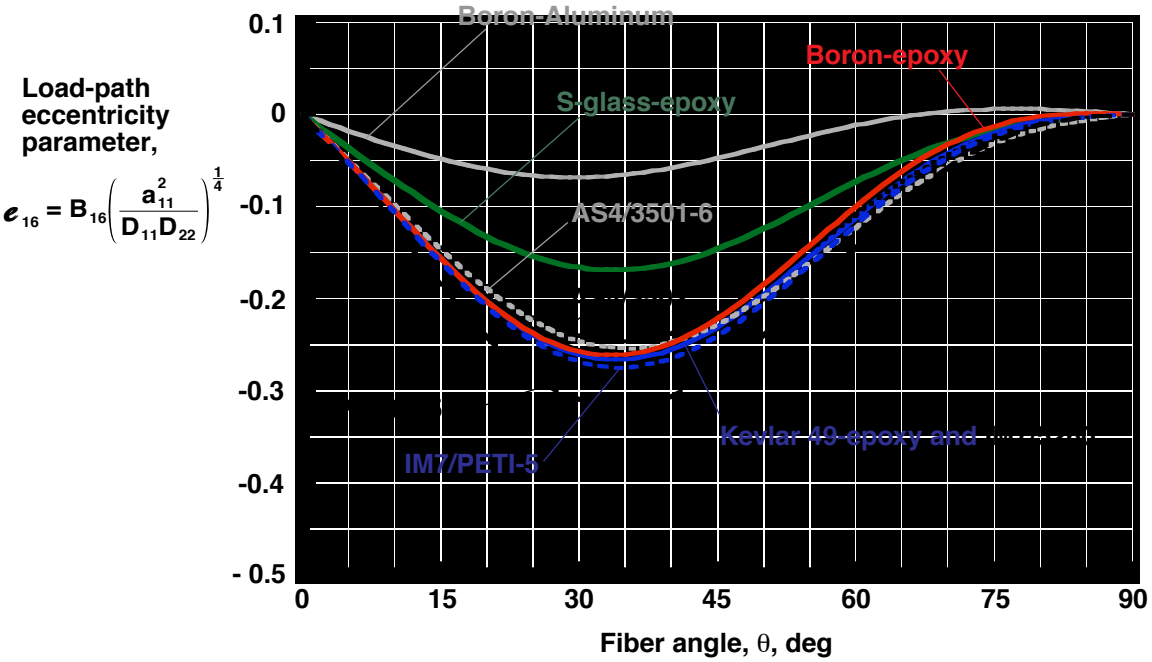

Figure 47. Effects of lamina material properties on nondimensional load-path eccentricity parameters e_{16} and $-e_{16}$ defined by equation (75) for $(+\theta/0/90)_m$ and $(-\theta/0/90)_m$ unbalanced, unsymmetric laminates, respectively (m = 1).

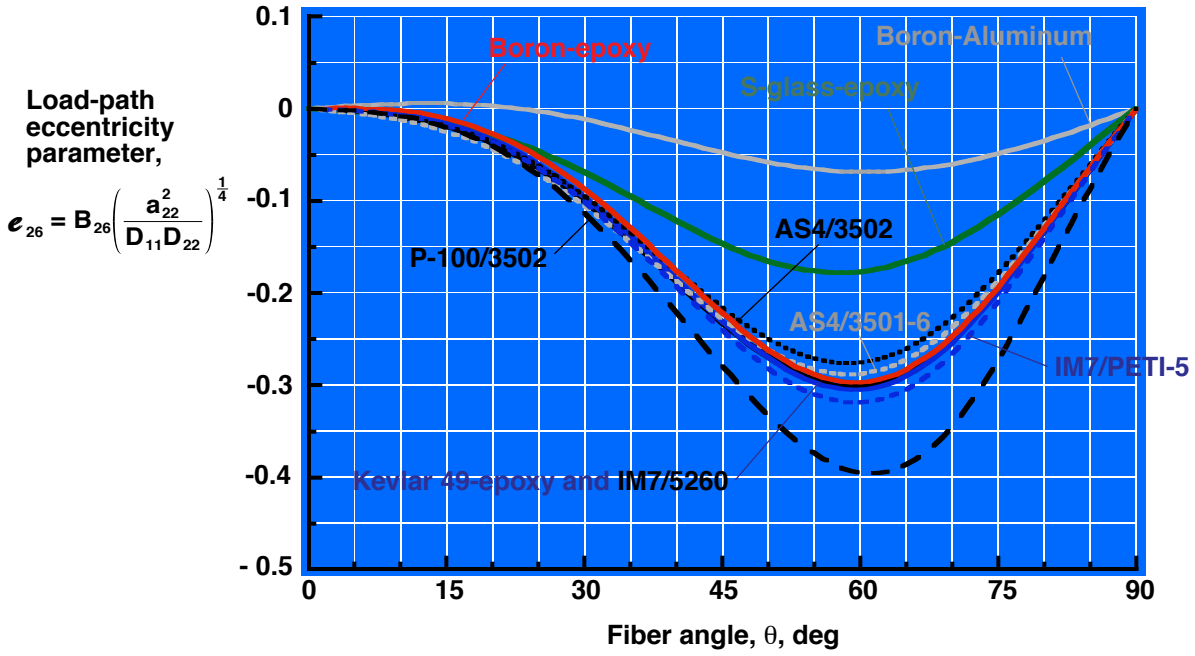

Figure 48. Effects of lamina material properties on nondimensional load-path eccentricity parameters e_{26} and $-e_{26}$ defined by equations (75) for $(+\theta\ /0/90)_m$ and $(-\theta\ /0/90)_m$ unbalanced, unsymmetric laminates, respectively (m = 1).

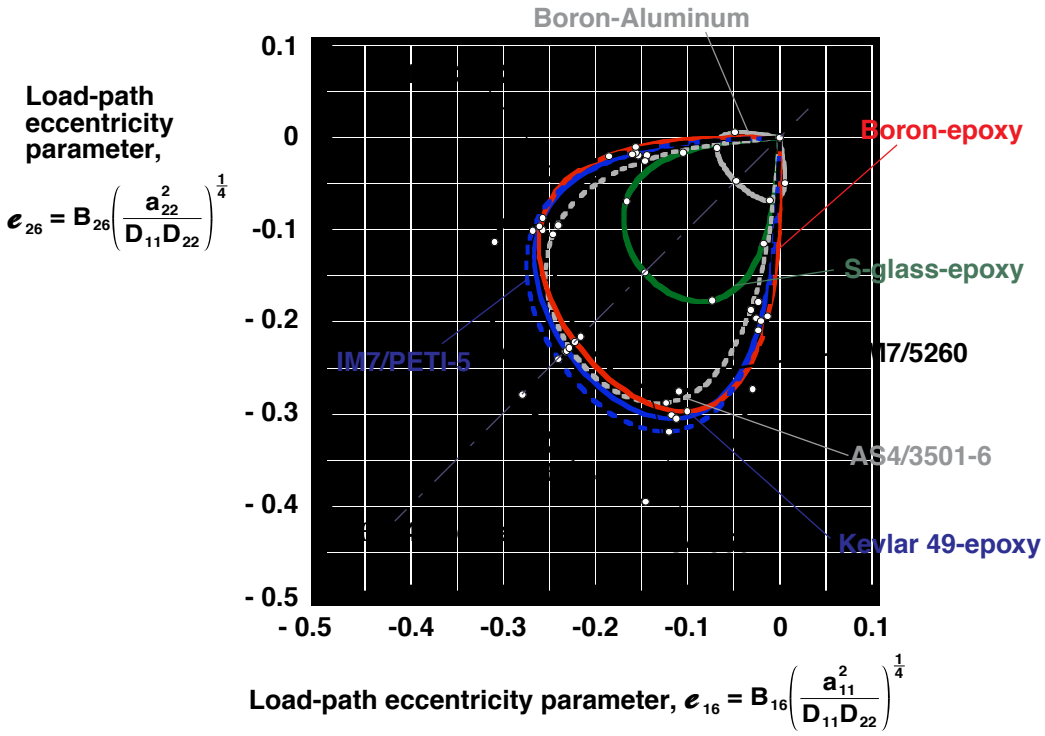

Figure 49. Effects of lamina material properties on nondimensional load-path eccentricity parameters e_{16} and e_{26} defined by equations (75) for $(+\theta\ /0/90)_m$ unbalanced, unsymmetric laminates (m = 1).

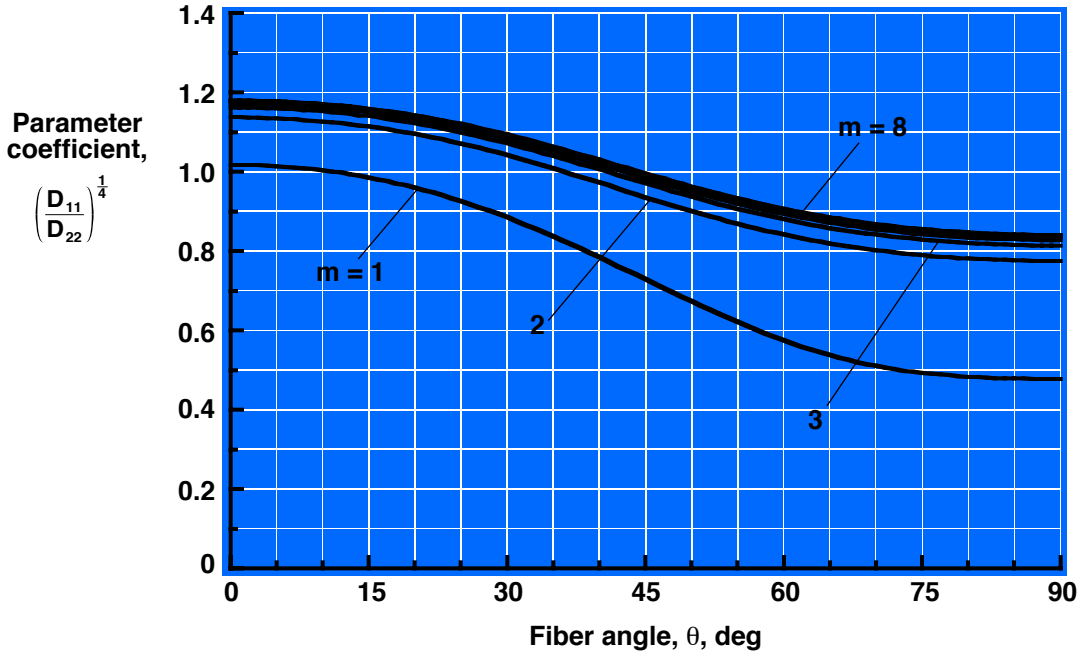

Figure 50. Effects of number of plies on parameter coefficients in equation (55) for $(+\theta/0/90)_m$ and $(-\theta/0/90)_m$ unbalanced, unsymmetric P-100/3502 laminates.

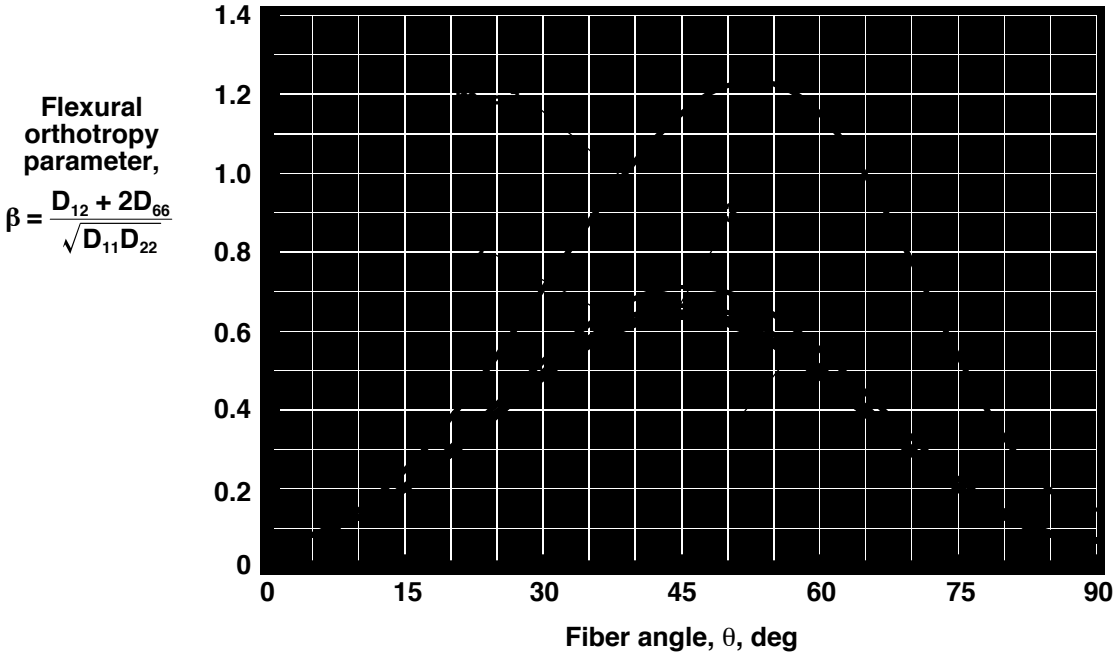

Figure 51. Effects of number of plies on the orthotropy parameter β for $(+\theta/0/90)_m$ and $(-\theta/0/90)_m$ unbalanced, unsymmetric P-100/3502 laminates.

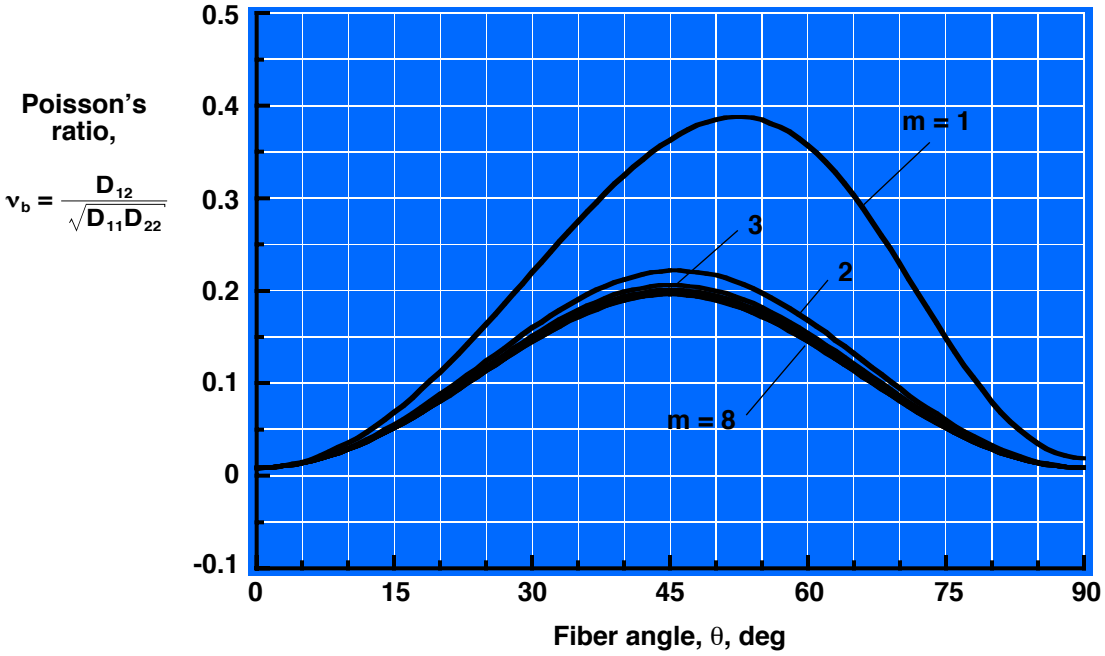

Figure 52. Effects of number of plies on Poisson's ratio defined by equation (59d) for $(+\theta/0/90)_m$ and $(-\theta/0/90)_m$ unbalanced, unsymmetric P-100/3502 laminates.

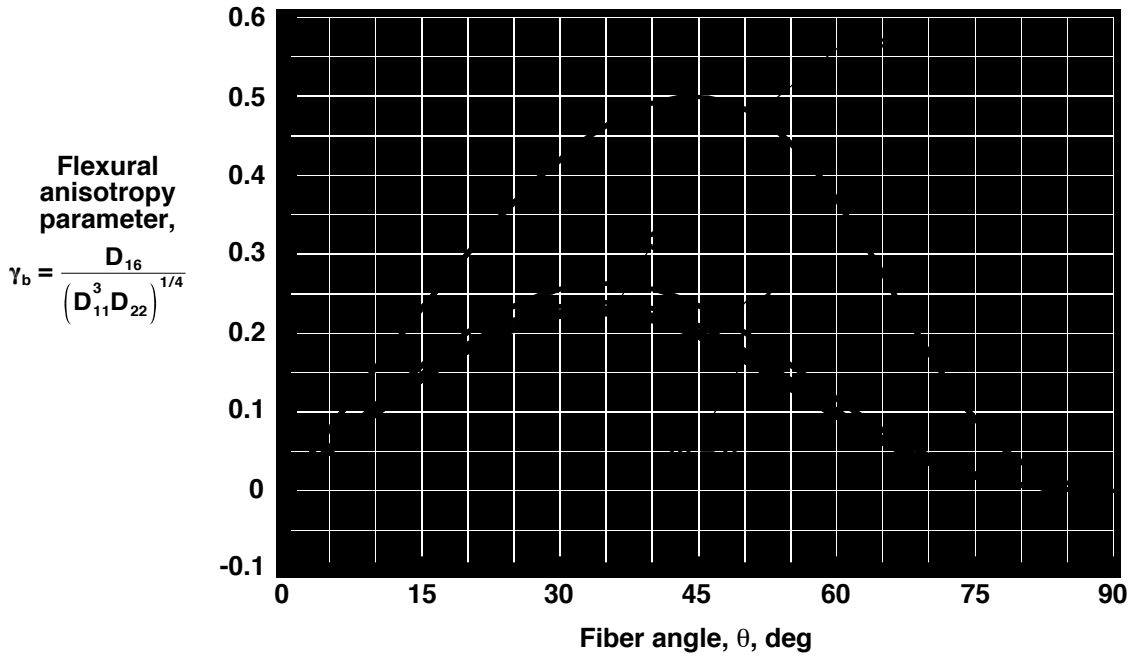

Figure 53. Effects of number of plies on flexural anisotropy parameters γ_b and $-\gamma_b$ for $(+\theta/0/90)_m$ and $(-\theta/0/90)_m$ unbalanced, unsymmetric P-100/3502 laminates, respectively.

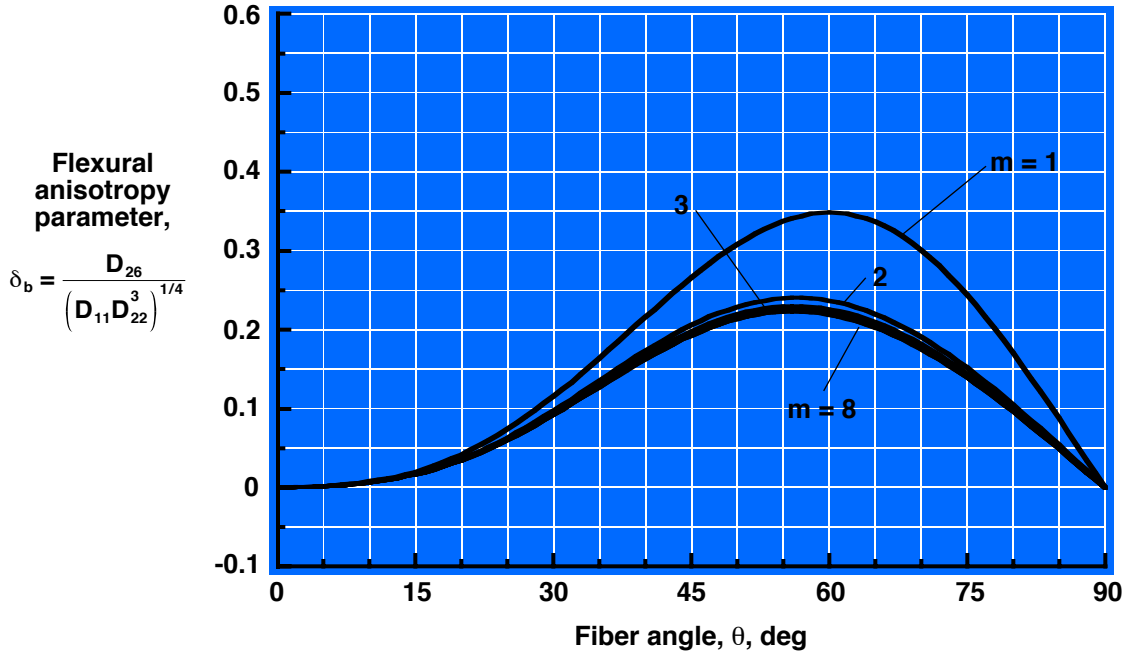

Figure 54. Effects of number of plies on flexural anisotropy parameters δ_b and $-\delta_b$ for $(+\theta/0/90)_m$ and $(-\theta/0/90)_m$ unbalanced, unsymmetric P-100/3502 laminates, respectively.

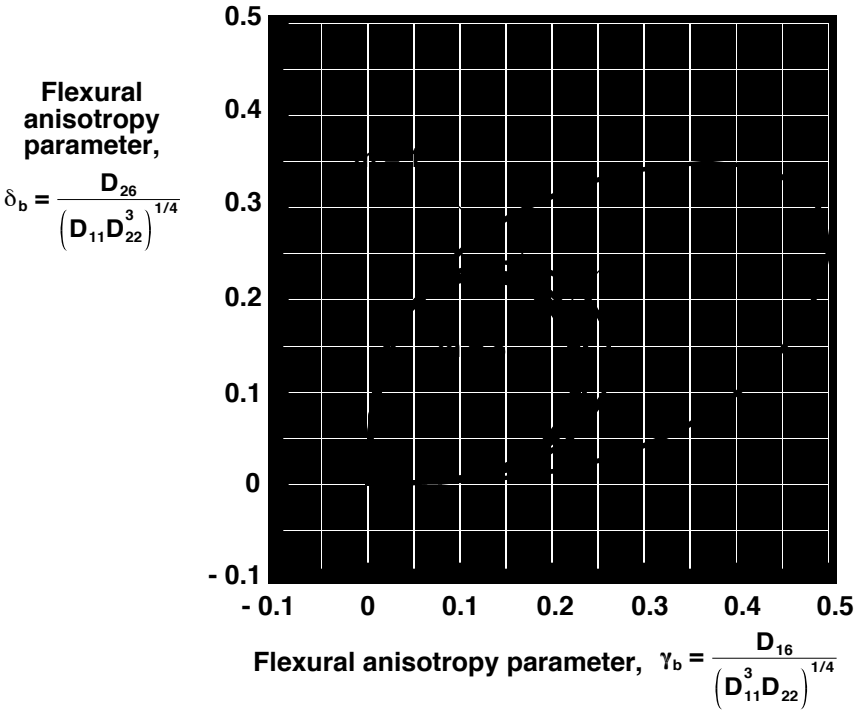

Figure 55. Effects of the number of plies on flexural anisotropy parameters γ_b and δ_b for $(+\theta/0/90)_m$ unbalanced, unsymmetric P-100/3502 laminates.

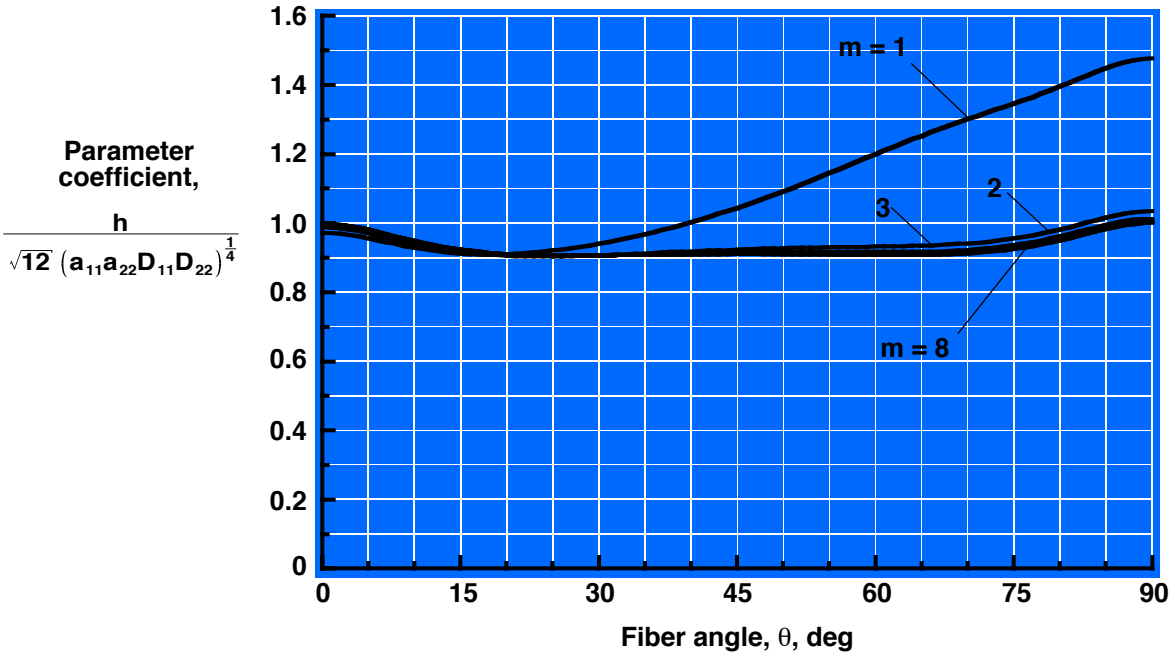

Figure 56. Effects of number of plies on Batdorf-Stein-parameter coefficients in equations (45) and (48) for $(+\theta/0/90)_m$ and $(-\theta/0/90)_m$ unbalanced, unsymmetric P-100/3502 laminates.

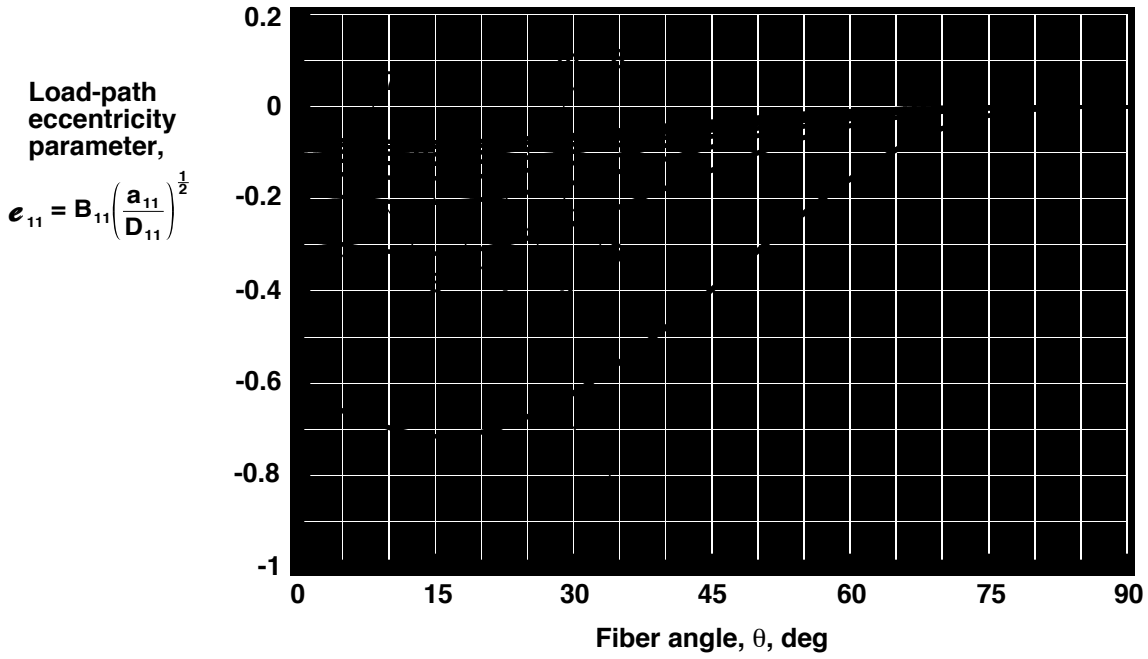

Figure 57. Effects of number of plies on nondimensional load-path eccentricity parameter e_{11} defined by equation (75b) for $(+\theta/0/90)_m$ and $(-\theta/0/90)_m$ unbalanced, unsymmetric P-100/3502 laminates.

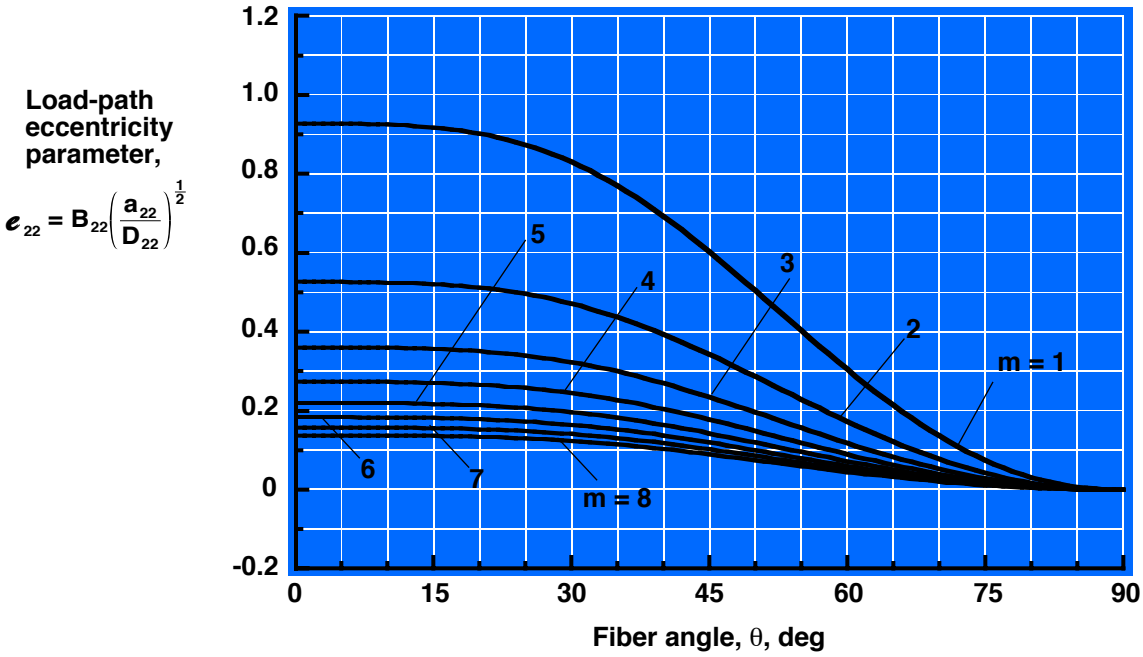

Figure 58. Effects of number of plies on nondimensional load-path eccentricity parameter e_{22} defined by equation (75d) for $(+\theta/0/90)_m$ and $(-\theta/0/90)_m$ unbalanced, unsymmetric P-100/3502 laminates.

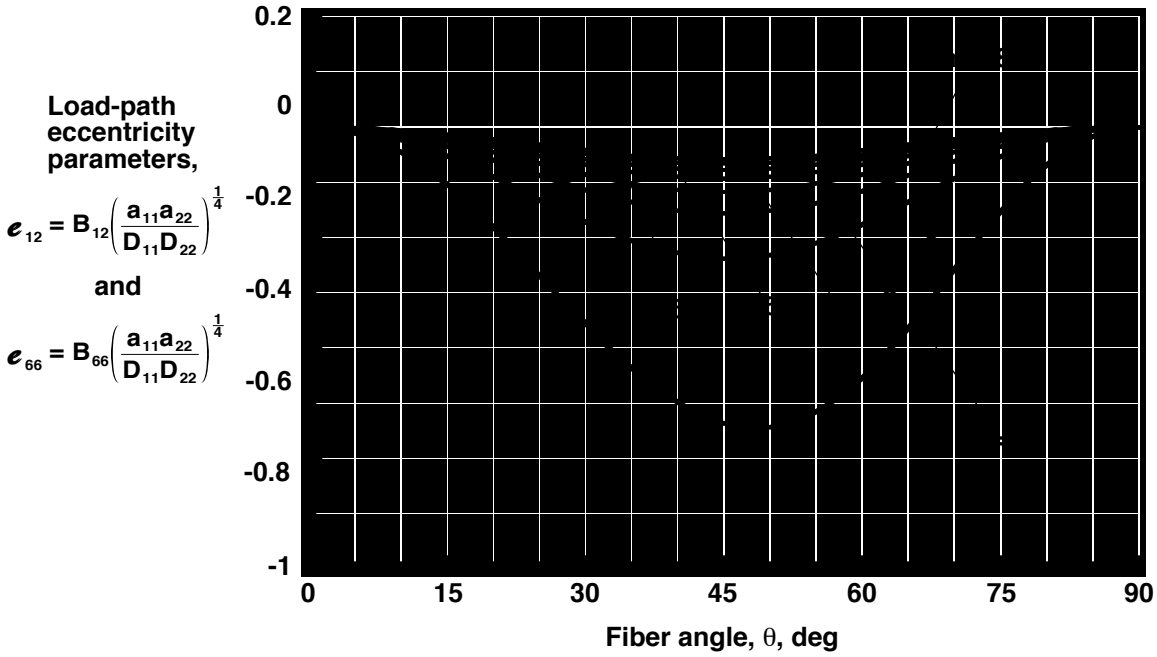

Figure 59. Effects of number of plies on nondimensional load-path eccentricity parameters e_{12} and e_{66} defined by equations (75) for $(+\theta/0/90)_m$ and $(-\theta/0/90)_m$ unbalanced, unsymmetric P-100/3502 laminates.

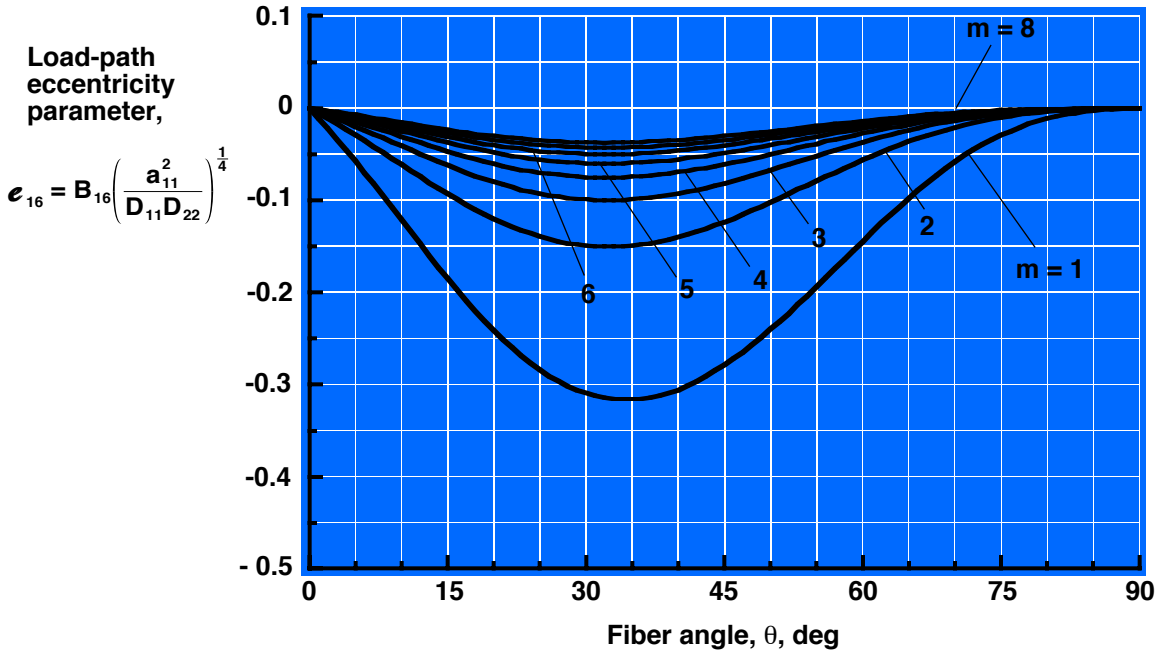

Figure 60. Effects of number of plies on nondimensional load-path eccentricity parameters e_{16} and $-e_{16}$ defined by equation (75) for $(+\theta/0/90)_m$ and $(-\theta/0/90)_m$ unbalanced, unsymmetric P-100/3502 laminates, respectively.

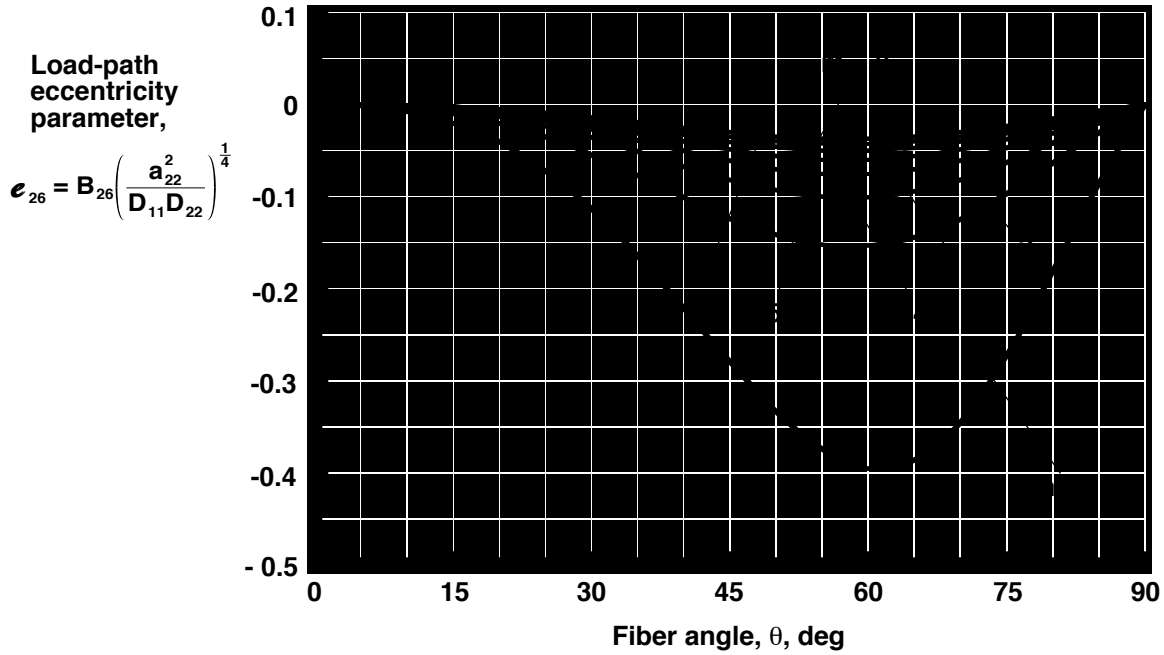

Figure 61. Effects of number of plies on nondimensional load-path eccentricity parameters e_{26} and $-e_{26}$ defined by equation (75) for $(+\theta/0/90)_m$ and $(-\theta/0/90)_m$ unbalanced, unsymmetric P-100/3502 laminates, respectively.

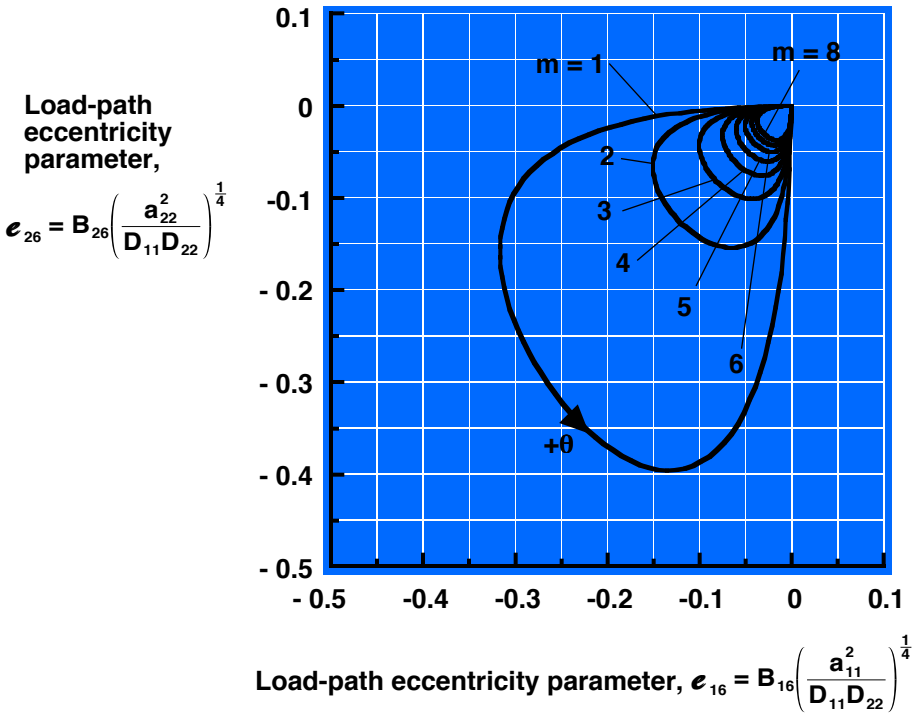

Figure 62. Effects of number of plies on nondimensional load-path eccentricity parameters e_{16} and e_{26} defined by equations (75) for $(+\theta/0/90)_m$ unbalanced, unsymmetric P-100/3502 laminates.

Appendix
Symbols

A	domain of the orthogonal Gaussian coordinates (ξ_1, ξ_2) for the shell reference surface, $\left[a_1, b_1\right] \times \left[a_2, b_2\right]$
a_1, a_2, b_1, b_2	constants that define the domain of the shell reference surface Gaussian coordinates; i. e., $a_1 \le \xi_1 \le b_1$ and $a_2 \le \xi_2 \le b_2$
$a_{11}, a_{12}, a_{16}, a_{22}, a_{26}, a_{66}$	membrane compliances defined by equation (21a), in./lb
$\mathcal{A}$	domain of the nondimensional orthogonal Gaussian coordinates (z_1, z_2) for the shell reference surface, $\left[\frac{a_1}{L_1}, \frac{b_1}{L_1}\right] \times \left[\frac{a_2}{L_2}, \frac{b_2}{L_2}\right]$
$A_1(\xi_1, \xi_2), A_2(\xi_1, \xi_2)$	metric coefficients of shell reference surface defined by equation (11)
$A_{11}, A_{12}, A_{16}, A_{22}, A_{26}, A_{66}$	membrane stiffnesses defined by equation (17), lb/in.
$[\mathcal{a}]$	matrix of constitutive constants defined by equation (154a)
$b_{11}, b_{12}, b_{16}, b_{22}, b_{26}, b_{66}$	constitutive constants defined by equation (21b), in.
$B_{11}, B_{12}, B_{16}, B_{22}, B_{26}, B_{66}$	coupling stiffnesses defined by equation (18), lb
$\mathcal{b}_{11}, \mathcal{b}_{12}, \mathcal{b}_{16}, \mathcal{b}_{22}, \mathcal{b}_{26}, \mathcal{b}_{66}$	constitutive constants defined by equation (69c)
$\mathcal{B}_{11}, \mathcal{B}_{12}, \mathcal{B}_{16}, \mathcal{B}_{21}, \mathcal{B}_{22}, \mathcal{B}_{26}, \mathcal{B}_{61}, \mathcal{B}_{62}, \mathcal{B}_{66}$	constitutive constants defined by equation (77)
$[\mathcal{B}]$	matix of constitutive constants defined by equation (139b)
ds	differential arc length defined in equation (11), in.
$d_{11}, d_{12}, d_{16}, d_{22}, d_{26}, d_{66}$	reduced bending stiffnesses defined by equation (21c), in-lb
$\mathcal{d}_{11}, \mathcal{d}_{12}, \mathcal{d}_{16}, \mathcal{d}_{22}, \mathcal{d}_{26}, \mathcal{d}_{66}$	constitutive constants defined by equations (79)
$[\mathcal{d}]$	matix of constitutive constants defined by equation (139c)
$D_{11}, D_{12}, D_{16}, D_{22}, D_{26}, D_{66}$	bending stiffnesses defined by equation (19), in-lb

$\mathcal{D}_b(\ ), \mathcal{D}_c(\ ), \mathcal{D}_{\varepsilon}(\ ), \mathcal{D}_m(\ ), \mathcal{D}_{\varphi}(\ )$	nondimensional linear differential operators defined by equations (122b), (122c), (122d), (124b), and (117b), respectively
E_L, E_T, G_{LT}	lamina moduli, psi
$E_{11}(z_1, z_2), E_{22}(z_1, z_2), G_{12}(z_1, z_2)$	nondimensional membrane strain fields defined by equations (46)
$\{E\}$	vector of nondimensional membrane strains defined by equation (151b)
$\left\{\overset{(1)}{E}\right\}$	vector of nondimensional membrane strains associated with adjacent equilibrium states and defined by equation (213a)
$e_{11}, e_{12}, e_{16}, e_{22}, e_{26}, e_{66}$	nondimensional load-path eccentricity parameters defined by equations (75)
$\overset{(0)}{E}_{11}(z_1, z_2, \tilde{p}), \overset{(0)}{E}_{22}(z_1, z_2, \tilde{p}),$ $\overset{(0)}{G}_{12}(z_1, z_2, \tilde{p})$	nondimensional membrane-strain fields associated with the primary equilibrium path and defined by equations (177)
$\overset{(1)}{E}_{11}(z_1, z_2), \overset{(1)}{E}_{22}(z_1, z_2), \overset{(1)}{G}_{12}(z_1, z_2)$	nondimensional membrane-strain fields associated with adjacent equilibrium states and defined by equations (193)
$\mathcal{F}(z_1, z_2)$	nondimensional stress function defined by equations (115)
$\overset{(1)}{\mathcal{F}}(z_1, z_2)$	nondimensional stress function associated with adjacent equilibrium states and defined by equations (214)
h	shell thickness, in.
$\mathcal{I}_1^B, \mathcal{I}_2^B$	boundary integrals defined by equations (134)
$\overset{(1)B}{\mathcal{I}}_1, \overset{(1)B}{\mathcal{I}}_2$	boundary integrals defined by equations (205)
$\mathcal{K}_{11}(z_1, z_2), \mathcal{K}_{22}(z_1, z_2), \mathcal{K}_{12}(z_1, z_2)$	nondimensional bending strain fields defined by equations (49)
$\overset{(0)}{\mathcal{K}}_{11}(z_1, z_2, \tilde{p}), \overset{(0)}{\mathcal{K}}_{22}(z_1, z_2, \tilde{p})$ $\overset{(0)}{\mathcal{K}}_{12}(z_1, z_2, \tilde{p})$	nondimensional bending-strain fields associated with the primary equilibrium path and defined by equations (178)

$\overset{(1)}{\mathcal{K}}_{11}(z_1, z_2), \overset{(1)}{\mathcal{K}}_{22}(z_1, z_2), \overset{(1)}{\mathcal{K}}_{12}(z_1, z_2)$	nondimensional bending-strain fields associated with adjacent equilibrium states and defined by equations (194)
$\{\mathcal{K}\}$	vector of nondimensional bending strains defined by equation (139a)
$\left\{\overset{(1)}{\mathcal{K}}\right\}$	vector of nondimensional bending strains associated with adjacent equilibrium states and defined by equation (213c)
L_1, L_2	characteristic dimensions used for scaling the (ξ_1, ξ_2) Gaussian coordinates
$\mathcal{L}(\ ,\ )$	nondimensional bilinear differential operator defined by equation (117c)
$M(\xi_1)$	moment per unit length applied to edges $\xi_2 = a_2$ and $\xi_2 = b_2$, as shown in figure 2, lb
$M(\xi_2)$	moment per unit length applied to edges $\xi_1 = a_1$ and $\xi_1 = b_1$, as shown in figure 2, lb
$M_{11}(\xi_1, \xi_2), M_{22}(\xi_1, \xi_2), M_{12}(\xi_1, \xi_2)$	bending stress resultants defined by equation (12b), lb
$\overline{M}(z_1)$	nondimensional loading applied to edges $\xi_2 = a_2$ and $\xi_2 = b_2$ and defined by equations (99)
$\overline{M}(z_2)$	nondimensional loading applied to edges $\xi_1 = a_1$ and $\xi_1 = b_1$ and defined by equations (98)
m_1, m_2, m_3	nondimensional functions defined by equation (121)
$\mathcal{M}_{11}(z_1, z_2), \mathcal{M}_{22}(z_1, z_2), \mathcal{M}_{12}(z_1, z_2)$	nondimensional bending stress resultants defined by equations (60)
$\overset{(0)}{\mathcal{M}}_{11}(z_1, z_2, \tilde{p}), \overset{(0)}{\mathcal{M}}_{22}(z_1, z_2, \tilde{p}),$ $\overset{(0)}{\mathcal{M}}_{12}(z_1, z_2, \tilde{p})$	nondimensional bending stress resultants associated with the primary equilibrium path (see equations (181) and (195))
$\overset{(1)}{\mathcal{M}}_{11}(z_1, z_2), \overset{(1)}{\mathcal{M}}_{22}(z_1, z_2), \overset{(1)}{\mathcal{M}}_{12}(z_1, z_2)$	nondimensional bending stress resultants associated with adjacent equilibrium states (see equations (195))
$\{m\}$	vector of nondimensional functions defined by equation (139d)
$\{\mathcal{M}\}$	vector of nondimensional stress resultants defined by equation (135b)

$\left\{\overset{(1)}{\mathcal{M}}\right\}$	vector of nondimensional stress resultants associated with adjacent equilibrium states (see equations (211))
$N(\xi_1)$	loads applied to edges $\xi_2 = a_2$ and $\xi_2 = b_2$, as shown in figure 2, lb/in.
$N(\xi_2)$	loads applied to edges $\xi_1 = a_1$ and $\xi_1 = b_1$, as shown in figure 2, lb/in.
$N_{11}(\xi_1, \xi_2), N_{22}(\xi_1, \xi_2), N_{12}(\xi_1, \xi_2)$	membrane stress resultants defined by equation (12a), lb/in.
$\mathcal{N}_{11}(z_1, z_2), \mathcal{N}_{22}(z_1, z_2), \mathcal{N}_{12}(z_1, z_2)$	nondimensional membrane stress resultants defined by equations (54)
$\overset{(0)}{\mathcal{N}}_{11}(z_1, z_2, \tilde{p}), \overset{(0)}{\mathcal{N}}_{22}(z_1, z_2, \tilde{p}),$ $\overset{(0)}{\mathcal{N}}_{12}(z_1, z_2, \tilde{p})$	nondimensional membrane stress resultants associated with the primary equilibrium path (see equations (181) and (195))
$\overset{(1)}{\mathcal{N}}_{11}(z_1, z_2), \overset{(1)}{\mathcal{N}}_{22}(z_1, z_2), \overset{(1)}{\mathcal{N}}_{12}(z_1, z_2)$	nondimensional membrane stress resultants associated with adjacent equilibrium states (see equations (195))
$\bar{N}(z_1)$	nondimensional loading applied to edges $\xi_2 = a_2$ and $\xi_2 = b_2$ and defined by equations (99)
$\bar{N}(z_2)$	nondimensional loading applied to edges $\xi_1 = a_1$ and $\xi_1 = b_1$ and defined by equations (98)
$\{\mathcal{N}\}$	vector of nondimensional stress resultants defined by equation (135a)
$[\mathcal{N}]$	matrix of nondimensional stress resultants defined by equation (135c)
$\left[\overset{(0)}{\mathcal{N}}(\tilde{p})\right]$	matrix of nondimensional stress resultants associated with the primary equilibrium path (see equations (211))
$\left\{\overset{(1)}{\mathcal{N}}\right\}$	vector of nondimensional stress resultants associated with adjacent equilibrium states (see equations (211))
P_m	force per unit area defined by equation (30), psi
$\mathcal{P}_m$	nondimensional value of P_m defined by equation (94)
$\mathcal{P}_T$	nondimensional function defined by equation (116b)

$\tilde{p}$, $\tilde{p}_{cr}$	nondimensional loading parameter and corresponding value at bifurcation, respectively
$\mathcal{P}_1, \mathcal{P}_2, \mathcal{P}_3$	nondimensional functions defined by equation (119)
$\{\mathcal{P}\}$	vector of nondimensional functions defined by equation (154b)
$q_1(\xi_1, \xi_2)$, $q_2(\xi_1, \xi_2)$, $q_3(\xi_1, \xi_2)$	applied tractions acting on shell reference surface, psi
$Q_1(\xi_1, \xi_2)$, $Q_2(\xi_1, \xi_2)$	transverse-shearing stress resultants defined by equation (13), lb/in.
$\overline{Q}_{11}, \overline{Q}_{12}, \overline{Q}_{16}, \overline{Q}_{22}, \overline{Q}_{26}, \overline{Q}_{66}$	transformed reduced stiffnesses for laminae in a state of plane stress, psi
$\mathcal{Q}_1(z_1, z_2)$, $\mathcal{Q}_2(z_1, z_2)$, $\mathcal{Q}_3(z_1, z_2)$	nondimensional applied tractions acting on shell reference surface and defined by equations (82), (84), and (92), respectively
$\mathcal{Z}_1(z_1, z_2)$, $\mathcal{Z}_2(z_1, z_2)$	nondimensional transverse-shear stress resultants defined by equations (86)-(89)
$\overset{(0)}{\mathcal{Z}}_1(z_1, z_2, \tilde{p})$, $\overset{(0)}{\mathcal{Z}}_2(z_1, z_2, \tilde{p})$	nondimensional shear stress resultants associated with the primary equilibrium path (see equations (181) and (195))
$\overset{(1)}{\mathcal{Z}}_1(z_1, z_2)$, $\overset{(1)}{\mathcal{Z}}_2(z_1, z_2)$	nondimensional shear stress resultants associated with adjacent equilibrium states (see equations (195))
$\{\tilde{\mathcal{F}}\}$	vector of nondimensional functions defined by equation (140b)
$[\tilde{\mathcal{F}}]$	matrix of nondimensional functions defined by equation (142b)
R_1, R_2	principal radii of curvature of the shell reference surface, in.
$S(\xi_1)$	loads applied to edges $\xi_2 = a_2$ and $\xi_2 = b_2$, as shown in figure 2, lb/in.
$S(\xi_2)$	loads applied to edges $\xi_1 = a_1$ and $\xi_1 = b_1$, as shown in figure 2, lb/in.
$\overline{S}(z_1)$	nondimensional loading applied to edges $\xi_2 = a_2$ and $\xi_2 = b_2$ and defined by equations (99)

$\bar{S}(z_2)$	nondimensional loading applied to edges $\xi_1 = a_1$ and $\xi_1 = b_1$ and defined by equations (98)
$\mathcal{U}_1(\xi_1,\xi_2,\zeta)$, $\mathcal{U}_2(\xi_1,\xi_2,\zeta)$, $\mathcal{U}_3(\xi_1,\xi_2,\zeta)$	components of the displacement vector field of the material points comprising a shell, in.
$u_1(\xi_1, \xi_2)$, $u_2(\xi_1, \xi_2)$, $w(\xi_1, \xi_2)$	displacement components of points of the two-dimensional shell reference surface defined by $\zeta = 0$
$U_1(z_1, z_2)$, $U_2(z_1, z_2)$	nondimensional displacement fields defined by equations (44) and (47), respectively
$\overset{(0)}{U}_1(z_1, z_2, \tilde{p})$, $\overset{(0)}{U}_2(z_1, z_2, \tilde{p})$, $\overset{(0)}{W}(z_1, z_2, \tilde{p})$	nondimensional displacement fields associated with the primary equilibrium path and defined by equations (175)
$\overset{(1)}{U}_1(z_1, z_2)$, $\overset{(1)}{U}_2(z_1, z_2)$, $\overset{(1)}{W}(z_1, z_2)$	nondimensional displacement fields associated with adjacent equilibrium states and defined by equations (175)
$V(\xi_1)$	loads applied to edges $\xi_2 = a_2$ and $\xi_2 = b_2$, as shown in figure 2, lb/in.
$V(\xi_2)$	loads applied to edges $\xi_1 = a_1$ and $\xi_1 = b_1$, as shown in figure 2, lb/in.
$\bar{V}(z_1)$	nondimensional loading applied to edges $\xi_2 = a_2$ and $\xi_2 = b_2$ and defined by equations (98)
$\bar{V}(z_2)$	nondimensional loading applied to edges $\xi_1 = a_1$ and $\xi_1 = b_1$ and defined by equations (99)
$W(z_1, z_2)$	nondimensional displacement defined by $w \equiv \left[a_{11}a_{22}D_{11}D_{22}\right]^{\frac{1}{4}} W$
$w_I(\xi_1, \xi_2)$	distribution of small geometric deviations in the ζ-coordinate direction, measured perpendicular to the tangent plane at each point of the shell reference surface
$W_I(z_1, z_2)$	nondimensional geometric imperfection function defined by $w_I \equiv \left[a_{11}a_{22}D_{11}D_{22}\right]^{\frac{1}{4}} W_I$
(z_1, z_2)	Nondimensional orthogonal Gaussian coordinates for shell reference surface given by $\xi_1 = L_1 z_1$ and $\xi_2 = L_2 z_2$
Z_1, Z_2	Batdorf-Stein parameters defined by equations (45) and (48)

α_b, α_m	nondimensional stiffness-weighted aspect ratios defined by equations (55) and (52a), respectively
β	nondimensional flexural orthotropy parameter defined by equation (59a)
$\beta_1(\xi_1, \xi_2)$, $\beta_2(\xi_1, \xi_2)$	fields defining rotation of material line elements tangent to the shell reference, defined by equations (10)
$\beta_1^I(\xi_1, \xi_2)$, $\beta_2^I(\xi_1, \xi_2)$	fields defining rotation of material line elements tangent to the shell reference surface associated with "small" initial geometric imperfections
γ_b	nondimensional flexural-twist anisotropy parameter defined by equation (59b)
γ_m	nondimensional membrane anisotropy parameter defined by equation (52c)
$\gamma_{12}(\xi_1,\xi_2,\zeta)$, $\gamma_{13}(\xi_1,\xi_2,\zeta)$, $\gamma_{23}(\xi_1,\xi_2,\zeta)$	shearing-strain fields for a three-dimensional shell body
$\gamma_{12}^o(\xi_1, \xi_2)$	tangential, membrane shearing-strain fields of shell reference surface
$\gamma_{13}^o(\xi_1, \xi_2)$, $\gamma_{23}^o(\xi_1, \xi_2)$	transverse-shearing-strain fields of shell reference surface
δ	variational operator of the Calculus of Variations
δ_b	nondimensional flexural-twist anisotropy parameter defined by equation (59c)
δ_m	nondimensional membrane anisotropy parameter defined by equation (52d)
$\delta E_{11}(z_1, z_2)$, $\delta E_{22}(z_1, z_2)$, $\delta G_{12}(z_1, z_2)$	nondimensional virtual membrane strain fields defined by equations (107)
$\overset{(1)}{\delta E}_{11}(z_1, z_2)$, $\overset{(1)}{\delta E}_{22}(z_1, z_2)$, $\overset{(1)}{\delta G}_{12}(z_1, z_2)$	virtual membrane strains associated with adjacent equilibrium states and defined by equations (208)
$\left\{\overset{(1)}{\delta E}\right\}$	vector of nondimensional virtual membrane strains associated with adjacent equilibrium states and defined by equation (213b)
$\delta\mathcal{F}$	nondimensional virtual stress function (see equations (150))

$\delta\mathcal{K}_{11}(z_1, z_2)$, $\delta\mathcal{K}_{22}(z_1, z_2)$, $\delta\mathcal{K}_{12}(z_1, z_2)$	nondimensional virtual bending strain fields defined by equations (108)
$\overset{(1)}{\delta\mathcal{K}}_{11}(z_1, z_2)$, $\overset{(1)}{\delta\mathcal{K}}_{22}(z_1, z_2)$, $\overset{(1)}{\delta\mathcal{K}}_{12}(z_1, z_2)$	virtual bending strains associated with adjacent equilibrium states and defined by equations (209)
$\{\delta\mathcal{K}\}$	vector of nondimensional virtual bending strains defined by equation (136d)
$\left\{\overset{(1)}{\delta\mathcal{K}}\right\}$	vector of nondimensional virtual bending strains associated with adjacent equilibrium states and defined by equation (213d)
$\delta\mathcal{N}^*_{11}$, $\delta\mathcal{N}^*_{22}$, $\delta\mathcal{N}^*_{12}$	nondimensional virtual stress resultants used in equations (143)
$\delta u_1(\xi_1, \xi_2)$, $\delta u_2(\xi_1, \xi_2)$, $\delta w(\xi_1, \xi_2)$	virtual-displacement fields of the two-dimensional shell reference surface defined by $\zeta = 0$
$\delta U_1(z_1, z_2)$, $\delta U_2(z_1, z_2)$, $\delta W(z_1, z_2)$	nondimensional virtual-displacement fields defined by equations (106)
δW	nondimensional radial-displacement field at buckling (see equations (1) and (2))
δW_{ext}	external virtual work per unit area defined by equation (23b), lb/in.
δW^{B}_{ext}	external virtual work per unit length defined by equations (23c), lb
δW_{int}	internal virtual work per unit area defined by equation (23a), lb/in.
$\overset{(1)}{\delta W}$	nondimensional virtual work associated with adjacent equilibrium states (see equations (203))
$\delta\mathcal{W}_{iext}$	nondimensional external virtual work per unit area defined by equation (109b)
$\overset{(1)}{\delta\mathcal{W}}$	nondimensional virtual work per unit area associated with adjacent equilibrium states and defined by equation (204a)
$\delta\mathcal{W}^{B}_{ext}$	external virtual work per unit length defined by equations (113)
$\overset{(1)}{\delta\mathcal{W}}^{B}_{1}$, $\overset{(1)}{\delta\mathcal{W}}^{B}_{2}$	nondimensional virtual work per unit length associated with adjacent equilibrium states and defined by equations (204)

$\delta\mathcal{W}^{*B}$, $\delta\tilde{\mathcal{W}}^{*B}$	complementary virtual work defined by equationa (147b) and (149b), respectively
$\delta\mathcal{W}_{int}$	nondimensional internal virtual work per unit area defined by equation (109a)
$\delta\overset{(1)}{\mathcal{W}}_{int}$	nondimensional internal virtual work per unit area associated with adjacent equilibrium states and defined by equation (206b)
$\delta\overset{(1)}{\mathcal{W}}'_{int}$	nondimensional internal virtual work per unit area associated with adjacent equilibrium states and defined by equation (206c)
$\delta\mathcal{W}^*_{int}$, $\delta\tilde{\mathcal{W}}^*_{int}$	nondimensional complementary internal virtual work per unit area defined by equations (147a) and (149a), respectively
$\delta\overset{(1)}{\mathcal{W}}^*_{int}$	nondimensional complementary internal virtual work per unit area associated with adjacent equilibrium states and defined by equation (234)
$\delta\overset{(1)}{\mathcal{W}}^{*B}$	nondimensional complementary virtual work associated with adjacent equilibrium states and defined by equation (232c)
$\delta\varepsilon^{\circ}_{11}(\xi_1, \xi_2)$, $\delta\varepsilon^{\circ}_{22}(\xi_1, \xi_2)$, $\delta\gamma^{\circ}_{12}(\xi_1, \xi_2)$	virtual membrane-strain fields of shell reference surface
$\delta\gamma^{\circ}_{13}(\xi_1, \xi_2)$, $\delta\gamma^{\circ}_{23}(\xi_1, \xi_2)$	virtual transverse-shearing-strain fields of shell reference surface
$\delta\kappa^{\circ}_{11}(\xi_1, \xi_2)$, $\delta\kappa^{\circ}_{22}(\xi_1, \xi_2)$, $\delta\kappa^{\circ}_{12}(\xi_1, \xi_2)$	fields defining virtual changes in shell reference-surface curvature and torsion
$\delta\psi_1(\xi_1, \xi_2)$, $\delta\psi_2(\xi_1, \xi_2)$	virtual rotation fields of the shell reference surface (see equations (27) and (28))
$\overset{(1)}{\delta\Omega}_1(z_1, z_2)$, $\overset{(1)}{\delta\Omega}_2(z_1, z_2)$	virtual rotations associated with adjacent equilibrium states and defined by equations (207)
$\{\delta\Omega\}$	vector of nondimensional virtual rotations defined by equation (136c)

$\left\{\delta\overset{(1)}{\Omega}\right\}$	vector of virtual rotations associated with adjacent equilibrium states and defined by equations (212c)
$\Delta_1(\xi_1)$, $\Delta_2(\xi_1)$, $\Delta_n(\xi_1)$	displacements applied to edges $\xi_2 = a_2$ and $\xi_2 = b_2$; positive in the positive ξ_1, ξ_2, and ζ directions, respectively, in.
$\Delta_1(\xi_2)$, $\Delta_2(\xi_2)$, $\Delta_n(\xi_2)$	displacements applied to edges $\xi_1 = a_1$ and $\xi_1 = b_1$; positive in the positive ξ_1, ξ_2, and ζ directions, respectively, in.
$\overline{\Delta}_1(z_1)$, $\overline{\Delta}_2(z_1)$, $\overline{\Delta}_n(z_1)$	nondimensional displacements applied to edges $\xi_2 = a_2$ and $\xi_2 = b_2$ and defined by equations (99)
$\overline{\Delta}_1(z_2)$, $\overline{\Delta}_2(z_2)$, $\overline{\Delta}_n(z_2)$	nondimensional displacements applied to edges $\xi_1 = a_1$ and $\xi_1 = b_1$ and defined by equations (98)
ε	"small" parameter used in bifurcation analysis, see equations (175)
$\varepsilon_{11}(\xi_1,\xi_2,\zeta)$, $\varepsilon_{22}(\xi_1,\xi_2,\zeta)$, $\varepsilon_{33}(\xi_1,\xi_2,\zeta)$	normal-strain fields for a three-dimensional shell body
$\varepsilon^{\circ}_{11}(\xi_1, \xi_2)$, $\varepsilon^{\circ}_{22}(\xi_1, \xi_2)$	tangential, membrane normal-strain fields of shell reference surface
θ	lamina fiber angle (see figure 3), degrees
$\kappa^{\circ}_{11}(\xi_1, \xi_2)$, $\kappa^{\circ}_{22}(\xi_1, \xi_2)$, $\kappa^{\circ}_{12}(\xi_1, \xi_2)$	fields defining changes in shell reference-surface curvature and torsion
μ	nondimensional orthotropy parameter defined by equation (52b)
ν_{LT}	lamina major Poisson's ratio
ν_b, ν_m	generalized laminate Poisson's ratios associated with membrane and bending action, respectively (see equations (52e) and (59d))
(ξ_1, ξ_2)	orthogonal Gaussian coordinates for shell reference surface
(ξ_1, ξ_2, ζ)	orthogonal curvilinear coordinates for points of three-dimensional Euclidean space
ρ	stiffness-weighted radius-to-thickness ratio defined by equations (10) and (20)
σ_{11}, σ_{12}, σ_{22}, σ_{13}, σ_{22}	shell stresses, psi

$\Phi(\xi_1)$	rotation applied to edges $\xi_2 = a_2$ and $\xi_2 = b_2$; positive about the positive ξ_1 direction
$\Phi(\xi_2)$	rotation applied to edges $\xi_1 = a_1$ and $\xi_1 = b_1$; positive about the negative ξ_2 direction
$\overline{\Phi}(z_1)$	nondimensional rotation applied to edges $\xi_2 = a_2$ and $\xi_2 = b_2$ and defined by equation (99d)
$\overline{\Phi}(z_2)$	nondimensional rotation applied to edges $\xi_1 = a_1$ and $\xi_1 = b_1$ and defined by equation (98d)
$\psi_1(\xi_1, \xi_2)$, $\psi_2(\xi_1, \xi_2)$	fields defining rotations of material line elements perpendicular to the shell reference surface
$\Omega_1(z_1, z_2)$, $\Omega_2(z_1, z_2)$	nondimensional rotation fields defined by equations (38)-(42)
$\{\Omega\}$	vector of nondimensional rotations defined by equation (136a)
$[\Omega]$	matrix of nondimensional rotations defined by equation (151c)
$\{\Omega_I\}$	vector of nondimensional rotations associated with an initial geometric imperfection and defined by equation (136b)
$[\Omega_I]$	matrix of nondimensional rotations associated with an initial geometric imperfection and defined by equation (151d)
$\overset{(0)}{\Omega}_1(z_1, z_2, \tilde{p})$, $\overset{(0)}{\Omega}_2(z_1, z_2, \tilde{p})$	nondimensional rotation fields associated with the primary equilibrium path and defined by equations (176)
$\overset{(1)}{\Omega}_1(z_1, z_2)$, $\overset{(1)}{\Omega}_2(z_1, z_2)$	nondimensional rotation fields associated with adjacent equilibrium states and defined by equations (192)
$\left\{ \overset{(0)}{\Omega}(\tilde{p}) \right\}$	vector of nondimensional rotation fields associated with the primary equilibrium path and defined by equations (212a)
$\left[\overset{(0)}{\Omega}(\tilde{p}) \right]$	matrix of nondimensional rotation fields associated with the primary equilibrium path and defined by equations (237)
$\left\{ \overset{(1)}{\Omega} \right\}$	vector of nondimensional rotation fields associated with adjacent equilibrium states and defined by equations (212b)
∂A	general boundary curve enclosing the reference surface domain

$\{\partial\mathcal{F}\}$	vector of nondimensional stress-function derivatives defined by equation (139e)
$[\partial\mathcal{F}]$	matrix of nondimensional stress-function derivatives defined by equation (142a)
$\left\{\partial\overset{(1)}{\mathcal{F}}\right\}$	vector of nondimensional stress-function derivatives associated with adjacent equilibrium states and defined by equation (211a)
$\{\partial\delta\mathcal{F}\}$	vector of nondimensional virtual-stress-function derivatives defined by equation (151e)
$\left\{\partial\overset{(1)}{\delta\mathcal{F}}\right\}$	vector of nondimensional virtual-stress-function derivatives associated with adjacent equilibrium states and defined by equation (226b)

REPORT DOCUMENTATION PAGE

Form Approved
OMB No. 0704-0188

1. REPORT DATE *(DD-MM-YYYY)*	2. REPORT TYPE	3. DATES COVERED *(From - To)*
01- 07 - 2010	Technical Publication	

4. TITLE AND SUBTITLE

Nondimensional Parameters and Equations for Nonlinear and Bifurcation Analyses of Thin Anisotropic Quasi-Shallow Shells

5a. CONTRACT NUMBER

5b. GRANT NUMBER

5c. PROGRAM ELEMENT NUMBER

6. AUTHOR(S)

Nemeth, Michael P.

5d. PROJECT NUMBER

5e. TASK NUMBER

5f. WORK UNIT NUMBER

869021.04.07.01.13

7. PERFORMING ORGANIZATION NAME(S) AND ADDRESS(ES)

NASA Langley Research Center
Hampton, VA 23681-2199

8. PERFORMING ORGANIZATION REPORT NUMBER

L-19827

9. SPONSORING/MONITORING AGENCY NAME(S) AND ADDRESS(ES)

National Aeronautics and Space Administration
Washington, DC 20546-0001

10. SPONSOR/MONITOR'S ACRONYM(S)

NASA

11. SPONSOR/MONITOR'S REPORT NUMBER(S)

NASA/TP-2010-216726

12. DISTRIBUTION/AVAILABILITY STATEMENT

Unclassified - Unlimited
Subject Category 39
Availability: NASA CASI (443) 757-5802

13. SUPPLEMENTARY NOTES

An electronic version can be found at http://ntrs.nasa.gov

14. ABSTRACT

A comprehensive development of nondimensional parameters and equations for nonlinear and bifurcations analyses of quasi-shallow shells, based on the Donnell-Mushtari-Vlasov theory for thin anisotropic shells, is presented. A complete set of field equations for geometrically imperfect shells is presented in terms general of lines-of-curvature coordinates. A systematic nondimensionalization of these equations is developed, several new nondimensional parameters are defined, and a comprehensive stress-function formulation is presented that includes variational principles for equilibrium and compatibility. Bifurcation analysis is applied to the nondimensional nonlinear field equations and a comprehensive set of bifurcation equations are presented. An extensive collection of tables and figures are presented that show the effects of lamina material properties and stacking sequence on the nondimensional parameters.

15. SUBJECT TERMS

Buckling; Shell mechanics; Structural design; Stability analysis; Nondimensional parameters

16. SECURITY CLASSIFICATION OF:			17. LIMITATION OF ABSTRACT	18. NUMBER OF PAGES	19a. NAME OF RESPONSIBLE PERSON
a. REPORT	b. ABSTRACT	c. THIS PAGE			STI Help Desk (email: help@sti.nasa.gov)
					19b. TELEPHONE NUMBER *(Include area code)*
U	U	U	UU	189	(443) 757-5802